MOTION CUES IN MAN-VEHICLE CONTROL

by

RICHARD S. SHIRLEY

S.B., S.M., Massachusetts Institute of Technology
(1963)

SUBMITTED IN PARTIAL FULFILLMENT OF THE
REQUIREMENTS FOR THE DEGREE OF
DOCTOR OF SCIENCE
at the
MASSACHUSETTS INSTITUTE OF TECHNOLOGY

January 1968

Signature of Author Signature redacted
Department of Aeronautics and Astronautics, January 1968

Certified by Signature redacted
Thesis Supervisor

Certified by Signature redacted
Thesis Supervisor

Certified by
Thesis Supervisor

Certified by Signature redacted
Thesis Supervisor

Accepted by Signature redacted
Chairman, Departmental Graduate Committee

MOTION CUES IN MAN-VEHICLE CONTROL

by

Richard S. Shirley

Submitted to the Department of Aeronautics and Astronautics, Massachusetts Institute of Technology, on January 21, 1967, in partial fulfillment of the requirements for the degree of Doctor of Science.

ABSTRACT

An investigation is made to determine how the human operator makes use of roll motion cues in a man-vehicle control system. To this purpose the human operator's describing function is measured over a wide range of vehicle dynamics and under conditions of visual inputs only, motion inputs only, and combined visual and motion inputs. Both the describing function (amplitude and phase of the human operator's output relative to his input) and the remnant (power spectral density of that part of the human operator's output which is uncorrelated with his input) are measured as a function of frequency. The relative integral squared error is also measured. Visual inputs are made by means of a dot moving laterally on an oscilloscope, and roll motion inputs are made by means of a motion simulator.

An analytical method of correcting the experimental measurements for errors introduced by the remnant is developed and applied to the data. The corrections are generally small.

Examination of the describing function data leads to some conclusions about the human operator's use of angular motion cues in a man-vehicle control system. When the roll motion cues are added to the visual cues the human operator is able to increase his lead in the frequency range above one radian per second. This permits him to increase his gain and cross-over frequency without decreasing his phase margin. The net effect of these changes in the human operator's control behavior is to increase the open loop gain without a loss of stability, and thus to reduce the relative integral squared error for the closed loop system.

The percentage reduction of the relative integral squared error upon the addition of the motion cues to the

visual cues varies as a function of the controlled vehicle dynamics. The human operator can make the most use of motion cues for vehicle dynamics which lead to significant roll motions above one radian per second. Such vehicle dynamics include low order dynamics ($1/s$ as opposed to $1/s^2$) and dynamics with an associated high control stick gain.

It is possible, in some cases, to use the body of data obtained for this thesis to predict actual in-flight or moving-base measurements of the human operator's describing function from fixed-base measurements of the human operator's describing function.

Prof. L. R. Young, Chairman, thesis committee

Prof. Y. T. Li, Thesis Supervisor

Prof. W. Vander Velde, Thesis Supervisor

Prof. J. Meiry, Thesis Supervisor

ACKNOWLEDGMENTS

The author gratefully acknowledges the guidance and support from his thesis supervisors, Professors L. R. Young, Y. T. Li, W. E. Vander Velde, and J. L. Meiry. Professor Young was closely associated with the research in all phases. Professor Meiry was of particular help in solving the intricacies of balky computers and simulators. Professor Vander Velde helped greatly in the analysis of the effects of the remnant.

The author is grateful to Mr. John Barley for technical assistance and to all the patient subjects who worked long hours in the simulator: S.U., B.P., R.S., L.L., T.I., J.G., and S.F. The author is grateful to his parents for their encouragement and to his wife for her moral support and countless cups of coffee.

This research was supported in part by NASA Grant NsG-577.

TABLE OF CONTENTS

	page
CHAPTER I: INTRODUCTION	1
1.1 Motion Cues In Man-Vehicle Control	1
1.2 A Brief Review Of Results To Date	3
1.3 Objectives Of The Thesis	5
1.4 Results Of The Thesis	6
1.5 Outline Of The Thesis	8
CHAPTER II: THE EXPERIMENT	9
2.1 What The Experiment Will Accomplish	9
2.2 A Brief Outline Of The Experiment	10
2.3 Details Of The Experiment	10
2.4 Validation of the Experimental System	28
CHAPTER III: THE EFFECTS OF THE REMNANT ON THE MEASUREMENTS	42
3.1 Derivation Of An Analytical Expression For The Effects Of The Remnant On The Measurements	42
3.2 Application Of The Remnant Correction To The Data	49
3.3 Difficulties In Correcting For The Remnant	57
CHAPTER IV: EXPERIMENTAL RESULTS	61
4.1 Introduction	61
4.2 How Roll Motion Cues Affect The Human Operator's Describing Function	62
4.3 The Human Operator's Use Of Roll Motion Cues As A Function Of Vehicle Dynamics	77
4.4 Variation Of Some Other Experimental Parameters	88

TABLE OF CONTENTS (continued)

4.5 Where The Effects Of Roll Angular Motion Cues Are Known 94

4.6 The Beginning Of A Physiological Model For The Human Operator's Use Of Motion Cues 95

CHAPTER V: CONCLUSIONS AND SUGGESTIONS FOR FURTHER WORK 101

5.1 The Conclusions Of The Thesis 101

5.2 Suggestions For Further Work 103

APPENDIX A: THE HYBRID COMPUTER 105

A.1 Introduction 105

A.2 The Digital Computer 105

A.2 The Analog Computer 105

A.3 The Hybrid Components 106

APPENDIX B: THE EFFECTS OF THE .1-SECOND DELAY ON THE HUMAN OPERATOR'S DESCRIBING FUNCTION 107

B.1 Examination Of Some Data 107

B.2 How To Correct The Experimental Data For The Effects Of The Delay 111

APPENDIX C: THE MEASUREMENT BANDWIDTH 113

APPENDIX D: THE HYBRID COMPUTER PROGRAMS 116

APPENDIX E: COMPUTER PROGRAM LISTINGS 118

APPENDIX F: THE EXPERIMENTAL DATA 162

F.1 Index To The Data 163

F.2 Explanation Of The Data Presentation 167

F.3 The Experimental Data 172

F.4 Subject To Subject Differences 233

F.5 Models Of The Human Operator's Describing Functions 253

TABLE OF CONTENTS (continued)

BIBLIOGRAPHY 291

BIOGRAPHICAL SKETCH 294

LIST OF FIGURES

number	title	page
1.1	the human operator performing a compensatory task in a man-vehicle control loop	2
2.1	the experimental set-up: the human operator in a compensatory system with visual and motion cues	11
2.2	the model for the human operator	12
2.3	the NE-2 simulator used in the experiment	13
2.4	the interior of the NE-2 simulator used in the experiment	14
2.5	the hybrid computer used in the experiment	15
2.6	the input to the man-vehicle control system	25
2.7	example of the run to run variability of the data	35
2.8	comparison of results with McRuer, et al., for $Y_c=1$, visual cues only	38
2.9	comparison of results with McRuer, et al., for $Y_c=1/s$, visual cues only	39
2.10	comparison of results with McRuer, et al., for $Y_c=1/s^2$, visual cues only	40
2.11	comparison of results with Meiry, for $Y_c=1/s$, motion cues only	41
3.1	diagram used in the derivation of the expression for the effects of the remnant	43

LIST OF FIGURES (continued)

number	title	page
3.2	The effect of the remnant correction for Y_p for $Y_c=1/s^2$ (no delay) for a fifteen minute run time	50
3.3	the effect of the remnant correction for Y_p for $Y_c=e^{-.1s}/s$ for a 90 second run time	51
3.4	the effect of the remnant correction for Y_p for $Y_c=10e^{-.1s}/s(s^2+10)$ for a 90 second run time	52
3.5	the effect of the remnant correction for Y_p for $Y_c=15e^{-.1s}/s(s^2+3s+15)$ for a 90 second run time	53
4.1	division of the $2\zeta\omega_n-\omega_n^2$ plane by type of Y_p measured for $Y_c=\omega_n^2e^{-.1s}/(s^2+2\zeta\omega_n s+\omega_n^2)$ part A	64
4.2	division of the $2\zeta\omega_n-\omega_n^2$ plane by type of Y_p measured for $Y_c=\omega_n^2e^{-.1s}/(s^2+2\zeta\omega_n s+\omega_n^2)$ part B	65
4.3	division of the real axis of the s-plane by type of Y_p measured for $Y_c=Ke^{-.1s}/s(\tau s+1)$, part A	66
4.4	division of the real axis of the s-plane by type of Y_p measured for $Y_c=Ke^{-.1s}/s(\tau s+1)$, part B	67
4.5	division of the $2\zeta\omega_n-\omega_n^2$ plane by type of Y_p measured for $Y_c=\omega_n^2e^{-.1s}/s(s^2+2\zeta\omega_n s+\omega_n^2)$ part A	68
4.6	division of the $2\zeta\omega_n-\omega_n^2$ plane by type of Y_p measured for $Y_c=\omega_n^2e^{-.1s}/s(s^2+2\zeta\omega_n s+\omega_n^2)$ part B	69

LIST OF FIGURES (continued)

number	title	page
4.7	how the human operator changes his control behaviour upon the introduction of roll motion cues	76
4.8	effects of motion cues for $Y_c=\omega_n^2 e^{-.1s}/(s^2+2\zeta\omega_n s+\omega_n^2)$	78
4.9	effects of motion cues for $Y_c=Ke^{-.1s}/s(\tau s+1)$	79
4.10	effects of motion cues for $Y_c=\omega_n^2 e^{-.1s}/s(s^2+2\zeta\omega_n s+\omega_n^2)$	80
4.11	the effects of motion cues on system performance as the vehicle dynamics range from $1/s$ to $1/s^2$ to $1/s^3$	82
4.12	the effects of motion cues for $Y_c=\omega_n^2 e^{-.1s}/(s^2+2\zeta\omega_n s+\omega_n^2)$	84
4.13	the effects of motion cues for $Y_c=Ke^{-.1s}/s(\tau s+1)$	85
4.14	the effects of motion cues for $Y_c=\omega_n^2 e^{-.1s}/s(s^2+2\zeta\omega_n s+\omega_n^2)$	86
4.15	the effect of variation of the control stick gain on the human operator's describing function for $Y_c=e^{-.1s}/s(s+1)$	89
4.16	the effect of variation of the input gain on the human operator's describing function for $Y_c=e^{-.1s}/s^2$	92
4.17	the effect of variation of the input breakpoint on the human operator's describing function for $Y_c=e^{-.1s}/s^2$	93

LIST OF FIGURES (continued)

number	title	page
4.18	development of a physiological model of the human operator's use of motion cues in man-vehicle control, part A	97
4.19	development of a physiological model of the human operator's use of motion cues in man-vehicle control, part B	98
B.1	the effects of the .1-second delay for $Y_c=1$	108
B.2	the effects of the .1-second delay for $Y_c=1/s$	109
B.3	the effects of the .1-second delay for $Y_c=1/s^2$	110
C.1	the effective bandwidth of the experimental system	115

GLOSSARY OF SYMBOLS

A_{ab} the Fourier coefficient of the signal a of frequency ω_b defined by $A_{ab} = \int_{t_o}^{t_o+2\pi n\omega_b} a(t)\sin\omega_b t\,dt$

A_{ek} the Fourier coefficient of the signal, e, of frequency ω_k, see A_{ab} above

A_k the amplitude of a sinusoid of frequency ω_k

A_{Mj} the Fourier coefficient of the signal M_m of frequency ω_j, see A_{ab} above

A_{Mk} the Fourier coefficient of the signal M_m of frequency ω_k, see A_{ab} above

AR the amplitude ratio of the human operator's describing function, Y_p

B_{ab} the Fourier coefficient of the signal a of frequency ω_b defined by $B_{ab} = \int_{t_o}^{t_o+2\pi n\omega_b} a(t)\cos\omega_b t\,dt$

B_{ek} the Fourier coefficient of the signal e of frequency ω_k, see B_{ab} above

B_{Mj} the Fourier coefficient of the signal M_m of frequency ω_j, see B_{ab} above

B_{Mk} the Fourier coefficient of the signal M_m of frequency ω_k, see B_{ab} above

C the coefficient of a lead term in the numerator of the vehicle dynamics, appears as $(1 + Cs)$

e the error signal for the system, see figure 2.1, a function of time, $e(n\Delta t)$, and a function of frequency, $e(\omega_k)$

$e^{-.1s}$ the Laplace transform of a pure time delay of .1 seconds,

GLOSSARY OF SYMBOLS (continued)

$f(t)$ a general signal, defined in various ways in the development of the expression for the correction of the measurements for the remnant, see Chapter III

$F(\omega_k)$ the Fourier transform of $f(t)$

$F_{xe}(\omega)$ the transfer function from x to e as diagrammed in figure 3.1

$F_{xM}(\omega)$ the transfer function from x to M_m as diagrammed in figure 3.1

$i(t)$ the system input, defined in Chapter II section 2.3.7

ISE the system integral squared error

ISI the integral squared input

K the control stick gain, see Chapter II section 2.3.5

K' a gain which multiplies the input, equal to unity for the bulk of the experiment, see Chapter II section 2.3.7

$M_a(\omega)$ the output from the human operator's describing function, see figure 3.1

M_m the human operator's output, a function of frequency, $M_m(\omega)$

$M_{nn}(\omega)$ that portion of the human operator's output, M_m, which is due to the remnant

n an index over the data, ranging from 1 to 896

$o(t)$ the output of the man-vehicle control system

P_k the initial phase of a sinusoid, used in Chapter III in the derivation of the expression for the correction of the measurements for the remnant

rISE	the relative integral squared error for the man-vehicle control system, see Chapter II, section 2.3.8
$rISE_V$	the rISE for the case where the human operator receives visual cues only
$rISE_{V+M}$	the rISE for the case where the human operator receives simultaneous visual and motion cues
s	the Laplace operator
$s_{nn}(t)$	a general signal, characterized by a continuous, smooth power spectral density, $S_{nn}(\omega)$, used in Chapter III in the derivation of the expression for the correction of the measurements for the remnant
$S_{nn}(\omega)$	a continuous, smooth power spectral density which characterizes $s_{nn}(t)$
t	time, measured in seconds
$x_{nn}(t)$	the human operator's remnant, see figure 2.2
Y_c	the vehicle dynamics, a function of s, $Y_c(s)$, or of ω, $Y_c(\omega)$
Y_p	the human operator's describing function, a function of s, $Y_p(s)$, or of ω, $Y_p(\omega)$
Y_{pa}	the actual human operator's describing function, defined in figure 3.1
Y_{pm}	the measured human operator's describing function, defined in figure 3.1
$Y_{comp}(s)$	that portion of the model for the human operator's describing function normally associated with the compensation abilities of the human operator, see Chapter IV, section 4.6

Y_{musc} that portion of the model for the human operator's describing function normally associated with the human operator's muscular dynamics, see Chapter IV, section 4.6

Δt an increment of time, equal to .1 seconds for the calculations for the experiment

$\delta\omega_k$ the effective bandwidth of the measurements of the thesis, see Appendix C

ζ the damping ratio associated with the vehicle dynamics, see Chapter II, section 2.3.6

ζ_m the damping ratio associated with the models for the human operator's describing function, see Chapter IV section 4.2

ζ_N the damping ratio associated with the human operator's muscular dynamics, see Chapter IV section 4.6

$\theta(s)$ the angular position of the human operator's head with respect to the horizontal

σ one standard deviation

τ the time constant associated with some of the vehicle dynamics, see Chapter II, section 2.3.6

τ_d the time delay associated with the model for the human operator's describing function, see Chapter IV, section 4.2

τ_i the time constants (for i = 1, 2, 3, 4, or 5) associated with the models for the human operator's describing function, see Chapter IV section 4.2

τ_N the time constant associated with the human operator's muscular dynamics, see Chapter IV section 4.6

ω frequency, measured in rad/sec

ω_{co} the cross-over frequency, that frequency at which the open loop gain (the magnitude of the product of the human operator's describing function and the vehicle dynamics) crosses from greater than unity to less than unity

ω_j frequencies between the input frequencies, ω_k

ω_k the input frequencies, see Chapter II section 2.3.7

ω_n the natural frequency associated with the vehicle dynamics, see Chapter II section 2.3.6

ω_{nm} the natural frequency associated with the model for the human operator's describing function, see Chapter IV, section 4.2

ω_{Nn} the natural frequency associated with the human operator's muscular dynamics, see Chapter IV section 4.6

$\Phi_{nn}(\omega)$ the power spectral density of the human operator's remnant, assumed to be a smooth and continuous function of frequency

CHAPTER I: INTRODUCTION

1.1 Motion Cues In Man-Vehicle Control

As aerospace technology develops, humans are being put in control of an ever-increasing variety of vehicles. Today's airplanes, VTOL's, and spacecraft are complex. They have a large number of instruments which the human must monitor to ensure the proper operation of the vehicle. They also possess dynamics which demand a great deal of skill on the part of the human operator to be controlled safely. In fact, the control capabilities of the human operator, and the interface between the human operator and the vehicle, have become so critical that they must be of prime concern in the development of new vehicles in which manual control is to be considered as a primary or back-up system.

In order to evaluate the dynamics of a proposed vehicle from the point of view of human operator control, the dynamics can be simulated on an analog computer. A pilot is then asked to control the dynamics in the laboratory on the ground. For example, the pilot could be placed in the compensatory system shown in figure 1.1. However, the results obtained from such a laboratory experiment are found to differ from the results of actual flight tests when the vehicle is developed. The differences are due to many things. In the fixed-base laboratory experiment the pilot does not receive motion cues, and the visual cues he receives are vastly different from actual flight experience. The noises, sights, and the entire atmosphere of actual flight are lacking in the laboratory. In order to over-come such differences, more realistic simulation is used. By simulating the conditions of the vehicle in flight it is possible to obtain a better prediction of

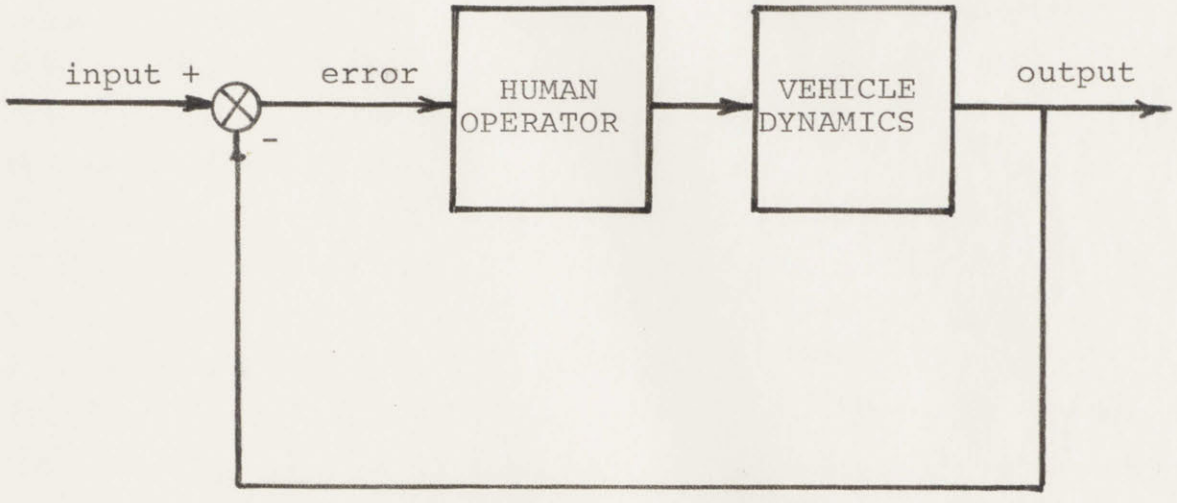

THE HUMAN OPERATOR PERFORMING A COMPENSATORY TASK IN A MAN-VEHICLE CONTROL LOOP: A SITUATION OFTEN USED TO TEST VEHICLE DYNAMICS, AND USED IN THIS THESIS TO INVESTIGATE THE HUMAN OPERATOR'S USE OF MOTION CUES

Figure 1.1

how well the pilot will be able to control the actual vehicle.

By experience it has been learned that the simulation of vehicle motions is most important. When vehicle motions are simulated in the laboratory, experiments yield data for the human operator which are usually in close agreement with the data obtained later from the actual vehicle. The motions involved are the classical six degrees of freedom (three degrees of translation and three degrees of rotation), vibrations, and sustained acceleration. Unfortunately it is expensive, often difficult, and sometimes impossible to simulate the motions of a given vehicle in the laboratory. Also difficult and expensive is the use of variable-stability aircraft to simulate a proposed vehicle. It would therefore be very useful to have sufficient knowledge about the effects of motion cues upon the human operator to be able to predict the actual flight data from fixed-base data taken in the laboratory without motion simulations. The purpose of this thesis is to take a step in that direction.

1.2 A Brief Review Of Results To Date

Simulation of vehicle motions has been perfected to the point where laboratory data for the human operator are very close to actual flight data for many situations. It has been learned that in the absence of high vibration levels or sustained acceleration the simulation of angular motions is generally (but not always) more important than translation simulation. Young (reference 28) points out the fact that stabilization of most vehicles requires attitude control prior to control of position, thus emphasizing rotational motions.

A great deal has been learned about man's primary motion sensors within the vestibular system. Meiry (reference 17) and Meiry and Young (reference 29) have developed models for the semicircular canals and otoliths. The model for the semicircular canals relates the human's subjective angular velocity to the actual angular velocity of his head. Thus the semicircular canals are primarily angular velocity sensors. The model for the otoliths relates the human's subjective angular position relative to the horizontal, (or the human's subjective linear acceleration), to the specific force on the human's head. Thus the otoliths are primarily linear acceleration sensors.

There is some knowledge of how the human operator uses motion to aid in vehicle control. Of particular interest is Meiry's conclusion (reference 17) that the human operator uses angular motion cues to generate more lead compensation at higher frequencies than can be generated with visual cues only. In a survey report (reference 28) which summarizes the results of most of the investigations of the human operator's use of motion cues as of January, 1966, Young concludes that:

"1. When vehicle dynamics are removed from the acceptable region, motion cues become more helpful to the pilot. Easily controlled vehicles do not require additional cues. Marginally stable or unstable vehicles, however, may require more lead compensation than is comfortably generated by pilots on the basis of instruments, and consequently the rate sensing elements of the vestibular system prove valuable in giving early indications of attitude changes.

2. Motion cues are more helpful with unstable

dynamics than with lightly damped oscillatory vehicles. As noted by others, the motion accompanying high frequency oscillations may shake the pilot about in the cockpit making precise control and accurate reading of the instruments difficult."

Knowledge of the human operator's use of motion cues in man-vehicle control is far from complete. Other than Meiry's result there is no clear understanding of how the human operator modifies his control behavior upon the addition of motion cues to visual cues, or of how this modification varies as a function of the vehicle dynamics. To a large extent the lack of knowledge is due to the fact that the data available on the human's use of motion cues comes from so many different sources. In trying to compare data from any two sources one often finds that so many experimental parameters differ between the two experiments that a direct comparison of the results is impossible. Furthermore, there is very little data available for the human operator's describing function while using motion cues.

1.3 Objectives Of The Thesis

The objectives of the thesis are twofold:

1) to develop a body of data on the human operator's use of roll motion cues, and
2) to use the data to to extend our knowledge of how the human operator uses angular motion cues in man-vehicle control situations.

In pursuing these a third objective is encountered:

3) to develop a method of analytically correcting the experimental measurements for errors introduced by the human operator's remnant (see Chapter II,

section 2.3.9, and Chapter III).

1.4 Results Of The Thesis

1.4.1 The Data

The data taken consist of the human operator's describing function and remnant and the system integral squared error for each of the experimental conditions studied. Data were taken for visual cues only, motion cues only, and simultaneous visual and motion cues for each set of vehicle dynamics considered. Visual cues were made by means of a dot moving laterally on an oscilloscope, and motion cues were made by means of a motion simulator in the roll mode. The vehicle dynamics studied included

$$Y_c = \frac{K}{s(\tau s + 1)} \text{ , } K \text{ and } \tau \text{ vary}$$

$$Y_c = \frac{\omega_n^2}{s^2 + 2\zeta\omega_n s + \omega_n^2} \text{ , } 2\zeta\omega_n \text{ and } \omega_n^2 \text{ vary}$$

$$Y_c = \frac{\omega_n^2}{s(s^2 + 2\zeta\omega_n s + \omega_n^2)} \text{ , } 2\zeta\omega_n \text{ and } \omega_n^2 \text{ vary}$$

Furthermore, for $Y_c = 1/s^2$, data were taken as other experimental parameters were varied in order to permit comparison of the data with previous and future work.

For complete details of the experiment see Chapter II. The data are presented on pages 161 to 288.

Prior to this work very few data were available on the human operator's describing function in the presence of motion cues.

In reference 17, Meiry states that the human's motion

sensor dynamics are the same in pitch as in roll in-so-far as orientation to the vertical is concerned. Hence the data and conclusions drawn from the data can be generalized from the roll-control studied to include pitch-control.

1.4.2 Conclusions About The Human Operator's Use Of Motion Cues

The data consistently confirm that the human operator uses roll motion cues to increase the phase lead of his describing function above 1 rad/sec. The increase in lead permits the human operator to increase his gain, and hence his cross-over frequency[1], without a loss of phase margin.(see Chapter IV, section 4.2). Figure 4.7, on page 76, illustrates the changes the human operator makes in his describing function when roll motion cues are added to visual cues.

The data also permit conclusions to be made as to which vehicle dynamics permit the human operator to make the best use of motion cues. "Best use" is measured as the greatest percentage reduction in the relative integral squared error when roll motion cues are added to visual cues. Better use of motion cues, as measured by percentage changes in the relative integral squared error, can be made for vehicle dynamics which are unstable or marginally stable, and for vehicle dynamics which cause rapid angular motions. Vehicle dynamics which cause rapid angular motions include low order dynamics (i.e. $1/s$ as opposed to $1/s^2$), and vehicle dynamics with a high gain between the control stick and roll angle.

1 cross-over frequency: that frequency at which the magnitude of the product of the vehicle dynamics and the human operator's describing function crosses from greater than unity to less than unity

1.5 Outline Of The Thesis

In Chapter II the experiment is described in detail, and then validated by comparison with known results from other experiments. Chapter III deals with the effect of the human operator's remnant (the human's output uncorrelated with his input) on the measurements taken, and derives a method by which the measurements can be corrected for the effect. In Chapter IV the experimental results are analyzed and some conclusions are made about the human operator's use of roll motion cues in vehicle control. Conclusions are also made as to just when the data can be used to predict the effects of roll motion cues on system performance, and thus permit prediction of moving-base data from fixed-base results. Finally, in Chapter V, the conclusions of the thesis are stated and some suggestions for further work are made.

CHAPTER II: THE EXPERIMENT

2.1 What The Experiment Accomplished

The purpose of the experiment was to obtain a body of data which would yield information about how a human operator utilizes angular motion cues while controlling a vehicle. Therefore, for each set of vehicle dynamics data were taken for the human operator as he received visual cues only, motion cues only, and simultaneous visual and motion cues. As will be seen in this chapter, all the parameters of the experiment were very carefully controlled so that differences among the data were due only to variations in the parameters of interest. The experiment was also designed to show how the human operator's use of angular motion cues in vehicle control varies as a function of the vehicle dynamics. For this purpose data were taken for a wide range of vehicle dynamics of practical interest (see section 2.3.6 of this chapter). Finally, the experiment was used to produce data for one set of vehicle dynamics as other experimental parameters were varied, thus permitting future extrapolation of all the data along these parameters for comparison with other data.

The actual data taken for each condition include:

1) the human operator's describing function as a function of frequency,
2) the human operator's remnant as a function of frequency, and
3) the system relative integral squared error.

For more details about the form of the data see sections 2.3.8 and 2.3.9 of this chapter.

2.2 A Brief Outline Of The Experiment

Figure 1.1 (page 2) shows a simple block diagram of the experiment: the human operator controlling a vehicle in a compensatory system. Figure 2.1 shows a few more details. The inputs to the human operator were visual and roll angular motion indications of the system error. The visual inputs were made by means of a dot moving laterally on an oscilloscope, the centered position on the scope face corresponding to zero system error. The motion inputs were made by means of a simulator in roll, the vertical position of the simulator cab corresponding to zero system error. The output from the human operator was by means of a spring-centered, pencil-type control stick. Figure 2.2 shows how the human operator is conventionally modelled by a describing function plus a remnant. In order to provide numbers for the human operator's describing function and remnant as a function of frequency, data were taken at the input to and at the output from the human operator. The data were stored digitally, and processed at the end of the run to yield values for the human operator's describing function and remnant (see sections 2.3.8 and 2.3.9 of this chapter and Chapter III). The vehicle dynamics were simulated on an analog computer, and are described in section 2.3.6 of this chapter. The system input was a pseudo-random sum of ten sinusoids provided by the digital computer, and is described in section 2.3.7 of this chapter. Figures 2.3 through 2.5 show the actual experimental apparatus.

2.3 Details Of The Experiment

2.3.1 The Method Of McRuer et al.

In reference 16, McRuer *et al.* model the human operator

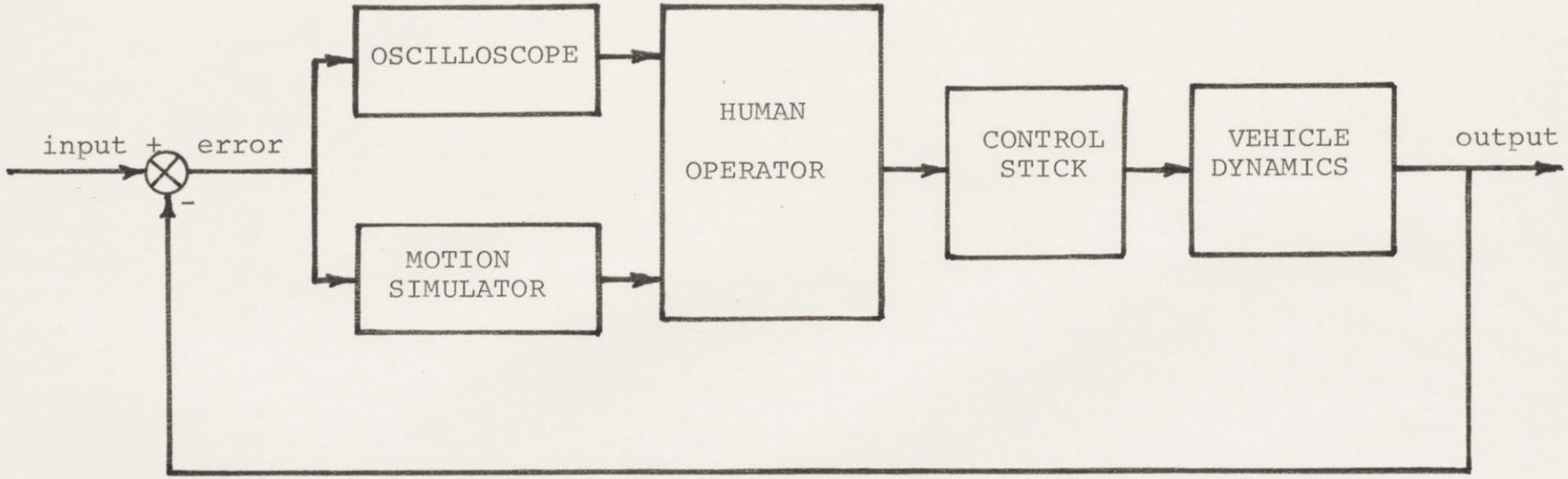

figure 2.1

THE EXPERIMENTAL SET-UP: THE HUMAN OPERATOR IN A COMPENSATORY SYSTEM WITH VISUAL AND MOTION CUES

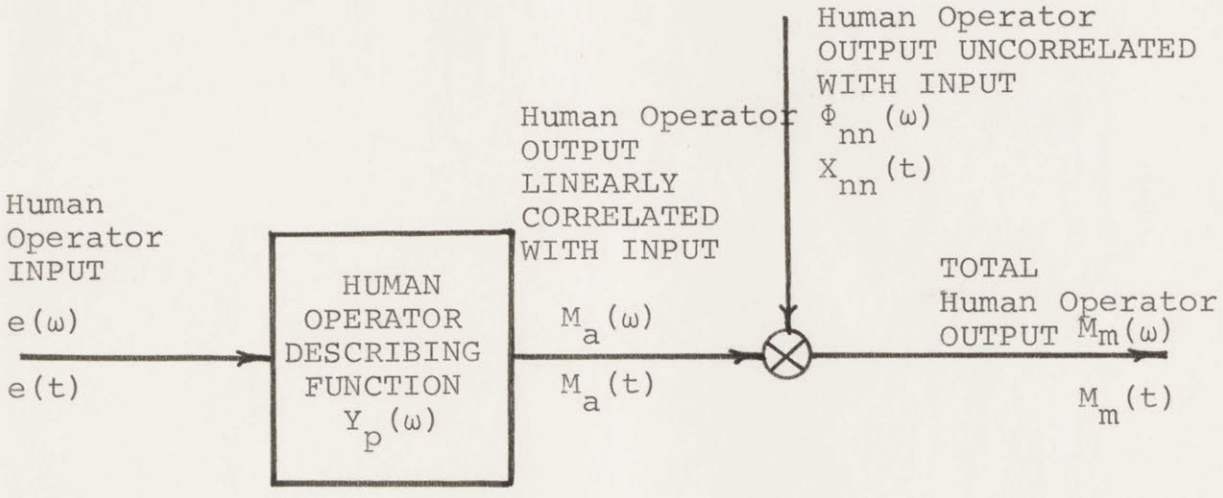

$M_m(\omega)$ = total human operator output

$\Phi_{nn}(\omega)$ = power spectral density of the human operator's output uncorrelated with his input

$M_a(\omega)$ = human operators output linearly correlated with his input

$Y_p(\omega)$ = the human operator's describing function relating $M_a(\omega)$ to $e(\omega)$

$e(\omega)$ = the input to the human operator

THE MODEL FOR THE HUMAN OPERATOR

Figure 2.2

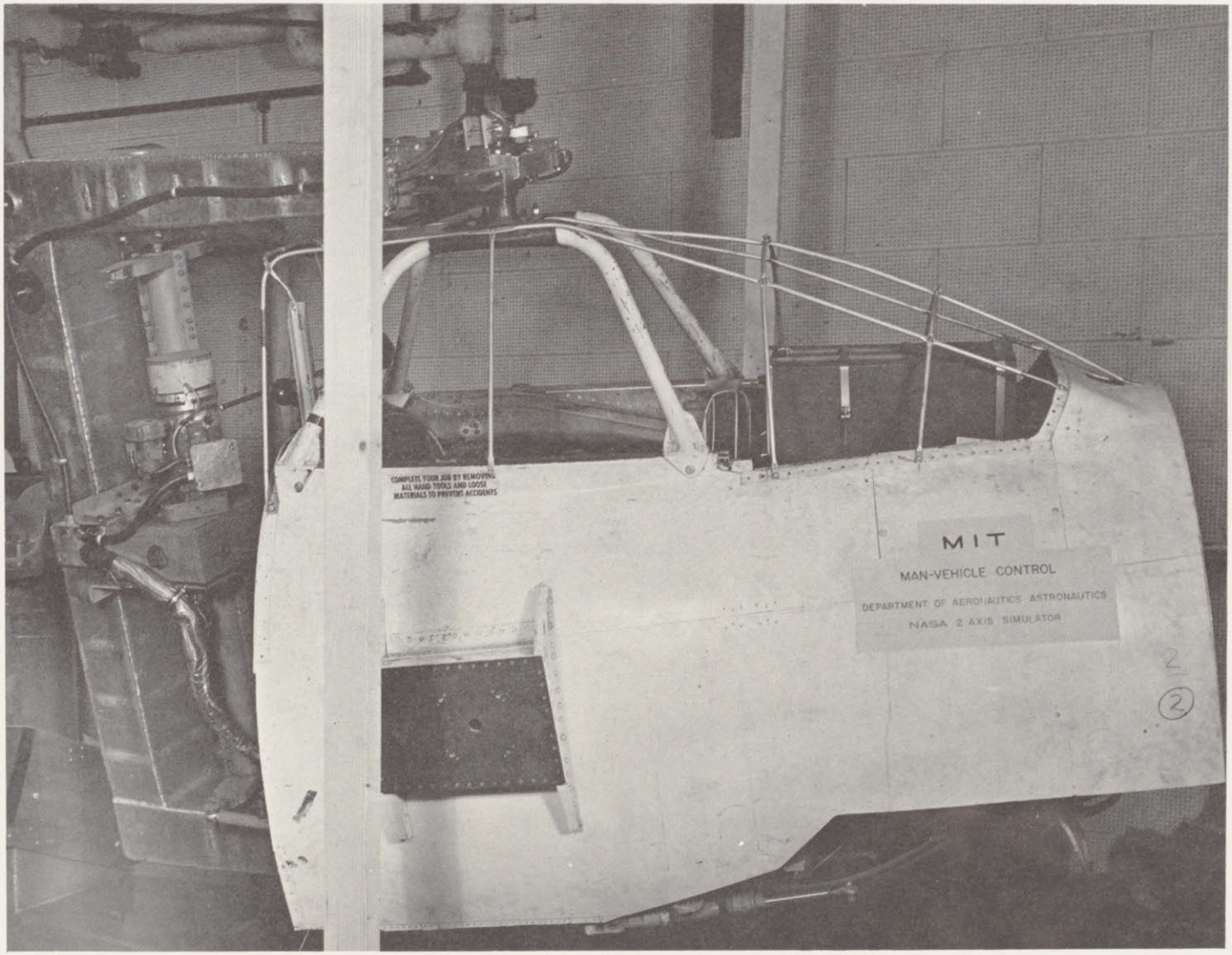

The NE-2 Simulator Used In The Experiment (see section 2.3.3)

figure 2.3

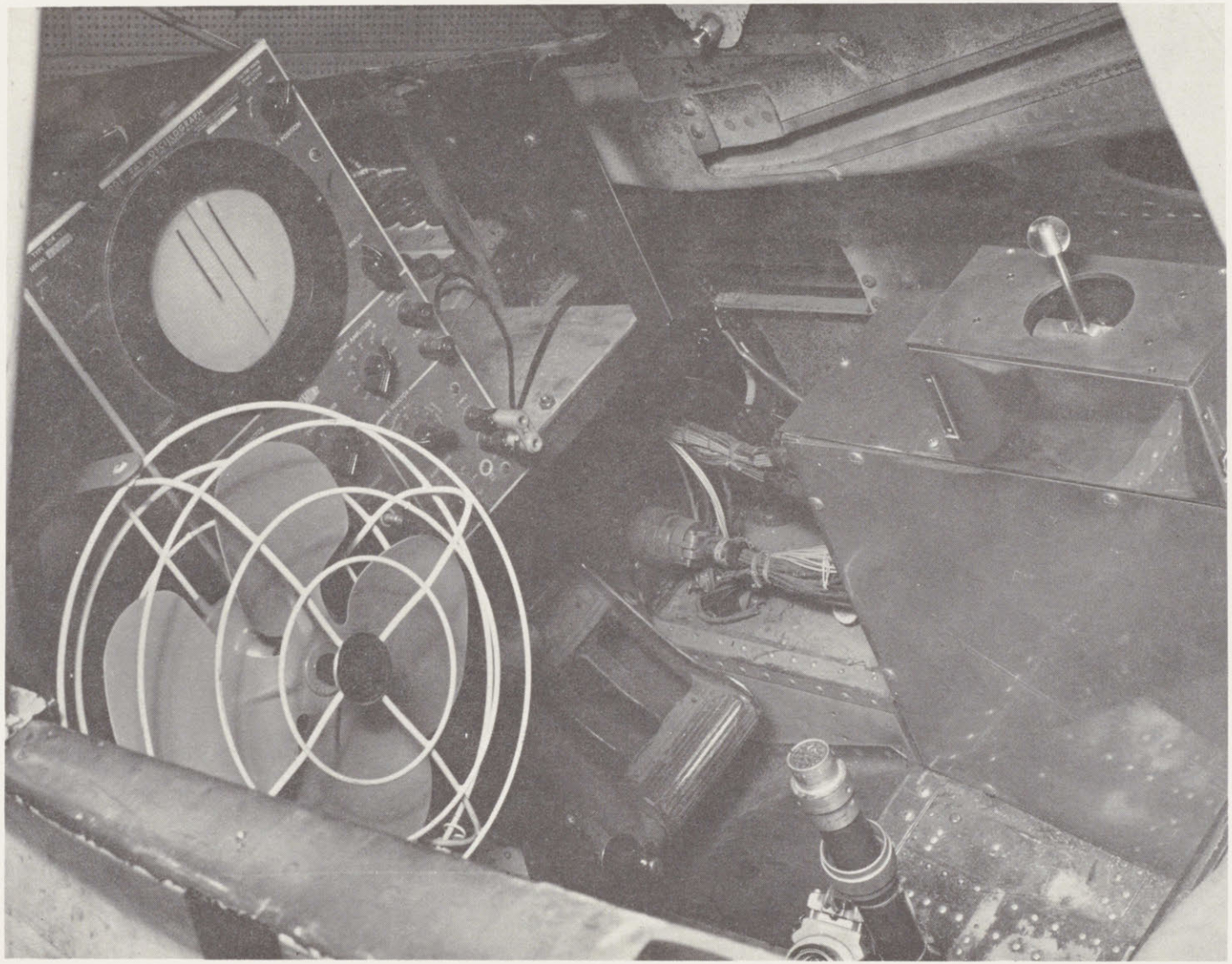

The Interior Of The NE-2 Simulator Used In The Experiment
Showing The Control Stick And Oscilloscope (see section 2.3.3)

figure 2.4

GPS 290T Hybrid Computer, Digital Portion

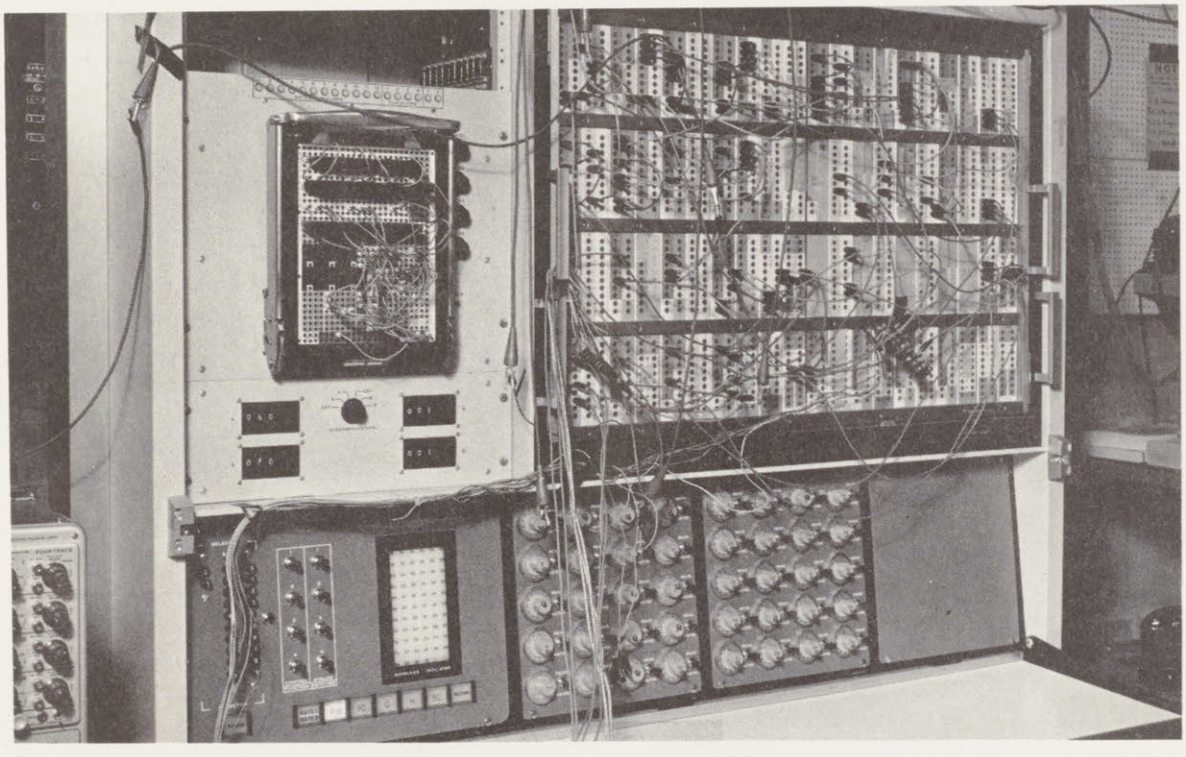

GPS 290T Hybrid Computer Analog Portion

Figure 2.5

as shown in figure 2.2, and perfect a method of measuring the human operator's describing function and remnant as a function of frequency. Their methods were heavily relied upon in setting up this experiment, although several modifications were made to correct for the effect of the remnant on the measurements (see Chapter III) and to allow for the hybrid computer used in the experiment (see Appendix A). In the following sections of this chapter the results of McRuer et al. will be used to justify some of the assumptions made.

2.3.2 The Human Operators

Seven subjects were used to take data and are identified as follows:

SU: a male MIT undergraduate student

JG: a male MIT undergraduate student

LL: a male MIT undergraduate student

BP: a female MIT undergraduate student

RS: a housewife

SF: a female MIT graduate student with a pilot's license

TI: a male MIT undergraduate student with a pilot's license and experience flying jet aircraft

The subjects were first trained with visual cues only for the vehicle dynamics $Y_c=1/s^2$. After they learned to maintain control of the system the 0.1-second delay (the simulated simulator dynamics mentioned in section 2.3.4 of this chapter) was introduced and training continued until consistent performance at an rISE of less than 1.00 was obtained. The rISE is explained in section 2.3.8 of this chapter, and stands for relative integral squared error. "Consistent performance" was

taken as meeting the performance criterion on the rISE five runs in a row on each of two consecutive days. After this initial training, practice continued for an average of twenty additional hours in order to train the subjects to use motion cues and to switch from one dynamics to another with facility. After that, frequent training periods were used as each new system was introduced.

The two subjects with flight experience, SF and TI, definitely proceeded faster than the others in the training period, both in the use of motion cues and of visual cues. For example, TI learned to control $e^{-.1s}/s^2$ to criterion in only two hours, as compared to an average of ten hours for the other subjects.

Throughout the experiment fairly high levels of motivation were maintained, contests between subjects occasionally springing up, and most subjects eager to best their previous low ISE for a given set of dynamics. At one time or another all the female subjects mentioned a desire "to prove I can do it" or "to show that all lady drivers aren't so bad".

If any subject appeared to be performing poorly they were asked why. Usually the explanation was a lack of sleep, and the subject was excused to remedy the situation. In some cases the reasons given were personal problems, and again the subject was excused until a later date.

Subject to subject differences exist, both in over-all ability, as well as in ability to improve performance with the addition of motion cues. Pages 231 to 250 show typical results for all the subjects for several sets of vehicle dynamics. The data on the

individual subjects permit the differences among the data due to subject differences to be allowed for. On each of the graphs showing the experimental results (pages 169 to 230) the subjects used to obtain the data as well as the number of runs they made are given. For example, TI-5, SU-3, RS-2 means that the data on that graph are an average of the results of five runs by TI, three runs by SU, and two runs by RS. In order to minimizes differences among the data due to temporal changes in the physical and psychological state of the experimental subjects, the data are always taken in sets of three runs by the same subject. Each of these sets of three runs consists of one run with visual cues only, one run with motion cues only, and one run with simultaneous visual and motion cues. For any given set of runs all three runs are taken on the same day, together, but in random order. See section 2.4.1.3 of this chapter for a discussion of run to run variations.

2.3.3 The Motion Cues

The motion simulator used was the NASA NE-2, two-degree-of-freedom motion simulator, built by Ames Research Center, and shown in figures 2.3 and 2.4. The moving cab of the simulator is mounted within two gimbals, the orientation of the gimbals and the mounting of the cab being variable to permit simultaneous motion about any two perpendicular axes, or, by locking one gimbal, motion about any one axis. Each gimbal of the simulator is driven as a DC position servomechanism by an electric amplidyne-motor set. The simulator was modified by the

Man-Vehicle Control Lab to make it capable of the desired angular accelerations for studies of the vestibular system. For this experiment the simulator was used in roll only. The characteristics of the simulator in roll are:

Maximum rotation:
possible: $\pm 360°$
used: $\pm 45°$

Maximum angular velocity: ± 8 rad/sec

Maximum angular acceleration: ± 15 rad/sec^2

Maximum rms acceleration noise: .05°/sec^2

Dynamics: $e^{-.1s}$, a pure delay, good to 10 rad/sec

In order that the only visual cues available to the human operator were by means of the oscilloscope, the simulator cab was completely enclosed with an opaque cloth cover.

The motion was about the roll axis, the angle of rotation from the vertical being directly proportional to the system error. The constant of proportionality was chosen for each set of vehicle dynamics so that the simulator motions were neither so small as to be useless, nor so large as to exceed $\pm 45°$ during the run. The size of the motions ranged from $\pm 5°$ for easy-to-control dynamics, to $\pm 15°$ for hard to control dynamics. Once the constant was chosen for one set of dynamics it was maintained throughout the experiment.

The simulator roll axis passed approximately through the subjects's belt line. The subjects' heads were not restrained, although the subjects were tightly strapped into the seat in the simulator cab, and their bodies could not move more than about an inch in any direction.

The subjects were told to keep their eyes open during all the runs, including runs with motion cues only, and thus had a visual reference of their head position relative to the simulator cab. Thus, if we consider the case for motion cues only, the subjects had the following complex task: to process 1) visual cues of their head position relative to the simulator cab, 2) neck proprioceptor cues of head position relative to their bodies, 3) vestibular system cues of roll angular position and velocity relative to the horizontal, and 4) their knowledge of the behavior of the vehicle dynamics, in order to make the proper control stick motions to stabilize and control the man-vehicle system. How all the cues brought about by the roll motions of the simulator interact was not a consideration of this thesis.

2.3.4 The Visual Cues

The visual cues were made by means of a dot moving laterally on an oscilloscope. The center position on the scope face corresponded to zero system error. A constant of proportionality between the system error and the dot's displacement from the centered position was determined so that the dot never reached the edge of the scope face during a run, yet at the same time did not just make minute perturbations about the center position. The scope face was ten centimeters wide, and typical motions of the dot during a run ranged from ± 1 to ± 3 centimeters depending on the degree of difficulty of the vehicle dynamics. The display sensitivity of the oscilloscope was kept in the same proportion to the roll motion throughout the experiment.

In order to make the visual cues correspond to the motion cues, which must pass through the simulator dynamics, the visual cues were passed through simulated simulator dynamics. As mentioned in section 2.3.3, the simulator dynamics in roll are a pure .1-second delay, $e^{-.1s}$. Taking advantage of the hybrid computer (see Appendix A) the error signal was sampled every .02 seconds and stored in the digital computer. It was then fed back to the analog computer and to the oscilloscope .1 seconds later, thus producing a .1-second delay in the visual loop which matched the simulator dynamics in the motion loop. Appendix B shows how the data, which were taken for dynamics with a factor of $e^{-.1s}$ included, can be modified so as to correspond to vehicle dynamics without the .1-second delay.

2.3.5 The Control Stick

Th control stick was a spring-centered, linear, pencil-type control stick mounted to the right of the simulator cab next to the human operator. The gain of the control stick was set such that the human operator's control motions were neither small perturbations about the centered position, nor continual full-scale motions to the $\pm 30°$ limit stops. A measure of the gain, the maximum voltage from the control stick at full 30° defelction, is called K, and the value of K for each case is given on all graphs of the data.

2.3.6 The Vehicle Dynamics

The vehicle dynamics were simulated on the analog computer described in Appendix A. The dynamics include three general cases:

1) $Y_c(s) = \dfrac{K}{s(\tau s + 1)}$, K and τ vary

2) $Y_c(s) = \dfrac{\omega_n^2}{s^2 + 2\zeta\omega_n s + \omega_n^2}$, ω_n and $2\zeta\omega_n$ vary

3) $Y_c(s) = \dfrac{\omega_n^2}{s(s^2 + 2\zeta\omega_n s + \omega_n^2)}$, ω_n and $2\zeta\omega_n$ vary

These three cases were chosen because they cover a wide range of vehicle dynamics of practical interest. To show this, some examples will be given.

The first set of vehicle dynamics, for $\tau = \infty$, corresponds to $Y_c(s) = K/s^2$, the relationship between control moment and angular position of a spacecraft in the absence of atmosphere. The various values of $1/\tau$ and K for which data were taken (see the list of data points on pages 161 to 164) also correspond to the dynamics of an airplane in roll, relating aileron position to roll angle, provided the Dutch roll mode is neglected.

The second set of dynamics, for low damping ratios, corresponds to a spacecraft during the early phases of re-entry into the atmosphere, relating control moment to vehicle pitch or yaw angle position.

The third set of dynamics corresponds to some compensated helicopters in hover, relating control stick position to horizontal velocity. These dynamics also correspond to the longitudinal dynamics of an airplane, relating control stick position to pitch angle, although there is often an additional lead term in the numerator for such cases.

A complete listing of the dynamics for which data were taken is given on pages 161 to 164.

2.3.7 The System Input

Following the work of McRuer, et al. (reference 16), the system input consisted of the sum of ten sinusoids of known amplitude, phase, and frequency. The ten frequencies chosen lay between .1 and 10 rad/sec, the range of interest in measuring the human operator's describing function. They were .1405, .2108, .3512, .6326, .9137, 1.4757, 2.1787, 2.8816, 4.2872, and 7.6605 rad/sec. All these frequencies were such that an integral number of cycles occurred during the period of data-taking, thus minimizing averaging errors (see section 2.3.9 of this chapter). In other words,

$$\frac{2\pi n}{\omega} = 89.6$$

where ω was in rad/sec, 89.6 seconds was the period of data-taking, and n was a positive integer. The amplitudes of the sinusoids were alternated positive and negative in order to avoid a large initial transient at the onset of data-taking. The amplitudes of the low frequency sinusoids were ± 1, and the amplitudes of the high frequency sinusoids were $\pm .1$. The frequency at which the amplitudes of the sinusoids change from 1 to .1 is called the breakpoint. The high frequency sinusoids were reduced in amplitude to simplify the task for the human operator without completely eliminating the input at these frequencies. The total input signal could further be multiplied by a gain, K', to vary the input power. The phases of the sinusoids were such that

all the sinusoids passed through zero-phase at the beginning and at the end of the data-taking period, again to minimize averaging errors. Finally, the input was given by

$$i(t) = \sum_{k=1}^{10} A_k \sin(\omega_k t + t_o)$$

and t_o was chosen as a negative value of about 28 seconds, such that $i(t_o) = 0$. This caused the human operator to be in the process of tracking at the onset of data-taking, avoiding taking data during the transients in his tracking which occur when the system is first turned on. Before any experimental runs were made the input was calculated on the digital computer and stored on magnetic tape. During the experimental runs the input was played back from the magnetic tape and converted to an analog voltage every .02 seconds, thus providing a pseudo-continuous, pseudo-random input for the system. Figure 2.6 shows the input.

For further details on the reasons for the nature of the input, see reference 16.

2.3.8 The Data Taken

Data were taken at the input to and at the output from the human operator, corresponding to the error and the total human operator's output shown in figure 2.2. The measurements taken were of voltages: the voltage from the control stick and the voltage corresponding to the system error. The voltages were scaled on the analog computer so as to be directly comparable, thus permitting calculation of the human operator's describing function and remnant as shown in section 2.3.9, without the necessity of a scale factor. The two signals

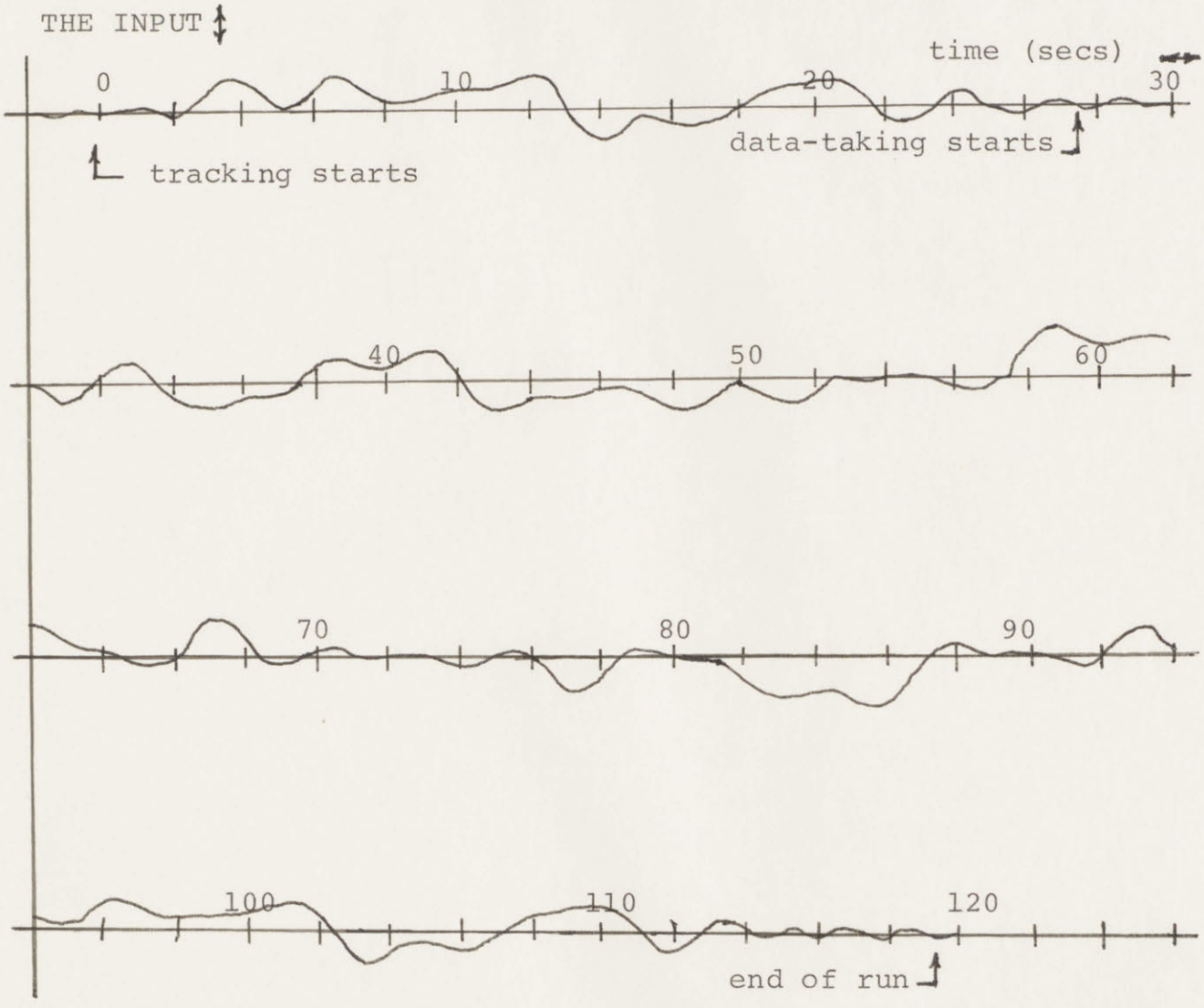

THE INPUT

Above is a tracing of the input which is not precise, but which gives an excellent indication of the nature of the input which is the sum of ten sines.

Figure 2.6

were sampled every .1 seconds and stored in the digital computer after analog to digital conversion, making a total of 896 samples of each signal during the 89.6-second run time. It should be recalled that the input was completely known (see section 2.3.7), and therefore it was not necessary to take data at the system input.

In addition the system error signal was squared and integrated on the analog computer during the run. At the end of the run the resulting voltage was converted to a digital value and saved in the digital computer. When this number is divided by the integral squared input, the relative integral squared error is obtained, (written as rISE in this thesis). The rISE is thus the ratio of total system error power to the total input power.

2.3.9 Processing The Data

The data was processed by the digital computer (see Appendix A). At the end of a run, stored in the digital computer, or on magnetic tape available to the digital computer, were:

1) $e(n\Delta t)$, the input to the human operator which is also the system error,
2) $M_m(n\Delta t)$, the total output from the human operator,
3) $\sin(\omega_k n\Delta t)$ and $\cos(\omega_k n\Delta t)$ for each of the ten frequencies of the system input, and
4) $\sin(\omega_j n\Delta t)$ and $\cos(\omega_j n\Delta t)$ for each of ten ω_j's between the ω_k's of the input.

The ω_j's and the ω_k's were chosen such that an integral number of cycles occurred during the period of data-taking in order to minimize averaging errors. The ω_k's

are listed in section 2.3.7. The ω_j's were .0702, .2810, .4920, .7732, 1.1947, 1.8977, 2.6004, 4.0060, 5.5523, and 9.6288 rad/sec. Δt was .1 seconds.

the data were processed as follows (following the work of McRuer, et al., but modified for the hybrid computer):

eq. 2.1) $$A_{ek} = \sum_{n=1}^{896} e(n\Delta t)\sin(\omega_k n\Delta t)$$

eq. 2.2) $$B_{ek} = \sum_{n=1}^{896} e(n\Delta t)\cos(\omega_k n\Delta t)$$

eq. 2.3) $$A_{Mk} = \sum_{n=1}^{896} M(n\Delta t)\sin(\omega_k n\Delta t)$$

eq. 2.4) $$B_{Mk} = \sum_{n=1}^{896} M(n\Delta t)\cos(\omega_k n\Delta t)$$

eq. 2.5) $$A_{Mj} = \sum_{n=1}^{896} M(n\Delta t)\sin(\omega_j n\Delta t)$$

eq. 2.6) $$B_{Mj} = \sum_{n=1}^{896} M(n\Delta t)\cos(\omega_j n\Delta t)$$

eq. 2.7) $$\left|e(\omega_k)\right|^2 = (A_{ek}^2 + B_{ek}^2)(\Delta t)^2$$

eq. 2.8) $$\angle e(\omega_k) = \tan^{-1}\left(\frac{B_{ek}}{A_{ek}}\right)$$

eq. 2.9) $$\left|M_m(\omega_k)\right|^2 = (A_{Mk}^2 + B_{Mk}^2)(\Delta t)^2$$

eq. 2.10) $$\angle M_m(\omega_k) = \tan^{-1}\left(\frac{B_{Mk}}{A_{Mk}}\right)$$

eq. 2.11) $$\left|M_{nn}(\omega_j)\right|^2 = (A_{Mj}^2 + B_{Mj}^2)(\Delta t)^2$$

Equations 2.7 and 2.8, and equations 2.9 and 2.10, give the amplitude and phase of the input and the output of the human operator. The human operator's describing function is thus given by

eq. 2.12) $$\left|Y_p(\omega_k)\right|^2 = \frac{\left|M_m(\omega_k)\right|^2}{\left|e(\omega_k)\right|^2}$$

eq. 2.13) $$\angle Y_p(\omega_k) = \angle M_m(\omega_k) - \angle e(\omega_k)$$

Equation 2.11 gives a measure of the magnitude of the remnant. How this number can be processed to give the actual remnant is discussed in Chapter III. The phase of the remnant was not calculated, as the remnant is a random signal possessing no fixed phase (see reference 16).

Thus we see that the data were processed to yield the human operator's describing function plus a measure of the human operator's remnant. In addition, for each run, the system integral squared error (ISE) is calculated on the analog computer during the run, and stored in the digital computer to be typed out with the rest of the data. The significance of the ISE and rISE are explained in section 2.3.8.

2.4 Validation Of The Experimental System

2.4.1 Variability Of The Data

2.4.1.1 Measurement Variability

The accuracy and variability of the measurements made by the experimental system were first checked by using the experimental system to take data across a known filter. To do this the system input was fed into the filter, and data were taken at the input and output of the filter, which was

$$Y_f(s) = \frac{1}{(s+1)^2}$$

The experimental measurements of the amplitude ratio of the filter all fall within 2% of the calculated values of the amplitude ratio, and the experimental measurements of the phase of the filter all fall within 2° of the calculated values of the phase. These error limits give the maximum measurement errors obtained in a series of five runs. It must be noted that this check on the system performance was made open loop with no noise injected into the system. When a human operator is involved in the loop his output is not simply the sum of ten sinusoids, but includes the remnant. Hence comparisons of actual human operator data with established results are made in sections 2.4.2 and 2.4.3 in order to further check the experimental system.

2.4.1.2 Subject To Subject Variability

Subject to subject variability was mentioned in section 2.3.2, and subject to subject differences are shown on pages 233 to 252. In taking the data, as many subjects were used at each point as possible in order to minimize the effects of subject to subject variability. Notable exceptions to this practice occur at data points where only the most skilled subjects were capable of

controlling the vehicle dynamics at that point. The subjects used at each point are listed on the graphs of the data (pages 169 to 230).

As was the case for McRuer, et al., subject to subject and run to run differences among the data are the most important sources of variations among the data. Table 2.1 and pages 231 to 250 show the subject to subject variability. The subject to subject differences among the data were controlled for in two ways. Wherever practical, the same subjects were used at each data point. When this was not possible, subjects of equal ability were used as judged by results of the type shown on pages 231 to 250. The fact that subject to subject differences were properly controlled for, and that the ability of the subjects used is representative of the general range of ability of human operators is borne out by the close correspondence between data taken for this thesis and previous established results (see sections 2.4.2 and 2.4.3 of this chapter.

2.4.1.3 Run To Run Variability

Figure 2.7 and tables 2.2 through 2.4 show typical run to run variability for one subject. The variability in the data from run to run is comparable to that obtained by McRuer, et al., in reference 16, and is due to the innate characteristics of the human operator, whose performance varies as a function of time, and to the run time of 89.6 seconds, which does not average the human operator's response over a long enough period to smooth out the human operator's time variations. As in reference 16, the effect of the run to run variability was

TABLE 2.1

freq. rad/sec	SU mean: 3 runs		RS mean: 5 runs		TI mean: 2 runs		JG mean: 5 runs	
	Y_p		Y_p		Y_p		Y_p	
	Data for visual and motion cues							
	AR	PH	AR	PH	AR	PH	AR	PH
.14	1.16	+21	.50	-39	.49	-31	1.1	-48
.21	.94	-45	.90	+3	.17	+9	.40	-15
.35	.64	+50	.58	+40	.69	-24	.87	+6
.63	2.73	+11	2.54	+3	3.00	+37	1.78	+23
.91	2.87	+48	2.76	+49	3.70	+50	2.62	+52
1.48	4.37	+50	4.76	+60	5.90	+41	3.84	+46
2.18	7.20	+52	6.92	+47	7.80	+38	6.54	+46
2.88	9.17	+42	8.82	+37	10.2	+29	8.28	+37
4.29	14.6	+30	13.9	+25	12.6	+22	12.3	+18
7.66	24.2	-2	27.4	-13	23.5	-5	16.3	-14
	Data for visual cues only							
.14	.23	+28	.23	-25	.31	+51	.32	+1
.21	.45	-16	.20	+2	.36	-43	.36	-17
.35	.69	+8	.76	+28	.38	-10	.64	-10
.63	2.50	+31	3.03	+24	2.80	+27	1.64	+19
.91	2.53	+46	2.28	+48	4.55	+38	1.32	+62
1.48	3.73	+63	3.44	+54	4.05	+62	3.12	+65
2.18	6.27	+50	5.90	+50	6.20	+44	5.50	+51
2.88	7.50	+43	8.34	+42	7.90	+33	7.50	+40
4.29	14.2	+28	13.7	+16	11.4	+26	12.2	-1
7.66	28.1	-28	29.9	-49	22.0	-45	20.6	-50

SUBJECT TO SUBJECT DIFFERENCES IN THE MEASURED VALUES

FOR Y_p FOR $Y_c = e^{-.1s}/s^2$

TABLE 2.2

	RS Y_p									
	visual cues only									
freq. rad/sec	AR_1	AR_2	AR_3	AR_4	AR_5	PH_1	PH_2	PH_3	PH_4	PH_5
.14	.12	.32	.14	.37	.22	-48	-58	-138	+69	+48
.21	.11	.28	.11	.12	.37	-12	-72	+47	+41	+2
.35	1.2	.36	1.1	.5	.66	-71	+57	+68	+23	+63
.63	1.2	.95	4.6	7.3	1.1	+31	+24	---	+43	-1
.91	2.2	2.2	2.1	2.9	2.0	+44	+48	+49	+52	+46
1.48	3.3	3.1	3.6	3.7	3.5	+52	+59	+55	+54	+49
2.18	5.3	6.2	6.0	6.0	6.0	+46	+52	+54	+47	+50
2.88	7.9	6.0	10.7	9.6	6.0	+36	+38	+35	+49	+52
4.29	14.	13.2	13.7	13.9	13.5	+6	+18	+17	+15	+22
7.66	32.4	27.5	30.0	29.1	30.5	-54	-61	-36	-47	-47
	visual and motion cues									
.14	1.6	.1	.36	.36	.12	-105	-31	-32	+3	-31
.21	.42	.25	.69	2.8	.35	+51	+31	+43	-62	-47
.35	.72	.8	.61	.48	.27	+39	+76	+1	+33	+52
.63	1.8	2.5	1.7	2.9	3.8	+41	-44	-5	-68	+91
.91	3.4	2.2	3.5	2.2	2.5	+81	+36	+48	+41	+38
1.48	4.9	4.3	3.9	5.1	5.6	+67	+57	+51	+57	+70
2.18	6.7	6.9	6.9	7.1	7.0	+53	+47	+47	+44	+45
2.88	9.2	8.4	10.1	8.5	7.9	+35	+34	+40	+34	+41
4.29	13.7	13.4	13.9	13.9	14.8	+29	+25	+25	+25	+22
7.66	25.8	30.0	36.0	28.5	26.8	-15	-9	-16	-12	-12

RUN TO RUN VARIATION OF THE VALUE OF Y_p MEASURED FOR

$$Y_c = e^{-.1s}/s^2$$

TABLE 2.3

freq. rad/sec	SU Y_p visual cues only						TI Y_p visual cues only			
	AR_1	AR_2	AR_3	PH_1	PH_2	PH_3	AR_1	AR_2	PH_1	PH_2
.14	.14	.33	.21	+37	-5	+52	.44	.18	+108	-6
.21	.2	.29	.87	-81	+18	+14	.57	.15	-59	-26
.35	.3	.66	1.1	-56	+5	+76	.27	.50	+51	-70
.63	3.2	1.5	2.8	+26	+16	+51	4.2	1.4	+28	+27
.91	1.6	2.3	3.7	+9	+46	+34	2.6	6.5	+25	+52
1.48	3.6	3.5	4.1	+65	+60	---	4.2	3.9	+60	+64
2.18	6.1	6.0	6.7	+49	+45	+56	6.5	5.9	+43	+44
2.88	6.4	9.0	7.1	+42	+40	+46	8.9	6.9	+34	+33
4.29	12.9	14.7	15.0	+24	+29	+31	10.8	12.1	+26	+26
7.66	21.4	31.2	31.8	-43	-25	-17	23.9	20.1	-31	-59
	visual and motion cues									
.14	2.6	.52	.37	+82	+43	-63	.06	.93	-100	+39
.21	.13	2.3	.39	-47	-43	---	.24	.10	-8	+25
.35	.37	.55	1.0	+92	+31	+27	.57	.81	-24	---
.63	2.5	1.9	3.8	+39	-22	+15	3.7	2.3	+60	+14
.91	2.4	2.8	3.4	+63	+46	+36	3.4	4.0	+50	+50
1.48	4.1	4.1	4.9	+50	+50	+51	6.1	5.7	+39	+44
2.18	7.4	7.4	6.8	+58	+50	+49	7.7	7.9	+39	+37
2.88	9.6	8.9	9.0	+40	+39	+46	11.4	9.0	+29	+29
4.29	13.9	14.4	15.4	+33	+23	+35	13.2	12.0	+20	+25
7.66	22.1	22.7	17.9	-14	+3	+5	19.7	27.2	+1	-11

RUN TO RUN VARIATION OF THE VALUE OF Y_p MEASURED FOR

$$Y_c = e^{-.1s}/s^2$$

TABLE 2.4

JG										
Y_p visual cues only										
freq. rad/sec	AR_1	AR_2	AR_3	AR_4	AR_5	PH_1	PH_2	PH_3	PH_4	PH_5
.14	67.67	.15	.45	.21	.10	+53	+5	+19	-90	+19
.21	.38	.83	.19	.15	.27	-85	+31	+23	-38	-18
.35	.79	.24	.55	.43	1.2	-81	+20	+48	+34	-69
.63	1.6	1.1	1.1	3.1	1.3	+42	+4	+22	-5	+31
.91	1.6	1.5	1.3	1.2	1.0	+42	+64	+36	+86	+83
1.48	4.3	2.6	2.8	2.7	3.2	+64	+54	+65	+74	+70
2.18	6.0	5.2	5.3	5.3	5.7	+47	+50	+50	+50	+60
2.88	7.2	8.0	7.0	7.4	7.9	+38	+37	+33	+33	+59
4.29	14.7	9.8	11.3	11.2	13.8	+12	-2	-11	-6	+3
7.66	25.4	17.9	18.4	18.7	22.4	-48	-24	-47	-86	-47
visual and motion cues										
.14	.27	2.2	.27	.37	2.6	-50	+38	-74	-105	-48
.21	.21	.32	.9	.15	.4	+4	-15	-26	+27	-63
.35	1.2	1.3	.54	.4	.9	+56	-10	-75	+47	+11
.63	1.5	1.6	1.7	2.4	1.7	+33	+11	+15	+76	-17
.91	2.4	2.9	2.7	2.3	2.8	+66	+63	+31	+50	+51
1.48	3.2	4.4	4.1	3.5	4.0	+45	+49	+43	+47	+46
2.18	6.5	6.9	6.5	5.9	6.9	+45	+47	+46	+44	+46
2.88	9.8	7.6	7.6	8.9	7.5	+41	+32	+37	+34	+39
4.29	11.8	11.4	12.6	10.5	15.	+16	+12	+24	+15	+21
7.66	15.4	16.	15.9	15.4	18.6	-26	-6	-21	-6	-9

RUN TO RUN VARIATION OF THE VALUE OF Y_p MEASURED FOR

$$Y_c = e^{-.1s}/s^2$$

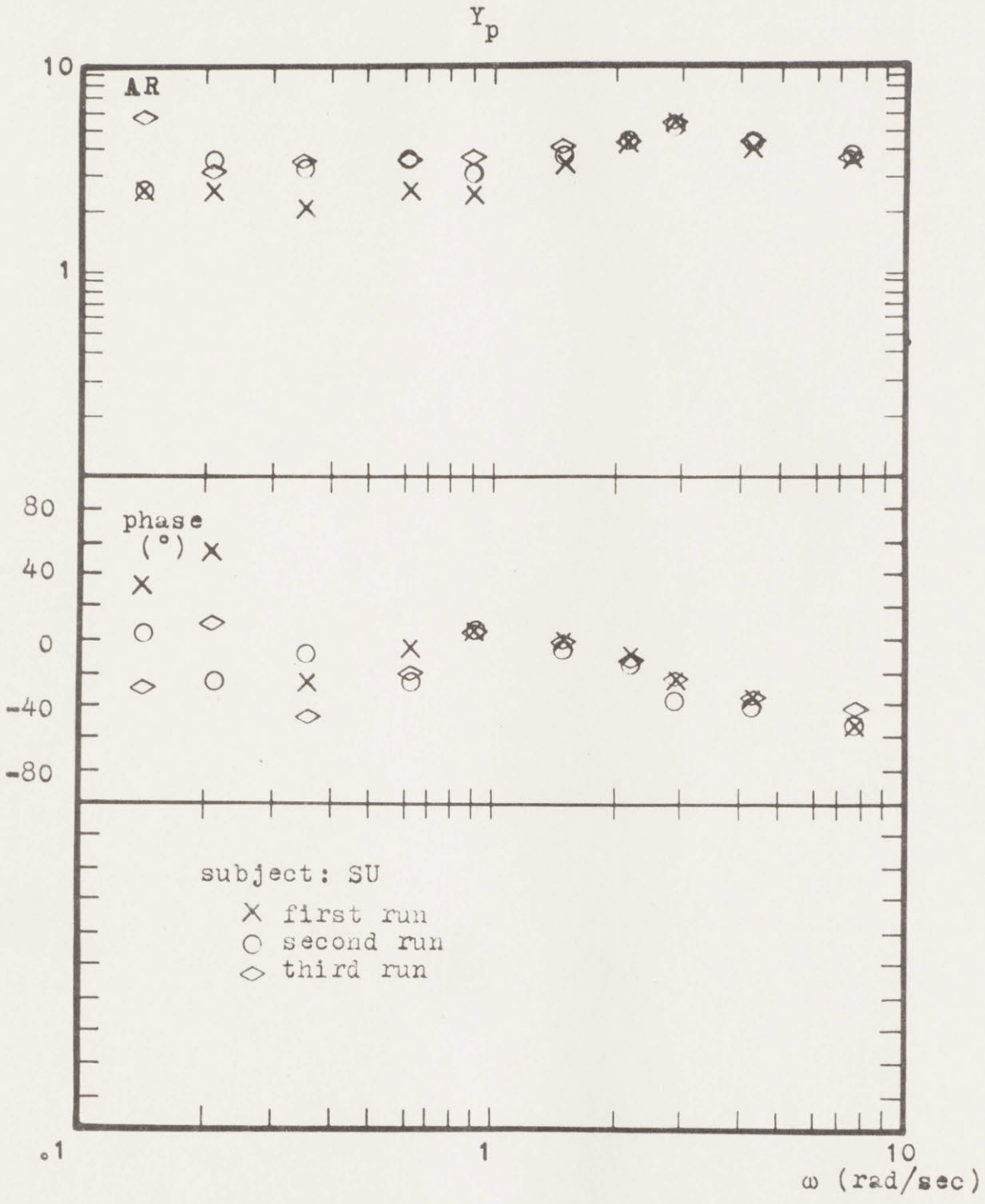

EXAMPLE OF THE RUN-TO-RUN VARIABILITY OF THE DATA

$Y_c = 1/s$

figure
2.7

reduced by averaging the results over several runs. For example, the standard deviations, σ, of the data shown in figures 2.8 through 2.10, are related to the standard deviations of the averaged data, σ_N, by

$$\sigma_N = \frac{\sigma}{\sqrt{N}}$$

where N is the number of data averaged. In the data presented on pages 171 to 232 from five to fifteen sets of data were averaged. A minimum of ten sets of data were averaged except for those vehicle dynamics which could be controlled by only one subject, in which case five sets of data were averaged. The number of runs averaged for each experimental condition is listed on the graphs of the data. The averaging performed was of the calculated values of the human operator's describing function and remnant for each run as follows:

$$\overline{|Y_p(\omega_k)|} = \frac{\sum_{l=1}^{m} |Y_{pl}(\omega_k)|}{m}$$

$$\overline{\angle Y_p(\omega_k)} = \frac{\sum_{l=1}^{m} \angle Y_{pl}(\omega_k)}{m}$$

$$\overline{M_{nn}(\omega_k)} = \frac{\sum_{l=1}^{m} M_{nnl}(\omega_k)}{m}$$

where m is the number of runs averaged.

2.4.2 Comparison Of The Results With The Literature: Fixed-Base Data

Fixed-base data (data for the human operator con-

trolling the simulated vehicle dynamics in the absence of motion cues) was taken for comparison with results obtained by other investigators. The controlled vehicle dynamics chosen were Y_c=1, 1/s, and 1/s^2, because results for these dynamics were well-known, and because these dynamics require three widely varying modes of control behavior from the human operator. The experimental results as well as the results of McRuer, et al., (reference 16), and of Elkind (reference 6), are shown in figures 2.8 through 2.10. An explanation of the format of these graphs is given on pages 165 to 168. As can be seen, the experimental results are in close agreement with previous results.

2.4.3 Comparison Of The Results With The Literature: Moving-Base Data

Figure 2.11 shows data for the human operator's describing function while he is controlling the vehicle dynamics $Y_c(s) = 1/s$ with motion cues only. Data taken by Meiry (reference 17) using the same simulator but an entirely different method of measurement and data-processing, are also shown. As can be see, the results are in very close agreement.

Thus, the close agreement between the preliminary experimental results and known results for both fixed-base and moving base data for the human operator's describing function shows that the experimental system was performing as desired.

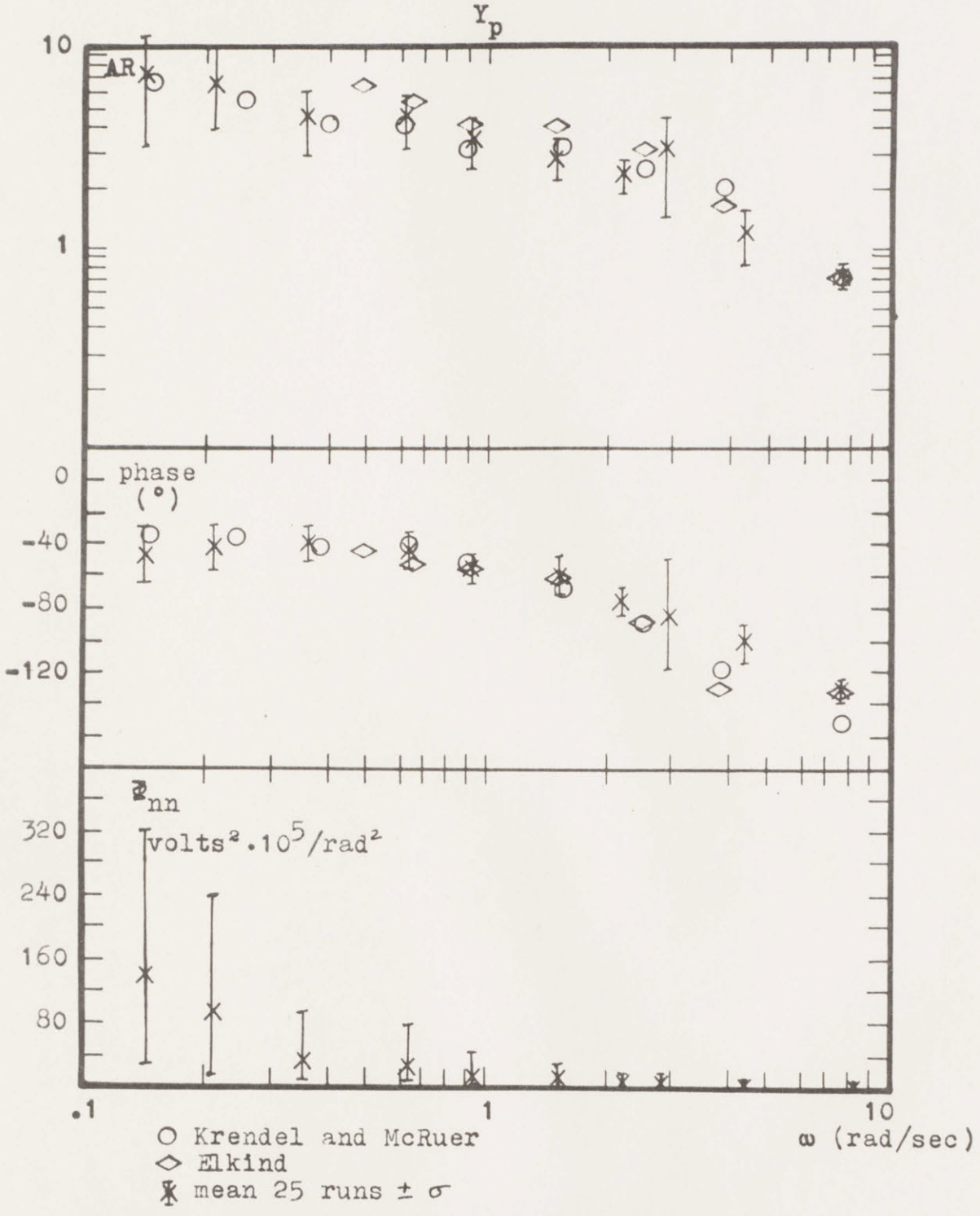

COMPARISON OF RESULTS WITH MCRUER ET AL.

$Y_c = 1$

(fixed-base data only)

figure 2.8

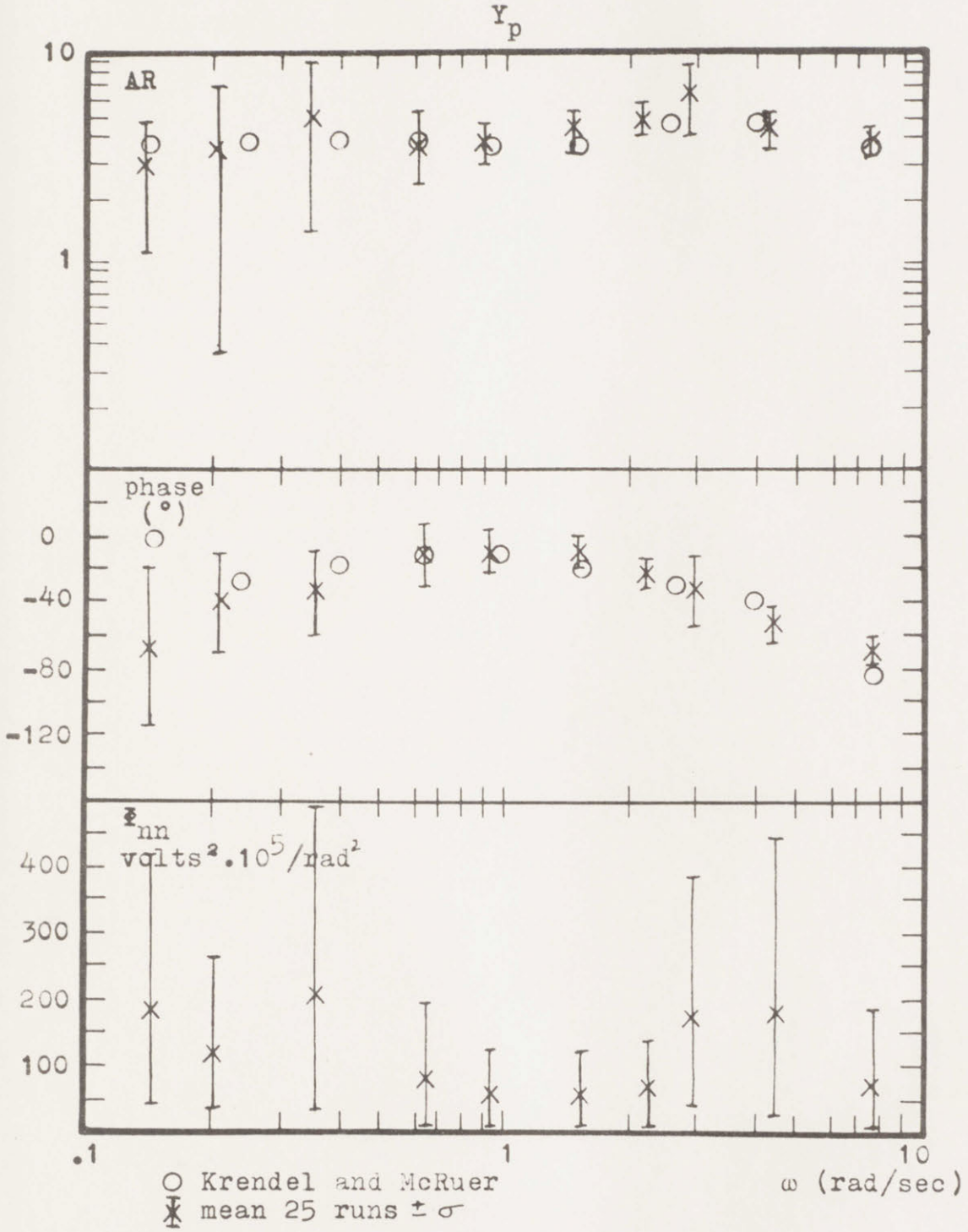

COMPARISON OF RESULTS WITH MCRUER, ET AL.

$Y_c = 1/s$

(fixed-base data only)

figure 2.9

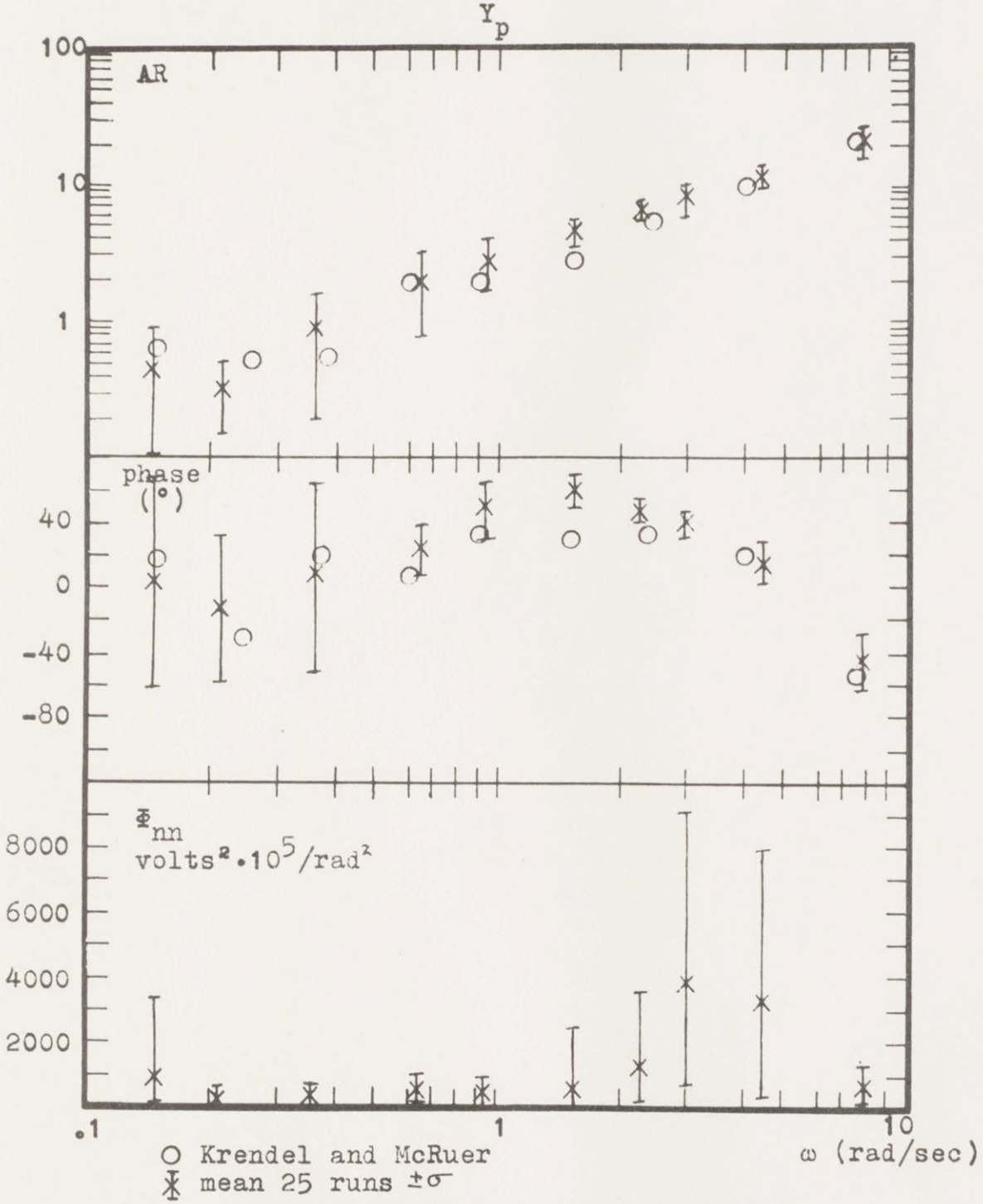

COMPARISON OF RESULTS WITH MCRUER ET AL.

$Y_c = 1/s^2$

(fixed-base data only)

figure 2.10

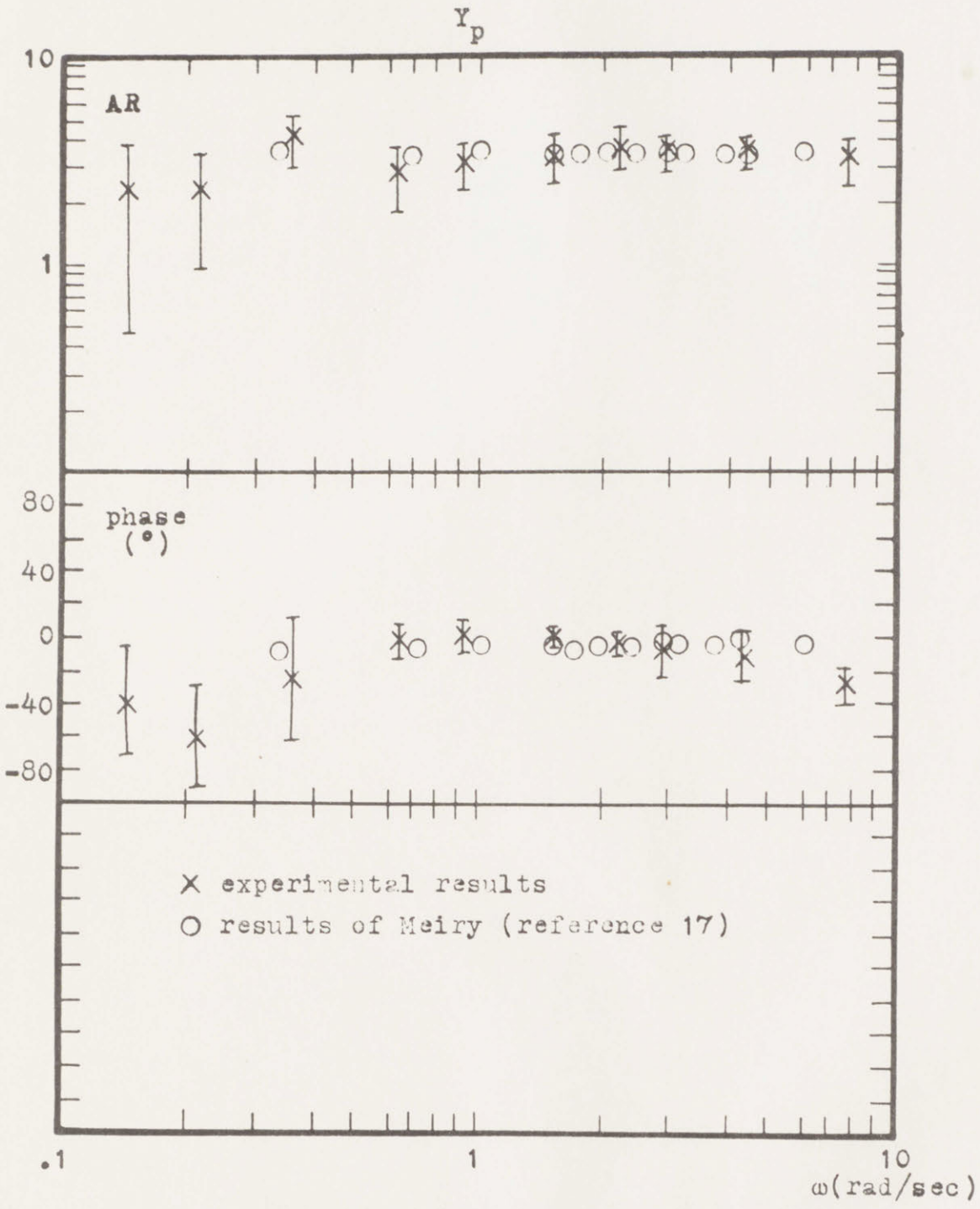

COMPARISON OF RESULTS WITH MEIRY

$Y_c = 1/s$

(motion cues only)

figure
2.11

CHAPTER III: THE EFFECTS OF THE REMNANT ON THE MEASUREMENTS

3.1 Derivation Of An Analytical Expression For The Effects Of The Remnant On The Measurements

The remnant is of importance not only for itself, but also because it affects the measurement of $Y_p(\omega)$, the human operator's describing function (see figure 2.2, page 12). With reference to figure 3.1 we see that

eq. 3.1) $$Y_{pa}(\omega) = \frac{M_a(\omega)}{e(\omega)}$$ = the actual human operator's describing function

eq. 3.2) $$Y_{pm}(\omega) = \frac{M_m(\omega)}{e(\omega)}$$ = the measured human operator's describing function

To see how $Y_{pa}(\omega)$ and $Y_{pm}(\omega)$ differ we must examine the quantities measured and the method of measurement in more detail.

Consider any signal, f(t). The measurements and calculations made on f(t) by the experimental program would be (see Chapter II, sections 2.3.8 and 2.3.9)

eq. 3.3) $$\frac{|F(\omega_k)|^2}{(\Delta t)^2} = \left(\sum_{n=1}^{896} f(n\Delta t)\sin(\omega_k n\Delta t)\right)^2 + \left(\sum_{n=1}^{896} f(n\Delta t)\cos(\omega_k n\Delta t)\right)^2$$

eq. 3.4) $$\angle F(\omega_k) = \tan^{-1}\left(\frac{\sum_{n=1}^{896} f(n\Delta t)\cos(\omega_k n\Delta t)}{\sum_{n=1}^{896} f(n\Delta t)\sin(\omega_k n\Delta t)}\right)$$

If f(t) were given by

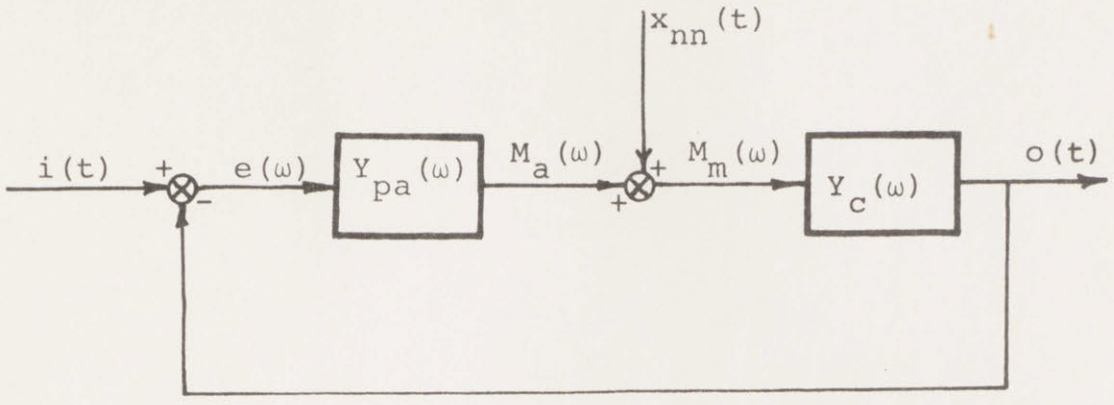

$$i(t) = \sum_{k=1}^{10} A_k \sin \omega_k t$$

$x_{nn}(t)$ = the human operator's remnant, that part of his output not linearly correlated with his input

$\Phi_{nn}(\omega)$ = the continuous power spectrum of $x_{nn}(t)$

$$Y_{pa}(\omega) = \frac{M_a(\omega)}{e(\omega)}$$ = the actual human operator's describing function

$$Y_{pm}(\omega) = \frac{M_m(\omega)}{e(\omega)}$$ = the measured human operator's describing function

$$F_{xM}(\omega) = \frac{1}{1 + Y_{pa}(\omega)\ Y_c(\omega)}$$ = transfer function between x and M_m

$$F_{xe}(\omega) = \frac{-Y_c(\omega)}{1 + Y_{pa}(\omega)\ Y_c(\omega)}$$ = transfer function between x and e

DIAGRAM USED IN THE DERIVATION OF THE EXPRESSION FOR THE EFFECTS OF THE REMNANT

Figure 3.1

$$f(t) = A_k \sin(\omega_k t + P_k)$$

the results of applying equations 3.3 and 3.4 to f(t) would be

$$\frac{|F(\omega_k)|}{(\Delta t)} = A_k$$

$$\angle F(\omega_k) = P_k$$

provided the ω_k's are chosen as integer multiples of 2π divided by the data-taking period to avoid averaging errors (see reference 16). If, however, f(t) were a random signal characterized by a continuous, smooth power spectral density $S_{nn}(\omega)$, the results of equations 3.3 and 3.4 would be

$$\frac{|F(\omega_k)|}{(\Delta t)} = (S_{nn}(\omega_k)\delta\omega_k)^{\frac{1}{2}}$$

$$\angle F(\omega_k) = 0$$

A word about the last two equations is in order. Because $\delta\omega_k$, the bandpass of equations 3.3 and 3.4, is narrow (about .14 rad/sec), and because $S_{nn}(\omega)$ is assumed smooth and continuous following the work of McRuer, et al., (reference 16),

$$\int_{-\infty}^{\infty} S_{nn}(\omega)\delta_k(\omega)d\omega \approx S_{nn}(\omega_k)\delta\omega_k$$

where $\delta_k(\omega)$ is the bandpass of the measurements at the frequency ω_k, and hence

$$\frac{|F(\omega_k)|}{(\Delta t)} = (S_{nn}(\omega_k)\delta\omega_k)^{\frac{1}{2}}$$

where $S_{nn}(\omega_k)$ is the average value of $S_{nn}(\omega)$ over the bandwidth $\delta\omega_k$ centered at ω_k. See Appendix C and figure C.1 for a derivation and discussion of $\delta\omega_k$. The average measurement of the phase of $F(\omega)$ is given as zero: if the angles are taken in the interval $-\pi$ to π, and because f(t) is a random variable, the expected value of the phase of $F(\omega_k)$ is zero.

If f(t) consisted of both the sinusoid and the random noise, i.e., if

$$f(t) = A_k \sin(\omega_k t + P_k) + s_{nn}(t)$$

then equations 3.3 and 3.4 would yield

$$\frac{|F(\omega_k)|}{(\Delta t)} = (A_k^2 + S_{nn}(\omega_k)\delta\omega_k)^{\frac{1}{2}}$$

$$\angle F(\omega_k) = P_k$$

In the actual case, measurements are made at $M_m(t)$ and at e(t) as shown in figure 3.1. It can be seen that both e(t) and $M_m(t)$ contain sinusoidal components due to i(t), the system input (see Chapter II, section 2.3.7), plus a random noise due to $x_{nn}(t)$, the human operator's remnant. By definition $x_{nn}(t)$ is uncorrelated with i(t), but the power spectrum of $x_{nn}(t)$, $\Phi_{nn}(\omega)$, is not necessarily zero at the input frequencies- in fact, it is assumed that $\Phi_{nn}(\omega)$ is a continuous, smooth function of ω. McRuer, et al., in reference 16, have shown by detailed analysis

of actual remnant data, that this assumption is justified.

With reference to figure 3.1, let us define the transfer functions from x to M_m and from x to e as

eq. 3.5) $$F_{xm}(\omega) = \frac{M_m(\omega)}{x(\omega)} = \frac{1}{1 + Y_{pa}(\omega)Y_c(\omega)}$$

eq. 3.6) $$F_{xe}(\omega) = \frac{e(\omega)}{x(\omega)} = \frac{-Y_c(\omega)}{1 + Y_{pa}(\omega)Y_c(\omega)}$$

and also let us define A_{ek} as the amplitude of the sinusoid of frequency ω_k at e due to the input, i(t). Then, the amplitude of the same sinusoid at M_m is $A_{ek}|Y_{pa}(\omega_k)|$. Using the same reasoning as we did for the general signal, f(t), equations 3.3 and 3.4, when applied at M_m and at e will yield

eq. 3.7) $$\frac{|M_m(\omega_k)|^2}{(\Delta t)^2} = \left[A_{ek}^2 |Y_{pa}(\omega_k)|^2 + \Phi_{nn}(\omega_k)\delta\omega_k |F_{xm}(\omega_k)|^2\right]$$

eq. 3.8) $$\angle M_m(\omega_k) = \angle M_a(\omega_k) = P_{mk}$$

eq. 3.9) $$\frac{|e(\omega_k)|^2}{(\Delta t)^2} = \left[A_{ek}^2 + \Phi_{nn}(\omega_k)\delta\omega_k |F_{xe}(\omega_k)|^2\right]$$

eq. 3.10) $$\angle e(\omega_k) = P_{ek}$$

where P_{mk} and P_{ek} are the phases of the sinusoids of frequency ω_k at M_m and at e relative to the system input, i(t). Similarly, if we measure $M_m(t)$ at frequen-

cies ω_j, between the input frequencies ω_k, then equations 3.3 and 3.4 give

eq. 3.11) $$\frac{|M(\omega_j)|^2}{(\Delta t)^2} = \Phi_{nn}(\omega_j)\delta\omega_j|F_{xm}(\omega_j)|^2$$

eq. 3.12) $$\angle M(\omega_j) = 0$$

Equation 3.12, which gives the phase of the remnant relative to the system input, represents the phase of a random signal characterized by the power spectral density $\Phi_{nn}(\omega)$. This measured phase angle is a random variable with expectation zero if the angles are taken in the interval $-\pi$ to π. Experiment shows that the average value of the phase measured does tend to zero.

Re-writing equation 3.11 we obtain

eq. 3.13) $$\Phi_{nn}(\omega_j) = \frac{|M(\omega_j)|^2}{\delta\omega_j|F_{xm}(\omega_j)|^2(\Delta t)^2}$$

Dividing equation 3.7 by equation 3.9 yields an expression for the measured value of the amplitude ratio of the human operator's describing function:

eq. 3.14) $$|Y_{pm}(\omega_k)|^2 = \frac{A_{ek}^2|Y_{pa}(\omega_k)|^2 + \Phi_{nn}(\omega_k)\delta\omega_k|F_{xm}(\omega_k)|^2}{A_{ek}^2 + \Phi_{nn}(\omega_k)\delta\omega_k|F_{xe}(\omega_k)|^2}$$

Subtracting equation 3.10 from 3.8 yields an expression for the measured value of the phase of the human operator's describing function:

3.15) $$\angle Y_{pm}(\omega_k) = \overline{P_{mk} - P_{ek}} = \angle Y_{pa}(\omega_k)$$

Equation 3.15 indicates that the expected value of the measured phase angle of the human operator's describing function is equal to the correct value. Furthermore, if the power of the remnant in the measurements made at M_m and at e is small relative to the power of the sinusoidal components, each measured value of the phase angle will be near the expected value, which is also the true value.

Following the work of McRuer, et al., reference 16, it is assumed that $\Phi_{nn}(\omega)$ is a smooth, continuous function of ω with no peaks at the input frequencies or at harmonics of the input frequencies. We can thus interpolate between the measured values of $M_m(\omega_j)$ (the ω_j's are frequencies between the input frequencies, ω_k) to obtain $M_{nn}(\omega_k)$, the signal level at M_m due to $x_{nn}(t)$ at the input frequencies ω_k. Then we can write equation 3.13 as

$$\text{eq. 3.16)} \quad \Phi_{nn}(\omega_k) = \frac{M_{nn}^2(\omega_k)}{\delta\omega_k \left|F_{xm}(\omega_k)\right|^2 (\Delta t)^2}$$

Now, realizing that

$$A_{ek}^2 = \frac{\left|e(\omega_k)\right|^2}{(\Delta t)^2} + \frac{M_{nn}^2(\omega_k)\left|Y_c(\omega_k)\right|^2}{(\Delta t)^2}$$

from equations 3.9 and 3.16, and that

$$\left|\frac{F_{xe}(\omega_k)}{F_{xm}(\omega_k)}\right|^2 = \left|Y_c(\omega_k)\right|^2$$

from equations 3.5 and 3.6, and that

$$\frac{M_{nn}^2(\omega_k)}{(\Delta t)^2} = \Phi_{nn}(\omega_k)\delta\omega_k \left|F_{xm}(\omega_k)\right|^2$$

from equation 3.16, and then substituting in equation 3.14 we obtain

eq. 3.17):
$$\left|Y_{pm}(\omega_k)\right|^2 = \frac{\left\{\left|e(\omega_k)\right|^2 - M_{nn}^2(\omega_k)\left|Y_c(\omega_k)\right|^2\right\}\left|Y_{pa}(\omega_k)\right|^2 + M_{nn}^2(\omega_k)}{\left|e(\omega_k)\right|^2}$$

which can be solved for $\left|Y_{pa}(\omega_k)\right|$ as

eq. 3.18) $$\left|Y_{pa}(\omega_k)\right|^2 = \frac{\left|e(\omega_k)\right|^2\left|Y_{pm}(\omega_k)\right|^2 - M_{nn}^2(\omega_k)}{\left|e(\omega_k)\right|^2 - M_{nn}^2(\omega_k)\left|Y_c(\omega_k)\right|^2}$$

where $\left|Y_{pa}(\omega_k)\right|$ is the desired actual amplitude of the human operator's describing function, unaffected by the human operator's remnant. Thus, equations 3.15, 3.16, and 3.18 now permit determination of $\Phi_{nn}(\omega_k)$ and $Y_{pa}(\omega_k)$, the measurements of $Y_{pa}(\omega_k)$ being unaffected by the remnant.

3.2 Application Of The Remnant Correction To The Data

Figures 3.2 through 3.5 and tables 3.1 through 3.3 show the effects of the remnant correction represented by equation 3.18. Figure 3.2 shows the effects of the remnant for some special cases involving $Y_c=1/s^2$, and will be discussed in section 3.3 of this chapter.

As can be seen from the figures and tables the corrections for the remnant are generally small compared to one standard deviation of the data, and may thus be neglected if desired. In general, the remnant

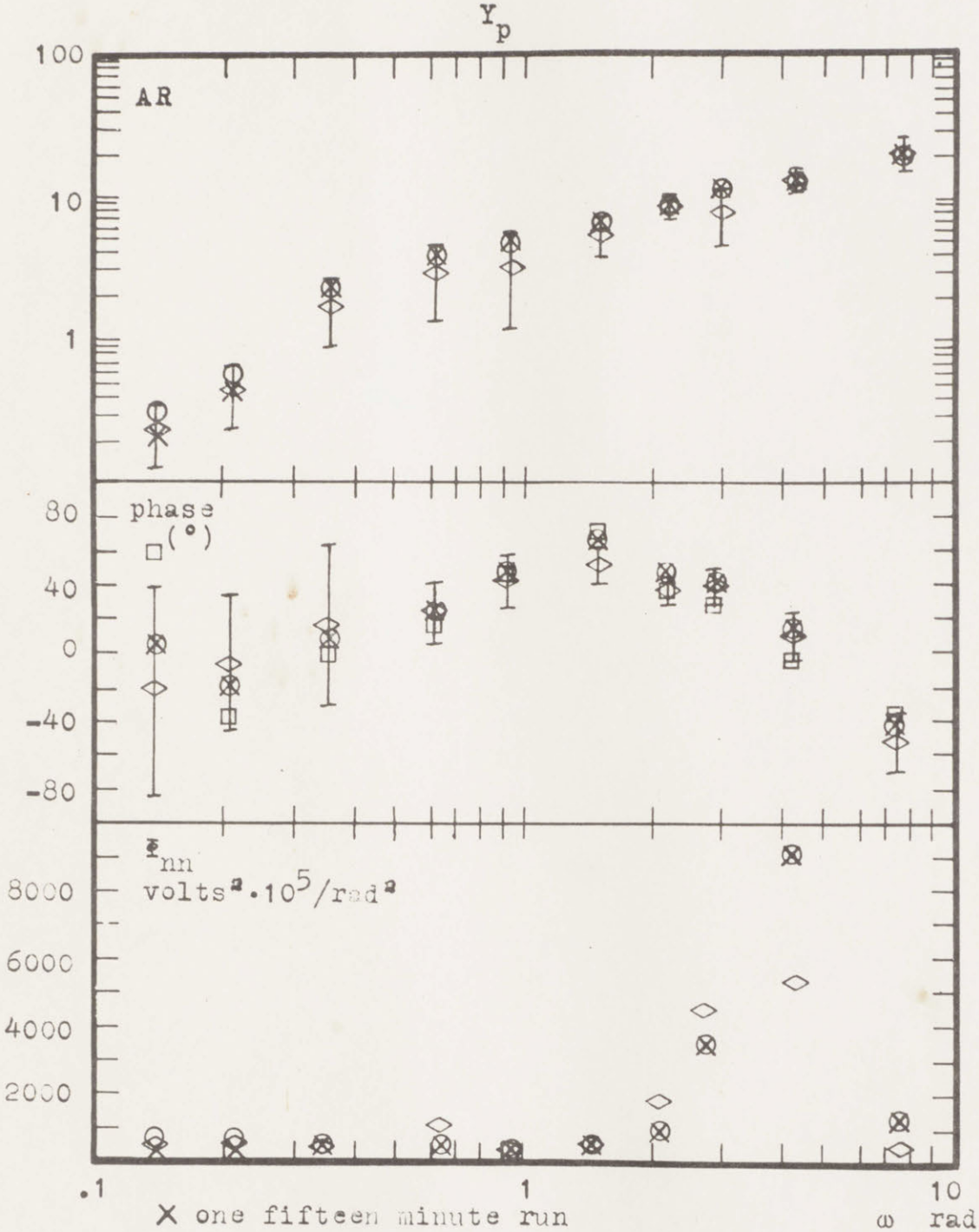

× one fifteen minute run

⊕ average of 10 90-second runs ± σ

○ one fifteen minute run corrected for remnant (phase by eq. 3.19)

□ one fifteen minute run, phase by eq. 3.20

THE EFFECT OF THE REMNANT CORRECTION TO Y_p FOR $Y_c = e^{-.1s}/s^2$

figure 3.2

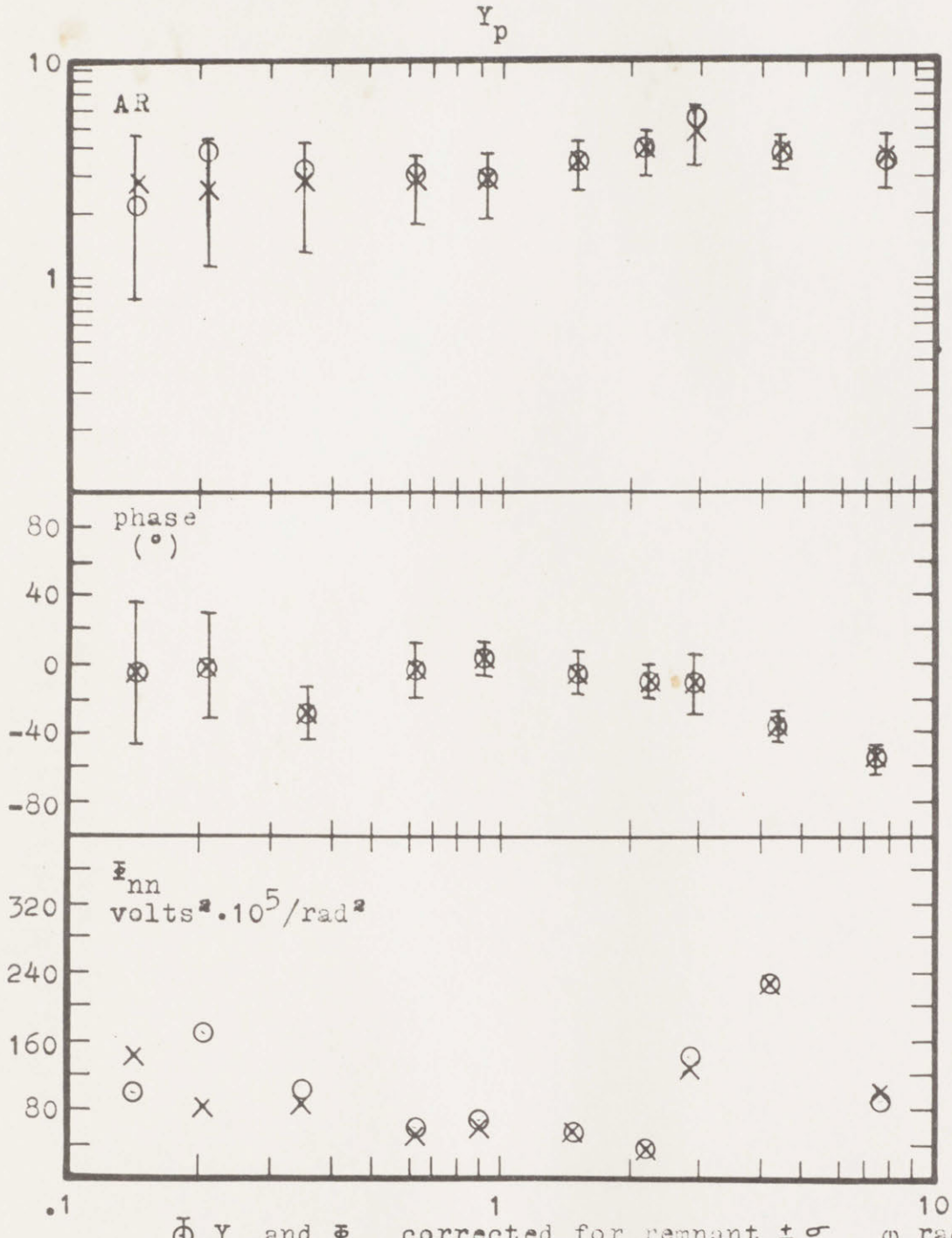

THE EFFECT OF THE REMNANT CORRECTION TO Y_p
FOR $Y_c = e^{-.1s}/s$

figure
3.3

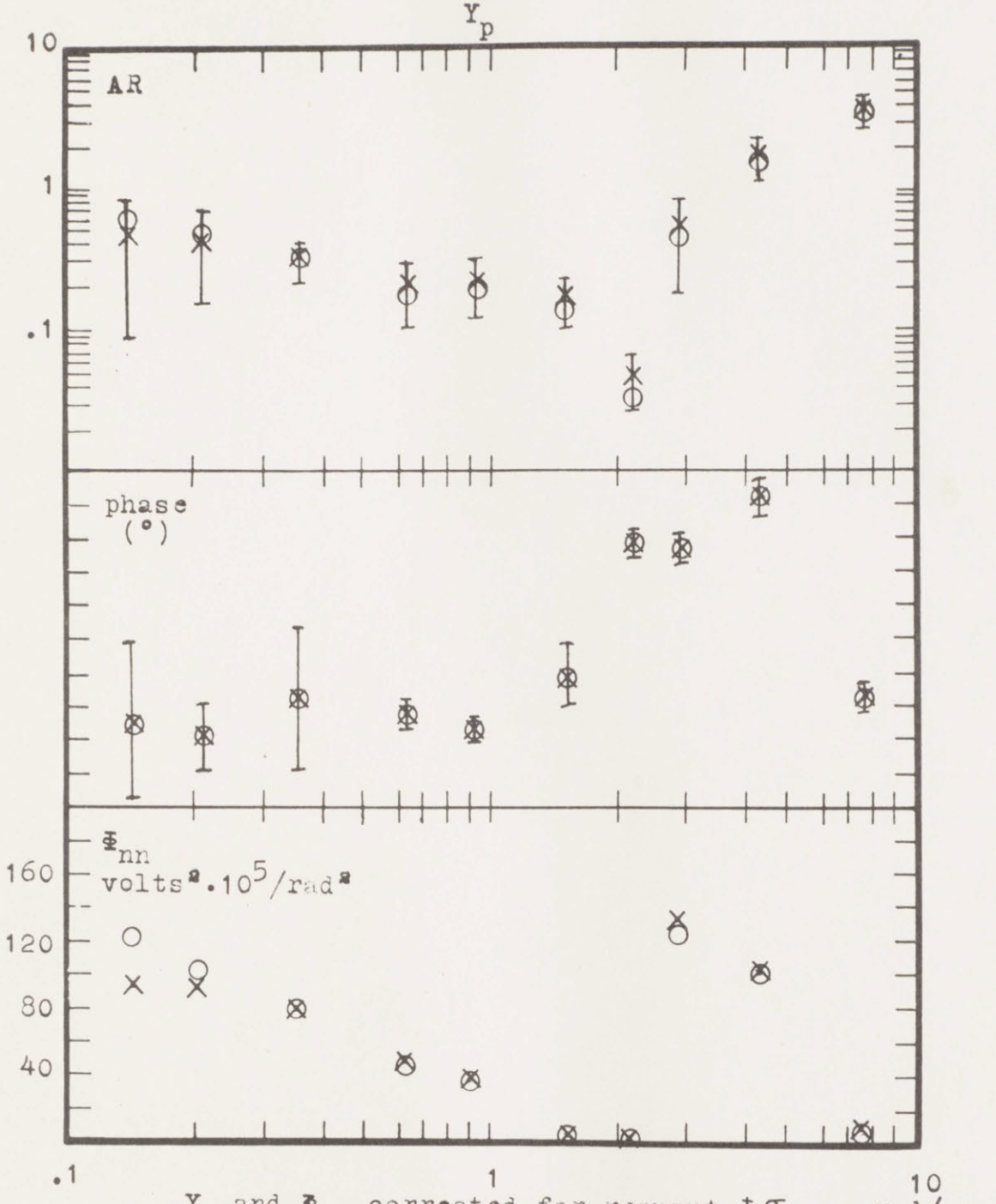

Y_p and Φ_{nn} corrected for remnant $\pm\sigma$

Y_p and Φ_{nn} uncorrected for remnant $\pm\sigma$

THE EFFECT OF THE REMNANT CORRECTION TO Y_p

$$\text{FOR } Y_c = \frac{10e^{-.1s}}{s(s^2 + 10)}$$

figure
3.4

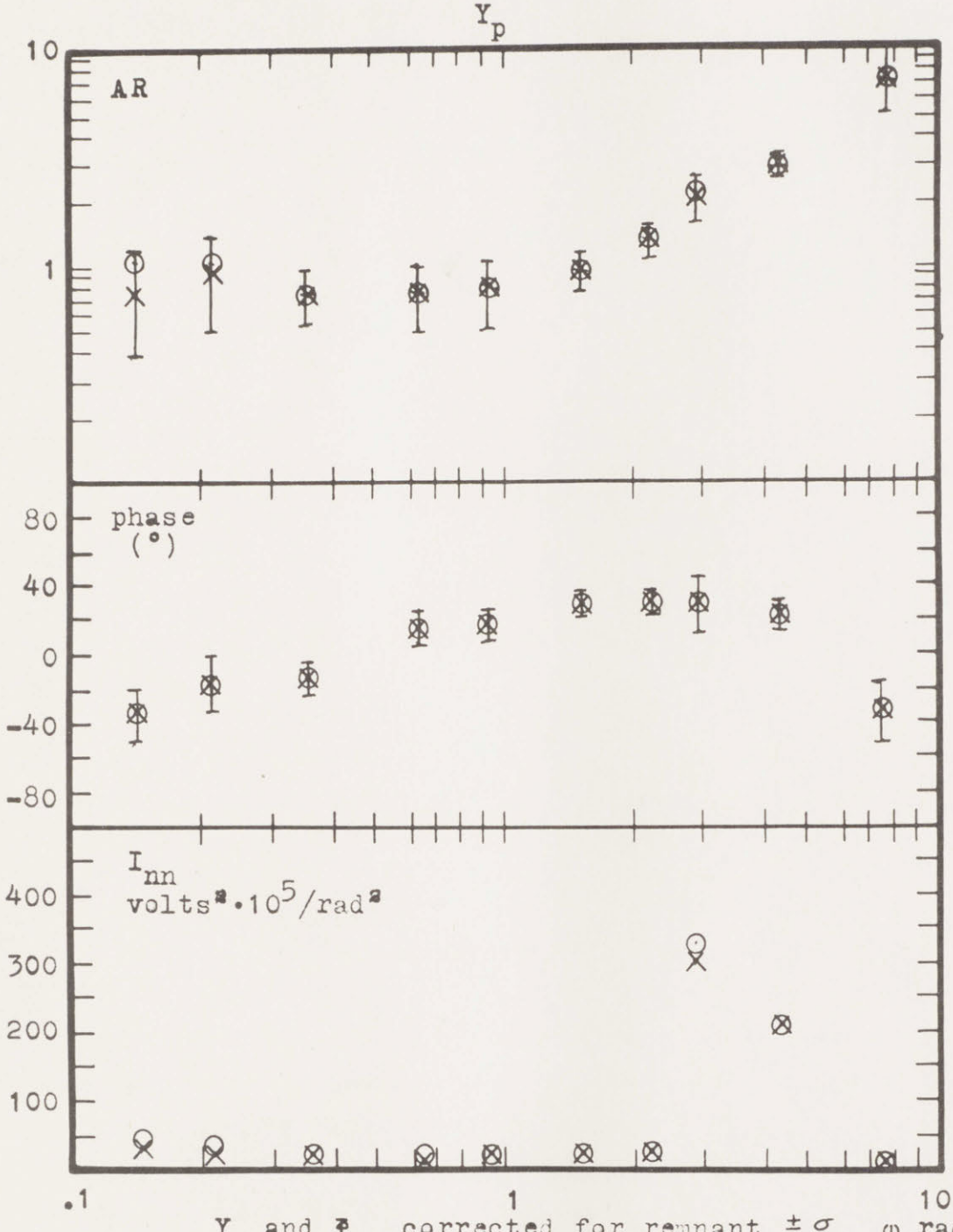

Y_p and $\bar{F}_{nn}$ corrected for remnant $\pm\sigma$

Y_p and $\bar{F}_{nn}$ uncorrected for remnant $\pm\sigma$

THE EFFECT OF THE REMNANT CORRECTION TO Y_p

FOR $Y_c = \dfrac{15e^{-.1s}}{s(s^2 + 3s + 15)}$

figure 3.5

TABLE 3.1

$Y_c = e^{-.1s}/s^2$

freq. rad/sec	$\lvert Y_n(\omega) \rvert$				$\angle Y_p(\omega)$				
	FMRU	NCFR	lSD	FMRC	FMRU	FCFR	lSD	FMRC	FMRP
.14	.22	.23	.18	.38	+5	-20	50	+60	+5
.21	.45	.45	.24	.66	-18	-5	56	-36	-18
.35	2.4	1.8	1.0	2.48	+10	+18	58	+2	+10
.63	4.4	3.0	1.7	4.4	+23	+25	38	+15	+23
.91	5.2	3.3	1.3	5.2	+50	+41	8	+49	+50
1.48	6.8	5.3	.16	6.8	+63	+53	7	+78	+63
2.18	9.3	9.0	1.5	9.3	+48	+38	5	+32	+48
2.88	11.4	8.3	3.5	11.4	+40	+40	16	+23	+40
4.29	14.3	14	1.5	14.3	+15	+12	8	-5	+15
7.66	22.9	21	5.1	22.9	-40	-50	23	-30	-40

FMRU = fifteen minute run not corrected for remnant

NCFR = average of ten 90-second runs not corrected for remnant

lSD = one standard deviation of the 10 90-second runs

FMRC = one fifteen minute run corrected for remnant, the phase calculated using eq. 3.20

FMRP = one fifteen minute run corrected for remnant, the phase calculated using eq. 3.19

TABLE 3.2

	$Y_c = e^{-.1s}/s$							
	$\lvert Y_p(\omega) \rvert$				$\angle Y_p(\omega)$			
freq. rad/sec	NCFR	1SD	CFR	$\frac{1SD}{\sqrt{n}}$	NCFR	1SD	CFR	$\frac{1SD}{\sqrt{n}}$
.14	2.8	2.0	2.2	.63	-3	43	-3	14
.21	2.6	1.8	4.1	.57	-1	31	-1	10
.35	2.9	1.5	3.2	.47	-28	15	-28	5
.63	2.9	1.0	3.0	.32	-2	14	-2	4
.91	3.0	1.0	3.0	.32	+4	7	+4	2
1.48	3.6	.9	3.6	.29	-3	11	-3	4
2.18	4.1	1.0	4.1	.32	-10	7	-10	2
4.29	4.0	.6	4.0	.19	-38	3	-38	1
7.66	3.9	1.1	3.8	.35	-52	6	-52	2
	$Y_c = \frac{10e^{-.1s}}{s(s^2 + 10)}$							
.14	.47	.41	.64	.18	-31	37	-31	16
.21	.43	.17	.50	.076	-39	19	-39	17
.35	.33	.10	.33	.045	-16	27	-16	12
.63	.22	.09	.18	.04	-25	14	-25	6
.91	.23	.10	.20	.045	-36	11	-36	5
1.48	.17	.06	.15	.027	-2	48	-2	21
2.18	.05	.02	.03	.009	+78	21	+78	9
2.88	.54	.34	.47	.15	+77	43	+77	19
4.29	1.9	.4	1.8	.18	+106	6	+106	3
7.66	3.9	1.0	3.8	.45	-14	3	-14	2

NCFR = not corrected for remnant (average of 5 to 10 runs)

1SD = one standard deviation of the data

CFR = corrected for remant (average 5 to 10 runs)

$1SD/\sqrt{n}$ = one standard deviation of the averaged data

TABLE 3.3

$$Y_c = \frac{15e^{-.1s}}{s(s^2 + 3s + 15)}$$

freq. rad/sec	$\lvert Y_p(\omega) \rvert$ NCFR	1SD	CFR	$\frac{1SD}{\sqrt{n}}$	$\angle Y_p(\omega)$ NCFR	1SD	CFR	$\frac{1SD}{\sqrt{n}}$
.14	.77	.32	1.1	.10	-32	16	-32	5
.21	.93	.47	1.0	.15	-14	15	-14	5
.35	.76	.18	.78	.057	-11	9	-11	3
.63	.79	.22	.79	.07	+18	10	+18	3
.91	.84	.22	.84	.07	+19	10	+19	3
1.48	1.0	.2	1.0	.063	+30	5	+30	2
2.18	1.4	.17	1.4	.054	+32	7	+32	2
2.88	2.2	.5	2.4	.16	+3-	14	+30	4
4.29	3.1	.35	3.1	.11	+24	11	+24	4
7.66	7.6	2.7	7.6	.86	-30	20	-30	6

NCFR = not corrected for remnant (average 10 runs)

1SD = one standard deviation of the data

CFR = corrected for remnant (average 10 runs)

$1SD/\sqrt{n}$ = one standard deviation of the averaged data

correction ranges up to 90% of one standard deviation of the data for frequencies below .5 rad/sec, and up to 30% (but generally less than 10%) of one standard deviation of the data above .5 rad/sec. Thus, if the measurements of the human operator's describing function are carefully made, following the work of McRuer, et al., they will be nearly free of any errors caused by remnant corruption of the experimental measurements.

All the data presented in this thesis are corrected for the effects of the remnant except data taken for vehicle dynamics which include a factor of $1/s^2$. Such data are clearly marked "NOT CORRECTED FOR REMNANT". Why these data are not corrected for the remnant is explained in section 3.3 of this chapter. Such corrections would be small, however, as is shown in figure 3.2 where corrections for the remnant were made to data taken for $Y_c=1/s^2$.

3.3 Difficulties In Correcting For The Remnant

3.3.1 Low Signal Levels

When both the remnant and the output from the human operator's describing function are low level signals, corrections cannot be made for the remnant with any reasonable accuracy. Such is the case for data taken below .5 rad/sec for vehicle dynamics with a factor of $1/s^2$.

Data were taken for the human operator's describing function for $Y_c=e^{-.1s}/s^2$ by measuring $Y_pY_c(\omega)$ instead of $Y_p(\omega)$ as was done for the bulk of the experiment. This was done in order to avoid measuring the low signal levels at the human operator's output which

signal levels below .5 rad/sec which exist at the output of the human operator. These data are shown on figure 3.2. Also shown are the same data corrected for the remnant, and data for the human operator's describing function obtained by measuring $Y_p(\omega)$ directly. Figure 3.2 shows two important results: 1) when data for the human operator's describing function for vehicle dynamics with a factor of $1/s^2$ are corrected for the remnant, the corrections are small as for the rest of the data taken, and 2) the data taken for $Y_p(\omega)$ directly are accurate, and it is not necessary to measure $Y_pY_c(\omega)$ to get the correct results. Chapter II, section 2.4.2, also verifies the second result. Finally,

3.3.2 Averaging The Phases

The phases of M_m and e relative to the system input are calculated according to

$$P_m(\omega_k) = \tan^{-1}\left(\frac{B_{mk}}{A_{mk}}\right)$$

$$P_e(\omega_k) = \tan^{-1}\left(\frac{B_{ek}}{A_{ek}}\right)$$

where we define the A's and B's, as in Chapter II, as

$$A_{ek} = \sum_{n=1}^{896} e(n\Delta t)\sin(\omega_k n\Delta t)$$

$$B_{ek} = \sum_{n=1}^{896} e(n\Delta t)\cos(\omega_k n\Delta t)$$

$$A_{mk} = \sum_{n=1}^{896} M_m(n\Delta t)\sin(\omega_k n\Delta t)$$

$$B_{mk} = \sum_{n=1}^{896} M_m(n\Delta t)\cos(\omega_k n\Delta t)$$

Because the derivation for the correction of $Y_p(\omega)$ was made after the data were taken, the data for the phase were averaged according to

$$\overline{\angle Y_p(\omega)} = \frac{1}{r}\sum_{n=1}^{r} \angle Y_{pn}(\omega)$$

where r is the number of runs over which the data are averaged. Since

$$\angle Y_p(\omega) = P_m - P_e$$

the calculated average of the data is given by

$$\overline{\angle Y_p(\omega_k)} = \overline{P_{mk} - P_{ek}}$$

or

$$\text{eq. 3.19)} \quad \overline{\angle Y_p(\omega_k)} = \overline{\tan^{-1}\left(\frac{B_{mk}}{A_{mk}}\right) - \tan^{-1}\left(\frac{B_{ek}}{A_{ek}}\right)}$$

Although the data typed out, and hence available for averaging, are of P_{mk} and P_{ek}, the actual experimental measurements made by the computer are of the A's and B's (see Chapter II, sections 2.3.8 and 2.3.9). Because the inverse tangent is a non-linear operator

$$\overline{\tan^{-1}\left(\frac{B}{A}\right)} \neq \tan^{-1}\left(\frac{\overline{B}}{\overline{A}}\right)$$

and hence the averaging of $\angle Y_p(\omega_k)$ should be done according to

eq. 3.20) $\angle Y_p(\omega_k) = \tan^{-1}\left(\frac{\bar{B}_{mk}}{\bar{A}_{mk}}\right) - \tan^{-1}\left(\frac{\bar{B}_{ek}}{\bar{A}_{ek}}\right)$

In figure 3.2 the results of treating the phase data in the proper manner are shown. Special data were taken for this purpose, as during the bulk of the experiment values of P_{mk} and P_{ek} were saved, but the actual Fourier coefficients (A's and B's) were not saved. On figure 3.2 and in table 3.1 it can be seen that except for the lowest frequency, the phase calculated according to equation 3.20 (the proper equation to use) is very nearly equal to the phase calculated according to equation 3.19 (the equation actually used). Thus the again we see that the effects of the remnant on the data are small.

CHAPTER IV: EXPERIMENTAL RESULTS

4.1 Introduction

A brief statement of the results of this thesis is given in Chapter I and in Chapter V. This chapter is devoted to a detailed explanation of how the data are analyzed to obtain information about the human operator's use of motion cues in man-vehicle control.

The actual experimental data are presented on pages 169 to 230. An index to the data and a complete description of the method of presentation of the data are given on pages 161 to 168.

Although the data are taken for roll motion cues, it should be remembered that very similar results can be expected for pitch motion cues (see reference 17).

In section 4.2 the describing function data are modelled and used to describe how the human operator uses roll motion cues in vehicle control.

In section 4.3 the rISE data (see section 2.3.8) are used to determine what vehicle dynamics permit the human operator to make the most use of roll motion cues.

In section 4.4 the describing function data are examined to determine the effects on the data of varying other experimental parameters.

In section 4.5 those vehicle dynamics for which the effects of roll motion cues on the human operator's describing function are known or can be predicted are summarized.

Finally, in section 4.6, the start of a physiologi-

cally based model for the human operator's use of motion cues in man-vehicle control is suggested.

4.2 How Roll Motion Cues Affect The Human Operator's Describing Function

The actual describing function data for the human operator are shown on pages 169 to 230. The data are taken for three sets of vehicle dynamics:

eq. 4.1) $$Y_c(s) = \frac{\omega_n^2}{s^2 + 2\zeta\omega_n s + \omega_n^2}$$, $2\zeta\omega_n$ and ω_n^2 vary

eq. 4.2) $$Y_c(s) = \frac{K}{s(\tau s + 1)}$$, K and $1/\tau$ vary

eq. 4.3) $$Y_c(s) = \frac{\omega_n^2}{s(s^2 + 2\zeta\omega_n s + \omega_n^2)}$$, $2\zeta\omega_n$ and ω_n^2 vary

As $2\zeta\omega_n$ and ω_n^2 vary, equation 4.1 represents many different vehicle dynamics. For the purposes of presenting data, it is possible to represent each such set of vehicle dynamics, corresponding to a given value of $2\zeta\omega_n$ and ω_n^2, by a point in the $2\zeta\omega_n$-ω_n^2 plane. Similarly, each of the vehicle dynamics given by equations 4.2 and 4.3 can be represented by points in the K-$1/\tau$ plane and in another $2\zeta\omega_n$-ω_n^2 plane. Thus each set of vehicle dynamics for which data were taken corresponds to a point in one of the three planes mentioned above. Examination of the data at these points within an area of one of the three planes shows that the human operator's describing functions assume a very similar shape. In fact, it is possible to divide the three planes into areas according

to the shape of the human operator's describing function as shown in figures 4.1 through 4.6. Representative points are chosen from each of the areas in the three planes, and the data for visual cues only and for simultaneous visual and motion cues are fitted using one of the two following models:

$$\text{eq. 4.4)} \quad Y_p(s) = \frac{Ke^{-\tau_3 s}(\tau_1 s + 1)(\tau_2 s + 1)}{(\tau_3 s + 1)(\tau_4 s + 1)(\tau_5 s + 1)}$$

$$\text{eq. 4.5)} \quad Y_p(s) = \frac{Ke^{-\tau_3 s}(\tau_1 s + 1)(s^2 + 2\xi_m \omega_{nm} s + \omega_{nm}^2)}{\omega_{nm}^2(\tau_2 s + 1)(\tau_3 s + 1)}$$

The values of the parameters used are shown in tables 4.1 through 4.3, and the actual frequency response of the models and the data points for the human operator's describing function are shown on pages 251 to 288. As can be seen, the model fits of the data are quite good except for one area: for vehicle dynamics given by $Y_c=1/s(s+1)$, $1/s^2$, or $-1/s(s-1)$, the phase curves are poor fits below 3 rad/sec. A better fit cannot be obtained using the models represented by equations 4.4 and 4.5. A third model is not used for three reasons:

1) It is desired to use as few and as simple models for Y_p as possible in order to more easily examine the differences in the model parameters between the fixed-base and moving-base cases.
2) The phase of Y_p, where it does not agree with the model used, does not change upon the addition of roll motion cues to the visual cues.

Y_p

Type Number	General Shape of the Curves AR	Phase
I		 0°
II		 0°
III		 0°
IV		 0°

Classification of Y_c's, the vehicle dynamics:

I: $\frac{20e^{-.1s}}{s^2+20}$, $\frac{10e^{-.1s}}{s^2+10}$, $\frac{5e^{-.1s}}{s^2+5}$, $\frac{-2.5e^{-.1s}}{s^2-2.5}$

$\frac{15e^{-.1s}}{s^2-s+15}$, $\frac{5e^{-.1s}}{s^2+s+5}$

II: $\frac{25e^{-.1s}}{s^2+5s+25}$, $\frac{15e^{-.1s}}{s^2+5s+15}$, $\frac{15e^{-.1s}}{s^2+3s+15}$, $\frac{20e^{-.1s}}{s^2+2s+20}$

$\frac{10e^{-.1s}}{s^2+2s+10}$

III: $\frac{5e^{-.1s}}{s^2+5s+5}$, $\frac{5e^{-.1s}}{s^2+3s+5}$

IV: $\frac{-2.5e^{-.1s}}{s^2+s-2.5}$, $\frac{-5e^{-.1s}}{s^2+3s-5}$, $\frac{-5e^{-.1s}}{s^2+s-5}$

DIVISION OF THE $2\xi\omega_n-\omega_n^2$ PLANE BY TYPE OF Y_p MEASURED FOR

$$Y_c = \frac{\omega_n^2 e^{-.1s}}{s^2 + 2\xi\omega_n s + \omega_n^2}$$ (see fig. 4.2)

Figure 4.1

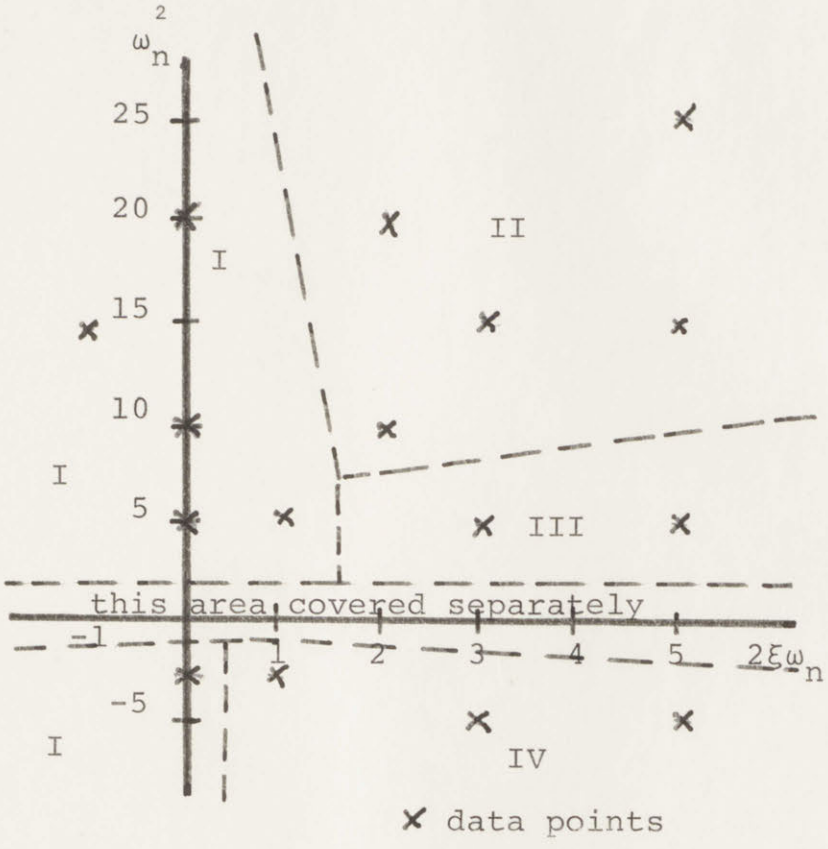

Dynamics: $$\frac{\omega_n^2 e^{-.1s}}{s^2 + 2\xi\omega_n s + \omega_n^2} = Y_c$$

DIVISION OF THE $2\xi\omega_n$-ω_n^2 PLANE BY TYPE OF Y_p MEASURED

FOR $$Y_c = \frac{\omega_n^2 e^{-.1s}}{s^2 + 2\xi\omega_n s + \omega_n^2}$$

(see figure 4.1)

Figure 4.2

Y_p

Type Number	General Shape of the Curves	
	AR	Phase
V		 0°
VI		 0°
VII		 0°
VIII		 0°
IX		 0°

Classification of Y_c's, the vehicle dynamics:

V: $\frac{e^{-.1s}}{s}$, $\frac{20e^{-.1s}}{s(s+20)}$

VI: $\frac{5e^{-.1s}}{s(s+5)}$

VII: $\frac{4e^{-.1s}}{s(s+4)}$

VIII: $\frac{2e^{-.1s}}{s(s+2)}$

IX: $\frac{-e^{-.1s}}{s(s-1)}$, $\frac{-.5e^{-.1s}}{s(s-.5)}$, $\frac{-.25e^{-.1s}}{s(s-.25)}$, Group C

$\frac{e^{-.1s}}{s^2}$ Group B

$\frac{e^{-.1s}}{s(s+1)}$ Group A

DIVISION OF THE REAL AXIS OF THE S-PLANE BY TYPE OF Y_p

MEASURED FOR $Y_c = \frac{Ke^{-.1s}}{s(\tau s + 1)}$ (see fig. 4.4)

Figure 4.3

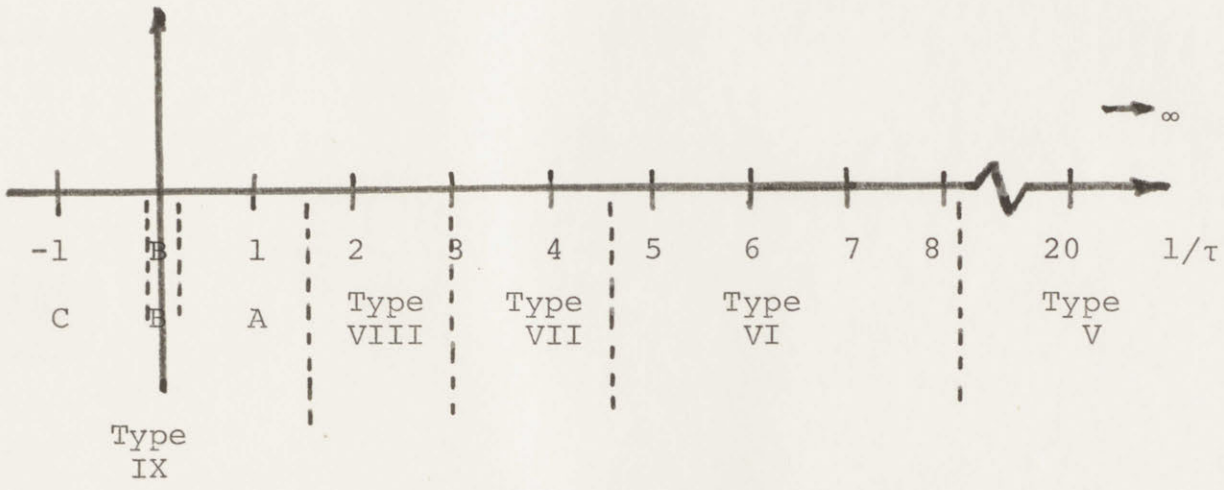

data points: location of the moving pole

DIVISION OF THE REAL AXIS OF THE S-PLANE BY TYPE OF Y_p

MEASURED FOR $Y_c = \frac{Ke^{-.1s}}{s(\tau s + 1)}$ (see fig. 4.3)

Figure 4.4

Y_p

Type — General Shape of the Curves

AR — Phase

X

0°

XI

0°

XII

0°

Classification of Y_c's, the vehicle dynamics

X: $\frac{2e^{-.1s}}{s^2(s+2)}$, $\frac{4e^{-.1s}}{s^2(s+4)}$

XI: $\frac{10e^{-.1s}}{s(s^2+10)}$, $\frac{20e^{-.1s}}{s(s^2+.5s+20)}$

XII: $\frac{15e^{-.1s}}{s(s^2+s+15)}$, $\frac{5e^{-.1s}}{s(s^2+s+5)}$, $\frac{20e^{-.1s}}{s(s^2+2s+20)}$

$\frac{10e^{-.1s}}{s(s^2+2s+10)}$, $\frac{15e^{-.1s}}{s(s^2+3s+15)}$, $\frac{5e^{-.1s}}{s(s^2+3s+5)}$

$\frac{20e^{-.1s}}{s(s^2+4s+20)}$, $\frac{10e^{-.1s}}{s(s^2+4s+10)}$, $\frac{15e^{-.1s}}{s(s^2+5s+15)}$

$\frac{5e^{-.1s}}{s(s^2+5s+5)}$

DIVISION OF THE $2\xi\omega_n$-ω_n^2 PLANE BY TYPE OF Y_p MEASURED

FOR $Y_c = \frac{\omega_n^2 e^{-.1s}}{s(s^2+2\xi\omega_n s+\omega_n^2)}$ (see fig. 4.6)

Figure 4.5

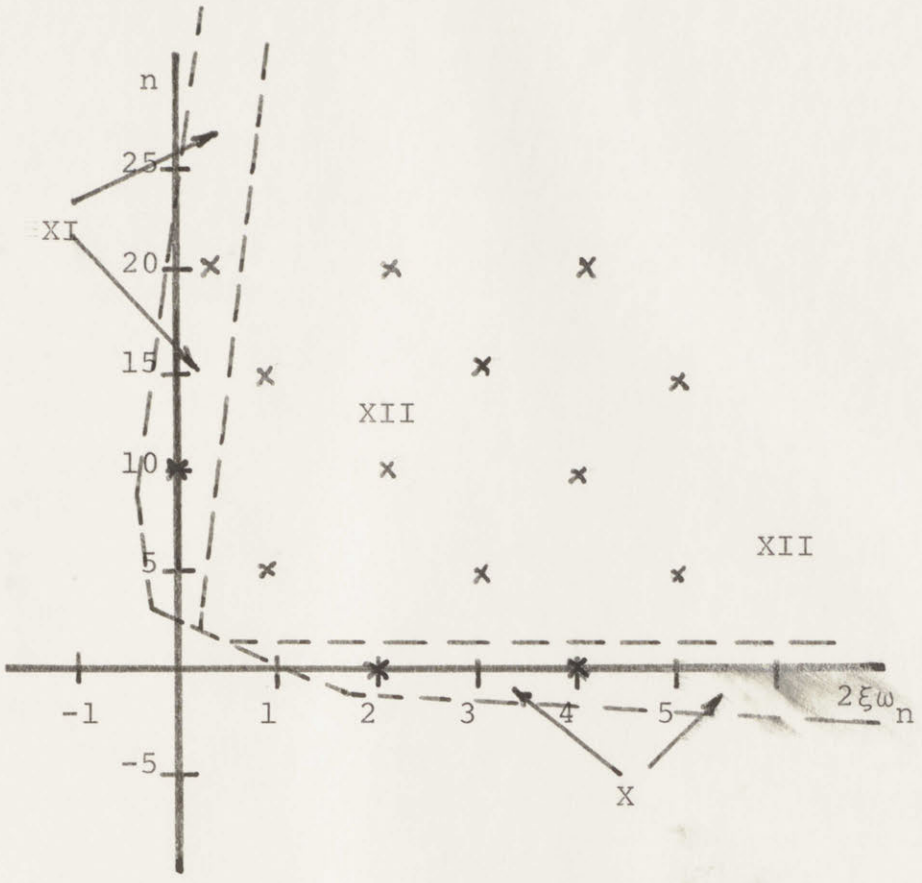

× data points

Dynamics: $Y_c = \dfrac{\omega_n^2 e^{-.1s}}{s(s^2 + 2\xi\omega_n s + \omega_n^2)}$

DIVISION OF THE $2\xi\omega_n - \omega_n^2$ PLANE BY TYPE OF Y_p MEASURED FOR

$$Y_c = \frac{\omega_n^2 e^{-.1s}}{s(s^2 + 2\xi\omega_n s + \omega_n^2)}$$ (see fig. 4.5)

Figure 4.6

3) The discrepancy between the models used and the actual data for the human operator's describing function occurs only for the three cases listed above.

Tables 4.1 through 4.3 give the parameters of the models (equations 4.4 and 4.5) for the human operator's describing function while he is controlling vehicle dynamics with visual cues only, and while he is controlling vehicle dynamics with simultaneous visual and motion cues. The changes in the model parameters when roll motion cues are added to the visual cues are summarized in table 4.4. From table 4.4 it can be seen that the human operator consistently uses the added roll motion cues to modify his fixed-base (visual cues only) behavior in two ways:

1) He increases his phase above 1 to 3 rad/sec as observed by Meiry (reference 17) and shown by the decreases in the lag, τ_4, and
2) he increases his gain, usually by increasing K, but sometimes by shifting the lead-lag compensation represented by τ_2 and τ_4.

These results lead to the following conclusions. When roll motion cues are added to the visual cues, the human operator controlling vehicle dynamics increases his phase lead above 1 rad/sec. This permits the human operator to also increase his gain, and hence the system cross-over[1] frequency, without a loss in phase margin (see

1) cross-over frequency: that frequency at which the magnitude of the product of the human operator's describing function and the vehicle dynamics crosses from greater than unity to less than unity.

TABLE 4.1

Type Number	Y_c		con-dition	model parameters						
	$2\xi\omega_n$	ω_n^2		K	τ_d	τ_1	τ_2	τ_3	$2\xi_m\omega_{nm}$	ω_{nm}^2
I	0	20	V V+M	9 20	.3 .2	1.5 1.5	14 14	.08 .08	1 1	20 20
I	0	5	V V+M	3 5	.38 .25	1.75 1.75	12 12	.08 .08	2 2	5 5
I	1	5	V V+M	11.5 20	.25 .14	1.9 1.9	7.5 7.5	.5 .5	4 4	5 5
II	5	25	V V+M	4.5 6.8	.3 .2	1.75 1.75	9 9	.17 .17	5 5	25 25
II	2	10	V V+M	19 23	.3 .2	2.5 2.5	10 10	.43 .43	3 3	10 10
III	5	5	V V+M	19 30	.28 .15	4.3 4.3	10 10	.65 .8	5 5	4.5 4.5
IV	1	-2.5	V V+M	3 5	.15 .05	0 0	.2 .38	.25 .3	1.5 1.5	2.5 2.5

$$\text{model:} \quad Y_p(s) = \frac{Ke^{-\tau_d s}(\tau_1 s + 1)(s^2 + 2\xi_m\omega_{nm}s + \omega_{nm}^2)}{\omega_{nm}^2(\tau_2 s + 1)(\tau_3 s + 1)}$$

$$\text{vehicle dynamics:} \quad Y_c(s) = \frac{\omega_n^2}{s^2 + 2\xi\omega_n s + \omega_n^2} \qquad \omega_n^2 \neq 0$$

For the meaning of the type numbers see fig. 4.1 and 4.2

V means visual cues only
V+M means simultaneous visual and roll motion cues

TABLE 4.2

ype umber	Y_c $1/\tau$	condi-tion	model parameters						
			K	τ_d	τ_1	τ_2	τ_3	τ_4	τ_5
V	∞	V V+M	4.5 4.5	.08 0	7 7	1.9 5	15 15	.85 1.75	.08 .08
V	20	V V+M	10 10	.07 0	6 6	1.1 2.5	27 27	.55 .9	.08 .08
VI	5	V V+M	8 8	.1 0	7 7	.85 1.6	31 31	.13 .29	.08 .08
VII	4	V V+M	16 16	.1 0	7 7	1.55 4	31 31	.15 .6	.08 .08
VIII	2	V V+M	10.5 15	.1 0	7 7	2 2	31 31	.23 .23	.08 .08
IX/A	1	V V+M	4.3 5.5	.1 0	7 7	3.8 3.8	31 31	.12 .12	.08 .08
IX/B	0	V V+M	.15 .18	.25 .15	10 10	3 3	.01 .01	1.5 1.5	.08 .08
IX/C	-1	V V+M	.2 .4	.2 0.15	10 10	3 1.8	.01 .01	1.5 1.5	0 0

$$\text{model: } Y_p(s) = \frac{Ke^{-\tau_d s}(\tau_1 s + 1)(\tau_2 s + 1)}{\omega_{nm}^2(\tau_3 s + 1)(\tau_4 s + 1)(\tau_5 s + 1)}$$

$$\text{vehicle dynamics: } Y_c(s) = \frac{K}{s(\tau s + 1)}$$

For the meaning of the type numbers, see fig. 4.3 and 4.4

V means visual cues only
V+M means simultaneous visual and roll motion cues

TABLE 4.3

Type Number	Y_c		condition	model parameters						
	$2\xi\omega_n$	ω_n^2		K	τ_d	τ_1	τ_2	τ_3	τ_4	τ_5
X	4	0	V	.4	.32	10	3	0	1.2	0
			V+M	.48	.25	10	3	0	1.2	0

$$\text{model:} \quad Y_p(s) = \frac{Ke^{-\tau_d s}(\tau_1 s + 1)(\tau_2 s + 1)}{\omega_{nm}^2(\tau_3 s + 1)(\tau_4 s + 1)(\tau_5 s + 1)}$$

Type Number	Y_c		condition	model parameters						
	$2\xi\omega_n$	ω_n^2		K	τ_d	τ_1	τ_2	τ_3	$2\xi_m\omega_{nm}$	ω_{nm}^2
XI	0	10	V	.9	.4	3	12	0	1	5
			V+M	1.5	.35	3	12	0	1	5
XII	2	10	V	.45	.43	.8	.15	.15	4	10
			V+M	.8	.43	.8	.15	.15	4	10
XII	4	10	V	1	.35	.9	.15	.25	4	10
			V+M	1.15	.35	.9	.15	.25	4	10

$$\text{model:} \quad Y_p(s) = \frac{Ke^{-\tau_d s}(\tau_1 s + 1)(s^2 + 2\xi_m\omega_{nm}s + \omega_{nm}^2)}{\omega_{nm}^2(\tau_2 s + 1)(\tau_3 s + 1)}$$

$$\text{vehicle dynamics for both cases:} \quad Y_c(s) = \frac{\omega_n^2}{s(s^2 + 2\xi\omega_n s + \omega_n^2)}$$

For meaning of type numbers see figures 4.5 and 4.6

V means visual cues only
V+M means simultaneous visual and roll motion cues

TABLE 4.4

Y_c example from the dynamics for which data were fitted	Y_p Type Number see figs. 4.1-4.6	Changes in the fixed base (visual cues only) model to fit the moving base (visual and motion cues) data for Y_p	Y_p the model used
$\frac{5e^{-.1s}}{s^2 + 5}$	I	1. increase K 85% 2. decrease lag (τ_d) 50%	eq. 4.5
$\frac{10e^{-.1s}}{s^2 + 2s + 10}$	II	1. increase K 25% to 50% 2. decrease lag (τ_d) 50%	eq. 4.5
$\frac{5e^{-.1s}}{s^2 + 5s + 5}$	III	1. increase K 50% 2. decrease lag (τ_d) 35% 3. increase $_3$ 20%	eq. 4.5
$\frac{-2.5e^{-.1s}}{s^2 + s - 2.5}$	IV	1. increase K 60% 2. decrease lag (τ_d) 60% 3. increase $_3$ 20%	eq. 4.5
$\frac{e^{-.1s}}{s}$	V	1. reduce lag (τ_d) to zero 2. increase $_2$ 150% 3. increase $_4$ 100%	eq. 4.4
$\frac{5e^{-.1s}}{s(s + 5)}$	VI	1. reduce lag (τ_d) to zero 2. increase $_2$ 90% 3. increase $_4$ 100%	eq. 4.4
$\frac{4e^{-.1s}}{s(s + 4)}$	VII	1. reduce lag (τ_d) to zero 2. increase $_2$ 150% 3. increase $_4$ 300%	eq. 4.4
$\frac{2e^{-.1s}}{s(s + 2)}$	VIII	1. reduce lag (τ_d) to zero 2. increase K 50%	eq. 4.4
$\frac{e^{-.1s}}{s(s + 1)}$	IX/A	1. reduce lag (τ_d) to zero 2. increase K 25%	eq. 4.4
$\frac{e^{-.1s}}{s^2}$	IX/B	1. reduce lag (τ_d) 40% 2. increase K 20%	eq. 4.4

continued on next page

TABLE 4.4 (continued)

Y_c example from the dynamics for which data were fitted	Y_p Type Number see figs. 4.1-4.6	Changes in the fixed base (visual cues only) model to fit the moving base (visual and motion cues) data for Y_p	Y_p the model used
$\frac{-e^{-.1s}}{s(s-1)}$	IX/C	1. reduce lag (τ_d) 40% 2. increase K 20% 3. decrease ζ 40%	eq. 4.4
$\frac{4e^{-.1s}}{s^2(s+4)}$	X	1. reduce lag (τ_d) 20% 2. increase K 20%	eq. 4.4
$\frac{10e^{-.1s}}{s(s^2+10)}$	XI	1. increase K 60% 2. reduce lag (τ_d) 20%	eq. 4.5
$\frac{10e^{-.1s}}{s(s^2+2s+10)}$	XII	1. increase K 15% to 90%	eq. 4.5

$$\text{eq. 4.4:} \quad Y_p(s) = \frac{Ke^{-\tau_d s}(\tau_1 s + 1)(\tau_2 s + 1)}{(\tau_3 s + 1)(\tau_4 s + 1)(\tau_5 s + 1)}$$

$$\text{eq. 4.5:} \quad Y_p(s) = \frac{Ke^{-\tau_d s}(\tau_1 s + 1)(s^2 + 2\xi_m \omega_{nm} s + \omega_{nm}^2)}{(\tau_2 s + 1)(\tau_3 s + 1)\omega_{nm}^2}$$

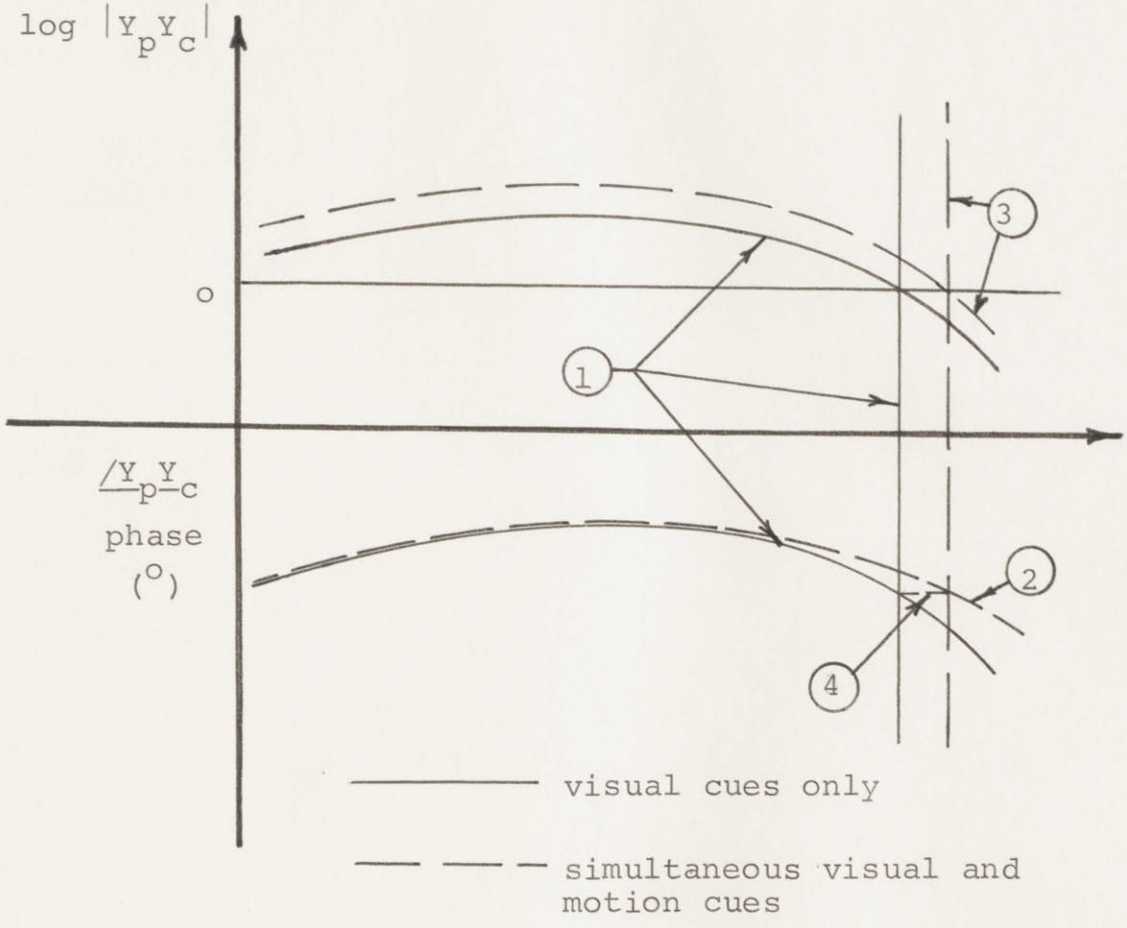

1. While controlling a vehicle with visual cues only, the human operator plant combination has a certain amplitude ratio, phase, and cross-over frequency.

2. The addition of roll motion cues to the visual cues permits the human operator to add lead at the higher frequencies and

3. thus permits him to increase the system gain and cross-over frequency without

4. a loss in phase margin.

HOW THE HUMAN OPERATOR CHANGES HIS CONTROL BEHAVIOR UPON THE INTRODUCTION OF ROLL MOTION CUES

Figure 4.7

figure 4.7).

4.3 The Human Operator's Use Of Roll Motion Cues As A Function Of Vehicle Dynamics

Along with the data on the human operator's describing function, data were taken for the system rISE (relative integral squared error, see Chapter II, section 2.3.8). By examining the data for the rISE, particularly the percent improvement in the rISE (measured for visual cues only) when motion cues are added, some conclusions can be reached about what vehicle dynamics permit the human operator to make the most use of motion cues. Figures 4.8 through 4.10 show all the data points, indicating at each point roughly how much motion cues helped the human operator. The classifications were made as follows:

DESCRIPTION "motion cues...	SYMBOL	CRITERIA significance of improvement of the rISE $\text{Prob}(rISE_V \; rISE_{V+M})$	CRITERIA %improvement of the rISE $100\left(\frac{rISE_V - rISE_{V+M}}{rISE_V}\right)$
are neutral"		$\text{Prob} < .05$	-
give slight improvement"		$\text{Prob} \geq .05$	-
are helpful"		$\text{Prob} \geq .01$	$\% < 30$
are very helpful"		$\text{Prob} > .01$	$\% \geq 30$
are extremely helpful"		$\text{Prob} > .01$	$\% \geq 40$

The classifications are chosen to fit obvious groupings in the data. It should be noted that at no point did motion cues actually harm system performance as measured by the rISE. It is felt that the rISE would increase with the addition of motion cues to the visual

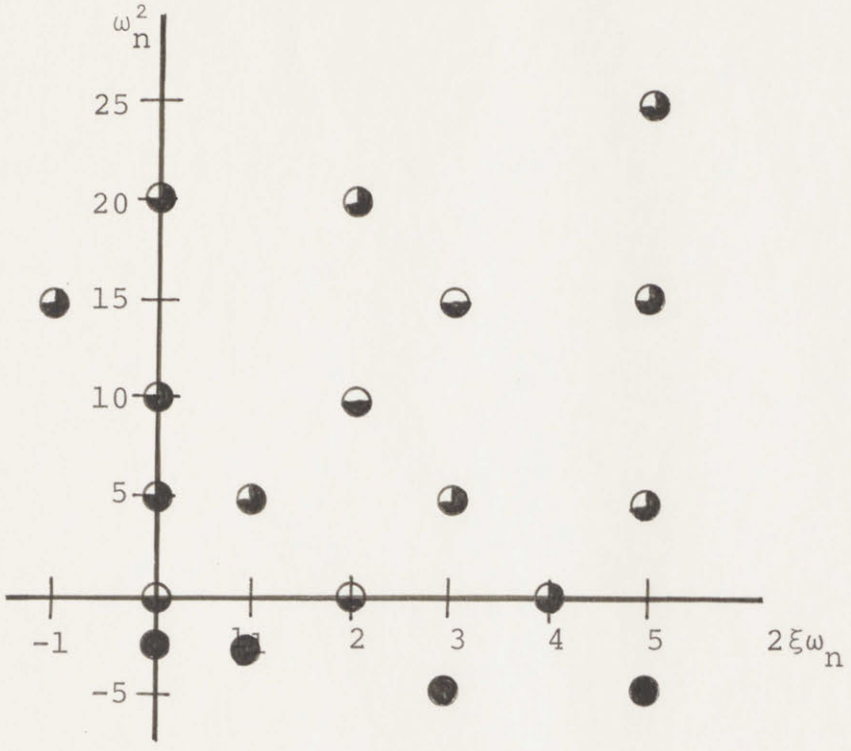

○ motion cues are neutral

◔ motion cues give slight improvement

◒ motion cues are fairly helpful

◕ motion cues are very helpful

● motion cues are extremely helpful

EFFECTS OF MOTION CUES FOR

$$Y_c = \frac{\omega_n^2 e^{-.1s}}{s^2 + 2\xi\omega_n s + \omega_n^2}$$

Figure 4.8

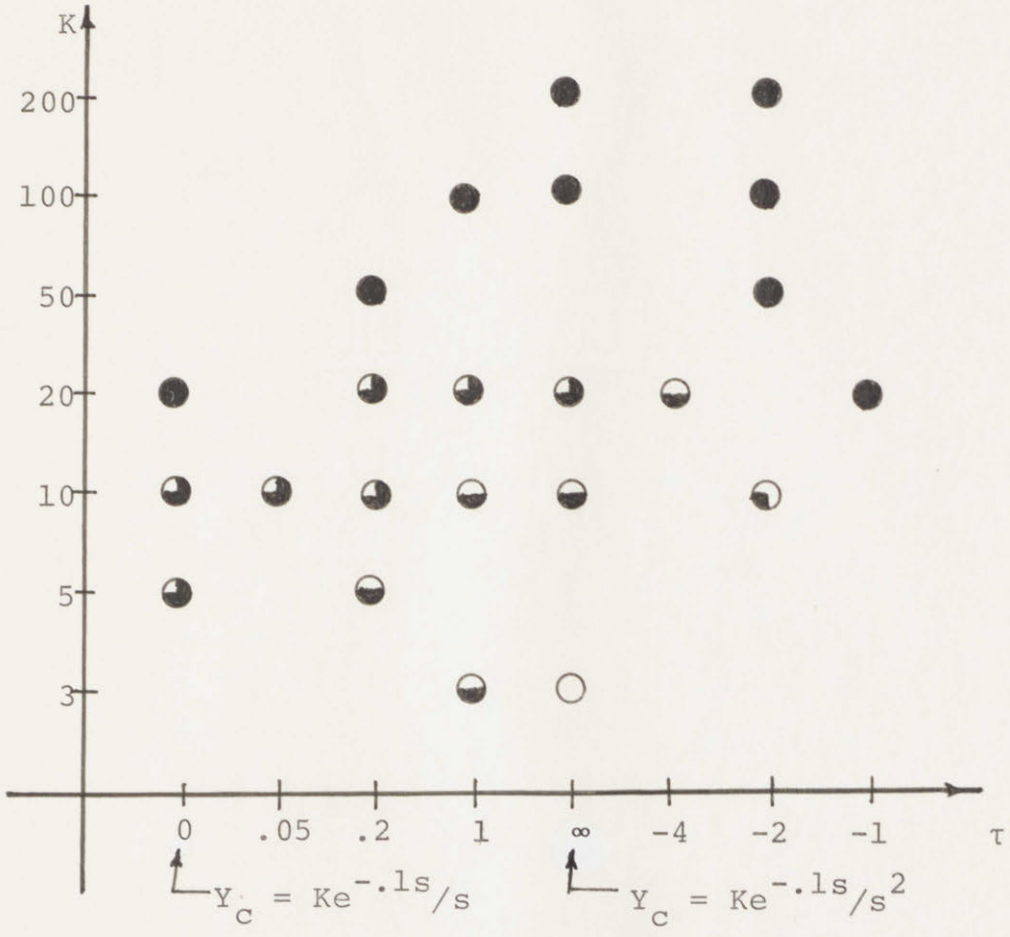

○ motion cues are neutral

◔ motion cues are slightly helpful

◒ motion cues are fairly helpful

◕ motion cues are very helpful

● motion cues are extremely helpful

EFFECTS OF MOTION CUES FOR

$$Y_c = \frac{Ke^{-.1s}}{s(\tau s + 1)}$$

Figure 4.9

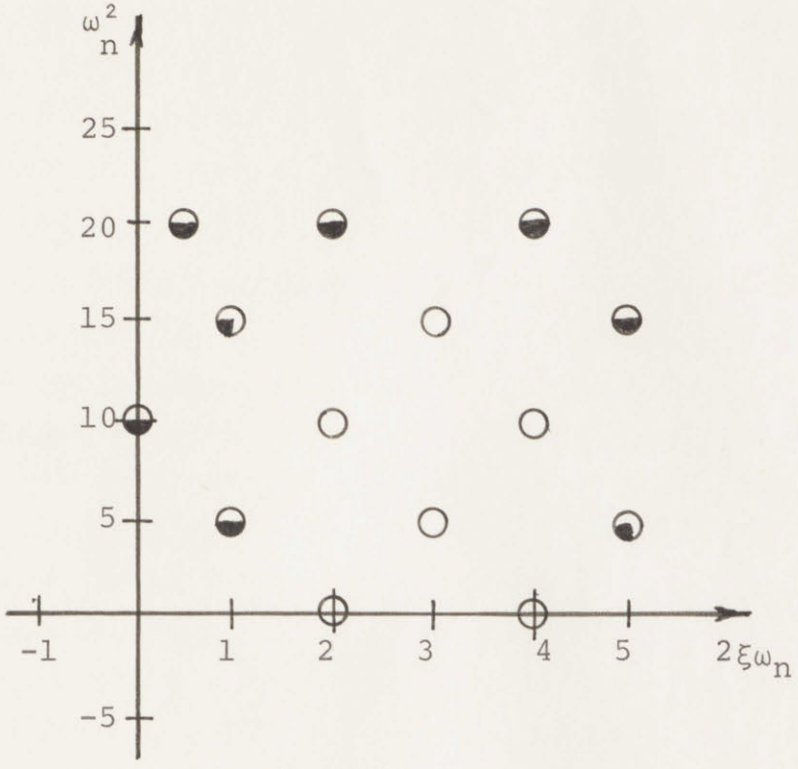

○ motion cues are neutral

◔ motion cues help slightly

◒ motion cues are fairly helpful

◕ motion cues are very helpful

● motion cues are extremely helpful

EFFECTS OF MOTION CUES FOR

$$Y_c = \frac{\omega_n^2 e^{-.1s}}{s(s^2 + 2\xi\omega_n s + \omega_n^2)}$$

Figure 4.10

cues for vehicle dynamics with low damping ratios and high natural frequencies. Data were not taken above $\omega_n = 20$ rad/sec for $\zeta = 0$ as the simulator was not capable of the accelerations associated with such vehicle dynamics.

In order to gain more information from figures 4.8 through 4.10, we will first examine figure 4.11. Here the usefulness of roll motion cues to the human operator is shown as the vehicle dynamics vary from $1/s^3$ to $1/s^2$ to $1/s$. It is important to note that for this figure the control stick gain, K, is constant at a value of ten volts maximum control stick output (see section 2.3.5). As will be seen in section 4.4.2, wide control stick gain variation can strongly affect the usefulness of motion cues to the human operator. As can be seen from figure 4.11, motion cues are of more help to the human operator as the vehicle dynamics decrease in order from $1/s^3$ to $1/s$. Furthermore, a comparison between figures 4.8 and 4.10 shows that for every value of $2\zeta\omega_n$ and ω_n^2 studied, the vehicle dynamics

$$Y_c(s) = \frac{\omega_n^2}{s(s^2 + 2\zeta\omega_n s + \omega_n^2)}$$

permit less use of motion cues by the human operator than the vehicle dynamics

$$Y_c(s) = \frac{\omega_n^2}{s^2 + 2\zeta\omega_n s + \omega_n^2}$$

Thus, for the range of vehicle dynamics studied (see

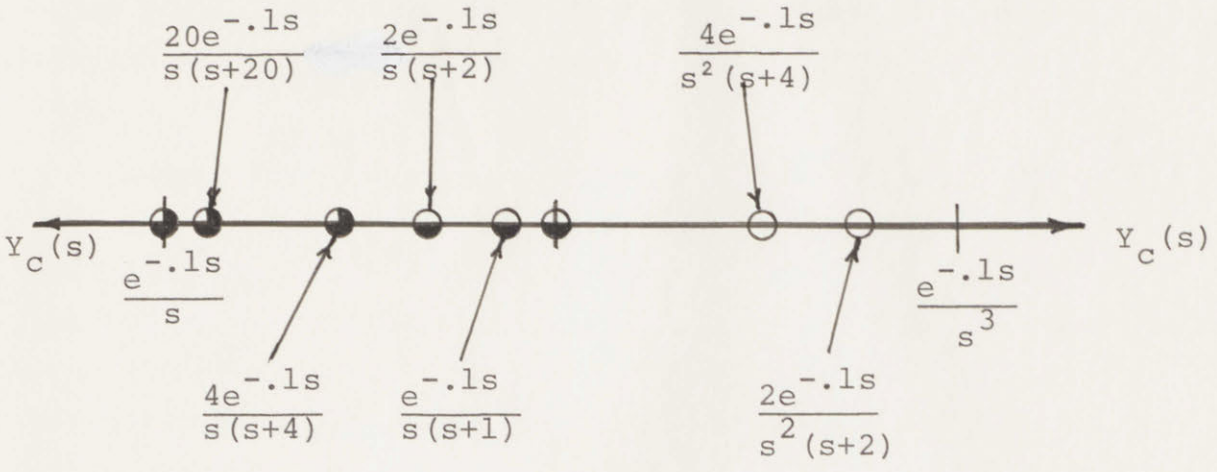

○ motion cues are neutral
◔ motion cues help slightly
◒ motion cues are helpful
◕ motion cues are very helpful
● motion cues are extremely helpful

THE EFFECTS OF MOTION CUES ON SYSTEM PERFORMANCE AS THE VEHICLE DYNAMICS RANGE FROM $1/s$ to $1/s^2$ to $1/s^3$

Figure 4.11

section 2.3.6 of Chapter II), and for constant control stick gain, the lower the order of the vehicle dynamics the more useful motion cues are to the human operator.

Lower order vehicle dynamics have a higher amplitude ratio above 1 rad/sec than higher order vehicle dynamics, and thus have a greater response to the control stick at the higher frequencies. As seen in section 4.2, the higher frequencies are where the human operator makes the most use of motion cues. Thus it is reasonable for the lower order vehicle dynamics, which respond more to the higher frequency inputs, to permit the human operator to make a greater use of angular motion cues.

Now let us further examine figures 4.8 through 4.10. When these figures are divided into areas according to the usefulness of roll motion cues to the human operator, they appear as in figures 4.12 through 4.14. On these figures loci of constant pilot opinion of the vehicle dynamics are also shown. These loci were obtained from references 1, 5, 19, and 28, as well as from some opinions stated by TI and SF, the two subjects for this experiment who were licensed pilots. From figures 4.12 through 4.14 we see that when vehicle dynamics are unstable or marginally stable (corresponding to negative or near-zero values of $1/\tau$, ω_n^2, or $2\zeta\omega_n$ in the figures), motion cues are very helpful to the pilot. Because very poor pilot opinion ratings correspond to unstable vehicle dynamics, we can conclude that motion cues are very helpful to the human operator for vehicle dynamics

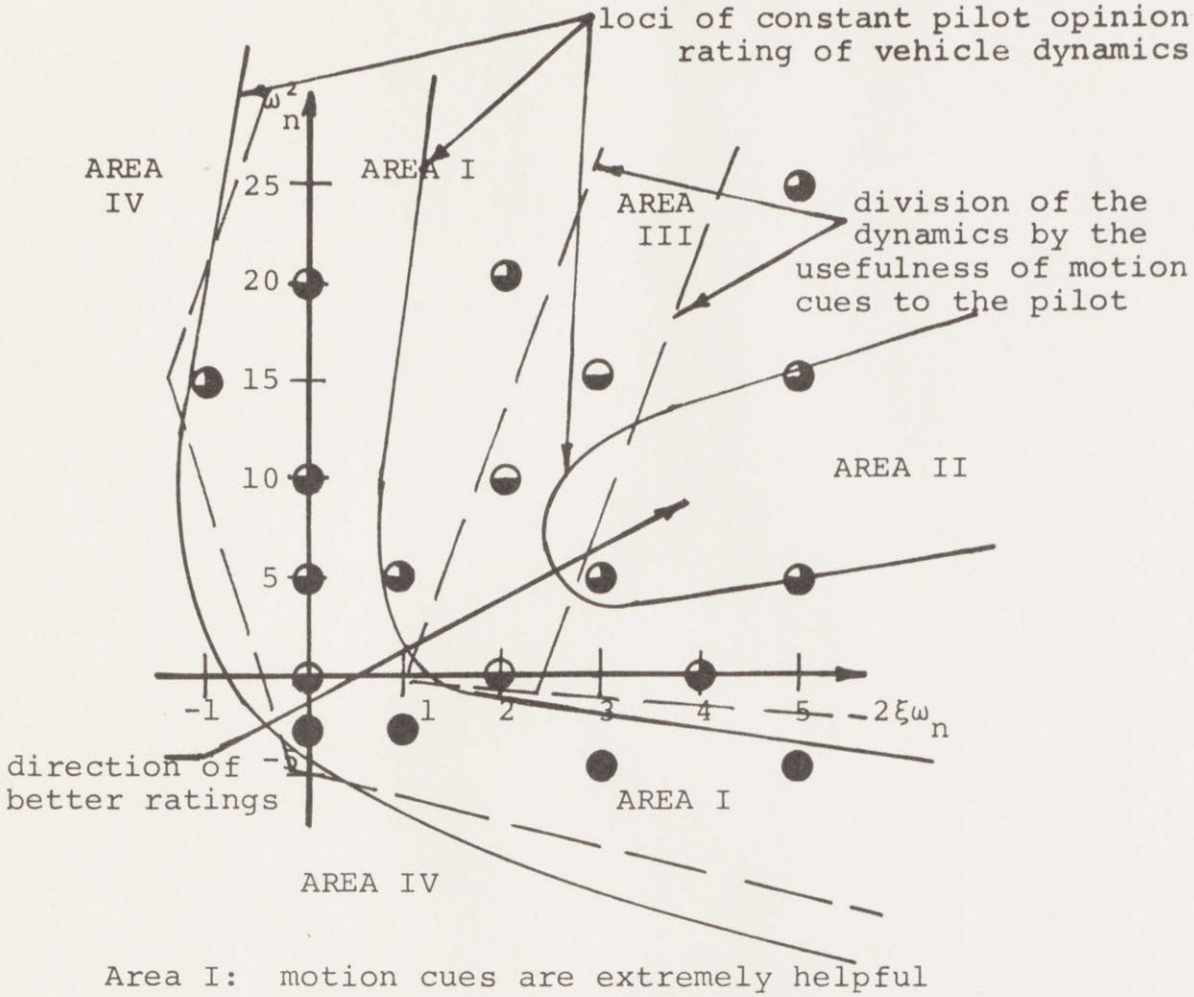

Area I: motion cues are extremely helpful

Area II: motion cues are very helpful

Area III: motion cues are helpful

Area IV: uncontrollable

DATA POINTS

- ○ motion cues are neutral
- ◔ motion cues help slightly
- ◒ motion cues are fairly helpful
- ◕ motion cues are very helpful
- ● motion cues are extremely helpful

THE EFFECTS OF MOTION CUES FOR

$$Y_c = \frac{\omega_n^2 e^{-.1s}}{s^2 + 2\xi\omega_n s + \omega_n^2}$$

Figure 4.12

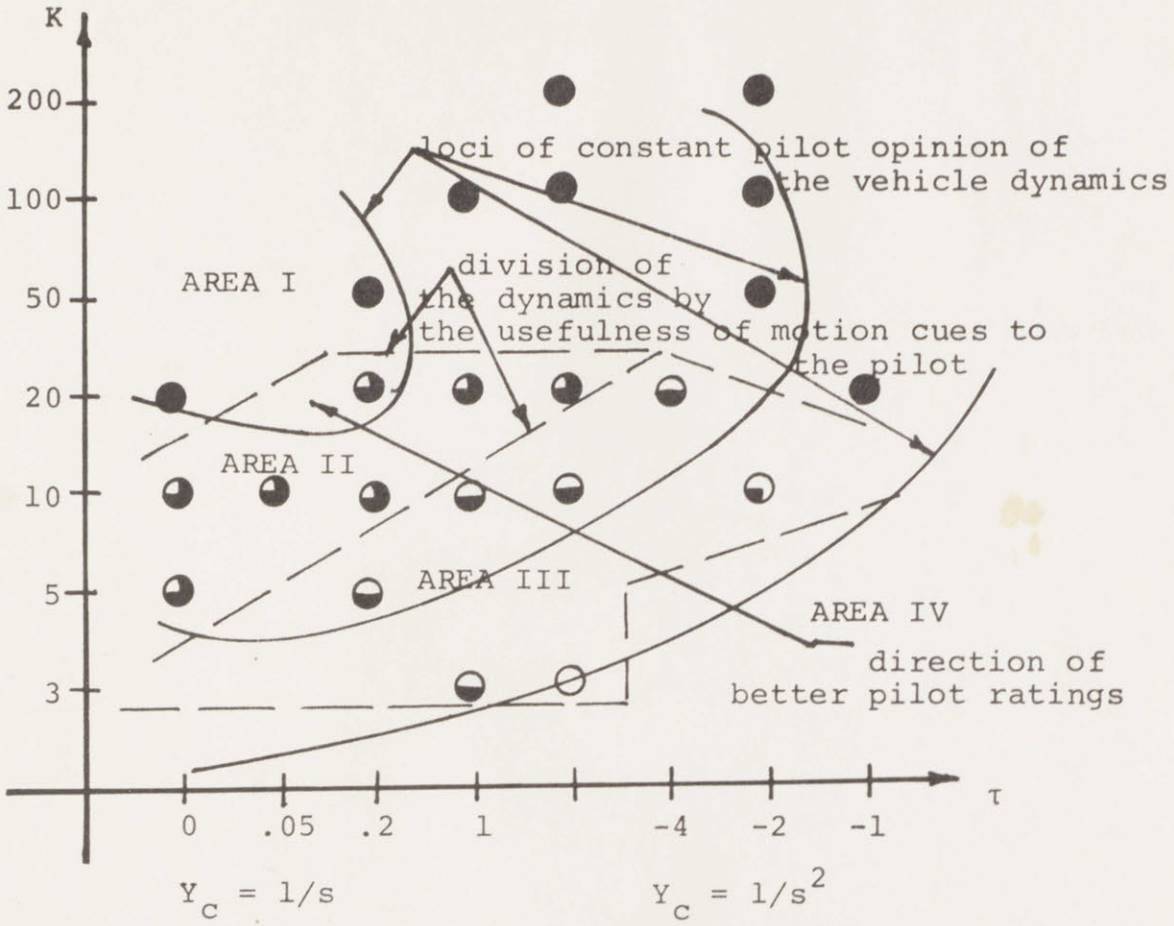

Area I: motion cues are extremely helpful
Area II: motion cues are very helpful
Area III: motion cues are helpful
Area IV: uncontrollable

○ motion cues are neutral
◔ motion cues help slightly
◒ motion cues are fairly helpful
◕ motion cues are very helpful
● motion cues are extremely helpful

THE EFFECTS OF MOTION CUES FOR

$$Y_c = \frac{Ke^{-.1s}}{s(\tau s + 1)}$$

Figure 4.13

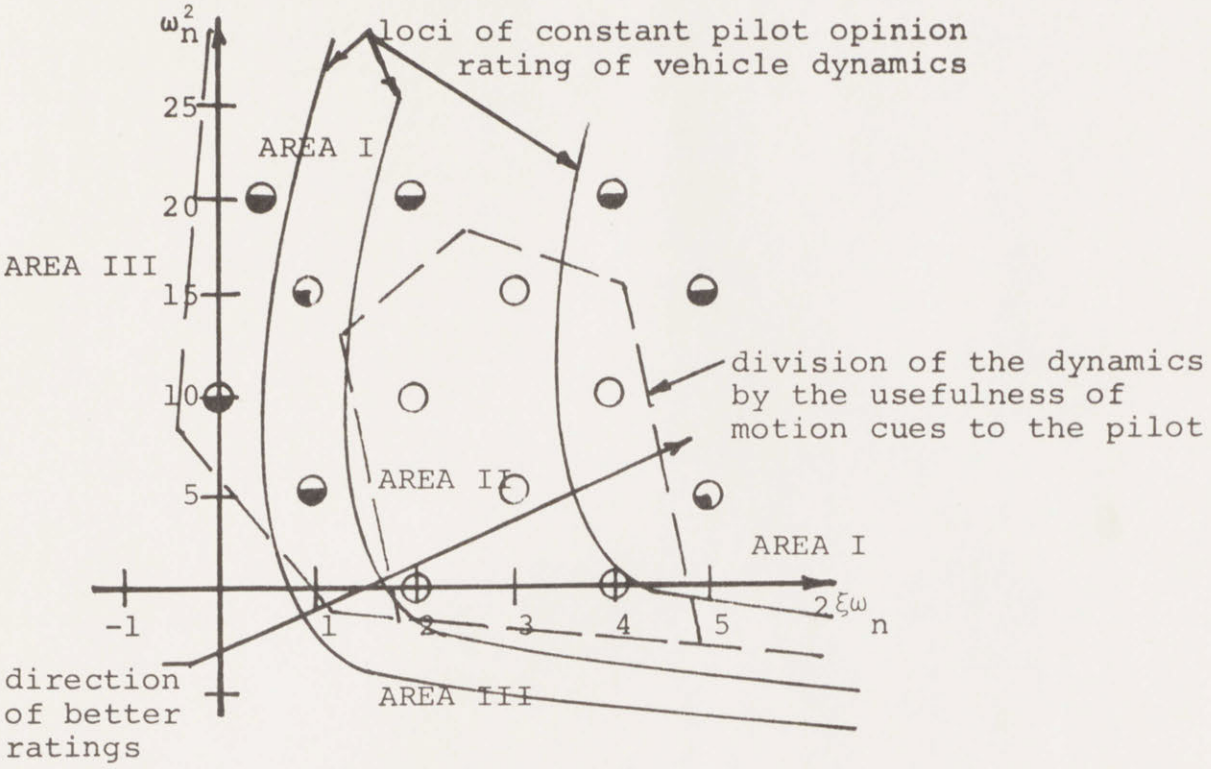

Area I: motion cues are helpful

Area II: motion cues are neutral

Area III: uncontrollable

DATA POINTS

○ motion cues are neutral
◔ motion cues are slightly helpful
◒ motion cues are fairly helpful
◕ motion cues are very helpful
● motion cues are extremely helpful

THE EFFECTS OF MOTION CUES FOR

$$Y_c = \frac{\omega_n^2 e^{-.1s}}{s(s^2 + 2\xi\omega_n s + \omega_n^2)}$$

Figure 4.14

with very poor pilot opinion ratings, as was stated by Young (reference 28).

However, figures 4.12 through 4.14 also show that motion cues are very helpful to the pilot for vehicle dynamics with very good pilot opinion ratings. In figure 4.13 the best pilot opinion ratings occur for $Y_c = 1/s$, the lowest order vehicle dynamics on the figure. In figures 4.12 and 4.14 the best pilot opinion ratings are for non-oscillatory vehicle dynamics with a fast response time ($1/\zeta\omega_n$ = one time constant). In all cases the vehicle dynamics receiving very good pilot opinion ratings correspond to the stable vehicle dynamics which best pass frequencies above 1 rad/sec. As mentioned earlier, frequencies above 1 rad/sec are the frequencies for which motion cues are the most useful to the human operator, and hence we would expect motion cues to be most helpful to the human operator for vehicle dynamics which best pass these frequencies.

In summary, motion cues are least helpful to the human operator for vehicle dynamics with intermediate pilot opinion ratings. For vehicle dynamics with very poor pilot opinion ratings, which correspond to vehicle dynamics with little or no stability margin, motion cues are helpful to the human operator as they help him maintain stability of the man-vehicle system. For vehicle dynamics with very good pilot opinion ratings, which correspond to vehicle dynamics which most readily pass frequencies above 1 rad/sec, motion cues are helpful to the human operator as they occur at frequencies where they are most readily used by the human operator.

4.4 Variation Of Some Other Experimental Parameters

Figures 4.15 through 4.17 are referred to in the following sections. The data for the human operator's describing function shown on these figures are straight line approximations to the data shown on pages 169 to 230. See Chapter II, section 2.4 for a discussion of the uncertainties and variability of these data.

4.4.1 Subject To Subject And Run To Run Variations

The subject to subject and run to run variations in the data are considered in Chapter II, section 2.4.1.2, page 29, and section 2.4.1.3, page 30. These variations are the most significant sources of error in the experimental measurements.

4.4.2 Control Stick Gain

Figure 4.15 shows the human operator's describing function and the system rISE for $Y_c = e^{-.1s}/s(s+1)$ as the control stick gain, K, is varied. As mentioned in Chapter II, section 2.3.5, K is used as a measure of the control stick gain, and is equal to the maximum voltage available to the human operator from the control stick. The control stick output voltage varied linearly from 0 to $\pm$K volts as the stick was displaced from the centered position to $\pm$30°. From figure 4.15 it can be seen that for very low control stick gain the gain of the human operator's describing function is reduced, and the rISE is increased. The lowest control stick gain for which data were taken was K=3, where K is the maximum control stick output and is just larger than the maximum input level of 2.8. It should be remembered (see

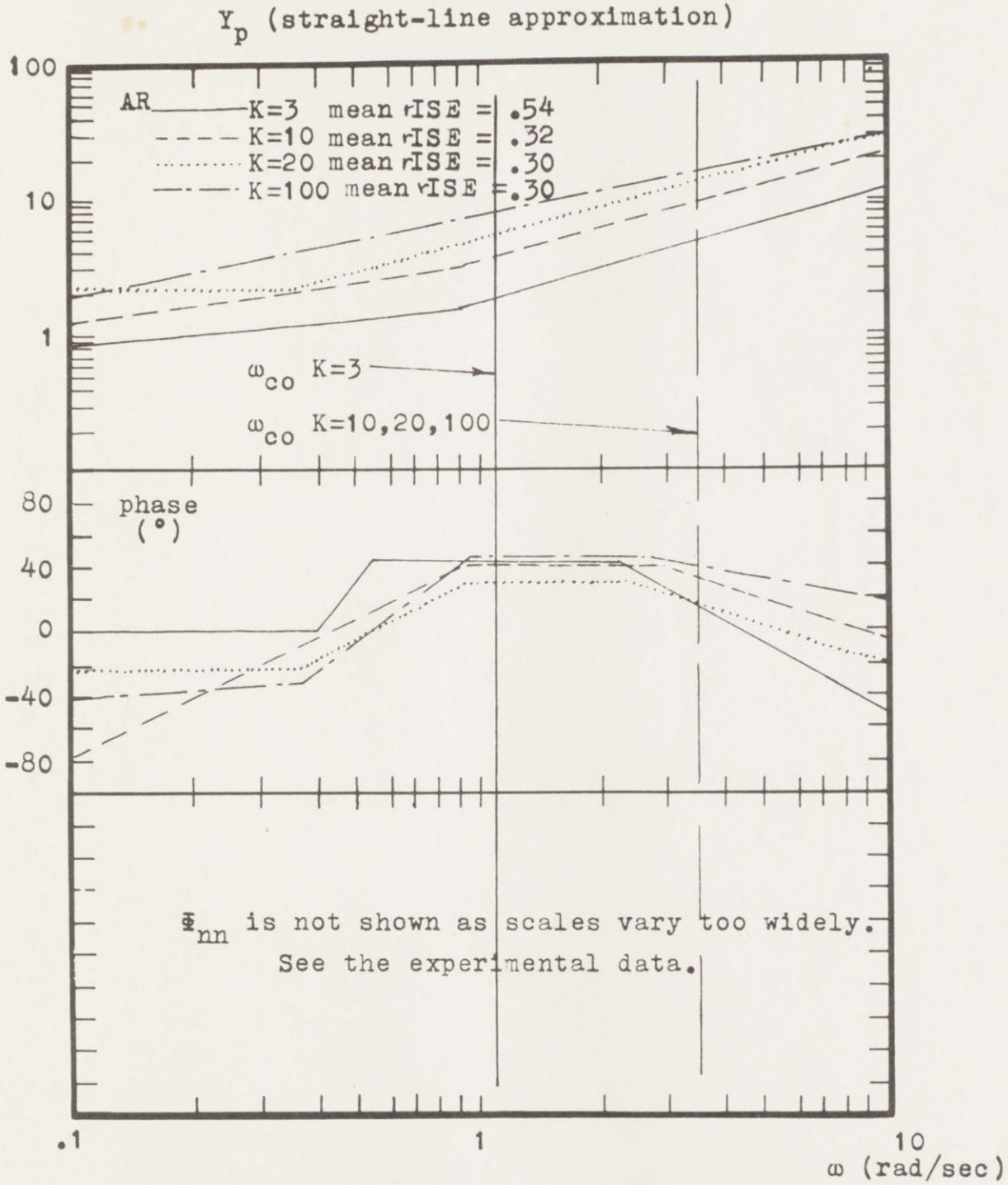

The Effect Of Variation Of The Control Stick Gain On The Human Operator's Describing Function

$$Y_c = \frac{e^{-.1s}}{s(s + 1)}$$

figure 4.15

section 2.3.5 of Chapter II) that the experimental measurements made were of the error voltage and of the control stick output voltage. Except for the lowest value of the control stick gain, as the control stick gain is increased the human operator's describing function shows a slight but consistent increase in gain, while the rISE remains relatively constant. The relatively small changes in the human operator's describing function (about a 50 to 100% maximum increase for a 1000% increase in the control stick gain) show the great adaptability of the human operator, and are consistent with the "indifference threshold" often attributed to the human operator. In other words, within a given range of the control stick gain, the human operator is capable of adjusting his gain so as to keep the system open-loop gain constant.

As the input gain is increased to very high levels, the human operator can easily over-power the vehicle dynamics, obtaining much faster vehicle responses than he can for low values of the control stick gain. In fact, the subjects reported that for high control stick gain they operated in a "bang-bang" control mode, continually making small perturbations of the control stcik from one side of the centered position to the other. Such control behavior led to a continual cycling of the simulator about the vertical position, and to motion cues which contained significant power above 1 rad/sec. As mentioned in section 4.3 of this chapter, motion cues above 1 rad/sec are of greatest use to the human operator. The truth of this is substantiated once more by the data presented in figure 4.11 (page 82), where it can be seen that motion cues proved more helpful to the human operator for high values of the control stick gain, which in turn

lead to higher frequency motion cues.

4.4.3 The Input Gain

The system input is multiplied by a gain, K', which is defined as unity for the system input level used throughout the bulk of the experiment. Figure 4.16 shows the human operator's describing function and the system rISE for $Y_c = e^{-.1s}/s^2$ as K' varies from .5 to 2.0. It can be seen from figure 4.16 that, except for the lowest value of K', there is very little change in the human operator's describing function as the input gain varies, but that the rISE decreases as the input gain increases. Once again the data show the great adaptability of the human operator, as he is able to compensate quite well for the changes in input gain.

4.4.4 The Input Breakpoint

The input breakpoint (see section 2.3.7 of Chapter II) is set at 2.5 rad/sec for the bulk of the experiment. The breakpoint is that frequency above which the amplitudes of the sinusoids comprising the input are reduced by 90% in amplitude. Figure 4.17 shows the human operator's describing function and the system rISE for the vehicle dynamics $Y_c = e^{-.1s}/s^2$ as the input breakpoint is varied from .7 to 5 rad/sec. The variation of the rISE is small over the middle range of the variation of the breakpoint, but the rISE increases markedly at the maximum values of the breakpoint for which data were taken. As the breakpoint frequency increases the human operator's describing function changes in two ways: there is an increase in lead at the higher frequencies, and an increase in gain at the higher frequencies coupled with a decrease

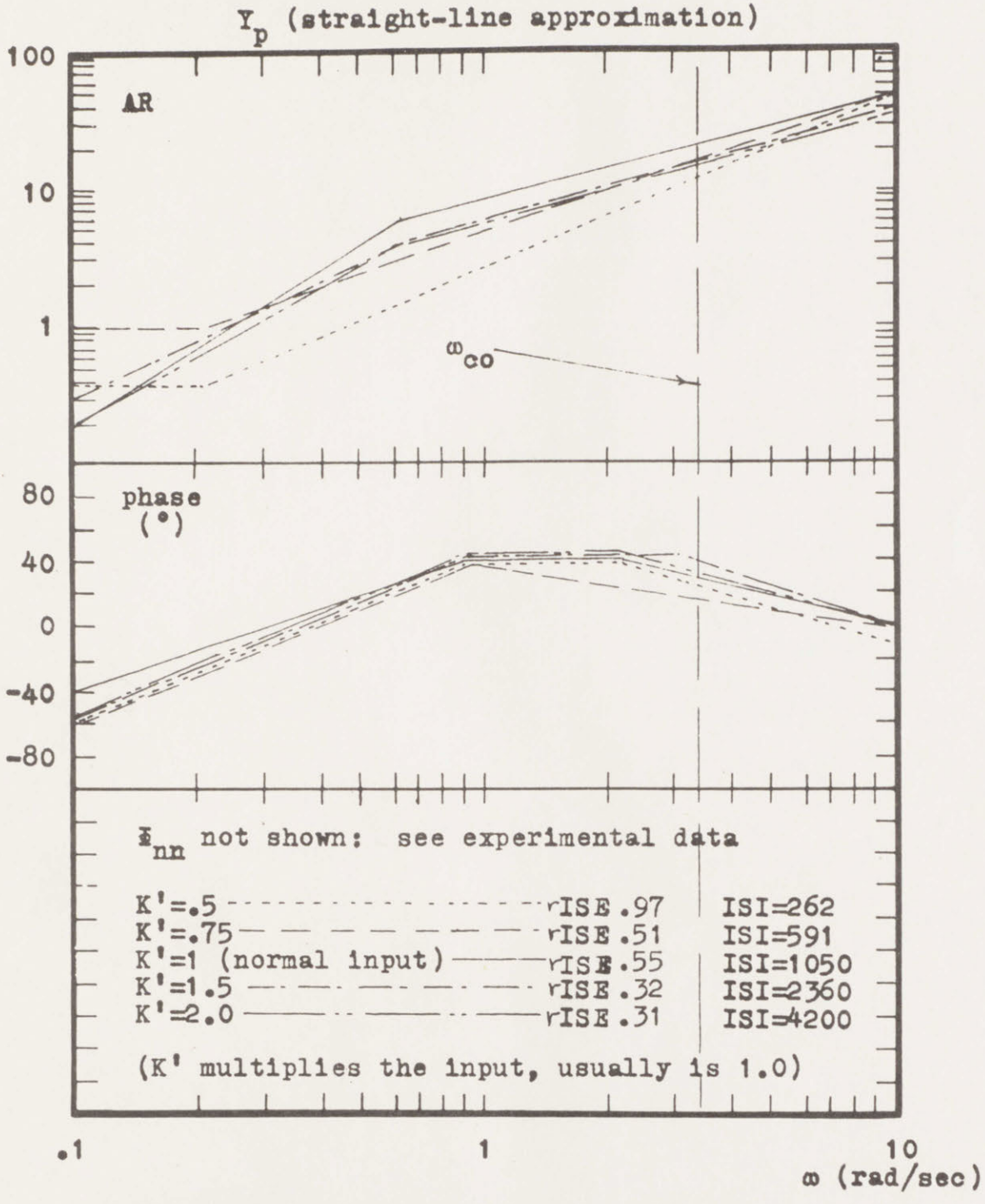

The Effect Of Variation Of The Input Gain On
The Human Operator's Describing Function

$$Y_c = \frac{e^{-.1s}}{s^2}$$

figure
4.16

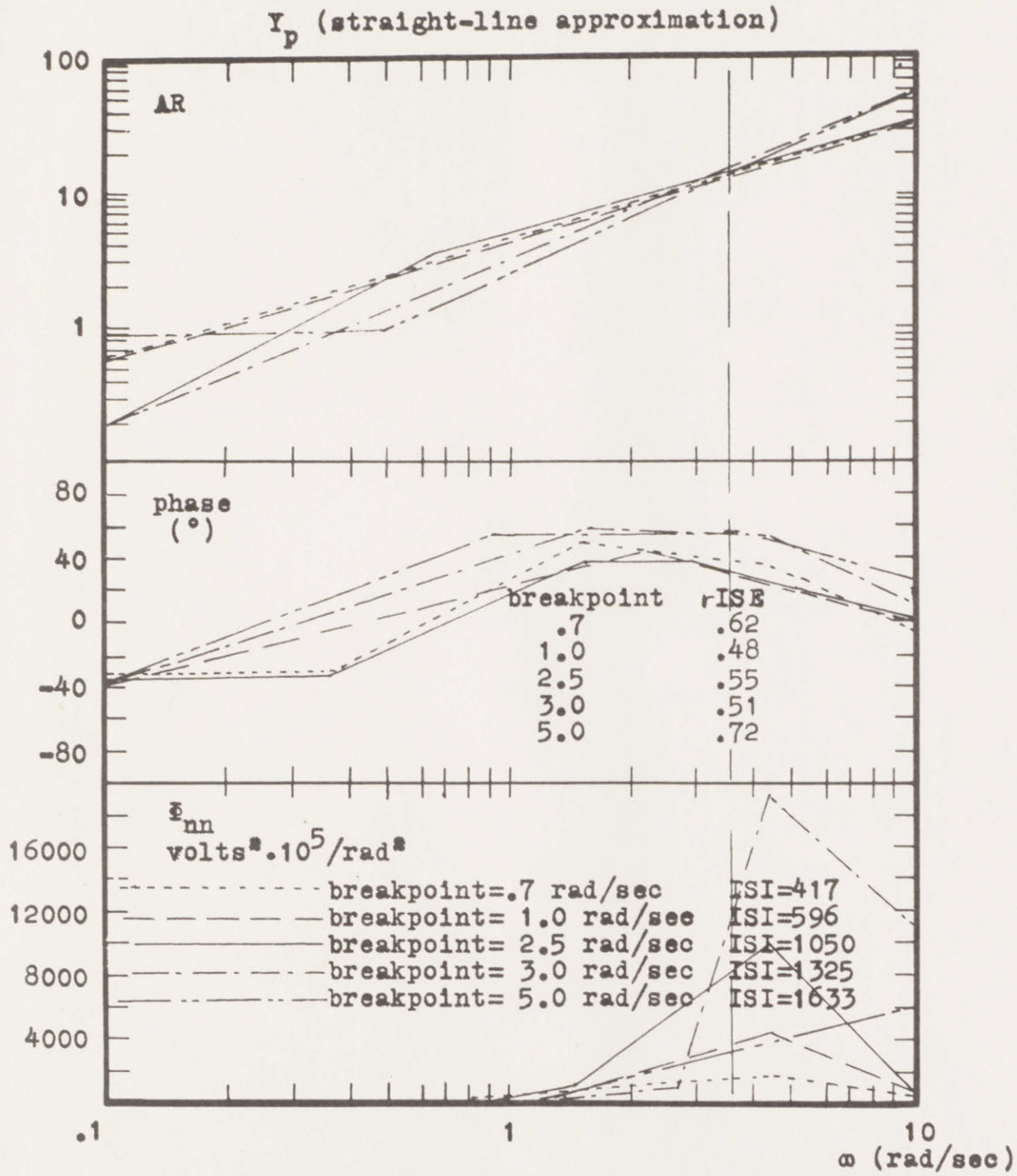

The Effect Of Variation Of The Input Breakpoint On The Human Operator's Describing Function

$$Y_c = \frac{e^{-.1s}}{s^2}$$

figure 4.17

in gain at the lower frequencies.

4.5 Where The Effects Of Roll Angular Motion Cues Are Known

For vehicle dynamics of the types

eq. 4.1) $$Y_c(s) = \frac{\omega_n^2 e^{-.15}}{s^2 + 2\zeta\omega_n s + \omega_n^2}$$, $2\zeta\omega_n$ and ω_n^2 vary

eq. 4.2) $$Y_c(s) = \frac{K e^{-.15}}{s(\tau s + 1)}$$, K and $1/\tau$ vary

eq. 4.3) $$Y_c(s) = \frac{\omega_n^2 e^{-.15}}{s(s^2 + 2\zeta\omega_n s + \omega_n^2)}$$, $2\zeta\omega_n$ and ω_n^2 vary

the effects of roll motion cues on the human operator's describing function were measured by the experiment for this thesis, and the human operator's describing functions for these dynamics are presented on pages 162 to 232. Furthermore, from these data it is possible to predict results for vehicle dynamics of the types

eq. 4.6) $$Y_c(s) = \frac{\omega_n^2(1 + Cs) e^{-.15}}{s(s^2 + 2\zeta\omega_n s + \omega_n^2)}$$

eq. 4.7) $$Y_c(s) = \frac{K(1 + Cs) e^{-.15}}{s^2}$$

To show this we will consider the example

$$Y_c(s) = \frac{K(1 + Cs)e^{-.15}}{s^2} = \frac{Ke^{-.15}}{s^2} + \frac{KCe^{-.15}}{s}$$

These vehicle dynamics will approximate K/s^2 for small values of C, and they will approximate K/s for very large values of C. As C varies from 0 to ∞, and thus as Y_c varies from K/s^2 to K/s, it would be expected that the human operator's describing function would vary from that for $Y_c = K/s^2$ to that for $Y_c = K/s$. Thus, the human operator's describing function for the vehicle dynamics

$$Y_c(s) = \frac{(1 + Cs)e^{-.15}}{s^2}$$

should be obtained by interpolating between the results for the human operator's describing functions for $Y_c = K/s^2$ and $Y_c = K/s$. Similarly the human operator's describing function for the vehicle dynamics

$$Y_c(s) = \frac{\omega_n^2(1 + Cs)\ e^{-.15}}{s(s^2 + 2\zeta\omega_n s + \omega_n^2)}$$

should be obtained by interpolating between the results for the human operator's describing function for

$$Y_c(s) = \frac{\omega_n^2\ e^{-.15}}{s(s^2 + 2\zeta\omega_n s + \omega_n^2)}$$

and the human operator's describing function for

$$Y_c(s) = \frac{\omega_n^2\ e^{-.15}}{s^2 + 2\zeta\omega_n s + \omega_n^2}$$

4.6 The Beginning Of A Physiological Model For The Human Operator's Use Of Motion Cues

It is not the purpose of this thesis to develop a

physiologically based model of the human operator controlling a vehicle with or without motion cues. It is appropriate, however, to mention something of what is known along these lines. Figures 4.18 and 4.19 show the possible development of such a model. Visual and vestibular paths are shown in these figures as they were of interest in the experiment for this thesis. Other non-visual paths, such as tactile or auditory paths, may also be included in a similar manner if desired.

The most recent model for the human operator's describing function while the human operator is using visual cues only is given by McRuer, et al. (reference 16), as

$$Y_p(s) = \frac{Ke^{-\tau_1 s}(\tau_1 s + 1)(\tau_2 s + 1)}{(\tau_3 s + 1)(\tau_4 s + 1)} Y_{musc}(s)$$

where the neuro-muscular dynamics, $Y_{musc}(s)$, are most commonly taken as

$$Y_{musc}(s) = \frac{1}{(\tau_N s + 1)}$$

but can be taken as the more precise form

$$Y_{musc}(s) = \frac{\omega_{Nn}^2}{(\tau_N s + 1)(s^2 + 2\zeta_N \omega_{Nn} s + \omega_{Nn}^2)}$$

All three loops (visual, otolith, and semicircular canal) must pass through the muscular dynamics. However, there is no reason to assume that the human operator processes all three loops in the same manner, and hence a different compensation network must be placed in each loop, the form of the compensation network

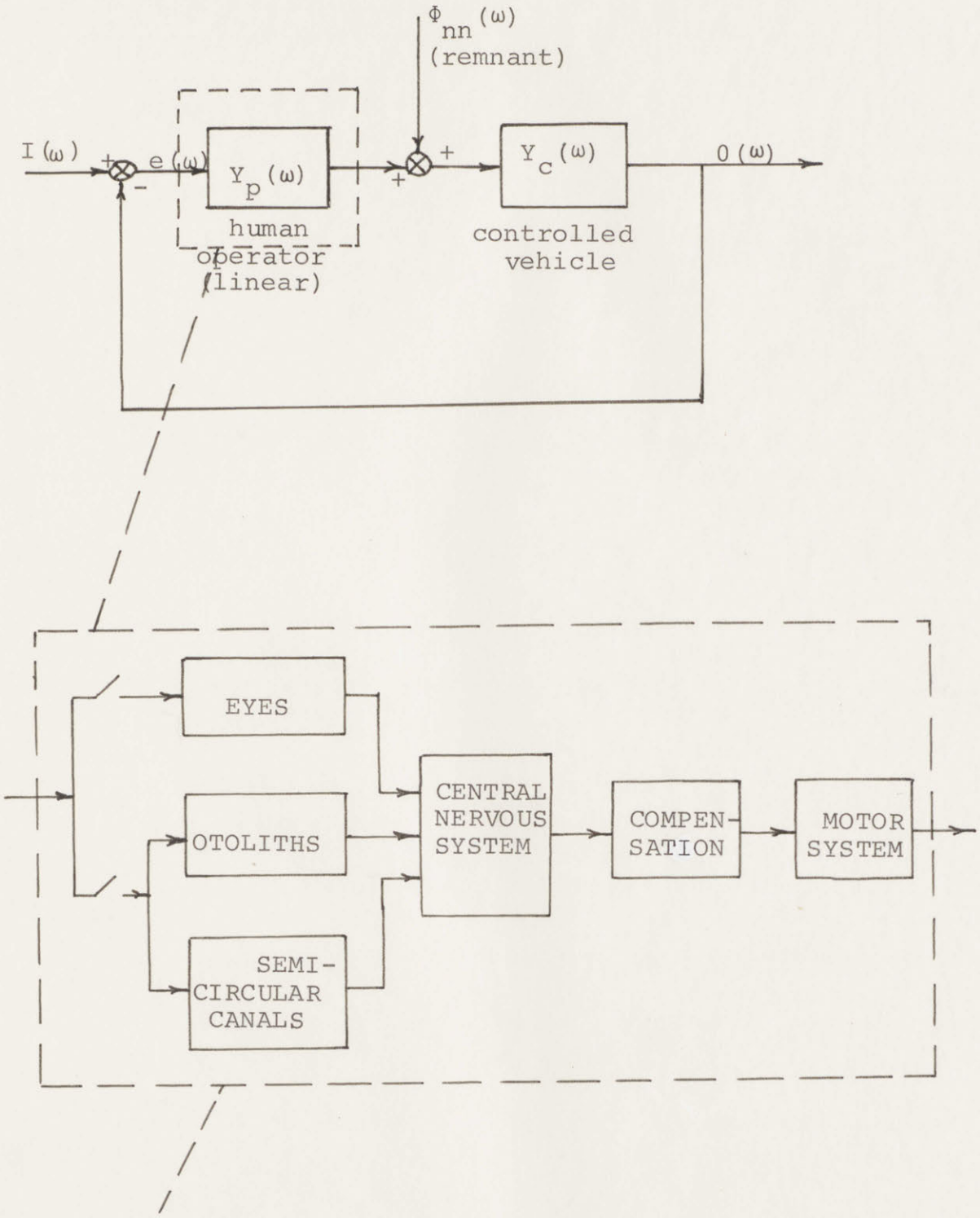

DEVELOPMENT OF A PHYSIOLOGICAL MODEL OF THE HUMAN OPERATOR'S USE OF MOTION CUES IN MAN-VEHICLE CONTROL: PART A

Figure 4.18

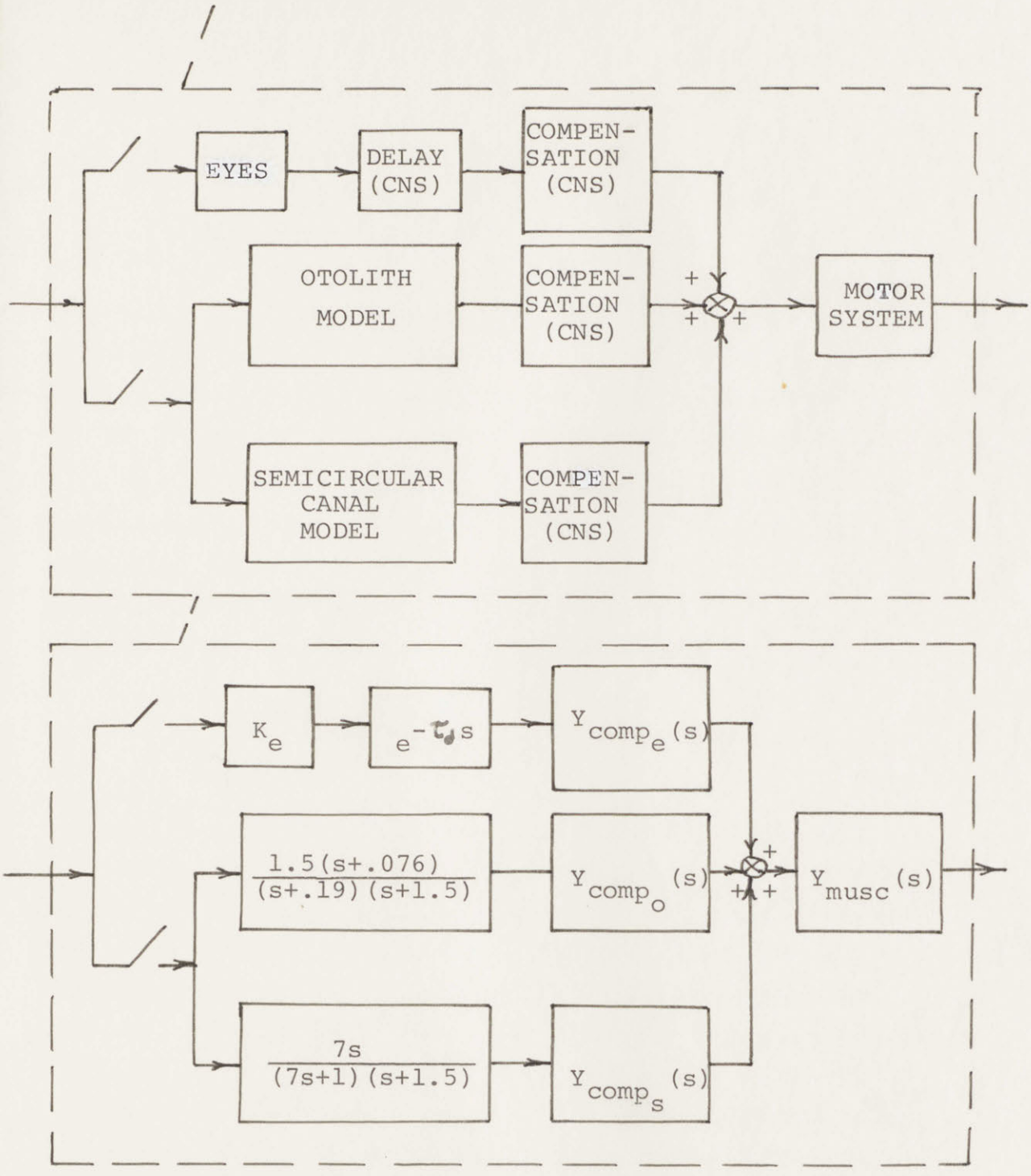

DEVELOPMENT OF A PHYSIOLOGICAL MODEL OF THE HUMAN OPERATOR'S USE OF MOTION CUES IN MAN-VEHICLE CONTROL: PART B

Figure 4.19

most generally applicable being

$$Y_{comp}(s) = \frac{K(\tau_1 s + 1)(\tau_2 s + 1)}{(\tau_3 s + 1)(\tau_4 s + 1)}$$

The delay term of the model for the human operator's describing function, given by $e^{-\tau_e s}$, is placed only in the visual loop, as it must be treated separately in the motion-sensing loops, as is discussed on page 100.

The two motion sensors of most importance to the human operator are the semicircular canals and the otoliths. The most recent model for the semicircular canals, relating sensed angular position to actual angular position, is given by Meiry (reference 17) as

$$\frac{\Theta(s)_{sensed}}{\Theta(s)_{actual}} = \frac{7s}{(7s + 1)(.1s + 1)}$$

It must be realized that strictly speaking this model cannot measure angular position. The lead term at the origin shows that, (over the frequency range of interest) the human senses angular velocity, and cannot sense a steady-state angular position, with his semicircular canals. Thus, unless the human operator has some source of information about his angular position, he cannot use his semicircular canals to control his angular position. Of course, the rate information he receives from his semicircular canals is very useful to him in controlling his angular position.

The most recent model for the otoliths, relating sensed angular position to actual angular position in relation to a gravity vector, is given by Young and Meiry (reference 29) as

$$\frac{\theta(s)_{\text{sensed}}}{\theta(s)_{\text{actual}}} = \frac{1.5(s + .076)}{(s + .19)(s + 1.5)}$$

Both the model for the otoliths and the model for the semicircular canals are valid over the frequency range of interest,.1 to 10 rad/sec. The models were determined primarily through eye movement measurements, but also from various subjective responses. Both these measures of the human operator's vestibular dynamics include the delay associated with the human's central nervous system, and hence the delay is already included in the models of the vestibular apparatus. That is why, in figures 4.18 and 4.19, the dead-time delay normally associated with the human operator's describing function, and present in the visual loop, is not placed in the motion-sensing loops.

CHAPTER V: CONCLUSIONS AND SUGGESTIONS FOR FURTHER WORK

5.1 The Conclusions Of The Thesis

The purpose of this thesis was to investigate the human operator's use of roll motion cues in man-vehicle control. Extensive data were taken of the human operator's describing function while he was controlling a wide range of vehicle dynamics with visual cues only, motion cues only, and simultaneous visual and motion cues. The data are presented on pages 171 to 232, and the experiment is outlined and described in detail in Chapter II. The data permit analysis to determine how the human operator modifies his control behavior when roll motion cues are added to visual cues. The data fill a void in the present knowledge of the human operator's performance, for there have been very little data taken on the human operator's describing function while the human operator is experiencing motion cues. The data may be used, under certain conditions, to predict actual flight or moving-base data for the human operator's describing function from fixed-base data for the human operator's describing function.

By examination of the data it was determined that the human operator uses roll motion cues to generate additional lead at high frequencies. The additional lead permits the human operator to increase his gain, and hence his cross-over frequency[1], without a loss in phase margin.

1) cross-over frequency: the frequency at which the open loop gain (the magnitude of the product of the vehicle dynamics and the human operator's describing function) crosses from greater than unity to less than unity.

Examination of the system integral squared errors for cases where the human operator receives visual cues only, motion cues only, and simultaneous visual and motion cues, permits determination of what vehicle dynamics permit the human operator to make the most use of roll motion cues. The human operator can make a greater percentage improvement in the system integral squared error, upon the introduction of roll motion cues, for vehicle dynamics which most readily respond to inputs above 1 rad/sec. Such vehicle dynamics include lower order dynamics. For example, the human operator can make greater use of roll motion cues for the vehicle dynamics $Y_c = 1/s$ than for $Y_c = 1/s^2$, for the vehicle dynamics

$$Y_c(s) = \frac{2}{s(s + 2)}$$

than for

$$Y_c(s) = \frac{2}{s^2(s + 2)}$$

and for the vehicle dynamics

$$Y_c(s) = \frac{\omega_n^2}{s^2 + 2\zeta\omega_n s + \omega_n^2}$$

than for

$$Y_c(s) = \frac{\omega_n^2}{s(s^2 + 2\zeta\omega_n s + \omega_n^2)}$$

It is also found that high control stick gains lead to more rapid vehicular responses and higher frequency motion cues, and hence motion cues are also very helpful to the human operator for vehicle dynamics with an

associated high control stick gain. Finally, it is noted that the human operator can take greater advantage of motion cues for vehicle dynamics which are unstable or marginally stable.

In the process of obtaining the data for the human operator's describing function, the effect of the remnant on the experimental measurements was considered. In Chapter III an expression which permits corrections of the data for the remnant is derived. When the corrections are applied to the data they are found to be small in relation to other experimental errors.

5.2 Suggestions For Further Work

At the end of Chapter IV, in section 4.6, the start of a physiologically based model of the human operator controlling a vehicle under the influence of both visual and motion cues was suggested. The development and completion of the model would be very useful to those involved with man-vehicle control.

The experiments of this thesis involved only roll angular motion cues, which can be extended to include pitch angular motion cues. It is recommended that further work be done with yaw angular motion cues, and also with linear accelerations, thus including all six degrees of freedom of motion.

The experiments of this thesis did not include vehicle dynamics with a lead term in the numerator, although a way of predicting results for certain such dynamics was suggested in Chapter IV, section 4.4. It is recommended that some data be taken to test these predictions, and to obtain data for vehicle dynamics [illegible]

with lead terms in the numerator which cannot be predicted from the data taken for this thesis.

It is further recommended that data be taken for vehicle dynamics for which the simulator used for the experiment for this thesis was incapable of providing the necessary angular accelerations. In particular, data should be taken for the human operator's describing function with and without roll motion cues for the vehicle dynamics $Y_c(s) = K/(s+a)$ as a varies from 0 to ∞, and thus as Y_c varies from K/s to 1. Of particular interest is information to show whether or not the human operator can continue to make still greater use of roll motion cues as the vehicle dynamics are reduced in order from 1/s to 1.

APPENDIX A: THE HYBRID COMPUTER

A.1) Introduction

The hybrid computer used for the experiment is the 290-T model built by GPS Instrument Co., composed of a PDP-8 digital computer, the GPS 200-T analog computer, some digital logic circuits, and the hybrid facilities permitting communication between the analog and digital computers.

A.2) The Digital Computer

The PDP-8 computer, made by Digital Electronics Corp., is a single address, fixed word length, 12-bit, 2's complement arithmetic computer with a cycle time of 1½ micro-seconds, an add time of 2 micro-seconds, and having an extended arithmetic element permitting 21 micro-second multiplication time and 37 micro-second division time. It also includes a very flexible input-output facility with interrupt capability. It has a 4096-word memory.

The Dectape (magnetic tape) system included with the digital computer permits addressable blocks of 128 words to be redd from tape into core, or vice-versa, operating by cycle-stealing (permitting data-transfer without interrupting the program in progress).

A.3) The Analog Computer.

The analog computer contains integrators, amplifiers, potentiometers, comparators, multipliers, electronic switches, limiters, and a digital voltmeter. Of interest is the fact that the amplifiers and integrators have a one megacycle response at the 3db level with a 200 ohm load at full amplitude (±10 volts), and the multi-

pliers have an 800KC response at the 3db level, thus making the analog computer compatible in frequency response with the digital computer's 1½ microsecond cycle time.

The digital logic supplied with the analog computer includes NAND gates, flip-flops, inverters, NOR gates, Schmitt triggers, and pulse delays. In addition, each integrator may be separately connected to a rate 1, 10, 100, or 1000 volts/sec, and may also be logically controlled as to mode, rather than necessarily having to follow the mode register.

A.4) The Hybrid Components

There are seven channels whereby, upon command from the digital or analog computer (as programmed), data may be converted or transferred from the digital to the analog computer. Similarly, there are eight channels, selected one at a time by a multiplexer, by which information is transferred on command from the analog to the digital computer. There are also control lines by which the digital computer can send pulses to the analog computer, and sense lines, by which the analog computer can send pulses to the digital computer.

Finally, there is the program interrupt, by which the program may be interrupted for any purpose, either at periodic times (using the analog clock) or when certain criteria are met (such as the digital computer has finished program A, or as voltage A exceeds voltage B, etc.).

APPENDIX B: THE EFFECTS OF THE .1-SECOND DELAY ON THE HUMAN OPERATOR'S DESCRIBING FUNCTION

B.1) Examination Of The Data

Figures B.1 through B.3 show the human operator's describing function for the vehicle dynamics Y_c=1, 1/s, and $1/s^2$ both with and without the .1-second delay ($e^{-.1s}$). For figure B.1 through B.3 the human operator receives visual cues only. See Chapter II section 2.3.4 for details of why the delay is in the motion and visual loops of the control system studied in this thesis. In looking for the effects of the delay on the human operator's describing function the three dynamics given above were chosen as they require three widely different modes of control behavior on the part of the human operator. Together, they are representative of most of the vehicle dynamics studied in the thesis.

From figures B.1 through B.3 the manner in which the human operator modifies his describing function when the .1-second delay is inserted in the visual loop can be seen to be fairly consistent.

A. Phase of the describing function
   1. Below the cross-over frequency: sufficient lead is generated to compensate for the delay (i.e. an extra $j\omega/10$ rad/sec).
   2. Above the cross-over frequency: some additional lead is generated, but far less than is needed to compensate for the delay. Roughly speaking, the phase above the cross-over frequency does not change when the delay is inserted into the visual loop.

B. Magnitude of the describing function
   1. Below the cross-over frequency: the delay is compensated for by a reduction of the amplitude ratio by about 75% of the amplitude

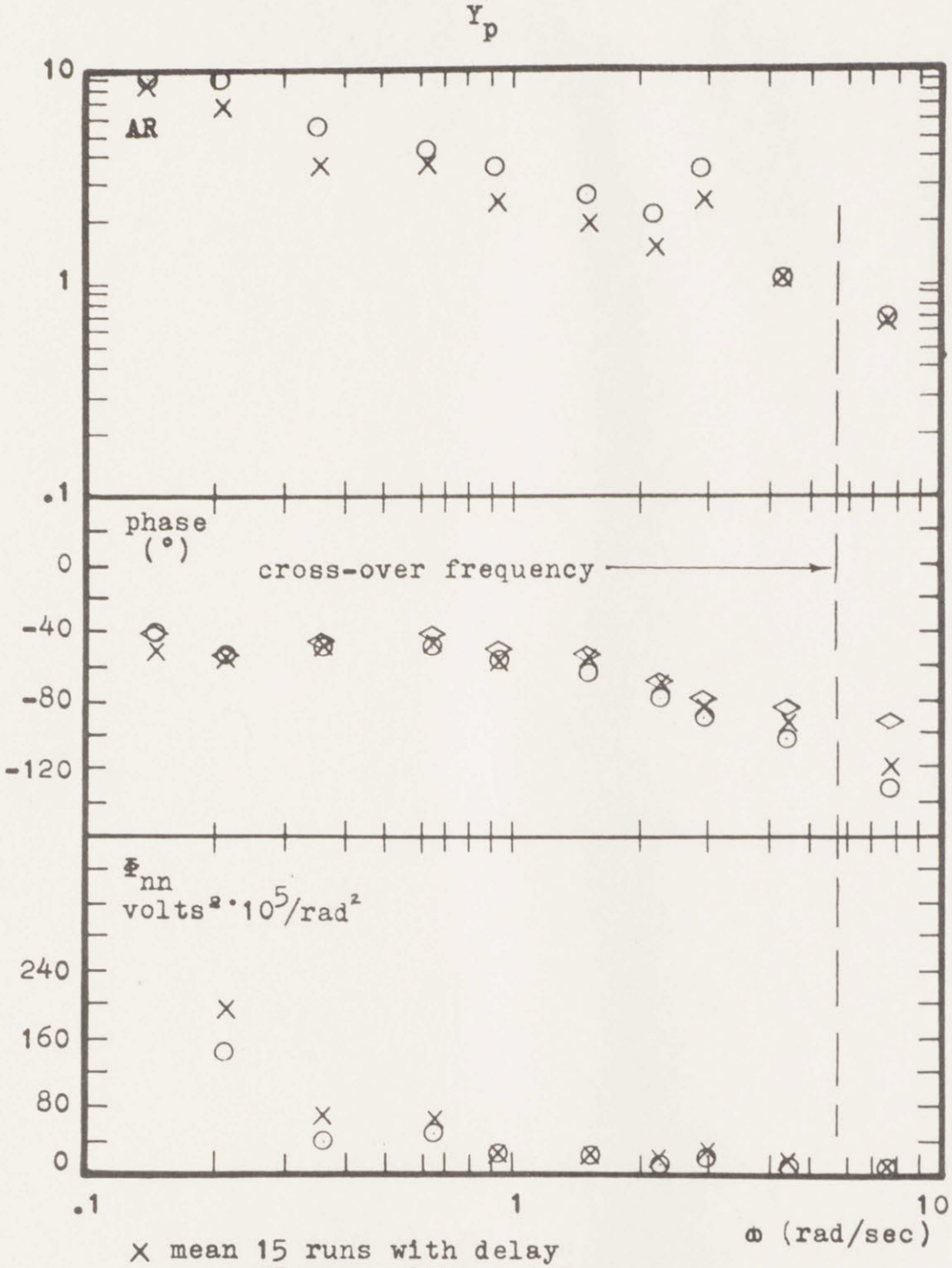

THE EFFECTS OF THE .1-SECOND DELAY FOR

$Y_c = 1$

figure
B.1

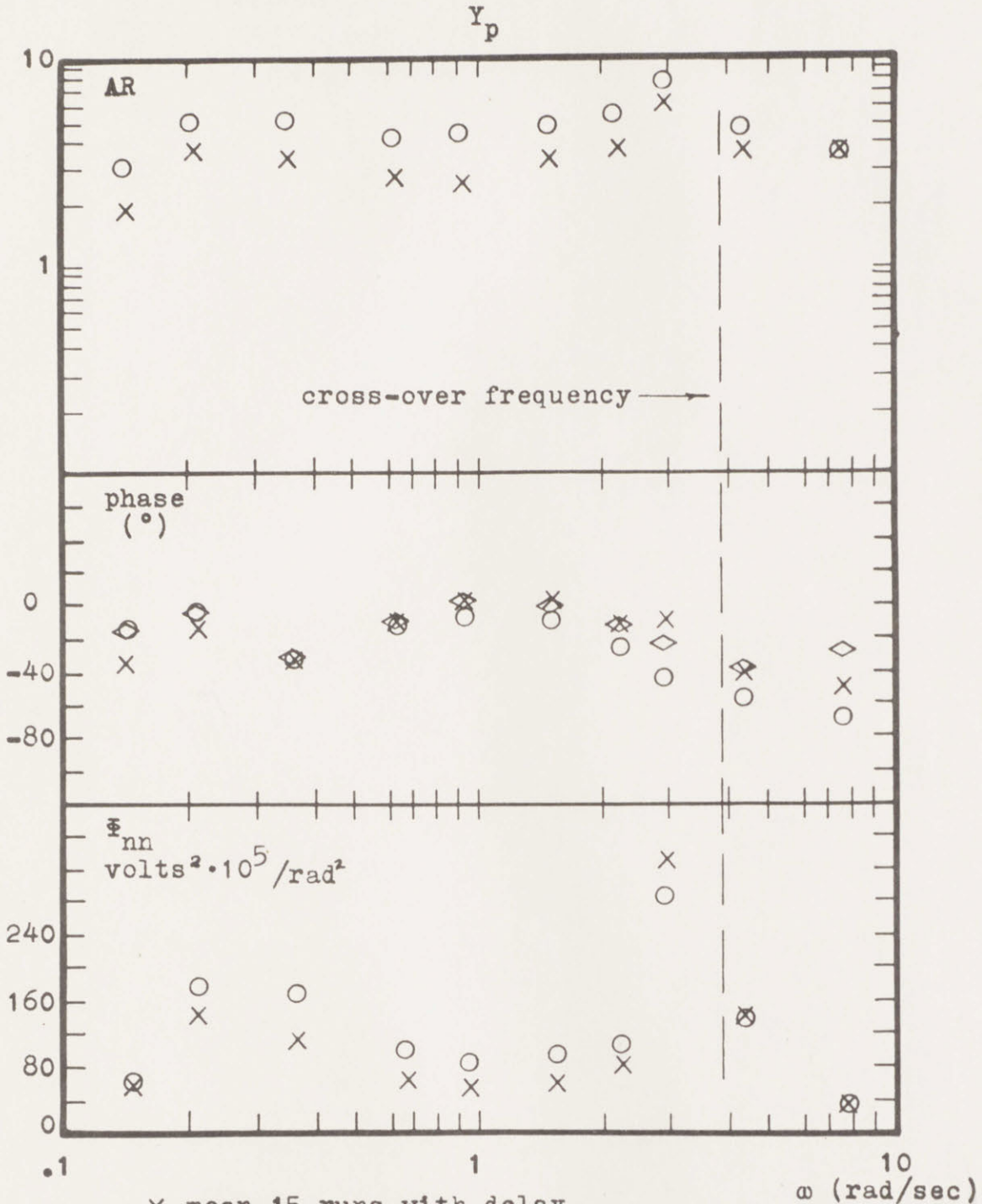

× mean 15 runs with delay
○ mean 15 runs without delay
◇ phase Y_p (without delay) $+j\omega/10$

THE EFFECTS OF THE .1-SECOND DELAY FOR

$Y_c = 1/s$

figure
B.2

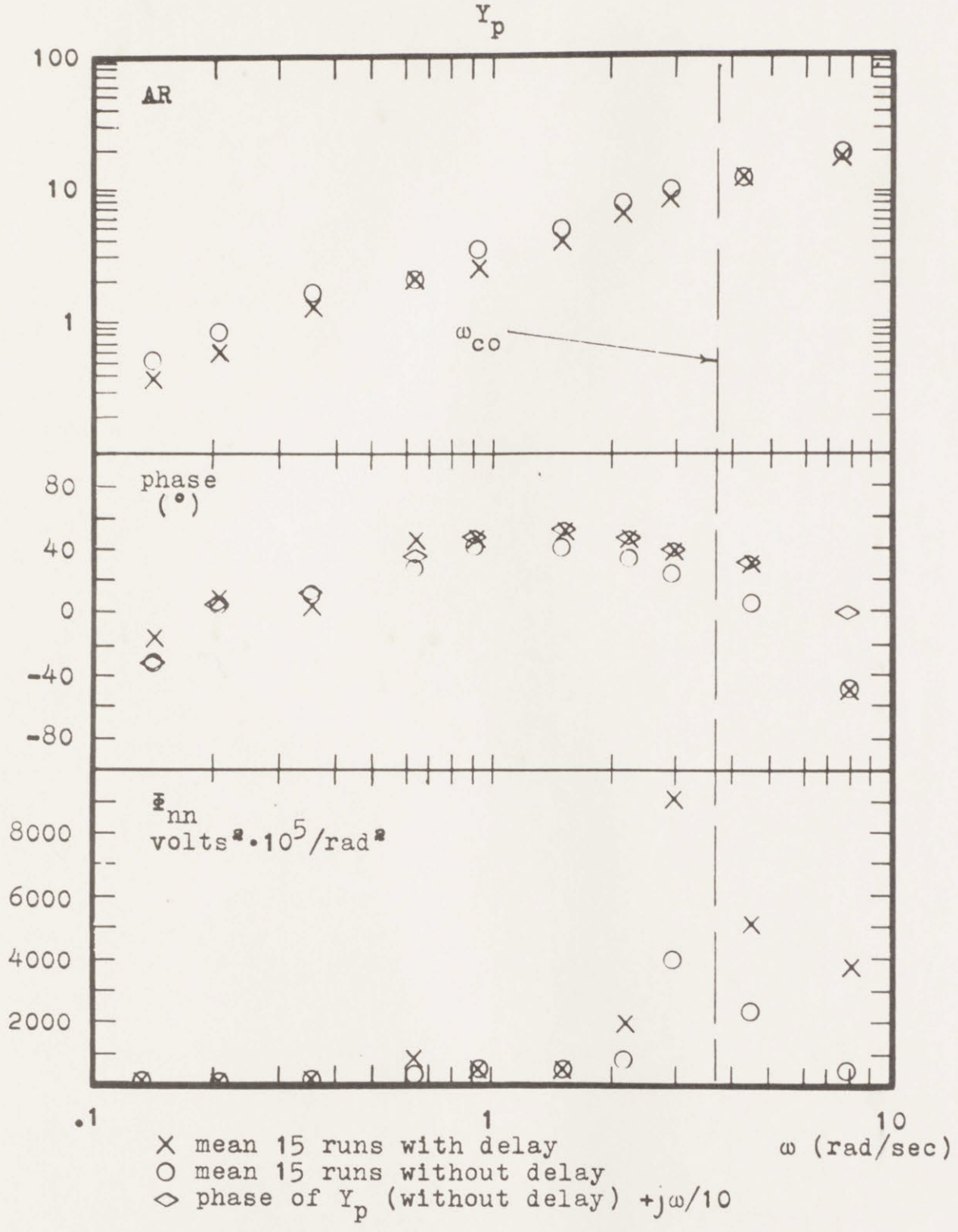

THE EFFECTS OF THE .1-SECOND DELAY

FOR $Y_c = 1/s^2$

figure
B.3

ratio without the delay.

2. Above the cross-over frequency: there is no significant change in the amplitude ratio of the human operator's describing function upon the introduction of the .1-second delay into the loop.

C. Remnant.

1. At and above the cross-over frequency: near or above the cross-over frequency, or at any critical frequency (such as at a resonant frequency of the vehical dynamics), the introduction of the .1-second delay into the loop consistantly causes an increase in the remnant, the size of the increase ranging from 10 to 150%.

2. Below the cross-over frequency: except for areas where the remnant levels are low (below 1×10^{-2} volts^2/rad^2), there is little change in the remnant when the .1-second delay is inserted into the loop. At the low remnant levels the remnant varies up to 50% in either direction.

B.2) How To Correct The Experimental Data For The Effects Of The Delay.

For reasons explained in Chapter II, section 2.3.4, all the data taken for this thesis include a .1-second delay ($e^{-.1s}$) in the loop. To obtain the approximate describing functions which would have been obtained without the delay we can use the results of section B.1 of this appendix. Thus, to approximately correct the data

of this thesis for the effects of the .1-second delay the following rules can be applied.

A. Above the cross-over frequency.

1) The magnitude and phase of the human operator's describing function remain unchanged.

2) The remnant should be decreased 50%.

B. Below the cross-over frequency.

1) The magnitude (amplitude ratio) of the human operator's describing function should be increased 33%.

2) The phase of the human operator's describing function should be decreased (i.e., lag introduced) by $j\omega/10$ rad/sec.

3) The remnant remains unchanged.

APPENDIX C: THE MEASUREMENT BANDWIDTH

The measurements made by the programs and represented by equations 2.1 through 2.6 of section 2.3.9 of Chapter II are of the form

$$\text{eq. C.1)}\quad X_k = \left[\left(\sum_{n=1}^{896} x(n\Delta t)\sin(n\Delta t\omega_k)\right)^2 + \left(\sum_{n=1}^{896} x(n\,t)\cos(n\,t\omega_k)\right)^2\right]^{\frac{1}{2}}$$

If $x(t)$ were of the form $A_k \sin\omega_k t$, where 89.6 is an even multiple of $2\pi/\omega_k$, the results of eq. C.1 are $X=k_p A_k$, where $k_p=44.75$. If, however, $x(t)$ were of the form

$$\text{eq. C.2)}\quad x(t) = A_k \sin(\omega_k + \Delta\omega_k)t$$

where ω_k is small, what would eq. C.1 yield? In other words, what is the bandwidth of eq. C.1?

The frequency range of interest is .1 to 10 rad/sec. Within this range and for the run time od 89.6 seconds, equation C.1 is very nearly equal to

$$\text{eq. C.3)}\quad X_k = \left[\left(\int_0^{89.6} x(t)\sin(\omega_k t)dt\right)^2 + \left(\int_0^{89.6} x(t)\cos(\omega_k t)dt\right)^2\right]^{\frac{1}{2}}$$

Substituting equation C.2 for $x(t)$ in equation C.3, and assuming $A_k = 1$,

$$\text{eq. C.4)}\quad X_k = \left[\left(\int_0^{89.6} \sin(\omega_k+\omega_k)t\,\sin(\omega_k t)dt\right)^2 + \left(\int_0^{89.6} \sin(\omega_k+\omega_k)t\,\cos(\omega_k t)dt\right)^2\right]^{\frac{1}{2}}$$

Evaluation of the integrals in equation C.4 gives

$$\text{eq. C.5)} \quad X_k = \left[\left(\frac{\sin(89.6\Delta\omega_k)}{2\Delta\omega_k} - \frac{\sin(89.6(2\omega_k+\Delta\omega_k))}{2(2\omega_k+\Delta\omega_k)}\right)^2 + \left(\frac{1}{2\Delta\omega_k} + \frac{1}{2(2\omega_k+\Delta\omega_k)} - \frac{\cos(89.6\Delta\omega_k)}{2\Delta\omega_k} - \frac{\cos(89.6(2\omega_k+\Delta\omega_k))}{292\omega_k+\Delta\omega_k)}\right)^2\right]^{\frac{1}{2}}$$

Equation C.5, when evaluated at each ω_k of interest as a function of ω_k gives the shape of the filter represented by equation C.1.

Figure C.1 shows the actual shape of the filters for ω_k equal to 7.66 rad/sec and .14 rad/sec. As can be seen the difference between the two is very slight, and the dependence upon ω_k may be neglected. Furthermore, since the filter goes to zero at each of the input frequencies, a fairly good approximation to the filter for the purposes of measuring the remnant and the human operator's describing function is the bandpass of .14 rad/sec shown in figure C.1.

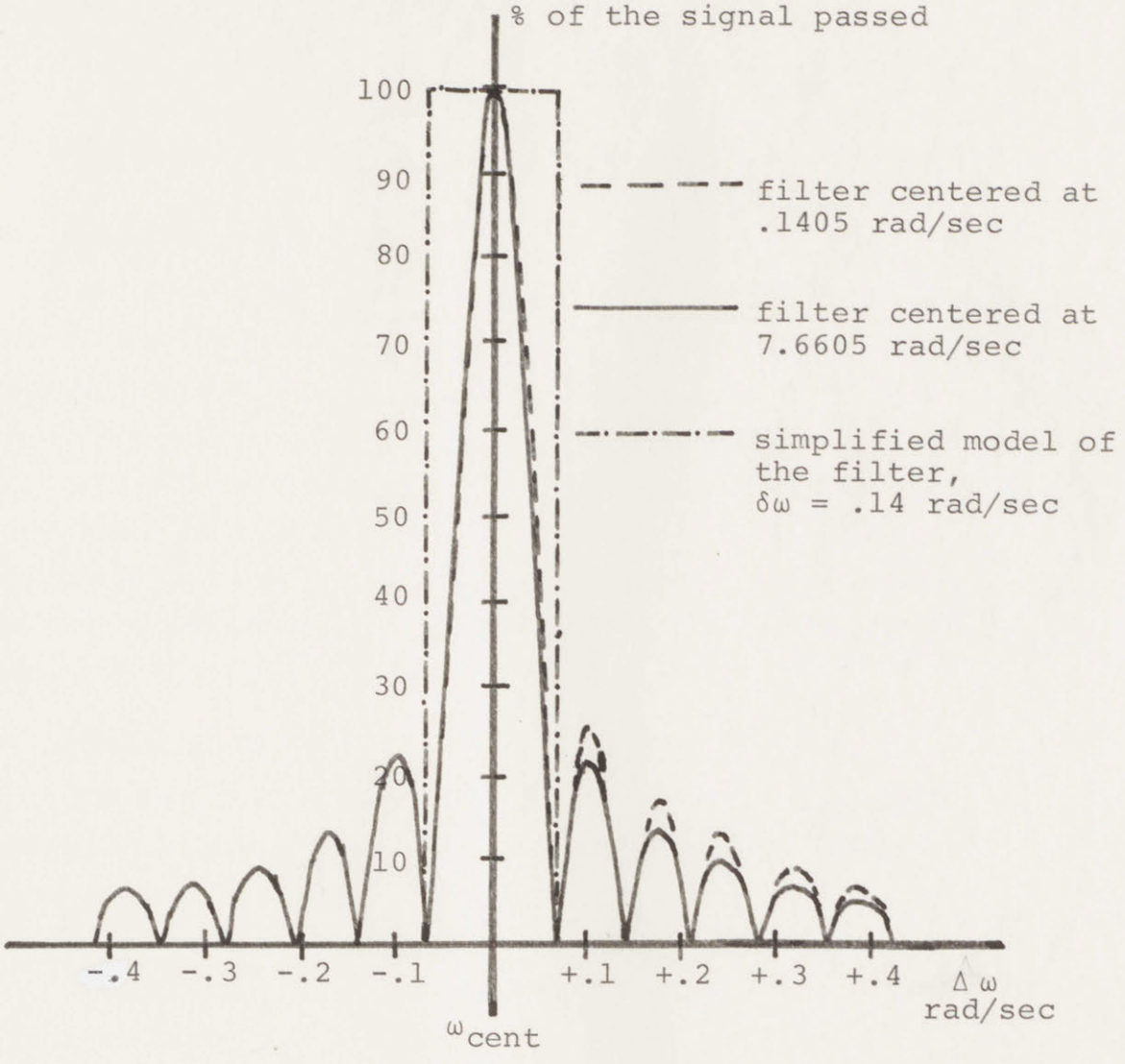

THE CURVE REPRESENTED BY EQUATION C.5: THE EFFECTIVE BANDWIDTH FOR MEASURING THE HUMAN OPERATOR'S DESCRIBING FUNCTION AND REMNANT

Figure C.1

APPENDIX D: THE HYBRID COMPUTER PROGRAMS

D.1 Introduction

The experiment for this thesis is described in detail in Chapter II. As mentioned in Chapter II, the hybrid computer described in Appendix A is used for the experiment. At the end of this appendix the actual computer programs used are listed. The programming language used is PAL (program assembly language), designed for the PDP-8 digital computer described in Appendix A. The following sections state briefly what each program does.

D.2 Run Routine

The run routine is the program which runs the experiment during the period of data-taking. The program does the following:

1) it reads the system input from magnetic tape and feeds it to the analog computer every .02 seconds,
2) after the 25 second delay it takes data at the input and output of the human operator every .1 seconds, and
3) it controls and records the measurement of the system integral squared error.

D.3 Conversion Routine

The conversion routine is used to move the data around in core and to move the various programs from tape to core and vice versa. Such manipulations are necessary because of the small core size of the PDP-8 computer.

D.4 F-C Routine

The F-C routine calculates the Fourier coefficients of the human operator's input and output at the ten frequencies of the system input (see Chapter II, section 2.3.9). It also calculates the Fourier coefficients of the human operator's output at ten frequencies between the input frequencies.

D.5 DFO And EO Routines

The DFO and EO routines calculate the human operator's describing function and remnant from the Fourier coefficients of his input and output, and then type the results out at each of the ten input frequencies.

D.6 Input Routine, SINCOS1, and SINCOS2

These programs calculate and store on magnetic tape the system input used by the run routine, and the sines and cosines used by the F-C routine (see Chapter II, section 2.3.9).

APPENDIX E: THE COMPUTER PROGRAM LISTINGS

The hybrid computer program listings are given on the following pages. The machine language used is PAL (Program Assembly Language) developed for the PDP-8 digital computer.

```
                    /RUN ROUTINE
                    /ERROR DATA GOES 2400-4177
                    /USES DECTP1
                    /INPUT DATA GOES 5000-6777
                    /INCLUDES TENTH SECOND DELAY
                    *1
0001   5402   JMP I .+1
0002   0130   INT
0003   4206   R128, 4206
0004   4200   W128, 4200
0005   0145   SCAT
0006   4341   ERCM, 4341
                    *20
0020   7402   ERROR, HLT
0021   5153   JMP START
0022   0000   SAVAC1, 0
0023   0000   SAVAC2, 0
0024   0000   SAVLK1, 0
0025   0000   SAVLK2, 0
0026   0000   SRET2, 0
0027   7776   M2, 7776
0030   7773   M5, 7773
0031   7766   M10, 7766
0032   7754   M20, 7754
0033   0130   INT1, INT
0034   0247   INT2, INTR
0035   6200   SEVPAG, 6200
0036   7000   FORPAG, 7000
0037   7354   HELDVL, 7354
                    *62
0062   0000   CNTR1, 0
0063   0000   CNTR2, 0
0064   0000   CNTR3, 0
0065   0000   CNTR4, 0
0066   0000   CNTR5, 0
0067   4777   INPGET, 4777
0070   2377   EDAT, 2377
0071   0577   HODAT, 577
0072   6000   LOC1, 6000
0073   5000   LOC2, 5000
0074   1072   RESET1, TAD LOC1
IR  0355  AT  0075
0075   5355   RESET2, JMP DOT
0076   2066   RESET3, ISZ CNTR5
0077   0105   TAPE0, 105
0100   0004   FOUR, 4
```

```
0101  0002  TWO, 2
0102  0003  THREE, 3
0103  0000  ERRSQ, 0
0104  0000  CONVRT, 0
0105  6543  ADCC ADSC
0106  6532  ADCV
0107  7200  CLA
0110  6531  ADSF
0111  5110  JMP .-1
0112  6534  ADRB
0113  5504  JMP I CONVRT
0114  0000  CVT, 0
0115  3045  DCA 45
0116  3046  DCA 46
0117  1122  TAD C13
0120  3044  DCA 44
0121  5514  JMP I CVT
0122  0013  C13, 13
0123  7300  BACK, CLA CLL
0124  1025  TAD SAVLK2
0125  7010  RAR
0126  1023  TAD SAVAC2
0127  5426  JMP I SRET2
0130  3022  INT, DCA SAVAC1
0131  7004  RAL
0132  3024  DCA SAVLK1
0133  6771  MMSC
0134  7410  SKP
0135  5406  JMP I ERCM
0136  6761  MMSF
0137  7410  SKP
0140  5406  JMP I ERCM
0141  6454  CLIF
0142  6032  KCC
0143  6042  TCF
0144  6534  ADRB
0145  7300  SCAT, CLA CLL
0146  1024  TAD SAVLK1
0147  7010  RAR
0150  1022  TAD SAVAC1
0151  6001  ION
0152  5400  JMP I Z 0
                *153
0153  6002  START, IOF
0154  1033  TAD INT1
0155  3002  DCA 2
0156  6554  DALB2
0157  6551  DALC1
0160  6452  CMR
0161  6401  AMIC
```

```
0162  6301  CCL01
0163  6311  SCL02
0164  6314  SCL03
0165  1030  TAD M5
0166  3062  DCA CNTR1
0167  4403  JMS I R128
0170  5000  5000
0171  0020  ERROR
0172  0700  0700
0173  0010  10
0174  0101  101
0175  7200  CLA
0176  1403  TAD I R128
0177  7650  SNA CLA
0200  5176  JMP .-2
0201  6002  IOF
0202  1034  TAD INT2
0203  3002  DCA 2
0204  1067  TAD INPGET
0205  3011  DCA Z 11
0206  1071  TAD HODAT
0207  3012  DCA Z 12
0210  1070  TAD EDAT
0211  3013  DCA Z 13
0212  1035  TAD SEVPAG
0213  3063  DCA CNTR2
0214  1036  TAD FORPAG
0215  3064  DCA CNTR3
0216  1027  TAD M2
0217  3065  DCA CNTR4
0220  1037  TAD HELDVL
0221  3066  DCA CNTR5
0222  1074  TAD RESET1
0223  3332  DCA CORE
0224  1077  TAD TAPE0
0225  3344  DCA TAPEAT
0226  1076  TAD RESET3
0227  3347  DCA HARE
0230  3103  DCA ERRSQ
0231  4646  JMS I DELAYS
0232  7402  HLT
0233  6534  ADRB
0234  6454  CLIF
0235  6032  KCC
0236  6042  TCF
0237  6302  SCL01
0240  6452  CMR
0241  6402  AMC
0242  6001  ION
0243  7200  CLA
```

```
0244  5243  JMP .-1
0245  0410  DELAY1, DELAY2
0246  0460  DELAYS, DELAYK
0247  6461  INTR, SKIF
0250  5271  JMP UP
0251  3022  DCA SAVAC1
0252  7004  RAL
0253  3024  DCA SAVLK1
0254  6771  MMSC
0255  7410  SKP
0256  5406  JMP I ERCM
0257  6761  MMSF
0260  7410  SKP
0261  5406  JMP I ERCM
0262  6531  ADSF
0263  7410  SKP
0264  5400  JMP I Z 0
0265  7200  CLA
0266  6032  KCC
0267  6042  TCF
0270  5145  JMP SCAT
0271  3023  UP, DCA SAVAC2
0272  7004  RAL
0273  3025  DCA SAVLK2
0274  1000  TAD Z 0
0275  6454  CLIF
0276  6001  ION
0277  3026  DCA SRET2
0300  2062  ISZ CNTR1
0301  5305  JMP INPGIV
0302  1030  TAD M5
0303  3062  DCA CNTR1
0304  5346  JMP DATGET
0305  7200  INPGIV, CLA
0306  4645  JMS I DELAY1
0307  1411  TAD I Z 11
0310  6554  DALB2
0311  6551  DALC1
0312  2064  ISZ CNTR3
0313  5123  JMP BACK
0314  7200  CLA
0315  1036  TAD FORPAG
0316  3064  DCA CNTR3
0317  2332  ISZ CORE
0320  2065  ISZ CNTR4
0321  5331  JMP TAPEIN
0322  1027  TAD M2
0323  3065  DCA CNTR4
0324  1067  TAD INPGET
```

```
0325  3011  DCA Z 11
0326  1027  TAD M2
0327  1332  TAD CORE
0330  3332  DCA CORE
0331  7300  TAPEIN, CLA CLL
0332  1072  CORE, TAD LOC1
0333  3340  DCA COREAT
0334  1344  TAD TAPEAT
0335  1100  TAD FOUR
0336  3344  DCA TAPEAT
0337  4403  JMS I R128
0340  0000  COREAT, 0
0341  0020  ERROR
0342  0700  0700
0343  0004  4
0344  0000  TAPEAT, 0
0345  5123  JMP BACK
0346  7300  DATGET, CLA CLL
0347  2066  HARE, ISZ CNTR5
0350  5305  JMP INPGIV
0351  7200  CLA
0352  1075  TAD RESET2
0353  3347  DCA HARE
0354  6312  CCL03
0355  7001  DOT, IAC
0356  4104  JMS CONVRT
0357  3412  DCA I Z 12
0360  1101  TAD TWO
0361  4104  JMS CONVRT
0362  3413  DCA I Z 13
0363  2063  ISZ CNTR2
0364  7410  SKP
0365  5370  JMP END
0366  6001  ION
0367  5305  JMP INPGIV
0370  6002  END, IOF
0371  6301  CCL01
0372  6304  CCL02
0373  6314  SCL03
0374  6452  CMR
0375  6411  AMH
0376  7200  CLA
0377  1102  TAD THREE
0400  4717  JMS I CENVRT
0401  3720  DCA I ORRS0
0402  6452  CMR
0403  6401  AMIC
0404  5605  JMP I .+1
0405  4600  4600
```

```
                *410
0410  0000  DELAY2, 0
0411  7200  CLA
0412  6002  IOF
0413  1306  TAD FOOR
0414  6543  ADCC ADSC
0415  6532  ADCV
0416  7200  CLA
0417  6531  ADSF
0420  5217  JMP .-1
0421  6534  ADRB
0422  6001  ION
0423  3321  HAP, DCA SCAN
0424  1333  TAD SCAN+12
0425  6552  DALB1
0426  6551  DALC1
0427  7200  CLA
0430  2223  ISZ HAP
0431  2224  ISZ HAP+1
0432  7200  CLA
0433  2315  ISZ NCNT
0434  5241  JMP ONW
0435  1307  TAD HAPTI
0436  3224  DCA HAP+1
0437  1312  TAD X20
0440  3315  DCA NCNT
0441  2316  ONW, ISZ LCNT
0442  5610  JMP I DELAY2
0443  1311  TAD HOPI
0444  3223  DCA HAP
0445  1312  TAD X20
0446  3316  DCA LCNT
0447  5610  JMP I DELAY2
                *460
0460  0000  DELAYK, 0
0461  7200  CLA
0462  6552  DALB1
0463  6551  DALC1
0464  1312  TAD X20
0465  3314  DCA XCNT
0466  1311  TAD HOPI
0467  3270  DCA HOP
0470  3321  HOP, DCA SCAN
0471  2270  ISZ HOP
0472  2314  ISZ XCNT
0473  5270  JMP HOP
0474  1311  TAD HOPI
0475  3223  DCA HAP
0476  1310  TAD HAPI
0477  3224  DCA HAP+1
```

```
0500  1313  TAD X10
0501  3315  DCA NCNT
0502  1312  TAD X20
0503  3316  DCA LCNT
0504  7200  CLA
0505  5660  JMP I DELAYK
0506  0004  FOOR, 4
0507  1321  HAPTI, TAD SCAN
0510  1333  HAPI, TAD SCAN+12
0511  3321  HOPI, DCA SCAN
0512  7766  X20, 7766
0513  7773  X10, 7773
0514  0000  XCNT, 0
0515  0000  NCNT, 0
0516  0000  LCNT, 0
0517  0104  CENVRT, CONVRT
0520  0103  ORRSO, ERRSQ
0521  0000  SCAN- 0
0522  0000  0
0523  0000  0
0524  0000  0
0525  0000  0
0526  0000  0
0527  0000  0
0530  0000  0
0531  0000  0
0532  0000  0
0533  0000  0
0534  0000  0
0535  0000  0
0536  0000  0
0537  0000  0
0540  0000  0
0541  0000  0
0542  0000  0
0543  0000  0
0544  0000  0
0545  0000  0

BACK    0123
CENVRT  0517
CNTR1   0062
CNTR2   0063
CNTR3   0064
CNTR4   0065
CNTR5   0066
CONVRT  0104
CORE    0332
COREAT  0340
CVT     0114
```

```
C13       0122
DATGET    0346
DELAYK    0460
DELAYS    0246
DELAY1    0245
DELAY2    0410
DOT       0355
EDAT      0070
END       0370
ERCM      0006
ERROR     0020
ERRSQ     0103
FOOR      0506
FORPAG    0036
FOUR      0100
HAP       0423
HAPI      0510
HAPTI     0507
HARE      0347
HELDVL    0037
HODAT     0071
HOP       0470
HOPI      0511
INPGET    0067
INPGIV    0305
INT       0130
INTR      0247
INT1      0033
INT2      0034
LCNT      0516
LOC1      0072
LOC2      0073
M10       0031
M2        0027
M20       0032
M5        0030
NCNT      0515
ONW       0441
ORRSO     0520
RESET1    0074
RESET2    0075
RESET3    0076
R128      0003
SAVAC1    0022
SAVAC2    0023
SAVLK1    0024
SAVLK2    0025
SCAN      0521
SCAT      0145
SEVPAG    0035
SRET2     0026
```

```
START    0153
TAPEAT   0344
TAPEIN   0331
TAPE0    0077
THREE    0102
TWO      0101
UP       0271
W128     0004
XCNT     0514
X10      0513
X20      0512
```

```
                    /FC-ROUTINE, 200-577
                    /CALCULATES FCS, PUTS THEM 500 ON
                    /10ALS, 10BLS, 10ARS, 10BRS,
                    /10EAS, 10EBS WITH STARTINGS AT
                    /500, 512, 524, 536, 550, 562
                    ERROR=20
                    R128=3
                    W128=4
                    *200
0200   7200   CLA
0201   1337   TAD ANSPUT
0202   3013   DCA Z 13
0203   1372   TAD RESET1
0204   3210   DCA RESET
0205   1367   TAD M2
0206   3370   DCA KNT
0207   7200   CLA
0210   1365   RESET, TAD M40
0211   3364   DCA CNTR
0212   1363   TAD BLOKO
0213   3222   DCA BLOK
0214   7200   BEGIN1, CLA
0215   4403   JMS I R128/SINCOS INTO CORE
0216   2400   2400
0217   0020   ERROR
0220   0700   0700
0221   0007   7
0222   0000   BLOK, 0
0223   7200   CLA
0224   1403   TAD I R128
0225   7450   SNA
0226   5223   JMP .-3
0227   6002   IOF
0230   7200   CLA
0231   1222   TAD BLOK
0232   1362   TAD SEVEN
0233   3222   DCA BLOK
0234   1361   TAD DATBEG
0235   3011   DCA Z 11
0236   1360   TAD SINBEG
0237   3012   DCA Z 12
0240   1356   TAD SEVPAG
0241   3357   DCA PAG
0242   4766   JMS I FPONTC
0243   5353   FGET ZERO
0244   6350   FPUT RUNSUM
```

```
0245  0000  FEXT
0246  7200  BEGIN2, CLA
0247  1411  TAD I Z 11
0250  3045  DCA 45
0251  3046  DCA 46
0252  1344  TAD C13
0253  3044  DCA 44
0254  4766  JMS I FPONTC
0255  7000  FNOR
0256  6345  FPUT DATFP
0257  0000  FEXT
0260  7200  CLA
0261  1412  TAD I Z 12
0262  3045  DCA 45
0263  3046  DCA 46
0264  1344  TAD C13
0265  3044  DCA 44
0266  4766  JMS I FPONTC
0267  7000  FNOR
0270  3345  FMPY DATFP
0271  1350  FADD RUNSUM
0272  6350  FPUT RUNSUM
0273  0000  FEXT
0274  2357  ISZ PAG
0275  5246  JMP BEGIN2
0276  4766  JMS I FPONTC
0277  5350  FGET RUNSUM
0300  3341  FMPY CONST
0301  0000  FEXT
0302  7200  CLA
3030 1044  TAD 44
0304  7540  SZA SMA
0305  5310  JMP .+3
0306  7200  CLA
0307  5324  JMP DONE+1
0310  1340  TAD M13
0311  7450  SNA
0312  5323  JMP DONE
0313  7500  SMA
0314  5020  JMP ERROR
0315  7040  CMA
0316  3321  DCA .+3
0317  1045  TAD 45
0320  7415  ASR
0321  0000  0
0322  7410  SKP
0323  1045  DONE, TAD 45
0324  3413  DCA I Z 13
```

```
0325  2364  ISZ CNTR
0326  5214  JMP BEGIN1
0327  7200  CLA
0330  2370  ISZ KNT
0331  5333  JMP ONE
0332  5335  JMP TWO
0333  5734  ONE, JMP I .+1
0334  0400  400
0335  5736  TWO, JMP I .+1
0336  4634  4634
0337  0477  ANSPUT, 477
0340  7765  M13, 7765
0341  7763  CONST, 7763
0342  2000  2000
0343  0000  0
0344  0013  C13, 13
0345  0000  DATFP, 0
0346  0000  0
0347  0000  0
0350  0000  RUNSUM, 0
0351  0000  0
0352  0000  0
0353  0000  ZERO, 0
0354  0000  0
0355  0000  0
0356  6200  SEVPAG, 6200
0357  0000  PAG, 0
0360  2377  SINBEG, 2377
0361  0577  DATBEG, 577
0362  0007  SEVEN, 7
0363  0300  BLOKO, 300
0364  0000  CNTR, 0
0365  7730  M40, 7730
0366  5600  FPONTC, 5600
0367  7776  M2, 7776
0370  0000  KNT, 0
0371  7754  M20, 7754
0372  1365  RESET1, TAD M40
            *400
0400  7200  CLA
0401  4403  JMS I R128/GET EDAT INTO CORE
0402  0600  600
0403  0020  ERROR
0404  0700  0700
0405  0007  7
0406  0740  740
0407  7200  CLA
0410  1403  TAD I R128
0411  7450  SNA
0412  5207  JMP .-3
```

```
0413  6002  IOF
0414  7200  CLA
0415  1222  TAD RESET2
0416  3621  DCA I RASAT
0417  5620  JMP I .+1
0420  0207  207
0421  0210  RASAT, RESET
IR  0371  AT  0422
0422  1371  RESET2, TAD M20

ANSPUT  0337
BEGIN1  0214
BEGIN2  0246
BLOK    0222
BLOKO   0363
CNTR    0364
CONST   0341
C13     0344
DATBEG  0361
DATFP   0345
DONE    0323
ERROR   0020
FPONTC  0366
KNT     0370
M13     0340
M2      0367
M20     0371
M40     0365
ONE     0333
PAG     0357
RASAT   0421
RESET   0210
RESET1  0372
RESET2  0422
RUNSUM  0350
R128    0003
SEVEN   0362
SEVPAG  0356
SINBEG  0360
TWO     0335
W128    0004
ZERO    0353
```

```
                    /DFO AND EO ROUTINES, 400-577
                    /REQUIRE DFO AND EO SUB-ROUTINES, 200-377
                    /OUTPUTS MAG OF REM, PHASE OF E-I,
                    /PHASE OF H-I, AND MAG OF H.O. DF
                    /10 TIMES, THEN INT ERRSQ WITH
                    /TYPICAL VALUE OF MAGN H-I
                    OUTPUT=14
                    *400
0400    6032        KCC
0401    6046        TLS
0402    7200        CLA
0403    1324        TAD ARBEG
0404    3011        DCA Z 11
0405    1325        TAD BRBEG
0406    3012        DCA Z 12
0407    1326        TAD ALBEG
0410    3013        DCA Z 13
0411    1327        TAD BLBEG
0412    3014        DCA Z 14
0413    1330        TAD EABEG
0414    3015        DCA Z 15
0415    1331        TAD EBBEG
0416    3016        DCA Z 16
0417    1332        TAD M10
0420    3333        DCA CNTR1
0421    7200        SPINIT, CLA
0422    1411        TAD I Z 11
0423    3734        DCA I AX
0424    1412        TAD I Z 12
0425    3735        DCA I BX
0426    4736        JMS I CONERT
0427    7200        CLA
0430    4737        JMS I MAGNIT
0431    7200        CLA
0432    4740        JMS I FPONTC
0433    5741        FGET I ASQ
0434    0014        OUTPUT
0435    0000        FEXT
0436    7200        CLA
0437    1415        TAD I Z 15
0440    3734        DCA I AX
0441    1416        TAD I Z 16
0442    3735        DCA I BX
0443    4736        JMS I CONERT
0444    7200        CLA
0445    473         JMS I MAGNIT
0446    7200        CLA
0447    4743        JMS I PHASE
0450    7200        CLA
0451    4740        JMS I FPONTC
```

```
0452  5744  FGET I ANG
0453  0014  OUTPUT
0454  5741  FGET I ASQ
0455  0014  OUTPUT
0456  6345  FPUT MAGN
0457  0000  FEXT
0460  7200  CLA
0461  1413  TAD I Z 13
0462  3734  DCA I AX
0463  1414  TAD I Z 14
0464  3735  DCA I BX
0465  4736  JMS I CONERT
0466  7200  CLA
0467  4737  JMS I MAGNIT
0470  7200  CLA
0471  4743  JMS I PHASE
0472  7200  CLA
0473  4740  JMS I FPONTC
0474  5744  FGET I ANG
0475  0014  OUTPUT
0476  5741  FGET I ASQ
0477  4345  FDIV MAGN
0500  3350  FMPY CONST
0501  0014  OUTPUT
0502  0000  FEXT
0503  7200  CLA
0504  4742  JMS I RET
0505  7200  CLA
0506  2333  ISZ CNTR1
0507  5221  JMP SPINIT
0510  7200  CLA
0511  1754  TAD I ERRSQ
0512  3734  DCA I AX
0513  4736  JMS I CONERT
0514  7200  CLA
0515  4740  JMS I FPONTC
0516  5753  FGET I A
0517  0014  OUTPUT
0520  0000  FEXT
0521  7200  CLA
0522  5723  JMP I .+1
0523  4670  4670
0524  4023  ARBEG, 4023
0525  4035  BRBEG, 4035
0526  3777  ALBEG, 3777
0527  4011  BLBEG, 4011
0530  4047  EABEG, 4047
0531  4061  EBBEG, 4061
0532  7766  M10, 7766
0533  0000  CNTR1, 0
0534  0250  AX, 250
```

```
0535  0251  BX, 251
0536  0226  CONERT, 226
0537  0301  MAGNIT, 301
0540  5600  FPONTC, 5600
0541  0317  ASQ, 317
0542  0207  RET, 207
0543  0260  PHASE, 260
0544  0273  ANG, 273
0545  0000  MAGN, 0
0546  0000  0
0547  0000  0
0550  0001  CONST, 1
0551  2000  2000
0552  0000  0
0553  0252  A, 252
0554  0103  ERRSQ, 103

A        0553
ALBEG    0526
ANG      0544
ARBEG    0524
ASQ      0541
AX       0534
BLBEG    0527
BRBEG    0525
BX       0535
CNTR1    0533
CONERT   0536
CONST    0550
EABEG    0530
EBBEG    0531
ERRSQ    0554
FPONTC   0540
MAGN     0545
MAGNIT   0537
M10      0532
OUTPUT   0014
PHASE    0543
RET      0542
SPINIT   0421
```

```
                /DFO AND EO SUB-ROUTINES,    200-377
                /CVT, RET, POUT, CONERT, PHASE, MAGNIT
                /PHASE GOES IN ANG, MAGNITUDE IN ASQ
                OUTPUT=14
                ARCTAN=5
                SQUARE=1
                SQROOT=2
                *200
0200  0000    CVT, 0
0201  3045    DCA 45
0202  3046    DCA 46
0203  1206    TAD C13
0204  3044    DCA 44
0205  5600    JMP I CVT
0206  0013    C13, 13
0207  0000    RET, 0
0210  7200    CLA
0211  1216    TAD RETURN
0212  4220    JMS POUT
0213  1217    TAD LINFED
0214  4220    JMS POUT
0215  5607    JMP I RET
0216  0215    RETURN, 215
0217  0212    LINFED, 212
0220  0000    POUT, 0
0221  6041    TSF
0222  5221    JMP .-1
0223  6046    TLS
0224  7200    CLA
0225  5620    JMP I POUT
0226  0000    CONERT, 0
0227  7200    CLA
0230  1250    TAD AX
0231  4200    JMS CVT
0232  4647    JMS I FPONTC
0233  7000    FNOR
0234  6252    FPUT A
0235  0000    FEXT
0236  7200    CLA
0237  1251    TAD BX
0240  4200    JMS CVT
0241  4647    JMS I FPONTC
0242  7000    FNOR
0243  6255    FPUT B
0244  0000    FEXT
0245  7200    CLA
```

```
0246  5626  JMP I CONERT
0247  5600  FPONTC, 5600
0250  0000  AX, 0
0251  0000  BX, 0
0252  0000  A, 0
0253  0000  0
0254  0000  0
0255  0000  B, 0
0256  0000  0
0257  0000  0
0260  0000  PHASE, 0
0261  7200  CLA
0262  4647  JMS I FPONTC
0263  5255  FGET B
0264  4252  FDIV A
0265  0005  ARCTAN
0266  3276  FMPY DEGREE
0267  6273  FPUT ANG
0270  0000  FEXT
0271  7200  CLA
0272  5660  JMP I PHASE
0273  0000  ANG, 0
0274  0000  0
0275  0000  0
0276  0006  DEGREE, 6
0277  3451  3451
0300  4632  4632
0301  0000  MAGNIT, 0
0302  7200  CLA
0303  4647  JMS I FPONTC
0304  5252  FGET A
0305  0001  SQUARE
0306  6317  FPUT ASQ
0307  5255  FGET B
0310  0001  SQUARE
0311  1317  FADD ASQ
0312  0002  SQROOT
0313  6317  FPUT ASQ
0314  0000  FEXT
0315  7200  CLA
0316  5701  JMP I MAGNIT
0317  0000  ASQ, 0
0320  0000  0
0321  0000  0

A        0252
ANG      0273
ARCTAN   0005
ASQ      0317
```

AX	0250
B	0255
BX	0251
CONERT	0226
CVT	0200
C13	0206
DEGREE	0276
FPONTC	0247
LINFED	0217
MAGNIT	0301
OUTPUT	0014
PHASE	0260
POUT	0220
RET	0207
RETURN	0216
SQROOT	0002
SQUARE	0001

```
                    /INPUT ROUTINE
                    *1
0001   5402   JMP I .+1
0002   0400   INT
0003   4243   4243
0004   4224   4224
0005   0411   SCAT
0006   0000   MCOM, 0
0007   5600   5600
               FSIN=3
               *20
0020   7766   INVAL1, 7766
0021   0000   INDEX1, 0
0022   0000   NULL, 0
0023   0003   THREE, 3
0024   5400   NUM128, 5400
0025   7765   M13, 7765
0026   7402   ERROR, HLT
0027   0577   START, 577
0030   5064   UPSIN, FGET W1
0031   3122   UPCON, FMPY A1
0032   0000   INDEX2, 0
0033   4361   A, 4361
0034   0012   BLOKTO, 12
0035   0101   BLOKAT, 101
0036   0000   INDEX3, 0
               *64
0064   7776   W1, 7776
0065   2176   2176
0066   7636   7636
0067   7776   W2, 7776
0070   3276   3276
0071   6773   6773
0072   7777   W3, 7777
0073   2636   2636
0074   4077   4077
0075   0000   W4, 0
0076   2417   2417
0077   4412   4412
0100   0000   W5, 0
0101   3517   3517
0102   2040   2040
0103   0001   W6, 1
0104   2747   2747
0105   2446   2446
0106   0002   W7, 2
0107   2133   2133
0110   3750   3750
```

```
0111  0002  W10, 2
0112  2703  2703
0113  3022  3022
0114  0003  W11, 3
0115  2111  2111
0116  4137  4137
0117  0003  W12, 3
0120  3651  3651
0121  0552  0552
0122  0001  A1, 1
0123  2000  2000
0124  0000  0
0125  0001  A2, 1
0126  6000  6000
0127  0000  0
0130  0001  A3, 1
0131  2000  2000
0132  0000  0
0133  0001  A4, 1
0134  6000  6000
0135  0000  0
0136  0001  A5, 1
0137  2000  2000
0140  0000  0
0141  0001  A6, 1
0142  6000  6000
0143  0000  0
0144  0001  A7, 1
0145  2000  2000
0146  0000  0
0147  7775  A10, 7775
0150  4361  4361
0151  4361  4361
0152  7775  A11, 7775
0153  3146  3146
0154  3147  3147
0155  7775  A12, 7775
0156  4361  4361
0157  4361  4361
0160  7400  7400
0161  7766  WOWZIR, 7766
0162  6064  RATS, FPUT W1
0163  6122  MOUSE, FPUT A1
0164  0000  SUM, 0
0165  0000  0
0166  0000  0
0167  0000  ZERO, 0
0170  0000  0
0171  0000  0
0172  0000  TIME, 0
```

```
0173  0000  0
0174  0000  0
0175  7773  DELTAT, 7773
0176  2436  2436
0177  5606  5606
            *200
0200  7300  CLA CLL
0201  6032  KCC
0202  6046  TLS
0203  1020  TAD INVAL1
0204  3161  DCA WOWZIR
0205  1162  TAD RATS
0206  3214  DCA SISO
0207  1163  TAD MOUSE
0210  3227  DCA DADO
0211  7300  CLA CLL
0212  4560  JMS I 160
0213  4407  JMS I 7
0214  6064  SISO, FPUT W1
0215  0000  FEXT
0216  1214  TAD SISO
0217  1023  TAD THREE
0220  3214  DCA SISO
0221  2161  ISZ WOWZIR
0222  5211  JMP 211
0223  1020  TAD INVAL1
0224  3161  DCA WOWZIR
0225  4560  JMS I 160
0226  4407  JMS I 7
0227  6122  DADO, FPUT A1
0230  0000  FEXT
0231  1227  TAD DADO
0232  1023  TAD THREE
0233  3227  DCA DADO
0234  2161  ISZ WOWZIR
0235  5225  JMP DADO-2
0236  1020  TAD INVAL1
0237  3161  DCA WOWZIR
0240  1020  TAD INVAL1
0241  3036  DCA INDEX3
0242  4407  JMS I 7
0243  5375  FGET TINIT
0244  6172  FPUT TIME
0245  0000  FEXT
0246  7200  BEGIN1, CLA
0247  1027  TAD START
0250  3010  DCA Z 10
0251  1024  TAD NUM128
0252  3032  DCA INDEX2
0253  7200  BEGIN2, CLA
```

```
0254  1020  TAD INVAL1
0255  3021  DCA INDEX1
0256  1030  TAD UPSIN
0257  3270  DCA .+11
0260  1031  TAD UPCON
0261  3273  DCA .+12
0262  4407  JMS I 7
0263  5167  FGET ZERO
0264  6164  FPUT SUM
0265  0000  FEXT
0266  7200  BEGIN3, CLA
0267  4407  JMS I 7
0270  5064  FGET W1
0271  3172  FMPY TIME
0272  0003  FSIN
0273  3122  FMPY A1
0274  1164  FADD SUM
0275  6164  FPUT SUM
0276  0000  FEXT
0277  7200  CLA
0300  1023  TAD THREE
0301  1270  TAD .-11
0302  3270  DCA .-12
0303  1023  TAD THREE
0304  1273  TAD .-11
0305  3273  DCA .-12
0306  2021  ISZ INDEX1
0307  5266  JMP BEGIN3
0310  4407  JMS I 7
0311  5164  FGET SUM
0312  3372  FMPY VOLTS
0313  6164  FPUT SUM
0314  0000  FEXT
0315  7200  CLA
0316  1164  TAD SUM
0317  7540  SZA SMA
0320  5323  JMP .+3
0321  7200  CLA
0322  5337  JMP FINE+1
0323  1025  TAD M13
0324  7450  SNA
0325  5336  JMP FINE
0326  7500  SMA
0327  5026  JMP ERROR
0330  7040  CMA
0331  3334  DCA .+3
0332  1165  TAD SUM+1
0333  7415  ASR
0334  0000  0
0335  7410  SKP
0336  1165  FINE, TAD SUM+1
0337  3410  DCA I Z 10
```

```
0340  4407  JMS I 7
0341  5175  FGET DELTAT
0342  1172  FADD TIME
0343  6172  FPUT TIME
0344  0000  FEXT
0345  2032  ISZ INDEX2
0346  5253  JMP BEGIN2
0347  7200  CLA
0350  1035  TAD BLOKAT
0351  3357  DCA .+6
0352  4404  JMS I 4
0353  0600  600
0354  0026  ERROR
0355  0700  0700
0356  0012  12
0357  0000  0
0360  7200  CLA
0361  1433  TAD I A
0362  7440  SZA
0363  5360  JMP .-3
0364  1035  TAD BLOKAT
0365  1034  TAD BLOKTO
0366  3035  DCA BLOKAT
0367  2036  ISZ INDEX3
0370  5246  JMP BEGIN1
0371  7402  HLT
0372  0010  VOLTS, 10
0373  3153  3153
0374  1463  1463
0375  0005  TINIT, 5
0376  4434  4434
0377  6315  6315
            *400
0400  3220  INT, DCA SAVAC
0401  7004  RAL
0402  3221  DCA SAVLK
0403  6771  MMSC
0404  7410  SKP
0405  5617  JMP I ERCM
0406  6761  MMSF
0407  7410  SKP
0410  5406  JMP I MCOM
0411  7300  SCAT, CLA CLL
0412  1221  TAD SAVLK
0413  7010  RAR
0414  1220  TAD SAVAC
0415  6001  ION
0416  5400  JMP I Z 0
0417  4201  ERCM, 4201
0420  0000  SAVAC, 0
0421  0000  SAVLK, 0
```

```
                *557
0557   6032   BEG, KCC
0560   6031   KSF
0561   5360   JMP .-1
0562   6036   KRB
0563   7106   CLL RTL
0564   7006   RTL
0565   7510   SPA
0566   5360   JMP BEG+1
0567   7006   RTL
0570   6031   KSF
0571   5370   JMP .-1
0572   6034   KRS
0573   7420   SNL
0574   3777   DCA I TEMP
0575   3377   DCA TEMP
0576   5357   JMP BEG
0577   0000   TEMP, 0

A          0033
A1         0122
A10        0147
A11        0152
A12        0155
A2         0125
A3         0130
A4         0133
A5         0136
A6         0141
A7         0144
BEG        0557
BEGIN1     0246
BEGIN2     0253
BEGIN3     0266
BLOKAT     0035
BLOKTO     0034
DADO       0227
DELTAT     0175
ERCM       0417
ERROR      0026
FINE       0336
FSIN       0003
INDEX1     0021
INDEX2     0032
INDEX3     0036
INT        0400
INVAL1     0020
MCOM       0006
MOUSE      0163
M13        0025
NULL       0022
NUM128     0024
RATS       0162
```

```
SAVAC    0420
SAVLK    0421
SCAT     0411
SISO     0214
START    0027
SUM      0164
TEMP     0577
THREE    0023
TIME     0172
TINIT    0375
UPCON    0031
UPSIN    0030
VOLTS    0372
WOWZIR   0161
W1       0064
W10      0111
W11      0114
W12      0117
W2       0067
W3       0072
W4       0075
W5       0100
W6       0103
W7       0106
ZERO     0167
```

```
                    /CONVERSION ROUTINE     4600-4757
                    /CONVERT1 RR TO FC, 4600
                    /CONVERT2 FC TO DFO, 4634
                    /CONVERT3 DFO TO RR, 4670
                    /RET SUB-ROUTINE, 4710
                    CNTR1=62
                    ERROR=20
                    R128=3
                    W128=4
                    INT1=33
                    *4600
4600   7200   CLA
4601   1033   TAD INT1
4602   3002   DCA 2
4603   4403   JMS I R128/GET F.C.
4604   0200   200
4605   0020   ERROR
4606   0700   0700
4607   0002   2
4610   0730   730
4611   7200   CLA
4612   1403   TAD I R128
4613   7650   SNA CLA
4614   5212   JMP .-2
4615   6002   IOF
4616   4404   JMS I W128/SAVE EDAT
4617   2400   2400
4620   0020   ERROR
4621   0700   0700
4622   0007   7
4623   0740   740
4624   7200   CLA
4625   1403   TAD I R128
4626   7650   SNA CLA
4627   5225   JMP .-2
4630   6002   IOF
4631   5330   JMP MISTAK
                    *4634
4634   7200   CLA
4635   1264   TAD ANSBEG/PUT FCS 4000 ON
4636   3011   DCA Z 11
4637   1265   TAD ANSPUT
4640   3012   DCA Z 12
4641   1266   TAD M60
4642   3062   DCA CNTR1
```

```
4643  1411  CYCLE, TAD I Z 11
4644  3412  DCA I Z 12
4645  2062  ISZ CNTR1
4646  5243  JMP CYCLE
4647  4403  JMS I R128/GET DFO AND EO
4650  0200  200
4651  0020  ERROR
4652  0700  0700
4653  0002  2
4654  0734  734
4655  7200  CLA
4656  1403  TAD I R128
4657  7650  SNA CLA
4660  5256  JMP .-2
4661  6002  IOF
4662  5663  JMP I .+1
4663  0400  400
4664  0477  ANSBEG, 477
4665  3777  ANSPUT, 3777
4666  7704  M60, 7704
            *4670
4670  7200  CLA
4671  4403  JMS I R128/GET RR
4672  0200  200
4673  0020  ERROR
4674  0700  0700
4675  0002  2
4676  0732  732
4677  7200  CLA
4700  1403  TAD I R128
4701  7650  SNA CLA
4702  5300  JMP .-2
4703  6002  IOF
4704  7200  CLA
4705  7402  HLT
4706  5707  JMP I .+1
4707  0153  153
            *4710
4710  0000  RET, 0
4711  7200  CLA
4712  1317  TAD RETURN
4713  4321  JMS POUT
4714  1320  TAD LINFED
4715  4321  JMS POUT
4716  5710  JMP I RET
4717  0215  RETURN, 215
4720  0212  LINFED, 212
4721  0000  POUT, 0
4722  6041  TSF
4723  5322  JMP .-1
```

```
4724  6046  TLS
4725  7200  CLA
4726  5721  JMP I POUT
            *4730
4730  7200  MISTAK, CLA
4731  4403  JMS I R128/GET CVT, FPONTC
4732  4600  4600
4733  0020  ERROR
4734  0700  0700
4735  0014  14
4736  0750  750
4737  7200  CLA
4740  1403  TAD I R128
4741  7650  SNA CLA
4742  5340  JMP .-2
4743  6002  IOF
4744  5745  JMP I .+1
4745  0200  200

ANSBEG   4664
ANSPUT   4665
CNTR1    0062
CYCLE    4643
ERROR    0020
INT1     0033
LINFED   4720
MISTAK   4730
M60      4666
POUT     4721
RET      4710
RETURN   4717
R128     0003
W128     0004
```

```
                    /SINCOS1, 1-577
                    /PUTS SINS, THEN COSS (7 PAGES EACH)
                    /ON TAPE, BLOCK 300 ON, AMPS +-1
                    *1
0001    5402        JMP I .+1
0002    0403        INT
0003    4243        4243
0004    4224        4224
0005    0414        SCAT
0006    0000        MCOM, 0
0007    5600        5600
                    FSIN=3
                    FCOS=4
                    *20
0020    7766        INVAL1, 7766
0021    0000        INDEX1, 0
0022    0007        SEVEN, 7
0023    0003        THREE, 3
0024    6200        SEVPAG, 6200
0025    7765        M13, 7765
0026    7402        ERROR, HLT
0027    0577        START, 577
0030    5064        UPSIN, FGET W1
0031    3122        UPCON, FMPY A1
0032    0000        INDEX2, 0
0033    4361        A, 4361
0034    0000        TINIT, 0
0035    0000        0
0036    0000        0
                    *64
0064    7776        W1, 7776
0065    2176        2176
0066    7636        7636
0067    7776        W2, 7776
0070    3276        3276
0071    6773        6773
0072    7777        W3, 7777
0073    2636        2636
0074    4077        4077
0075    0000        W4, 0
0076    2417        2417
0077    4412        4412
0100    0000        W5, 0
0101    3517        3517
0102    2040        2040
0103    0001        W6, 1
0104    2747        2747
0105    2446        2446
0106    0002        W7, 2
0107    2133        2133
```

```
0110  3750  3750
0111  0002  W10, 2
0112  2703  2703
0113  3022  3022
0114  0003  W11, 3
0115  2111  2111
0116  4137  4137
0117  0003  W12, 3
0120  3651  3651
0121  0552  0552
0122  0001  A1, 1
0123  2000  2000
0124  0000  0
0125  0001  A2, 1
0126  6000  6000
0127  0000  0
0130  0001  A3, 1
0131  2000  2000
0132  0000  0
0133  0001  A4, 1
0134  6000  6000
0135  0000  0
0136  0001  A5, 1
0137  2000  2000
0140  0000  0
0141  0001  A6, 1
0142  6000  6000
0143  0000  0
0144  0001  A7, 1
0145  2000  2000
0146  0000  0
0147  0001  A10, 1
0150  6000  6000
0151  0000  0
0152  0001  A11, 1
0153  2000  2000
0154  0000  0
0155  0001  A12, 1
0156  6000  6000
0157  0000  0
0160  7400  7400
0161  7766  WOWZIR, 7766
0162  6064  RATS, FPUT W1
0163  6122  MOUSE, FPUT A1
0164  0000  SUM, 0
0165  0000  0
0166  0000  0
0167  0000  ZERO, 0
0170  0000  0
```

```
0171  0000  0
0172  0000  TIME, 0
0173  0000  0
0174  0000  0
0175  7775  DELTAT, 7775
0176  3146  3146
0177  3147  3147
            *200
0200  7300  CLA CLL
0201  6032  KCC
0202  6046  TLS
0203  1020  TAD INVAL1
0204  3161  DCA WOWZIR
0205  1162  TAD RATS
0206  3214  DCA SISO
0207  1163  TAD MOUSE
0210  3230  DCA DADO
0211  7300  CLA CLL
0212  4560  JMS I 160
0213  4407  JMS I 7
0214  6064  SISO, FPUT W1
0215  0000  FEXT
0216  1214  TAD SISO
0217  1023  TAD THREE
0220  3214  DCA SISO
0221  2161  ISZ WOWZIR
0222  5211  JMP 211
0223  1020  TAD INVAL1
0224  3161  DCA WOWZIR
0225  7300  CLA CLL
0226  4560  JMS I 160
0227  4407  JMS I 7
0230  6122  DADO, FPUT A1
0231  0000  FEXT
0232  1230  TAD DADO
0233  1023  TAD THREE
0234  3230  DCA DADO
0235  2161  ISZ WOWZIR
0236  5225  JMP DADO-3
0237  1020  TAD INVAL1
0240  3161  DCA WOWZIR
0241  1371  TAD MTWO
0242  3372  DCA CRAT
0243  1373  TAD CREATE
0244  3275  DCA CLOD
0245  1377  TAD BLOKO
0246  3376  DCA BLOKAT
0247  7200  BEGIN1, CLA
0250  1020  TAD INVAL1
```

```
0251  3021  DCA INDEX1
0252  1030  TAD UPSIN
0253  3273  DCA DUMB
0254  1031  TAD UPCON
0255  3276  DCA TROD
0256  7200  BEGIN2, CLA
0257  4407  JMS I 7
0260  5167  FGET ZERO
0261  6164  FPUT SUM
0262  5034  FGET TINIT
0263  6172  FPUT TIME
0264  0000  FEXT
0265  1027  TAD START
0266  3010  DCA Z 10
0267  1024  TAD SEVPAG
0270  3032  DCA INDEX2
0271  7200  BEGIN3, CLA
0272  4407  JMS I 7
0273  5064  DUMB, FGET W1
0274  3172  FMPY TIME
0275  0003  CLOD, FSIN
0276  3122  TROD, FMPY A1
0277  3775  FMPY I VOLTS
0300  6164  FPUT SUM
0301  0000  FEXT
0302  7200  CLA
0303  1164  TAD SUM
0304  7540  SZA SMA
0305  5310  JMP .+3
0306  7200  CLA
0307  5324  JMP FINE+1
0310  1025  TAD M13
0311  7450  SNA
0312  5323  JMP FINE
0313  7500  SMA
0314  5026  JMP ERROR
0315  7040  CMA
0316  3321  DCA .+3
0317  1165  TAD SUM+1
0320  7415  ASR
0321  0000  0
0322  7410  SKP
0323  1165  FINE, TAD SUM+1
0324  3410  DCA I Z 10
0325  4407  JMS I 7
0326  5175  FGET DELTAT
0327  1172  FADD TIME
0330  6172  FPUT TIME
0331  0000  FEXT
0332  2032  ISZ INDEX2
0333  5271  JMP BEGIN3
0334  1376  TAD BLOKAT
0335  3343  DCA .+6
```

```
0336  4404  JMS I 4
0337  0600  600
0340  0026  ERROR
0341  0700  0700
0342  0007  7
0343  0000  0
0344  7200  CLA
0345  1433  TAD I A
0346  7440  SZA
0347  5344  JMP .-3
0350  7200  CLA
0351  1376  TAD BLOKAT
0352  1022  TAD SEVEN
0353  3376  DCA BLOKAT
0354  1273  TAD DUMB
0355  1023  TAD THREE
0356  3273  DCA DUMB
0357  1276  TAD TROD
0360  1023  TAD THREE
0361  3276  DCA TROD
0362  2021  ISZ INDEX1
0363  5256  JMP BEGIN2
0364  1374  TAD CRITER
0365  3275  DCA CLOD
0366  2372  ISZ CRAT
0367  5247  JMP BEGIN1
0370  7402  HLT
0371  7776  MTWO, 7776
0372  0000  CRAT, 0
0373  0003  CREATE, FSIN
0374  0004  CRITER, FCOS
0375  0400  VOLTS, VALTS
0376  0000  BLOKAT,-0
0377  0300  BLOKO, 300
              *400
0400  0010  VALTS, 10
0401  3153  3153
0402  1463  1463
0403  3223  INT, DCA SAVAC
0404  7004  RAL
0405  3224  DCA SAVLK
0406  6771  MMSC
0407  7410  SKP
0410  5622  JMP I ERCM
0411  6761  MMSF
0412  7410  SKP
0413  5406  JMP I MCOM
0414  7300  SCAT, CLA CLL
0415  1224  TAD SAVLK
0416  7010  RAR
0417  1223  TAD SAVAC
```

```
0420  6001  ION
0421  5400  JMP I Z 0
0422  4201  ERCM, 4201
0423  0000  SAVAC, 0
0424  0000  SAVLK, 0
            *557
0557  6032  BEG, KCC
0560  6031  KSF
0561  5360  JMP .-1
0562  6036  KRB
0563  7106  CLL RTL
0564  7006  RTL
0565  7510  SPA
0566  5360  JMP BEG+1
0567  7006  RTL
0570  6031  KSF
0571  5370  JMP .-1
0572  6034  KRS
0573  7420  SNL
0574  3777  DCA I TEMP
0575  3377  DCA TEMP
0576  5357  JMP BEG
0577  0000  TEMP, 0

A         0033
A1        0122
A10       0147
A11       0152
A12       0155
A2        0125
A3        0130
A4        0133
A5        0136
A6        0141
A7        0144
BEG       0557
BEGIN1    0247
BEGIN2    0256
BEGIN3    0271
BLOKAT    0376
BLOKO     0377
CLOD      0275
CRAT      0372
CREATE    0373
CRITER    0374
DADO      0230
DELTAT    0175
DUMB      0273
ERCM      0422
ERROR     0026
FCOS      0004
```

```
FINE      0323
FSIN      0003
INDEX1    0021
INDEX2    0032
INT       0403
INVAL1    0020
MCOM      0006
MOUSE     0163
MTWO      0371
M13       0025
RATS      0162
SAVAC     0423
SAVLK     0424
SCAT      0414
SEVEN     0022
SEVPAG    0024
SISO      0214
START     0027
SUM       0164
TEMP      0577
THREE     0023
TIME      0172
TINIT     0034
TROD      0276
UPCON     0031
UPSIN     0030
VALTS     0400
VOLTS     0375
WOWZIR    0161
W1        0064
W10       0111
W11       0114
W12       0117
W2        0067
W3        0072
W4        0075
W5        0100
W6        0103
W7        0106
ZERO      0167
```

```
                    /SINCOS2, 1-577 (REMNANT)
                    /PUTS SINS, THEN COSS BLOCK 514 ON
                    /AMPLITUDES ARE +-1
                    *1
0001   5402   JMP I .+1
0002   0403   INT
0003   4243   4243
0004   4224   4224
0005   0414   SCAT
0006   0000   MCOM, 0
0007   5600   5600
               FSIN=3
               FCOS=4
               *20
0020   7766   INVAL1, 7766
0021   0000   INDEX1, 0
0022   0007   SEVEN, 7
0023   0003   THREE, 3
0024   6200   SEVPAG, 6200
0025   7765   M13, 7765
0026   7402   ERROR, HLT
0027   0577   START, 577
0030   5064   UPSIN, FGET W1
0031   3122   UPCON, FMPY A1
0032   0000   INDEX2, 0
0033   4361   A, 4361
0034   0000   TINIT, 0
0035   0000   0
0036   0000   0
               *64
0064   7775   W1, 7775
0065   2176   2176
0066   1202   1202
0067   7777   W2, 7777
0070   2176   2176
0071   7636   7636
0072   7777   W3, 7777
0073   3737   3737
0074   1667   1667
0075   0000   W4, 0
0076   3057   3057
0077   4067   4067
0100   0001   W5, 1
0101   2307   2307
0102   2767   2767
```

```
0103  0001  W6, 1
0104  3627  3627
0105  1752  1752
0106  0002  W7, 2
0107  2463  2463
0110  3172  3172
0111  0003  W10, 3
0112  2001  2001
0113  4223  4223
0114  0003  W11, 3
0115  2615  2615
0116  3071  3071
0117  0004  W12, 4
0120  2320  2320
0121  3711  3711
0122  0001  A1, 1
0123  2000  2000
0124  0000  0
0125  0001  A2, 1
0126  6000  6000
0127  0000  0
0130  0001  A3, 1
0131  2000  2000
0132  0000  0
0133  0001  A4, 1
0134  6000  6000
0135  0000  0
0136  0001  A5, 1
0137  2000  2000
0140  0000  0
0141  0001  A6, 1
0142  6000  6000
0143  0000  0
0144  0001  A7, 1
0145  2000  2000
0146  0000  0
0147  0001  A10, 1
0150  6000  6000
0151  0000  0
0152  0001  A11, 1
0153  2000  2000
0154  0000  0
0155  0001  A12, 1
0156  6000  6000
0157  0000  0
0160  7400  7400
0161  7766  WOWZIR, 7766
0162  6064  RATS, FPUT W1
0163  6122  MOUSE, FPUT A1
0164  0000  SUM, 0
0165  0000  0
0166  0000  0
```

```
0167  0000  ZERO, 0
0170  0000  0
0171  0000  0
0172  0000  TIME, 0
0173  0000  0
0174  0000  0
0175  7775  DELTAT, 7775
0176  3146  3146
0177  3147  3147
            *200
0200  7300  CLA CLL
0201  6032  KCC
0202  6046  TLS
0203  1020  TAD INVAL1
0204  3161  DCA WOWZIR
0205  1162  TAD RATS
0206  3214  DCA SISO
0207  1163  TAD MOUSE
0210  3230  DCA DADO
0211  7300  CLA CLL
0212  4560  JMS I 160
0213  4407  JMS I 7
0214  6064  SISO, FPUT W1
0215  0000  FEXT
0216  1214  TAD SISO
0217  1023  TAD THREE
0220  3214  DCA SISO
0221  2161  ISZ WOWZIR
0222  5211  JMP 211
0223  1020  TAD INVAL1
0224  3161  DCA WOWZIR
0225  7300  CLA CLL
0226  4560  JMS I 160
0227  4407  JMS I 7
0230  6122  DADO, FPUT A1
0231  0000  FEXT
0232  1230  TAD DADO
0233  1023  TAD THREE
0234  3230  DCA DADO
0235  2161  ISZ WOWZIR
0236  5225  JMP DADO-3
0237  1020  TAD INVAL1
0240  3161  DCA WOWZIR
0241  1371  TAD MTWO
0242  3372  DCA CRAT
0243  1373  TAD CREATE
0244  3275  DCA CLOD
0245  1377  TAD BLOKO
0246  3376  DCA BLOKAT
0247  7200  BEGIN1, CLA
0250  1020  TAD INVAL1
```

```
0251  3021  DCA INDEX1
0252  1030  TAD UPSIN
0253  3273  DCA DUMB
0254  1031  TAD UPCON
0255  3276  DCA TROD
0256  7200  BEGIN2, CLA
0257  4407  JMS I 7
0260  5167  FGET ZERO
0261  6164  FPUT SUM
0262  5034  FGET TINIT
0263  6172  FPUT TIME
0264  0000  FEXT
0265  1027  TAD START
0266  3010  DCA Z 10
0267  1024  TAD SEVPAG
0270  3032  DCA INDEX2
0271  7200  BEGIN3, CLA
0272  4407  JMS I 7
0273  5064  DUMB, FGET W1
0274  3172  FMPY TIME
0275  0003  CLOD, FSIN
0276  3122  TROD, FMPY A1
0277  3775  FMPY I VOLTS
0300  6164  FPUT SUM
0301  0000  FEXT
0302  7200  CLA
0303  1164  TAD SUM
0304  7540  SZA SMA
0305  5310  JMP .+3
0306  7200  CLA
0307  5324  JMP FINE+1
0310  1025  TAD M13
0311  7450  SNA
0312  5323  JMP FINE
0313  7500  SMA
0314  5026  JMP ERROR
0315  7040  CMA
0316  3321  DCA .+3
0317  1165  TAD SUM+1
0320  7415  ASR
0321  0000  0
0322  7410  SKP
0323  1165  FINE, TAD SUM+1
0324  3410  DCA I Z 10
0325  4407  JMS I 7
0326  5175  FGET DELTAT
0327  1172  FADD TIME
0330  6172  FPUT TIME
0331  0000  FEXT
0332  2032  ISZ INDEX2
0333  5271  JMP BEGIN3
```

```
0334  1376  TAD BLOKAT
0335  3343  DCA .+6
0336  4404  JMS I 4
0337  0600  600
0340  0026  ERROR
0341  0700  0700
0342  0007  7
0343  0000  0
0344  7200  CLA
0345  1433  TAD I A
0346  7440  SZA
0347  5344  JMP .-3
0350  7200  CLA
0351  1376  TAD BLOKAT
0352  1022  TAD SEVEN
0353  3376  DCA BLOKAT
0354  1273  TAD DUMB
0355  1023  TAD THREE
0356  3273  DCA DUMB
0357  1276  TAD TROD
0360  1023  TAD THREE
0361  3276  DCA TROD
0362  2021  ISZ INDEX1
0363  5256  JMP BEGIN2
0364  1374  TAD CRITER
0365  3275  DCA CLOD
0366  2372  ISZ CRAT
0367  5247  JMP BEGIN1
0370  7402  HLT
0371  7776  MTWO, 7776
0372  0000  CRAT, 0
0373  0003  CREATE, FSIN
0374  0004  CRITER, FCOS
0375  0400  VOLTS, VALTS
0376  0000  BLOKAT, 0
0377  0514  BLOKO, 514
            *400
0400  0010  VALTS, 10
0401  3153  3153
0402  1463  1463
0403  3223  INT, DCA SAVAC
0404  7004  RAL
0405  3224  DCA SAVLK
0406  6771  MMSC
0407  7410  SKP
0410  5622  JMP I ERCM
0411  6761  MMSF
0412  7410  SKP
```

```
0413  5406  JMP I MCOM
0414  7300  SCAT, CLA CLL
0415  1224  TAD SAVLK
0416  7010  RAR
0417  1223  TAD SAVAC
0420  6001  ION
0421  5400  JMP I Z 0
0422  4201  ERCM, 4201
0423  0000  SAVAC, 0
0424  0000  SAVLK, 0
            *557
0557  6032  BEG, KCC
0560  6031  KSF
0561  5360  JMP .-1
0562  6036  KRB
0563  7106  CLL RTL
0564  7006  RTL
0565  7510  SPA
0566  5360  JMP BEG+1
0567  7006  RTL
0570  6031  KSF
0571  5370  JMP .-1
0572  6034  KRS
0573  7420  SNL
0574  3777  DCA I TEMP
0575  3377  DCA TEMP
0576  5357  JMP BEG
0577  0000  TEMP, 0

A         0033
A1        0122
A10       0147
A11       0152
A12       0155
A2        0125
A3        0130
A4        0133
A5        0136
A6        0141
A7        0144
BEG       0557
BEGIN1    0247
BEGIN2    0256
BEGIN3    0271
BLOKAT    0376
BLOKO     0377
CLOD      0275
CRAT      0372
CREATE    0373
CRITER    0374
```

```
DADO      0230
DELTAT    0175
DUMB      0273
ERCM      0422
ERROR     0026
FCOS      0004
FINE      0323
FSIN      0003
INDEX1    0021
INDEX2    0032
INT       0403
INVAL1    0020
MCOM      0006
MOUSE     0163
MTWO      0371
M13       0025
RATS      0162
SAVAC     0423
SAVLK     0424
SCAT      0414
SEVEN     0022
SEVPAG    0024
SISO      0214
START     0027
SUM       0164
TEMP      0577
THREE     0023
TIME      0172
TINIT     0034
TROD      0276
UPCON     0031
UPSIN     0030
VALTS     0400
VOLTS     0375
WOWZIR    0161
W1        0064
W10       0111
W11       0114
W12       0117
W2        0067
W3        0072
W4        0075
W5        0100
W6        0103
W7        0106
ZERO      0167
```

APPENDIX F: THE EXPERIMENTAL DATA

The experimental data are presented on the following pages as follows:

Index to the data, pages 163 to 166
The explanation of the data, pages 167 to 171
The experimental data, pages 172 to 232
Subject to subject differences, pages 233 to 252
Models of the human operator's describing functions, pages 253 to 290

INDEX TO THE DATA

(see Appendix B to correct for the factor $e^{-.1s}$)

	controlled vehicle dynamics $Y_c(\omega)$	human operator data: describing function and remnant $Y_p(\omega)$ and $\Phi_{nn}(\omega)$
1)	$\frac{1}{s} e^{-.1s}$	data-6 through data-8
2)	$\frac{-1}{s(s-1)} e^{-.1s}$	data-9
3)	$\frac{-.5}{s(s-.5)} e^{-.1s}$	data-10 through data-13
4)	$\frac{-.25}{s(s-.25)} e^{-.1s}$	data-14
5)	$\frac{1}{s^2} e^{-.1s}$	data-15 through data-27 data-77, data-78
6)	$\frac{1}{s(s+1)} e^{-.1s}$	data-28 through data-31
7)	$\frac{2}{s(s+2)} e^{-.1s}$	data-32, data-69 through data-70
8)	$\frac{4}{s(s+4)} e^{-.1s}$	data-33, data-71, data-72
9)	$\frac{5}{s(s+5)} e^{-.1s}$	data-34 through data-37, data-73 through data-76
10)	$\frac{20}{s(s+20)} e^{-.1s}$	data-38

data-1

INDEX TO THE DATA (continued)

controlled vehicle dynamics $Y_c(\omega)$	human operator data: describing function and remnant $Y_p(\omega)$ and $\Phi_{nn}(\omega)$
11) $\frac{20}{s^2+20} e^{-.1s}$	data-39
12) $\frac{10}{s^2+10} e^{-.1s}$	data-40 , data-79, data-80
13) $\frac{5}{s^2+5} e^{-.1s}$	data-41
14) $\frac{-2.5}{s^2-2.5} e^{-.1s}$	data-42
15) $\frac{25}{s^2+5s+25} e^{-.1s}$	data-43 , data-85, data-86
16) $\frac{15}{s^2+5s+15} e^{-.1s}$	data-44
17) $\frac{5}{s^2+5s+5} e^{-.1s}$	data-45
18) $\frac{-5}{s^2+5s-5} e^{-.1s}$	data-46
19) $\frac{15}{s^2+3s+15} e^{-.1s}$	data-47
20) $\frac{5}{s^2+3s+5} e^{-.1s}$	data-48

data-2

INDEX TO THE DATA (continued)

controlled vehicle dynamics $Y_c(\omega)$	human operator data: describing function and remnant $Y_p(\omega)$ and $\Phi_{nn}(\omega)$
21) $\frac{-5}{s^2+3s-5} e^{-.1s}$	data-49
22) $\frac{20}{s^2+2s+20} e^{-.1s}$	data-50 , data-81, data-82
23) $\frac{10}{s^2+2s+10} e^{-.1s}$	data-51
24) $\frac{5}{s^2+s+5} e^{-.1s}$	data-52
25) $\frac{-2.5}{s^2+s-2.5} e^{-.1s}$	data-53
26) $\frac{15}{s^2-s+15} e^{-.1s}$	data-54
27) $\frac{2}{s^2(s+2)} e^{-.1s}$	data-55
28) $\frac{4}{s^2(s+4)} e^{-.1s}$	data-56
29) $\frac{10}{s(s^2+10)} e^{-.1s}$	data-57
30) $\frac{20}{s(s^2+.5s+20)} e^{-.1s}$	data-58

data-3

INDEX TO THE DATA (continued)

controlled vehicle dynamics $Y_c(\omega)$	human operator data: describing function and remnant $Y_p(\omega)$ and $\Phi_{nn}(\omega)$
31) $\frac{15}{s(s^2+s+15)} e^{-.1s}$	data-59
32) $\frac{5}{s(s^2+s+5)} e^{-.1s}$	data-60
33) $\frac{20}{s(s^2+2s+20)} e^{-.1s}$	data-61
34) $\frac{10}{s(s^2+2s+10)} e^{-.1s}$	data-62, data-87, data-88
35) $\frac{15}{s(s^2+3s+15)} e^{-.1s}$	data-63
36) $\frac{5}{s(s^2+3s+5)} e^{-.1s}$	data-64
37) $\frac{20}{s(s^2+4s+20)} e^{-.1s}$	data-65 , data-83, data-84
38) $\frac{10}{s(s^2+4s+10)} e^{-.1s}$	data-66
39) $\frac{15}{s(s^2+5s+15)} e^{-.1s}$	data-67
40) $\frac{5}{s(s^2+5s+5)} e^{-.1s}$	data-68

data-4

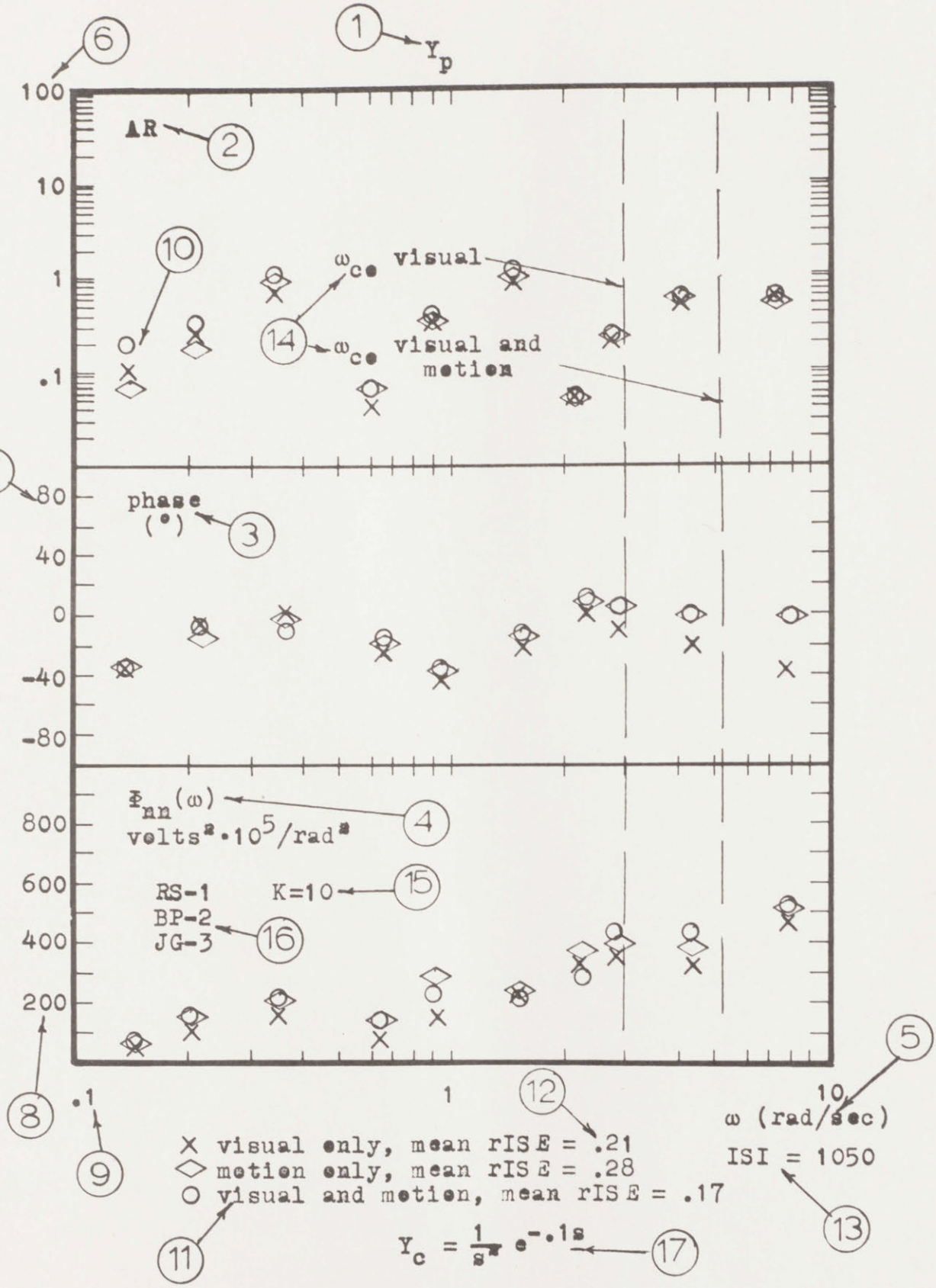

EXPERIMENTAL RESULTS
NOT ACTUAL DATA
EXPLANATION OF DATA PRESENTATION/A data-5/A

EXPLANATION OF THE DATA PRESENTATION

see previous page, data-5/A

1) Y_p, the human operator's describing function, consists of the magnitude and phase of the human operator's output relative to his input, and is shown in the upper two sections of each graph.

2) AR, the amplitude ratio or magnitude of the human operator's describing function.

3) phase, the phase of the human operator's describing function.

4) $\Phi_{nn}(\omega)$, the remnant, or that part of the human operator's output which is not correlated with his input, is presented as a power spectral density.

5) ω, frequency, is the horizontal axis for all three sections of each graph (2, 3, and 4 above).

6) the scale for the AR (2 above), always a log scale, but the labeled values changing from graph to graph.

7) the scale for the phase (3 above), always a linear scale, the values shown usually used, but occasionally other values are used. The scale is in degrees.

8) the scale for the remnant (4 above), always a linear scale, but the values widely varying from graph to graph.

9) the scale for the frequency on the horizontal axis, always a log scale with the values as shown. The scale is in radians per second.

10) the data points, presented at the ten frequencies of the input between .1 and 10 rad/sec.

data-5/B

EXPLANATION OF THE DATA PRESENTATION

see previous two pages, data-5/A and 5/B

11) key to the data points, showing which symbols are for visual cues only, motion cues only, and simultaneous visual and motion cues.

12) mean rISE, the mean value of the relative integral squared errors for all the runs for the conditions listed. The relative integral squared error is the integral squared error divided by the integral squared input, and hence is a measure of the ratio of the error power to the input power.

13) the ISI, or integral squared input, is a measure of the power of the system input, and is equal to 1050 unless the input is varied from the usual form. See Chapter II for more details about the ISE and rISE.

14) the cross-over frequencies, ω_{co}, listed separately for visual cues only and for simultaneous visual and motion cues if there is a data point between the two cross-over frequencies. The cross-over frequency is that frequency at which the product of the magnitudes of the human operator's describing function and of the vehicle dynamics crosses from greater than unity to less than unity. The cross-over frequency was determined as lying between two of the input frequencies (no closer determination of the cross-over frequency was attempted) by examination of the output of a digital computer program.

15) K, the control stick gain, is given for each set of data. The control stick gain is the maximum voltage available to the human operator from the control stick.

16) the listing of the subjects and the number of runs for each subject which go into the average values of the data which are presented. See Chapter II for more

EXPLANATION OF THE DATA PRESENTATION
see previous three data pages, data-5/A-C

details about the subjects and inter-subject differences.

17) Y_c, the vehicle dynamics, given as a function of s, the Laplace operator. The vehicle dynamics all include the factor $e^{-.1s}$, a pure delay of .1-seconds. To correct the data for this factor see Appendix B.

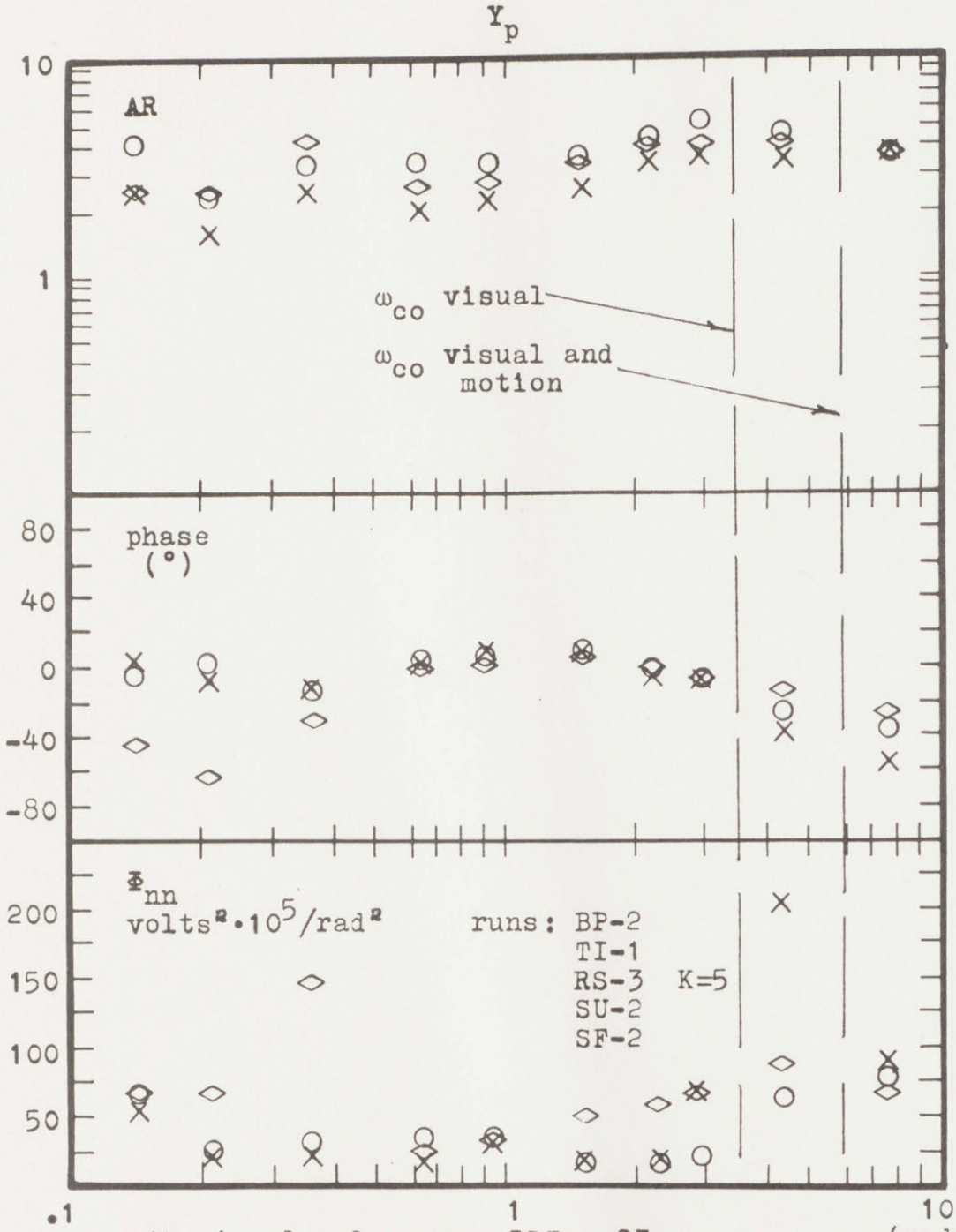

× visual only, mean rISE = .23
◇ motion only, mean rISE = .21
○ visual and motion, mean rISE = .16 **ISI=1050**

$$Y_c = \frac{e^{-.1s}}{s} \quad K=5$$

EXPERIMENTAL RESULTS

data-6

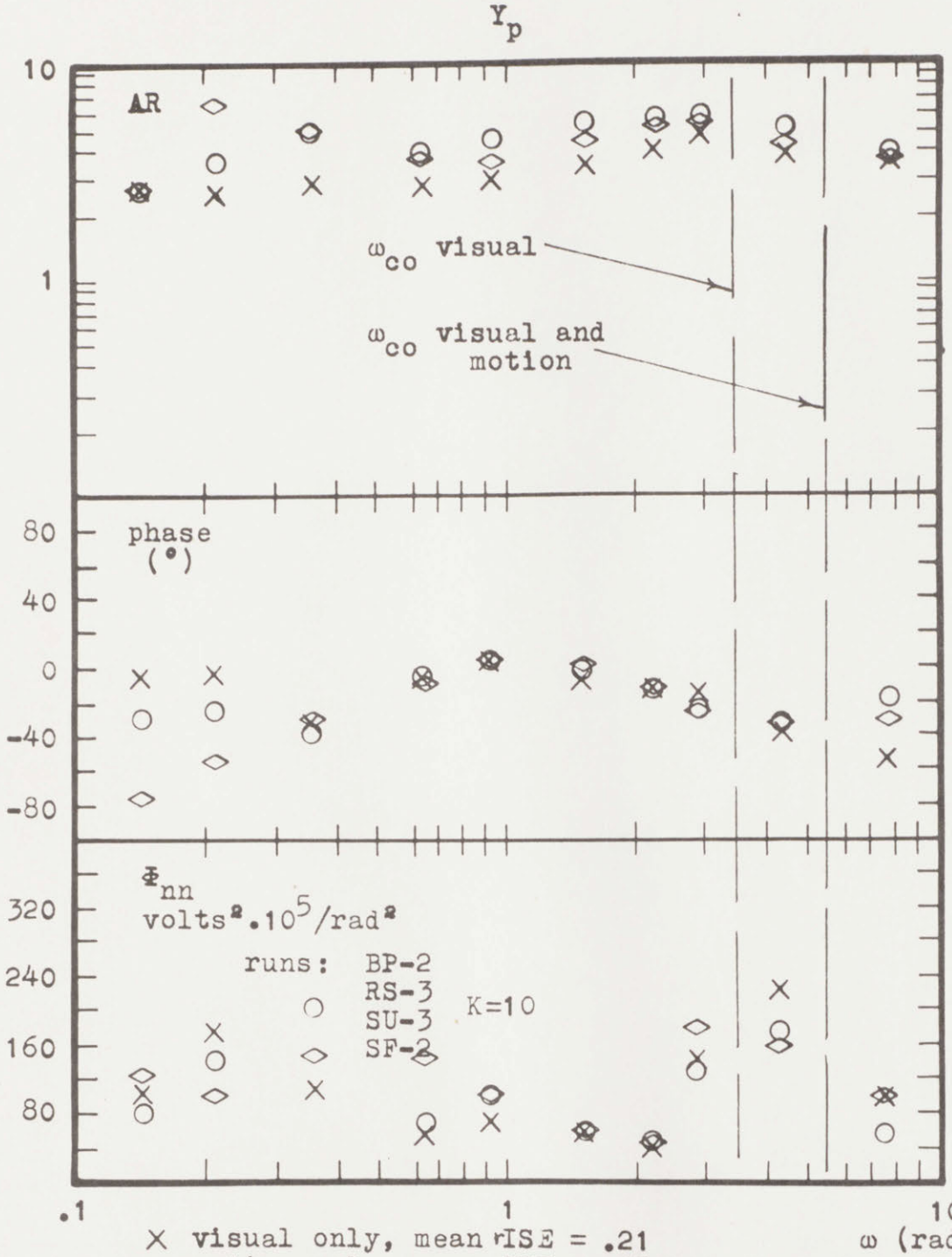

× visual only, mean rISE = .21
◇ motion only, mean rISE = .15
○ visual and motion, mean rISE = .13

ISI=1050

$$Y_c = \frac{e^{-.1s}}{s} \quad K=10$$

EXPERIMENTAL RESULTS

data-7

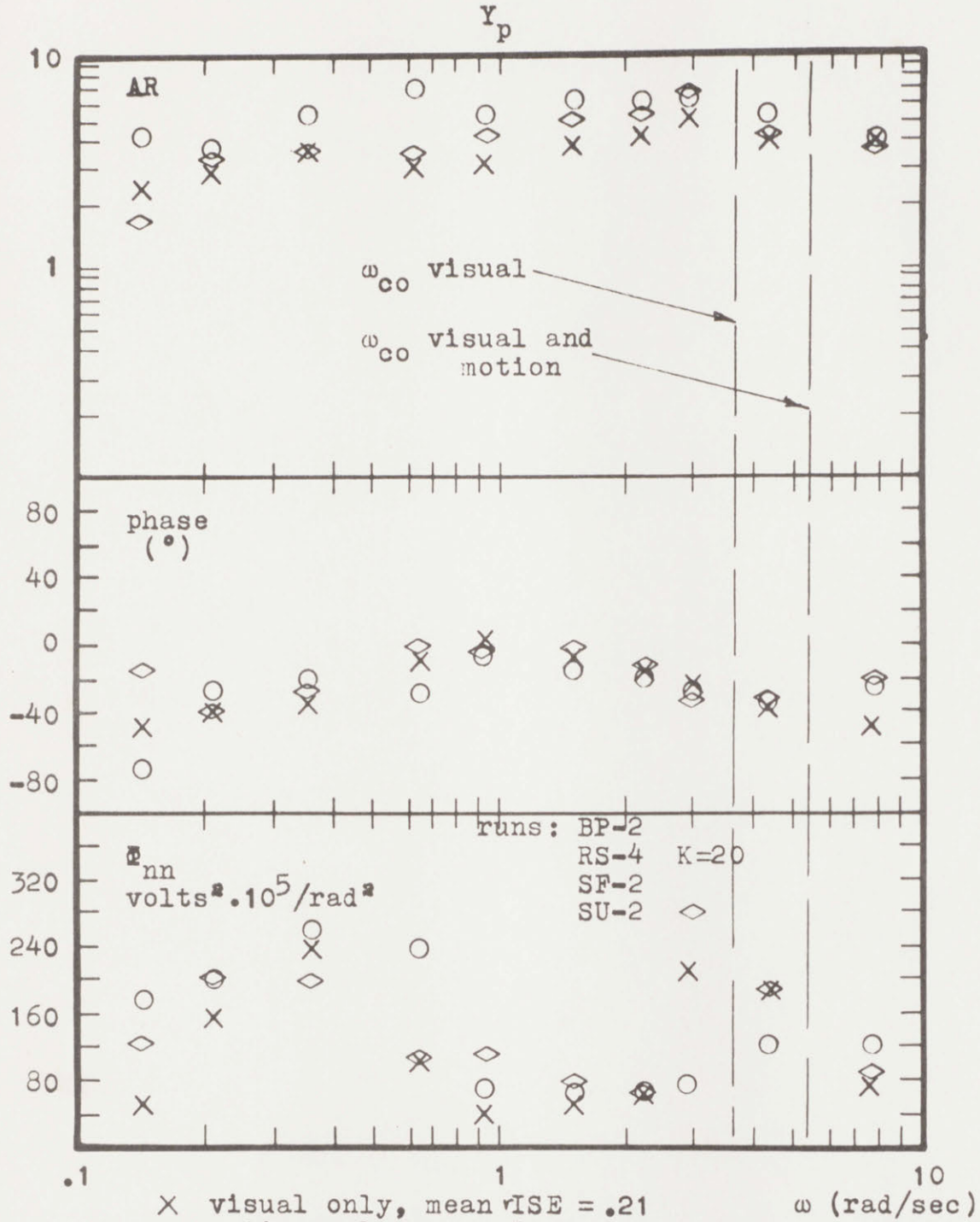

× visual only, mean rISE = .21
◇ motion only, mean rISE = .15
○ visual and motion, mean rISE = .12

ISI=1050

$$Y_c = \frac{e^{-.1s}}{s} \quad K=20$$

EXPERIMENTAL RESULTS

data-8

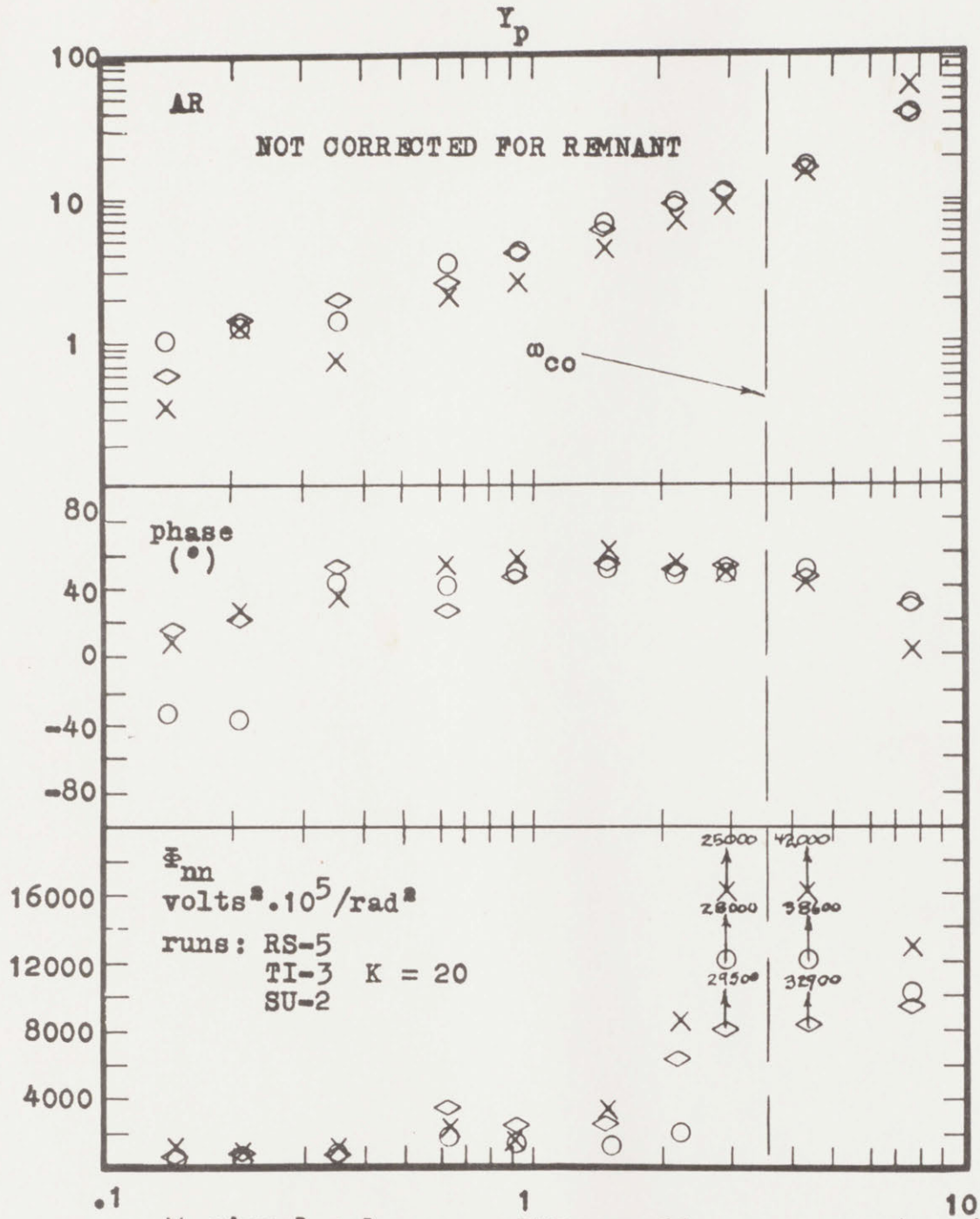

× visual only, mean rISE = 1.66
◇ motion only, mean rISE = 1.05
○ visual and motion, mean rISE = .83

ISI=1050

$$Y_c = \frac{-e^{-.1s}}{s(s-1)}, \quad K = 20$$

EXPERIMENTAL RESULTS

data-9

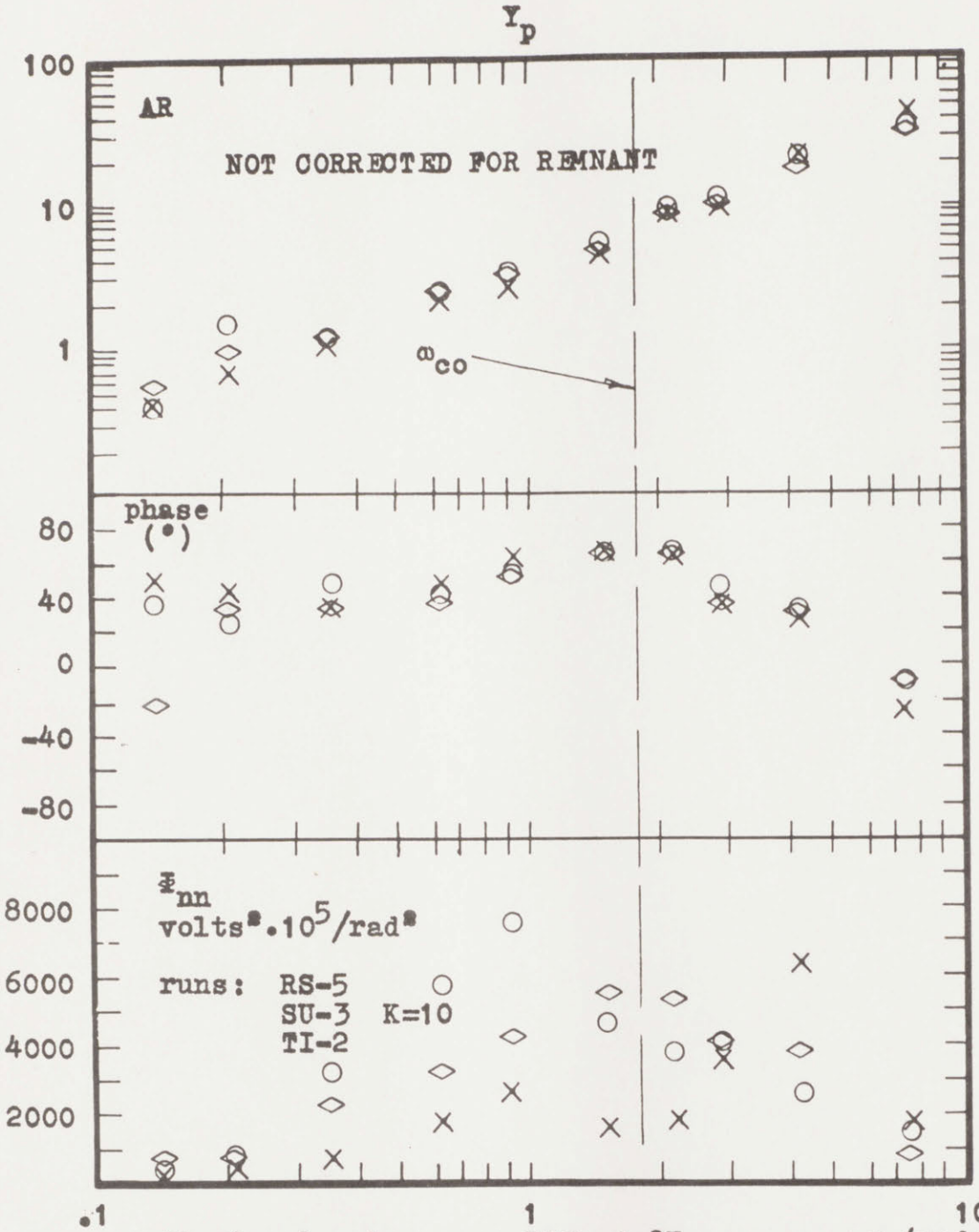

× visual only, mean rISE =1.87
◇ motion only, mean rISE =1.90
○ visual and motion, mean rISE =1.52

$$Y_c = \frac{-.5e^{-.1s}}{s(s - .5)}, \quad K=10$$

EXPERIMENTAL RESULTS

data-10

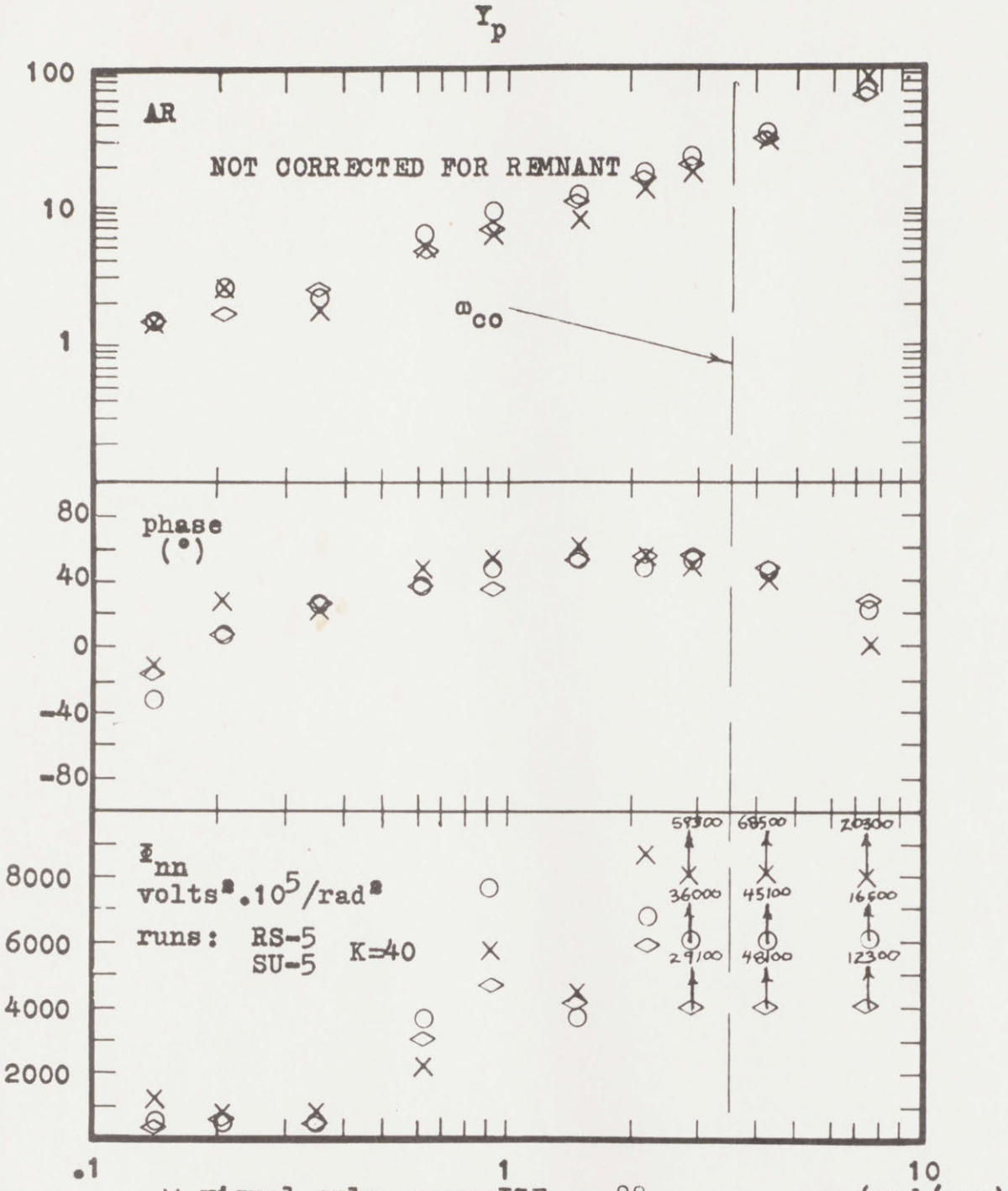

$$Y_c = \frac{-.5e^{-.1s}}{s(s - .5)}, \quad K=40$$

EXPERIMENTAL RESULTS

data-11

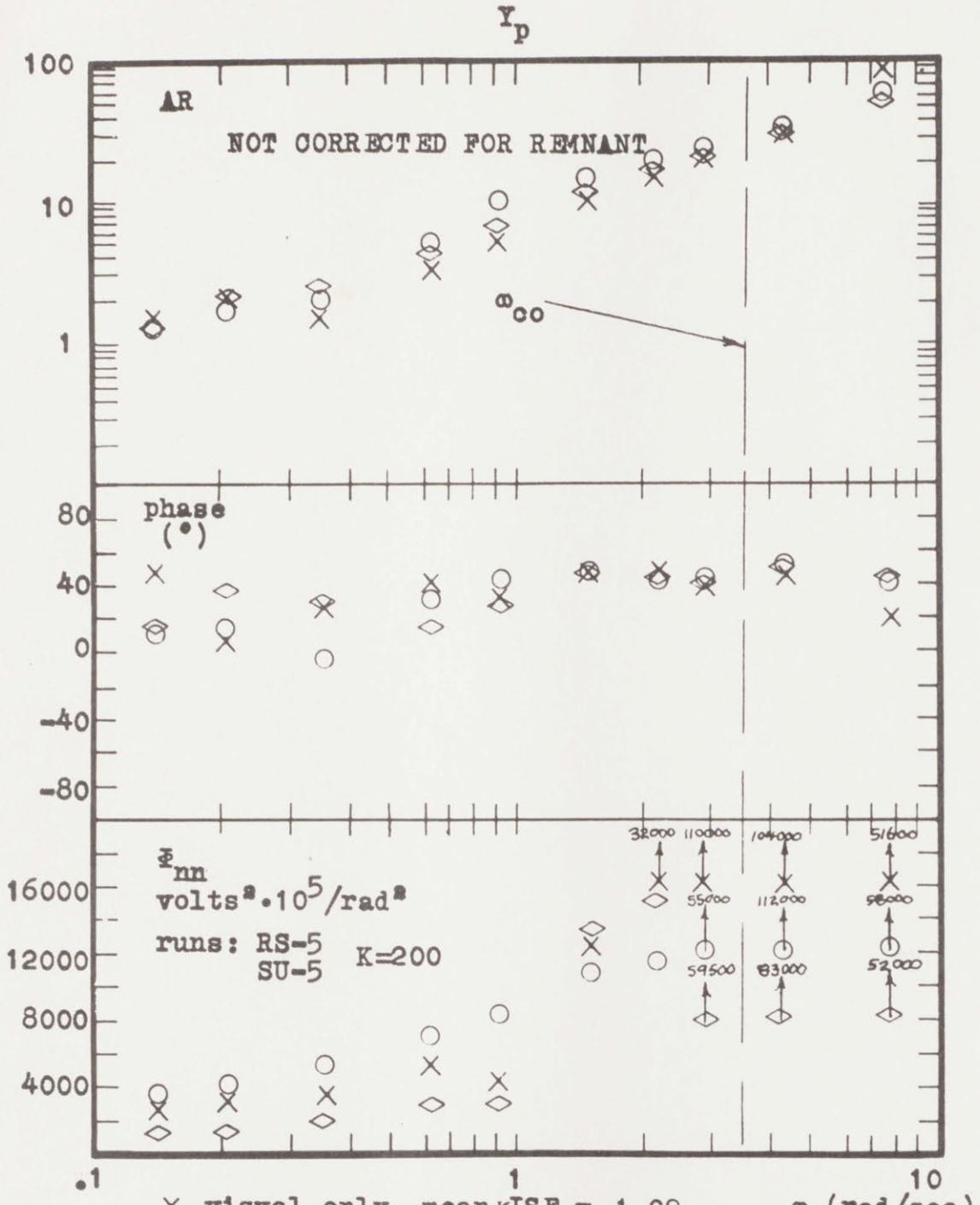

$$Y_c = \frac{-.5e^{-.1s}}{s(s - .5)}, \quad K=200$$

EXPERIMENTAL RESULTS

data-13

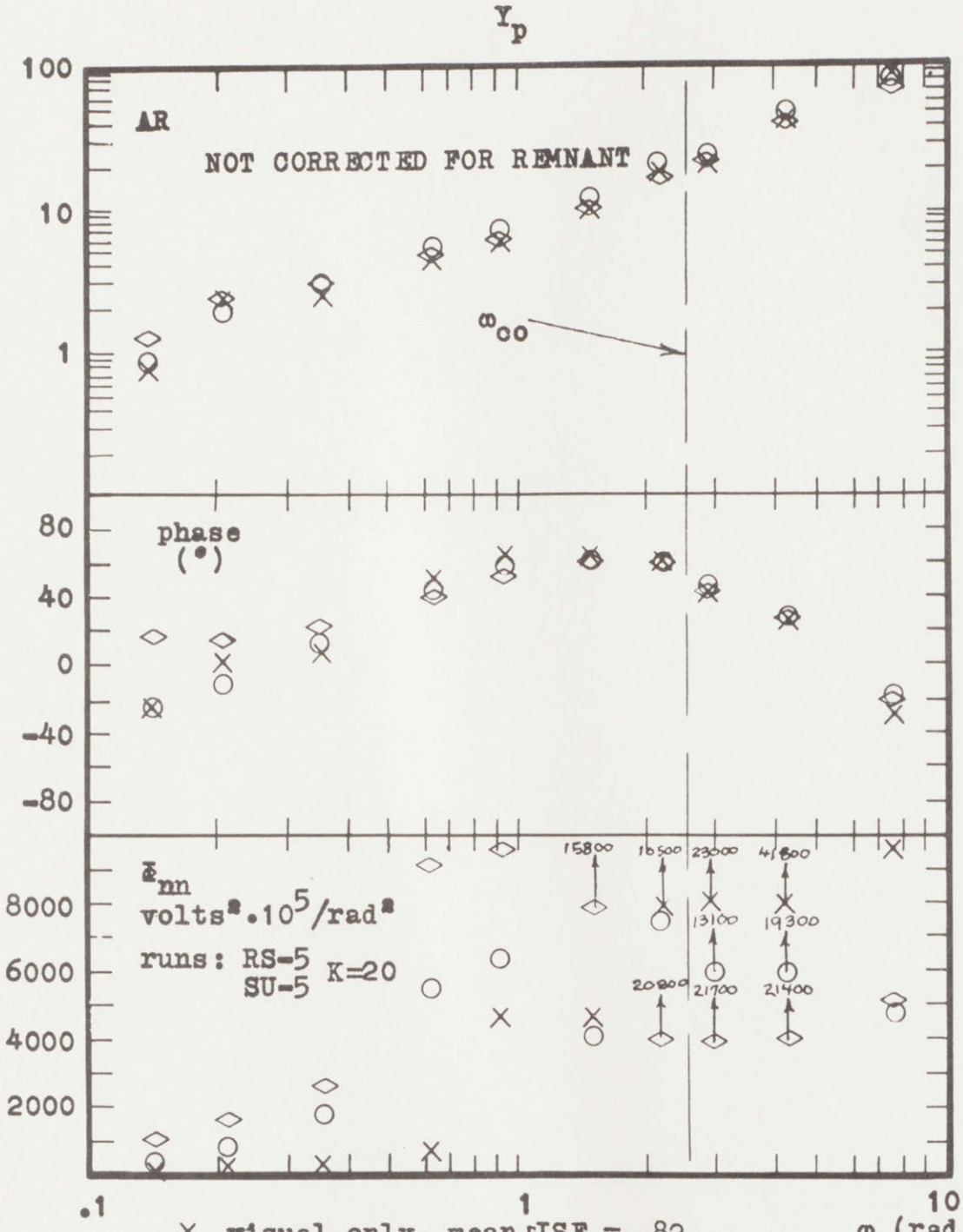

× visual only, mean rISE = .82
◇ motion only, mean rISE = .98
○ visual and motion, mean rISE = .65

ISI=1050

$$Y_c = \frac{-2.5e^{-.1s}}{s(s - .25)}, \quad K = 20$$

EXPERIMENTAL RESULTS

data-14

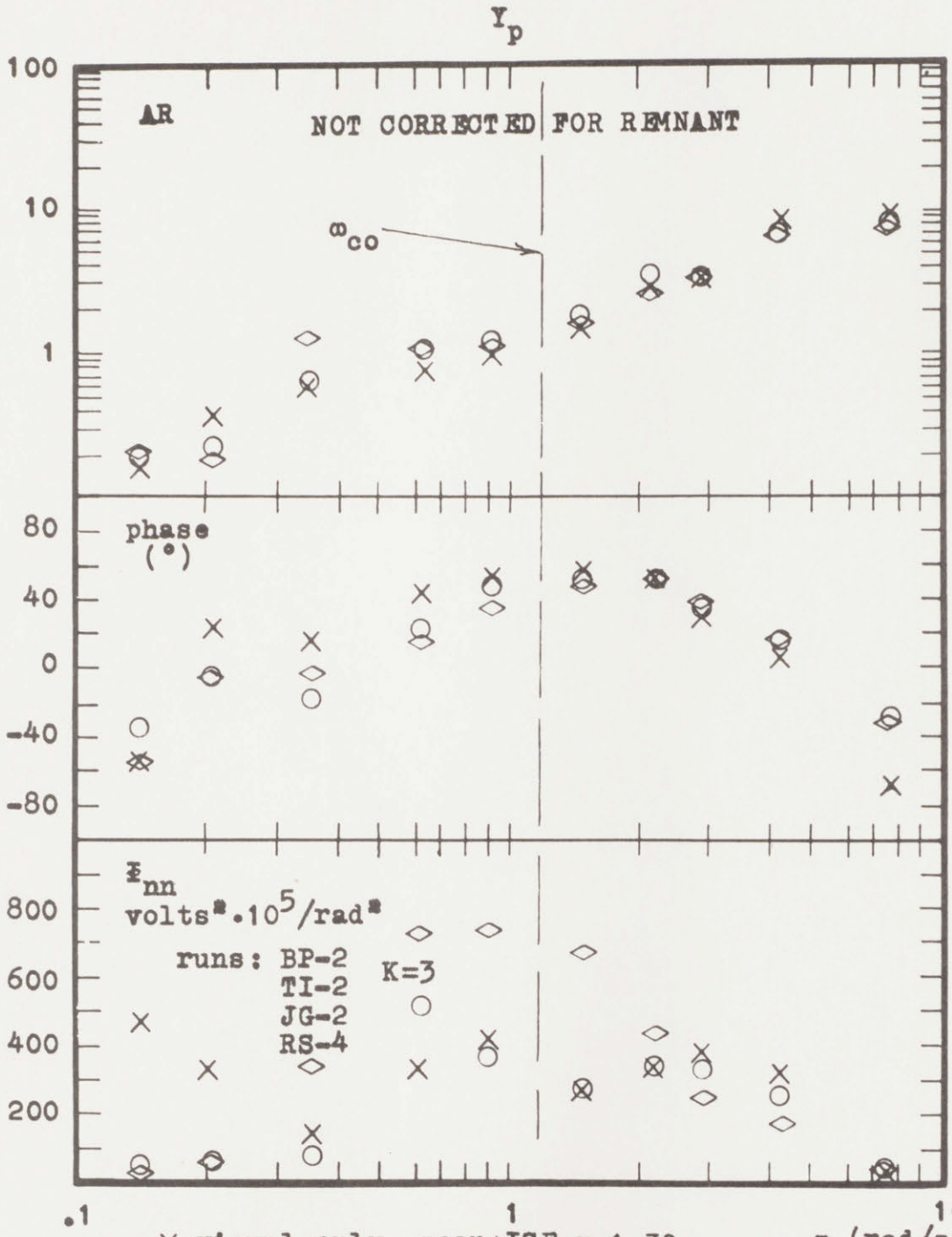

EXPERIMENTAL RESULTS

data-15

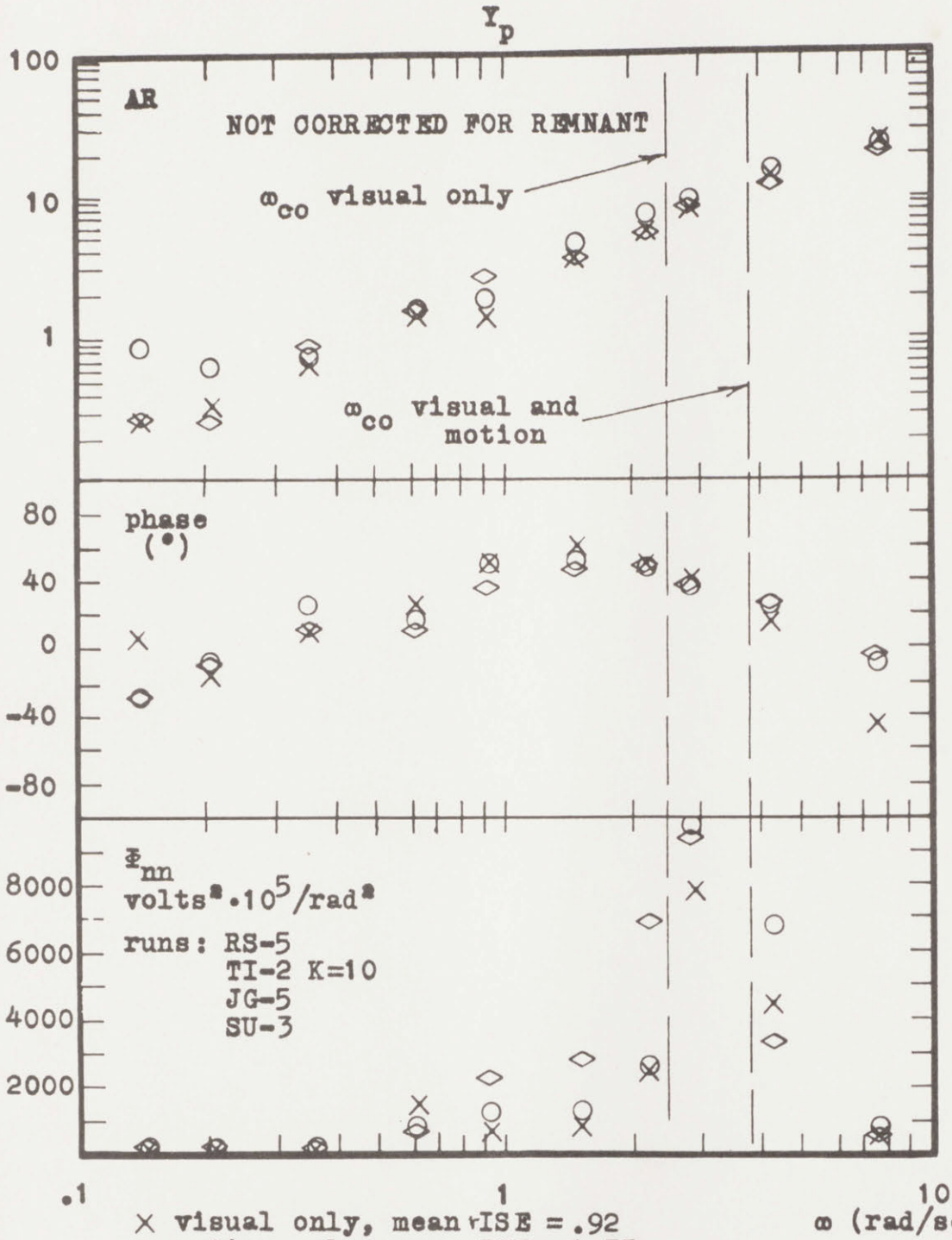

× visual only, mean rISE = .92
◇ motion only, mean rISE = 1.33
○ visual and motion, mean rISE = .75

ISI=1050

$$Y_c = \frac{e^{-.1s}}{s^2} \quad K=10$$

EXPERIMENTAL RESULTS

data-16

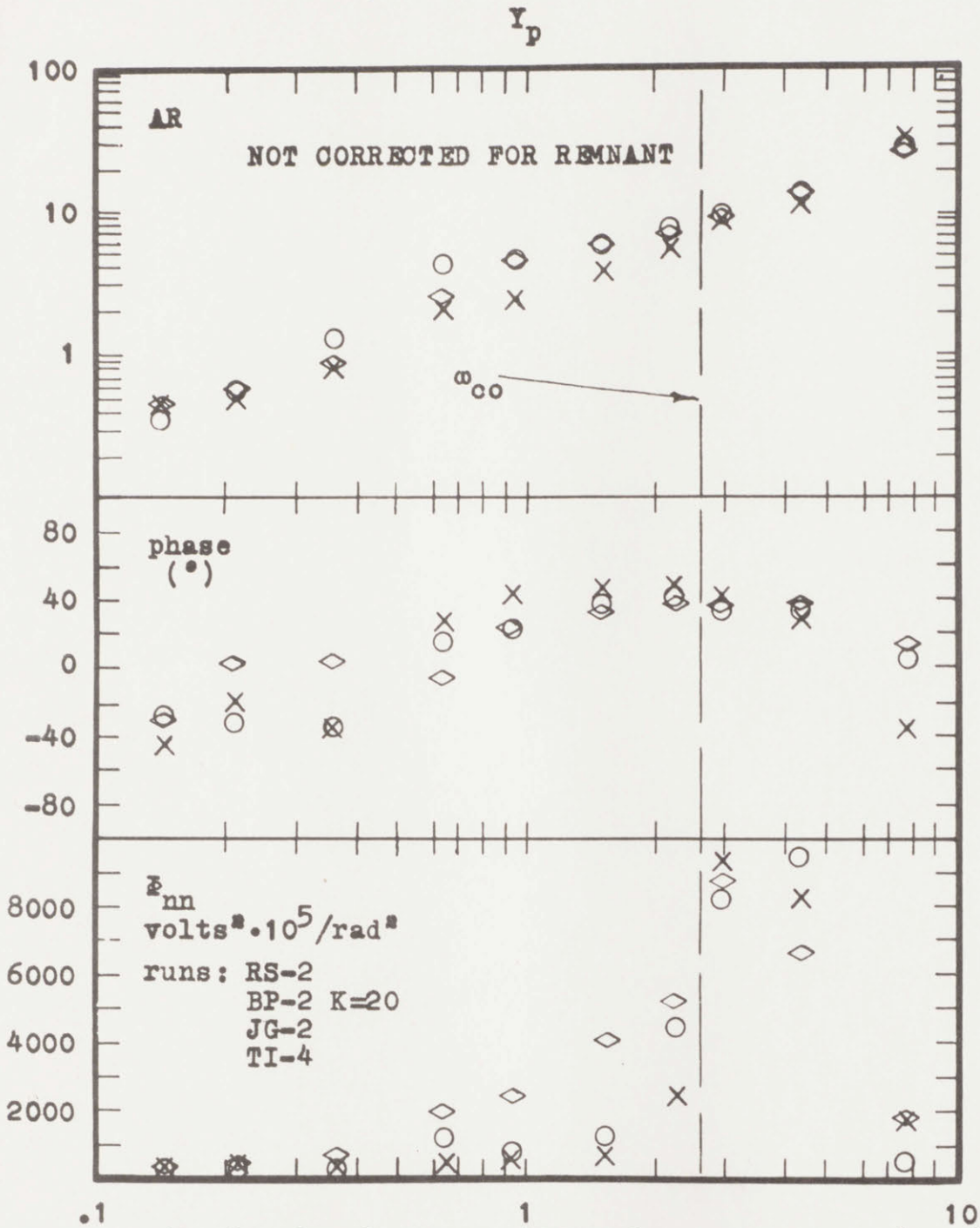

× visual only, mean rISE = .81
◇ motion only, mean rISE = .80
○ visual and motion, mean rISE = .55

ISI=1050

$$Y_c = \frac{e^{-.1s}}{s^2} \quad K=20$$

EXPERIMENTAL RESULTS

data-17

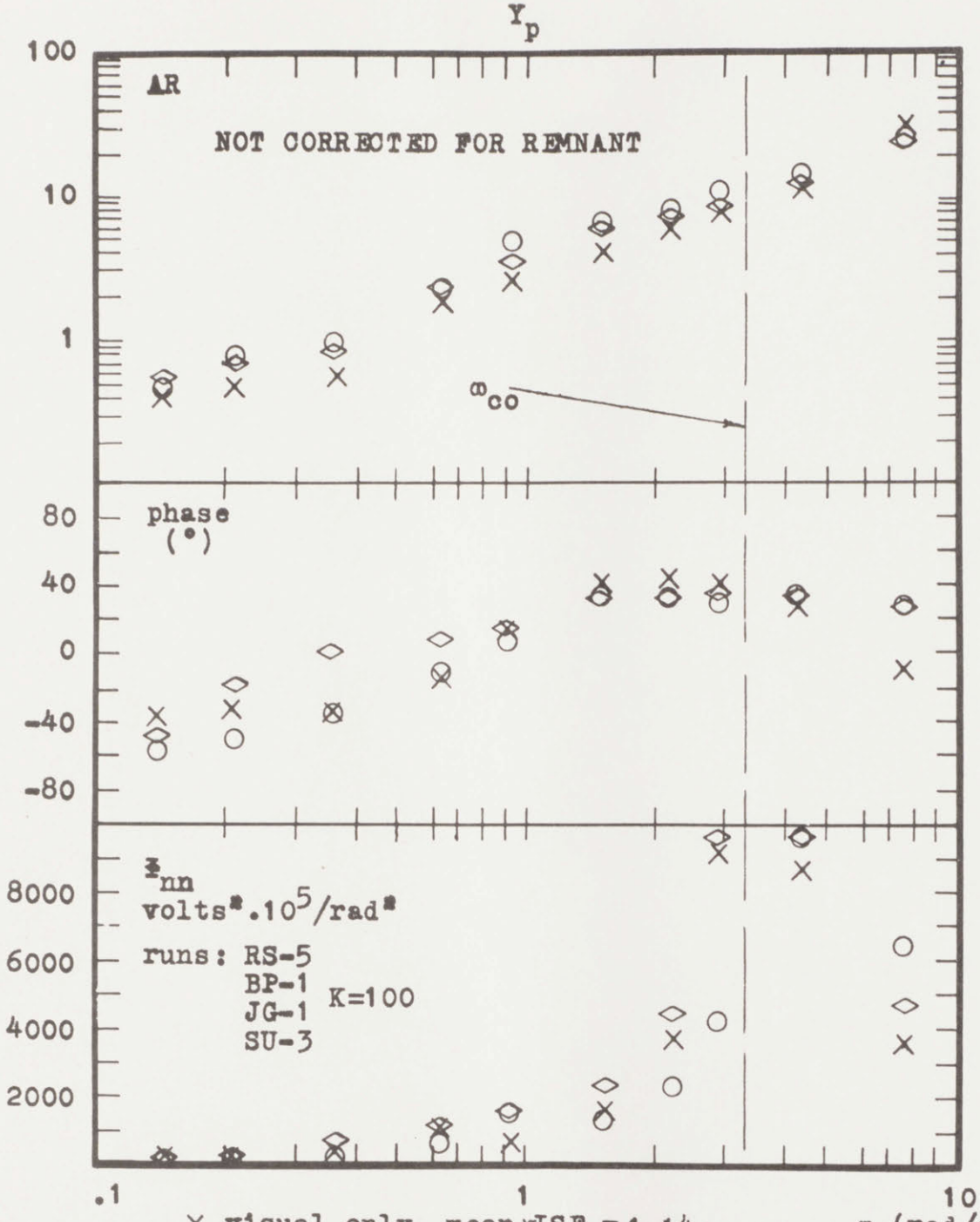

× visual only, mean rISE = 1.14
◇ motion only, mean rISE = 1.00
○ visual and motion, mean rISE = .51

ISI=1050

$$Y_c = \frac{e^{-.1s}}{s^2} \quad K=100$$

EXPERIMENTAL RESULTS

data-18

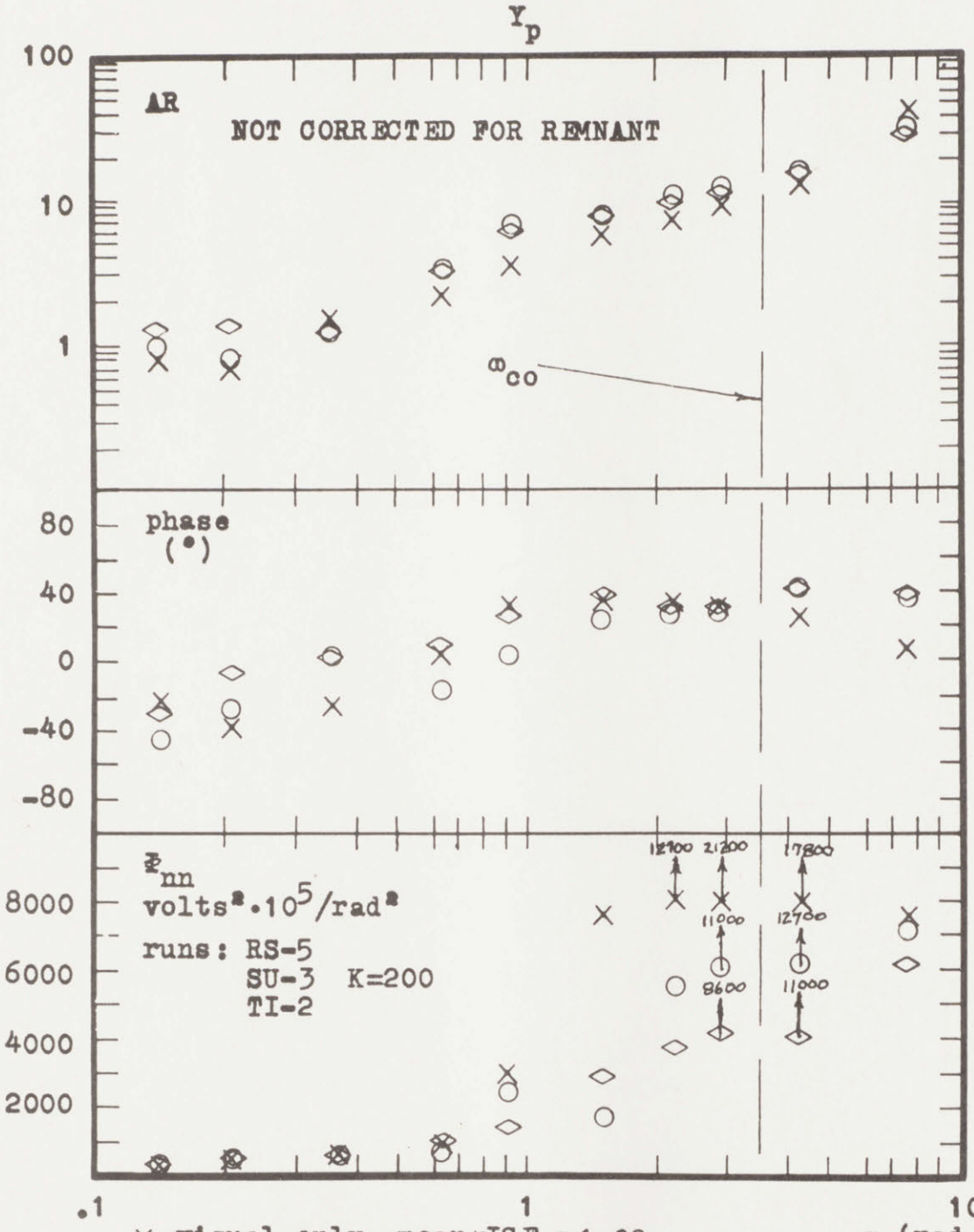

× visual only, mean rISE = 1.09
◇ motion only, mean rISE = .57
○ visual and motion, mean rISE = .44

ISI=1050

$$Y_c = \frac{e^{-.1s}}{s^2} \quad K=200$$

EXPERIMENTAL RESULTS

data-19

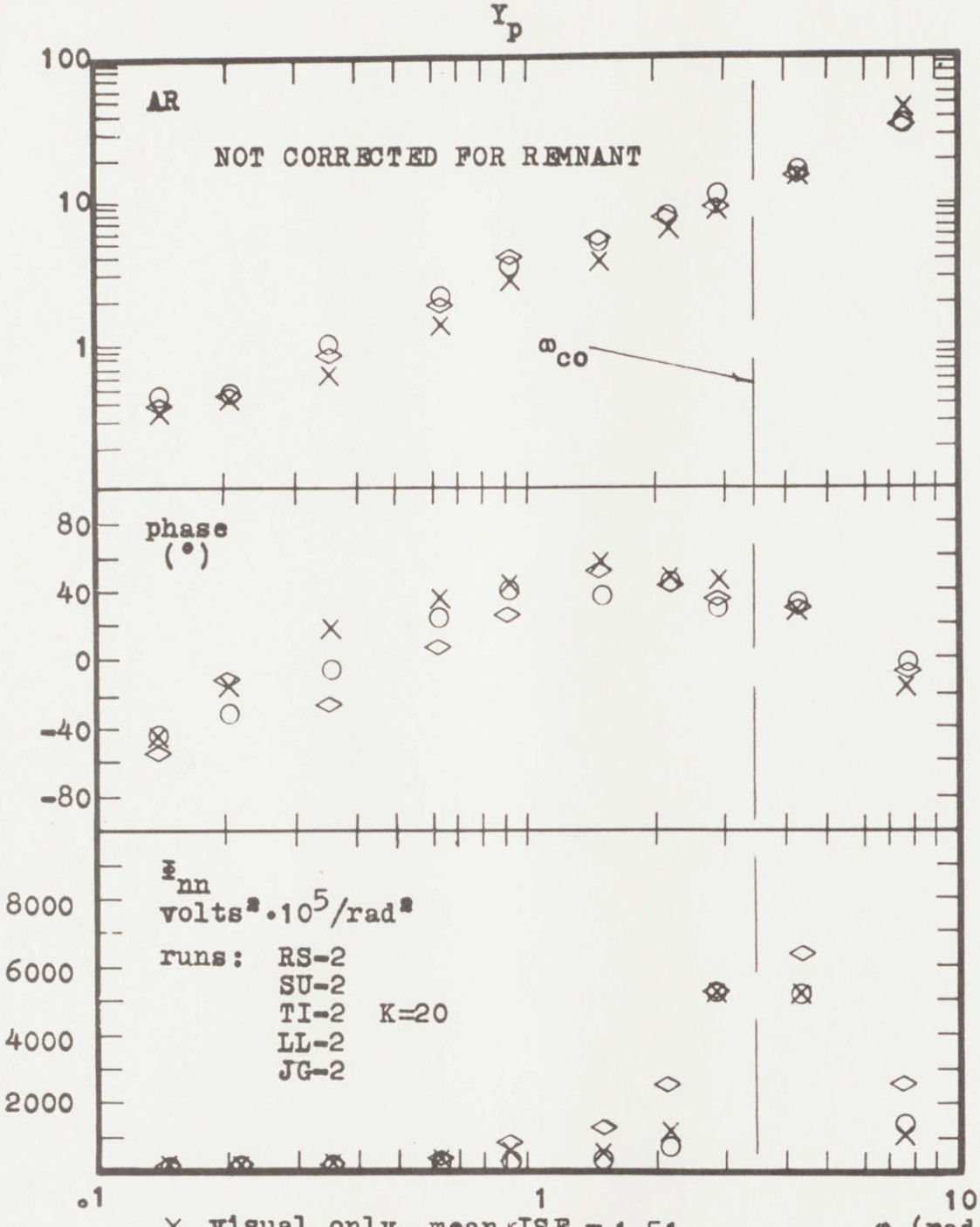

× visual only, mean rISE = 1.51
◇ motion only, mean rISE = 1.92
○ visual and motion, mean rISE = .97

ISI=262

$Y_c = \frac{e^{-.1s}}{s^2}$ K=20, K'=.5 (K' multiplies the input)

EXPERIMENTAL RESULTS

data-20

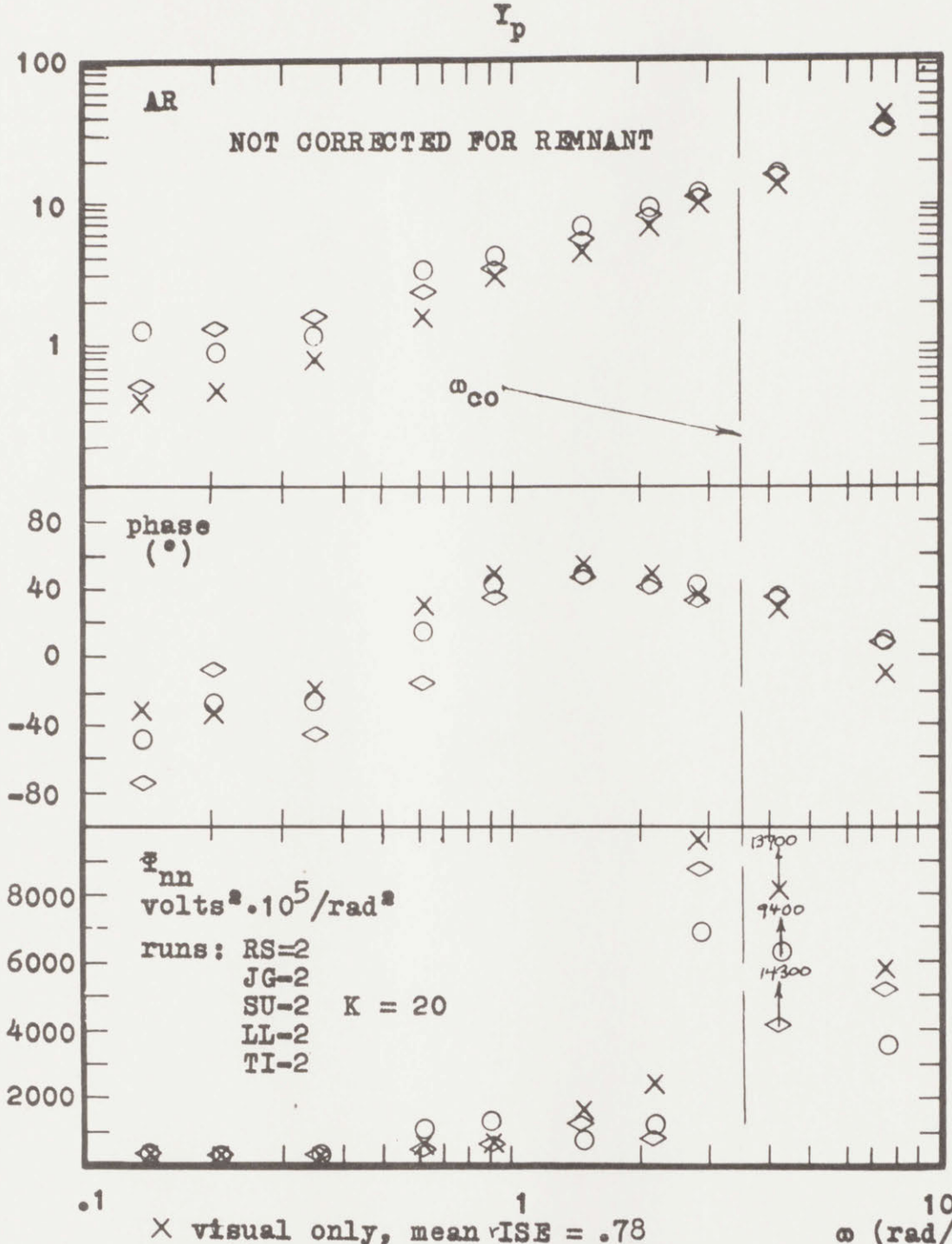

× visual only, mean rISE = .78
◇ motion only, mean rISE = .98
○ visual and motion, mean rISE = .51

ISI=591

$$Y_c = \frac{e^{-.1s}}{s^2} \quad K = 20,\ K' = .75$$

(K' multiplies the input)

EXPERIMENTAL RESULTS

data-21

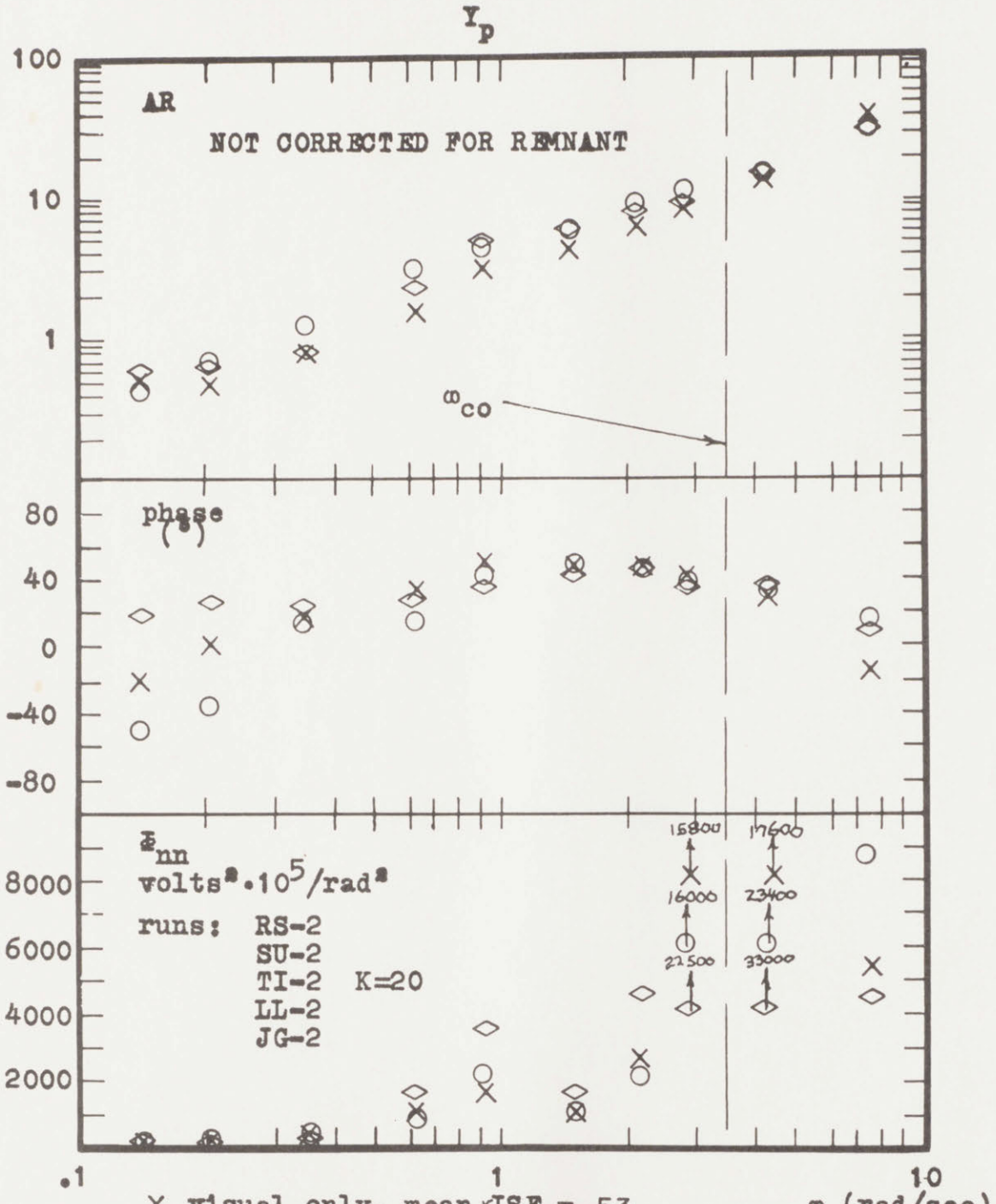

EXPERIMENTAL RESULTS

data-22

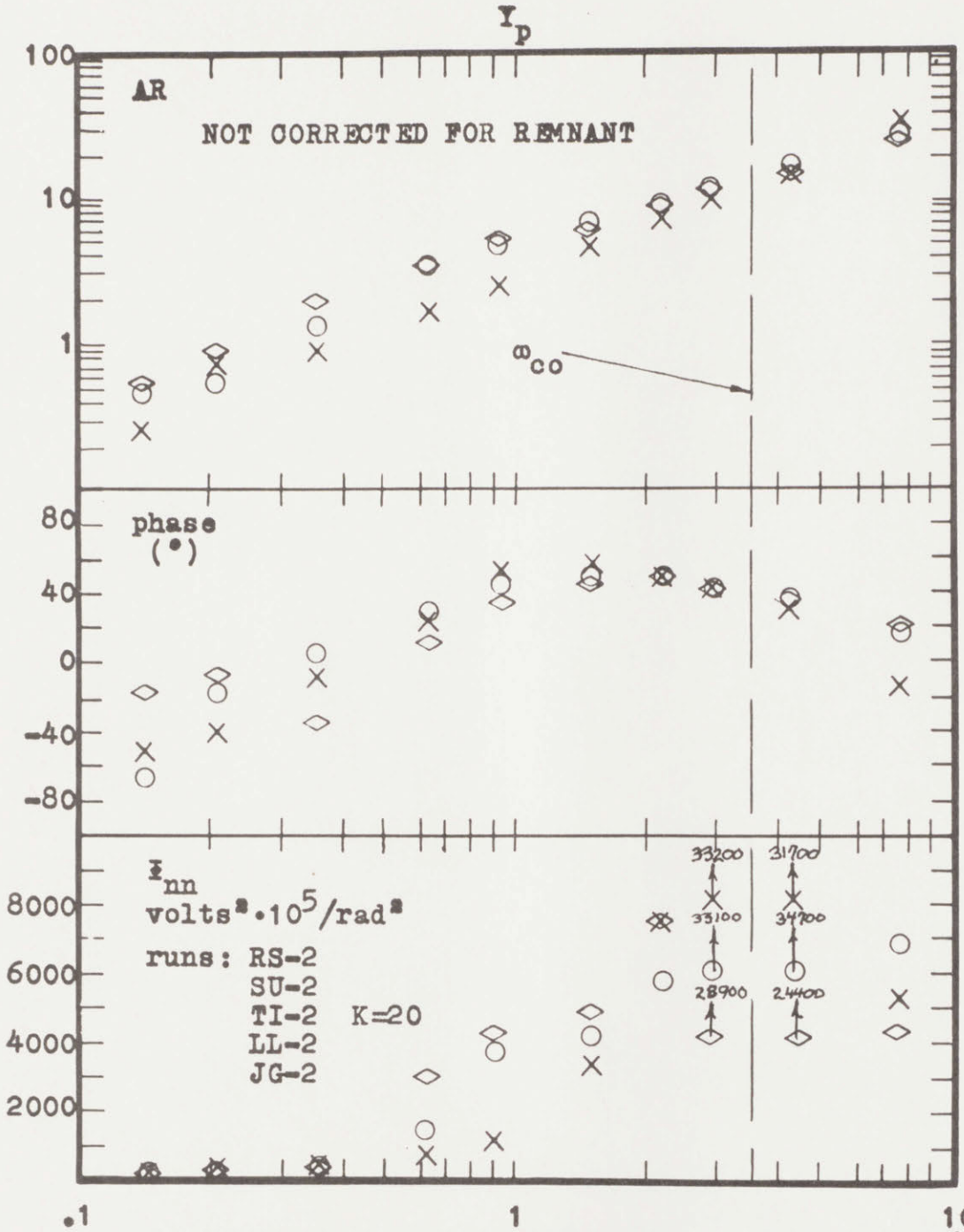

× visual only, mean rISE = .52
◇ motion only, mean rISE = .36
○ visual and motion, mean rISE = .31

$Y_c = \frac{e^{-.1s}}{s^2}$ K=20, K'=2 (K' multiplies the input)

EXPERIMENTAL RESULTS

data-23

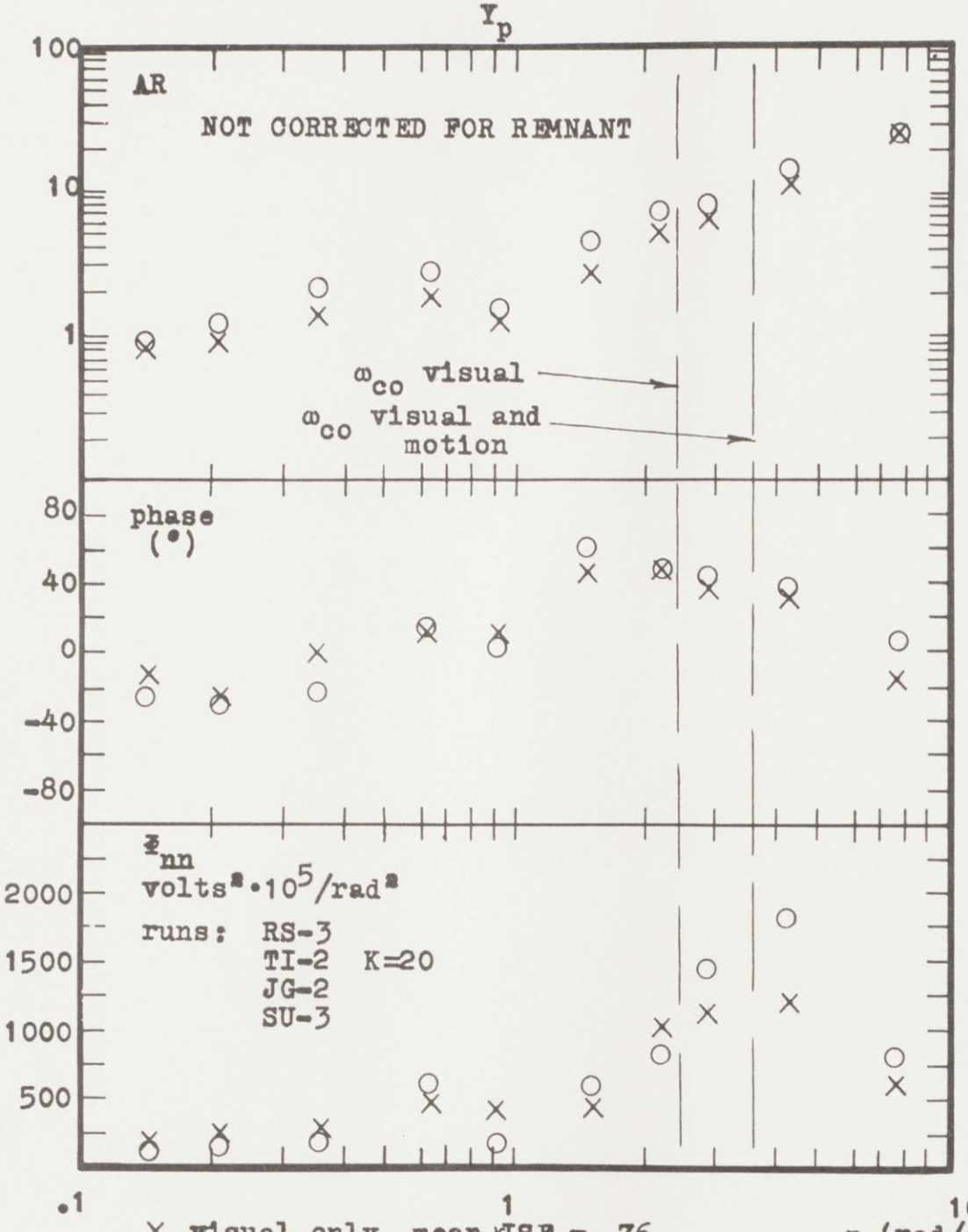

× visual only, mean rISE = .76
○ motion and visual, mean rISE =.62
ISI=417

$Y_c = \frac{e^{-.1s}}{s^2}$ K=20, breakpoint=.7 rad/sec

EXPERIMENTAL RESULTS

data-24

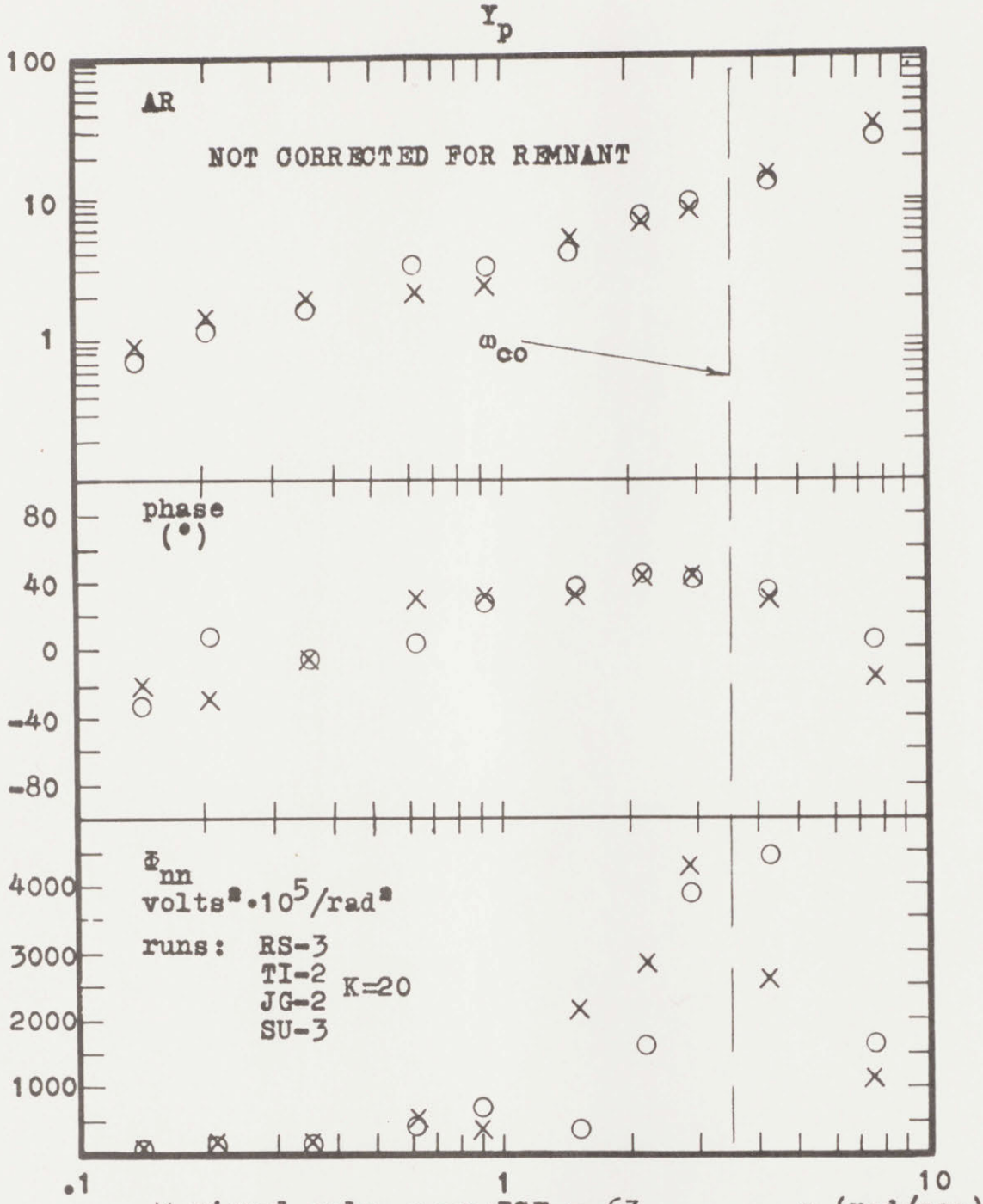

EXPERIMENTAL RESULTS

data-25

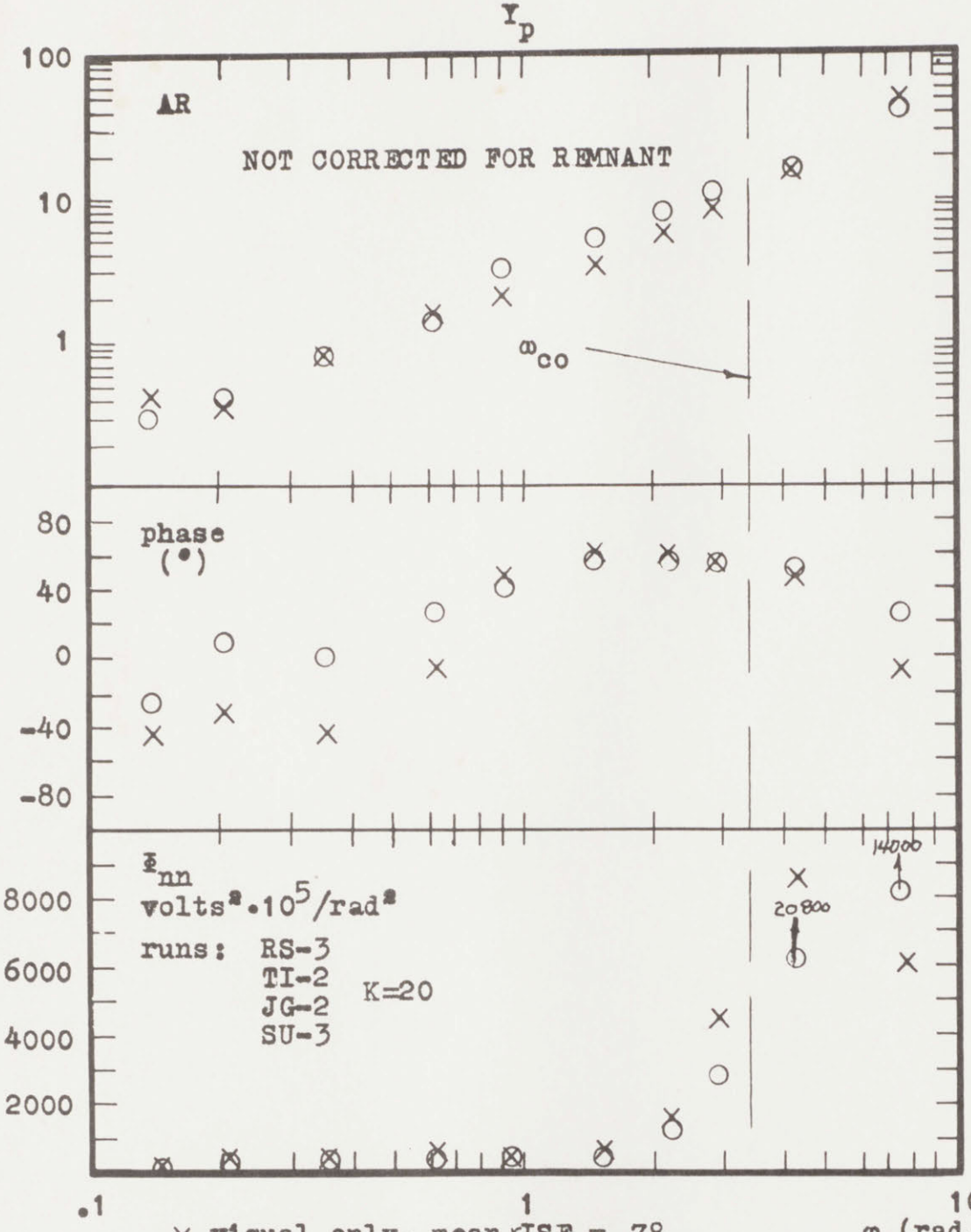

× visual only, mean rISE = .78

○ visual and motion, mean rISE = .51

ISI=1325

$Y_c = \frac{e^{-.1s}}{s^2}$ K=20, breakpoint=3.0 rad/sec

EXPERIMENTAL RESULTS

data-26

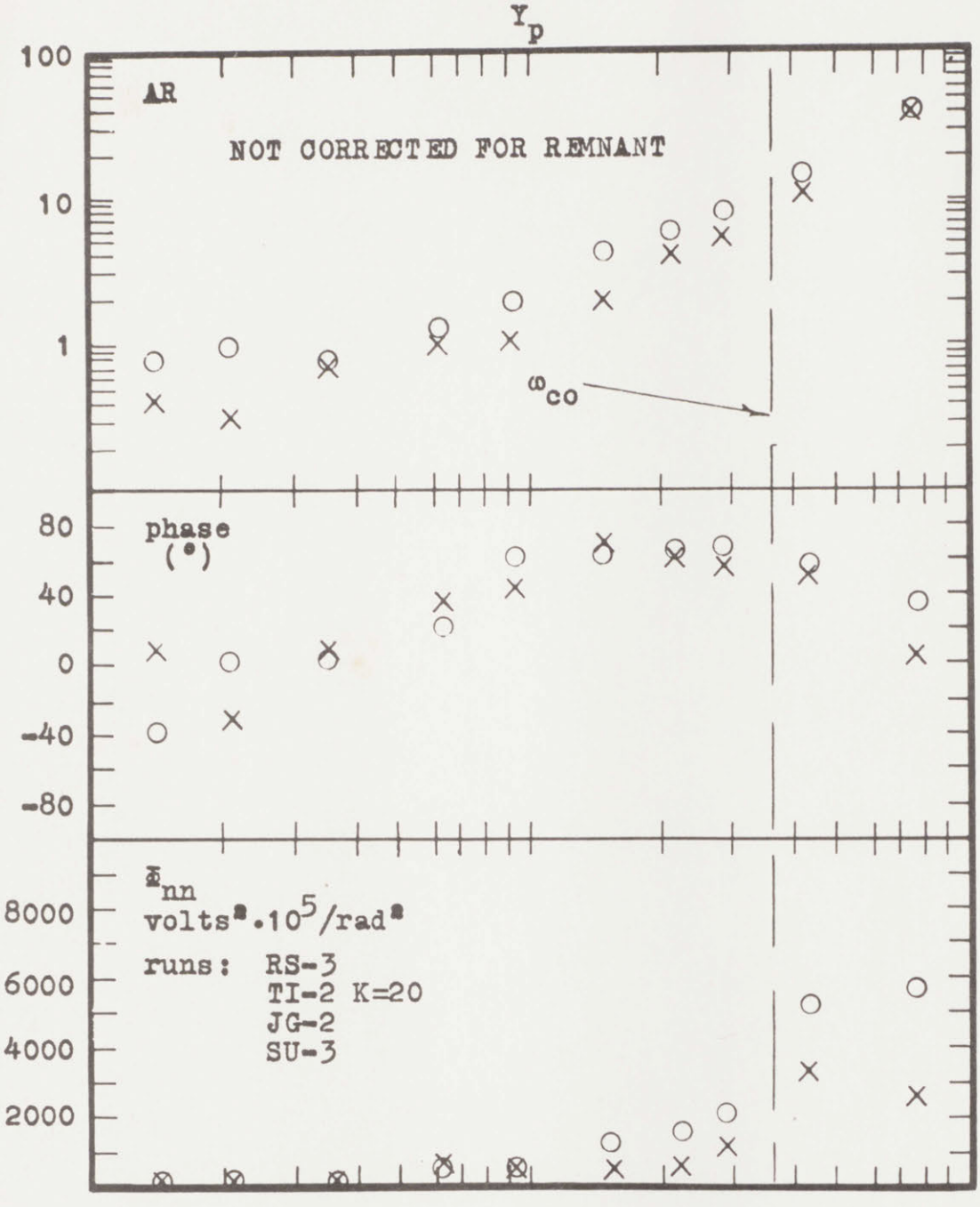

× visual only, mean rISE = 1.09

○ visual and motion, mean rISE = .68

ISI=1633

$Y_c = \frac{e^{-.1s}}{s^2}$ K=20, breakpoint=5.0 rad/sec

EXPERIMENTAL RESULTS

data-27

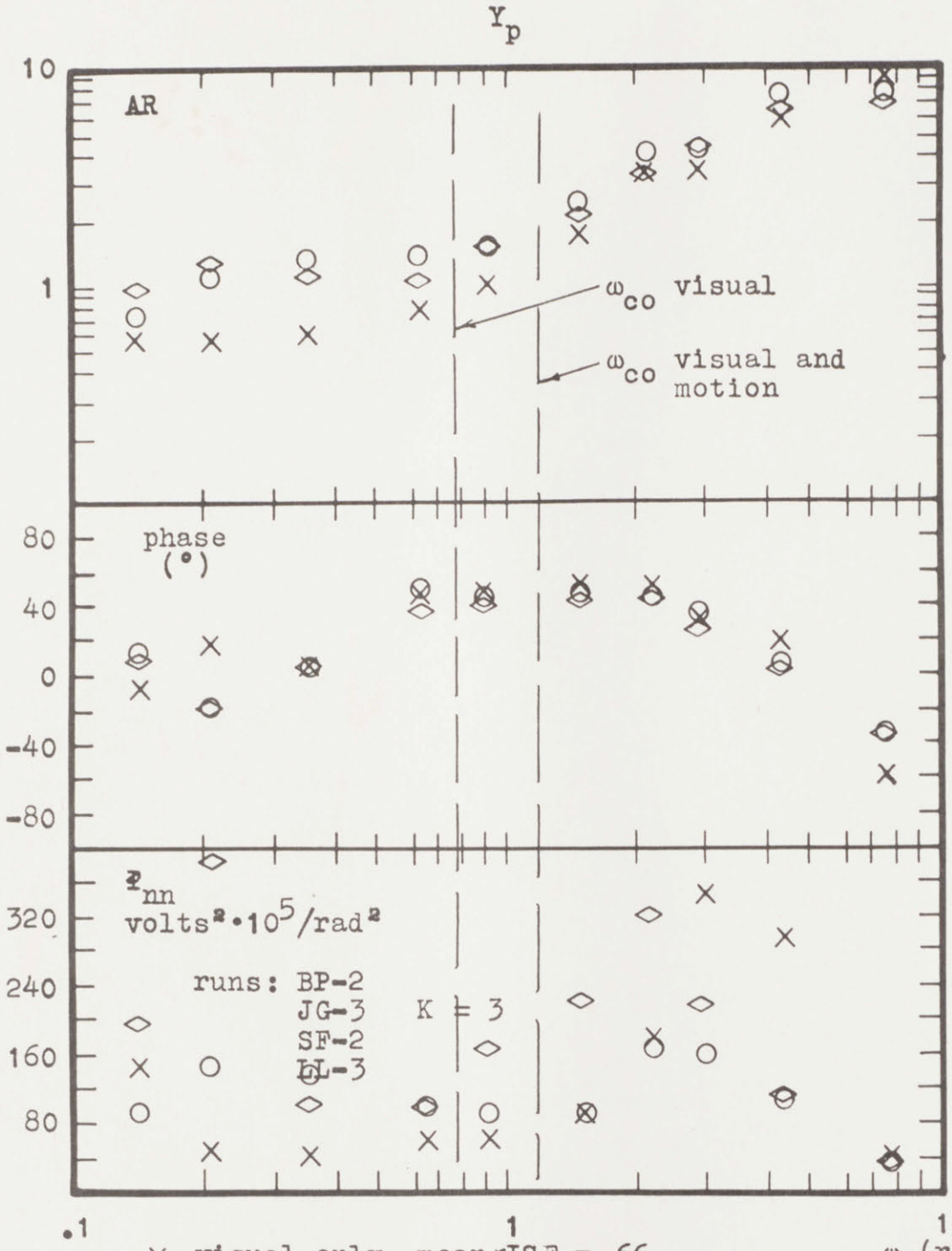

× visual only, mean rISE = .66
◇ motion only, mean rISE = .71
○ visual and motion, mean rISE = .54

ISI=1050

$$Y_c = \frac{e^{-.1s}}{s(s+1)}, \quad K = 3$$

EXPERIMENTAL RESULTS

data-28

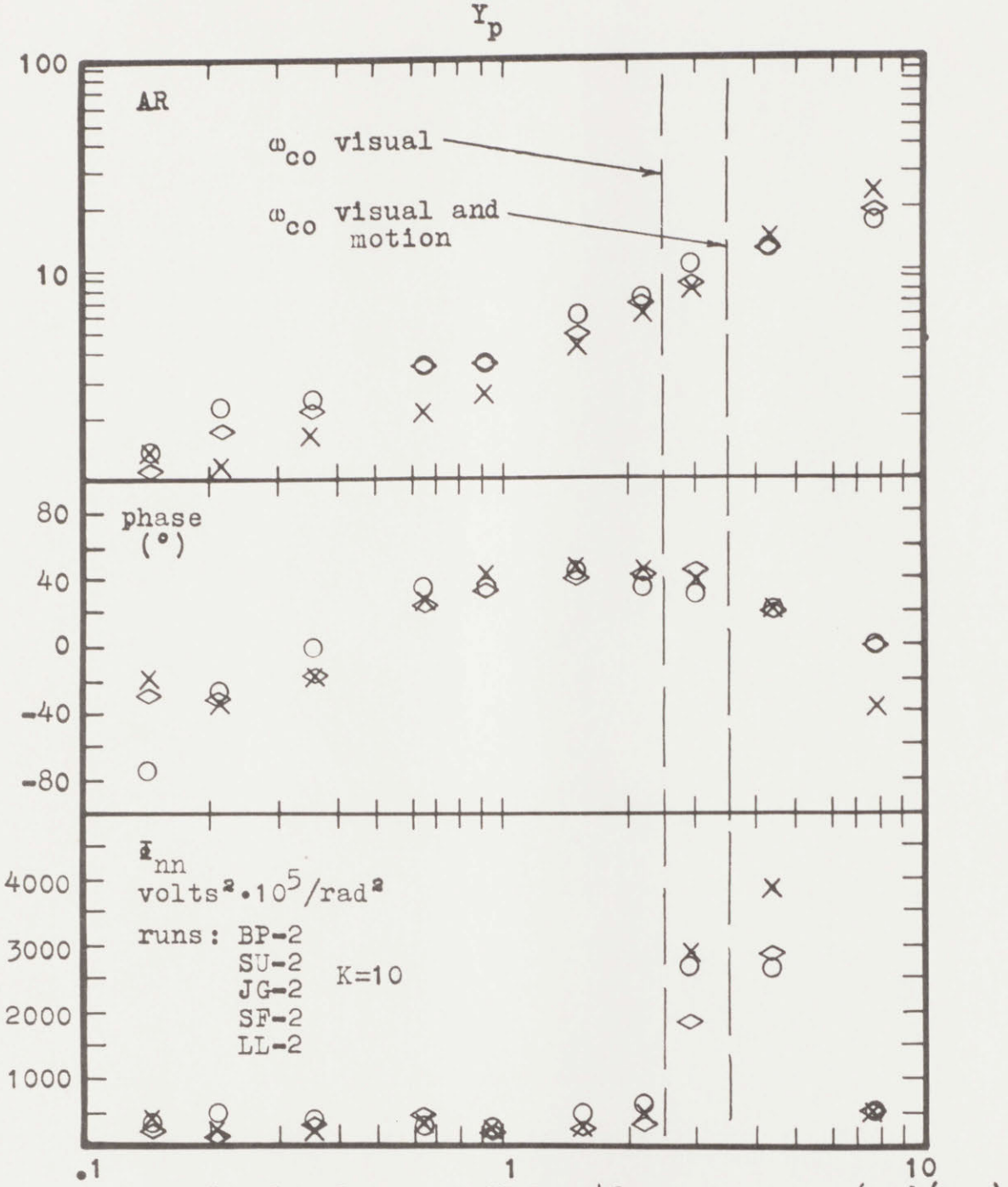

× visual only, mean rISE = .40
◇ motion only, mean rISE = .38
○ visual and motion, mean rISE = .32

$$Y_c = \frac{e^{-.1s}}{s(s+1)}, \quad K = 10$$

EXPERIMENTAL RESULTS

data-29

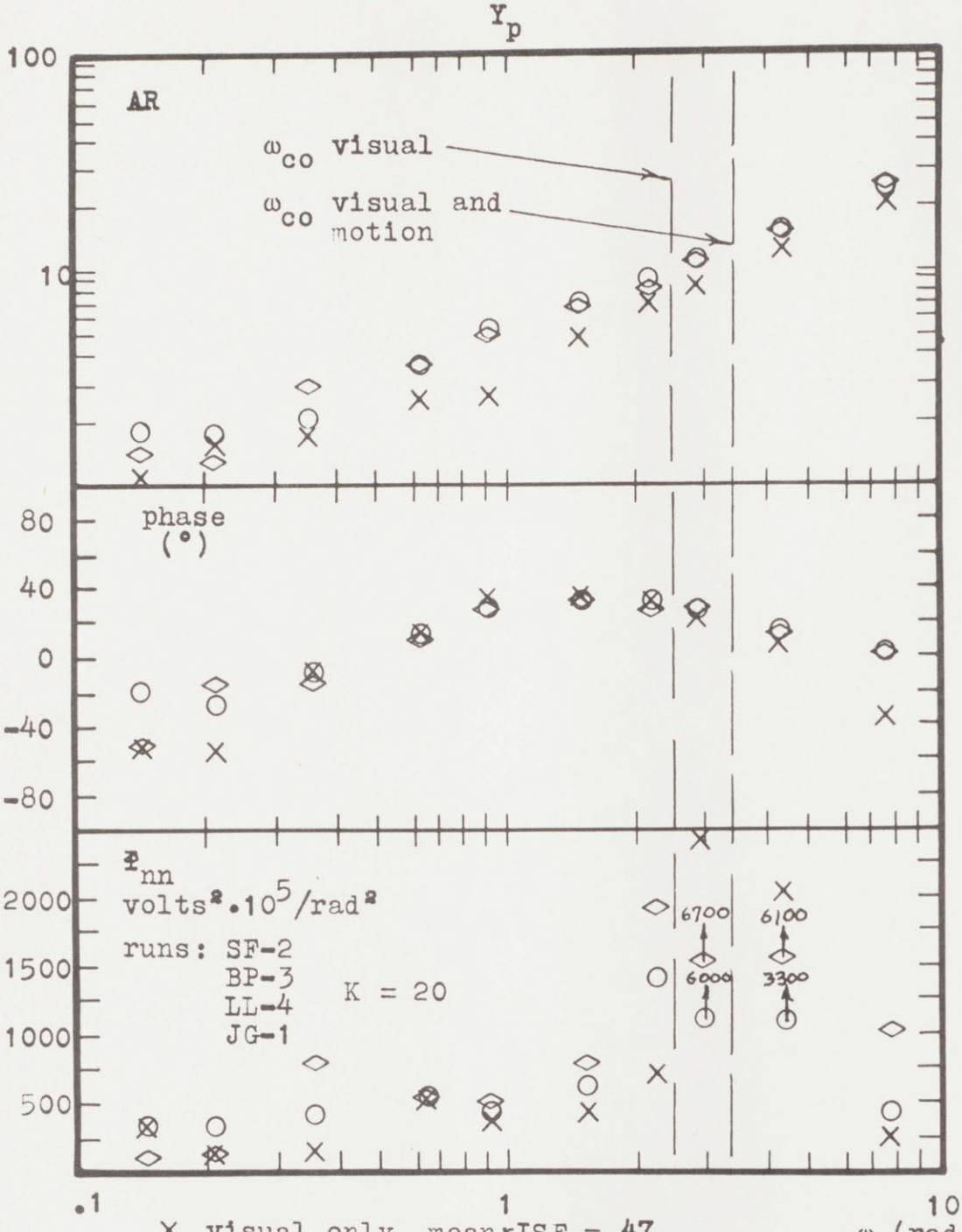

× visual only, mean rISE = .47
◇ motion only, mean rISE = .45
○ visual and motion, mean rISE = .30

ISI=1050

$$Y_c = \frac{e^{-.1s}}{s(s+1)}, \quad K = 20$$

EXPERIMENTAL RESULTS

data-30

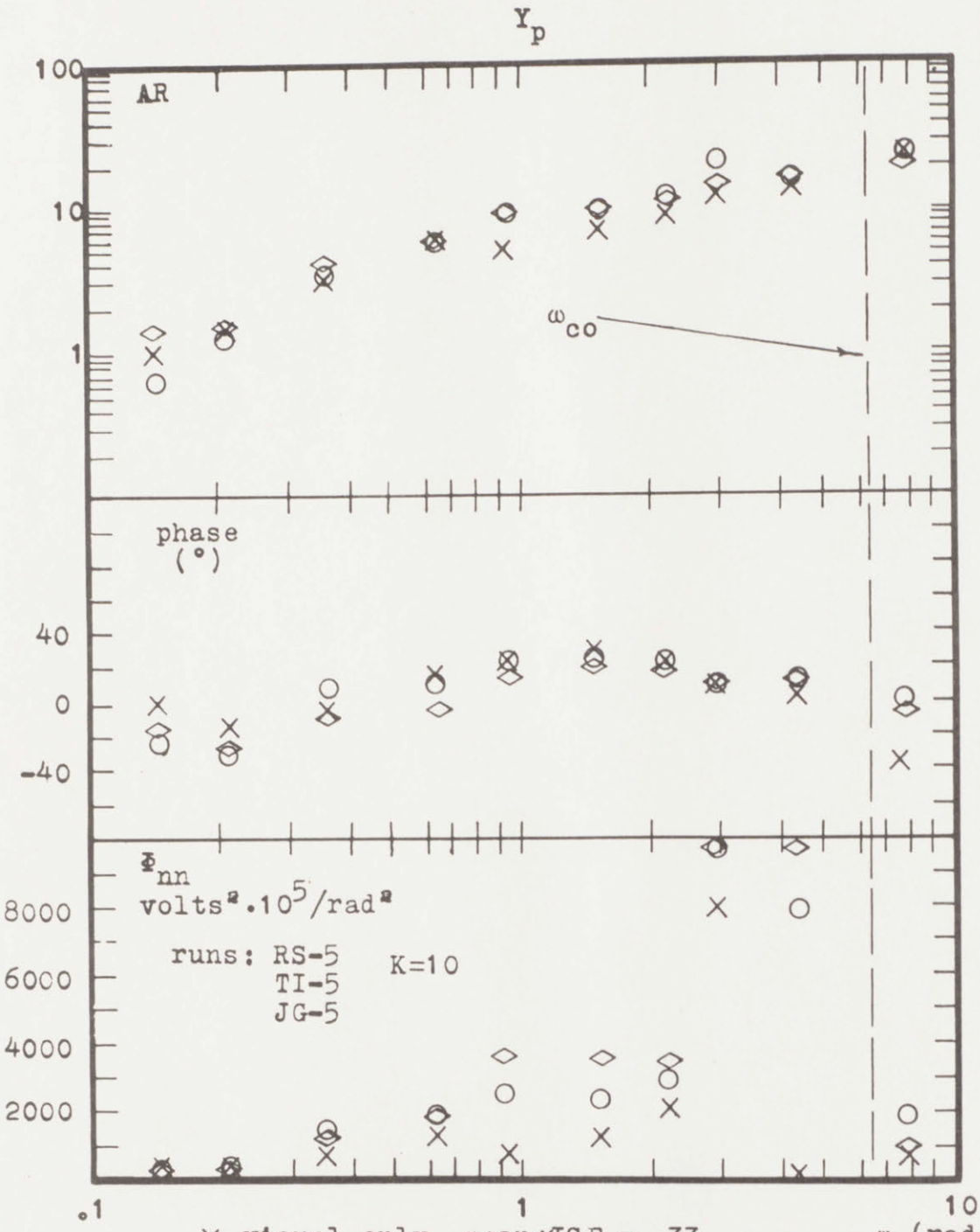

× visual only, mean rISE = .33
◇ motion only, mean rISE = .28
○ visual and motion, mean rISE = .24

$$Y_c = \frac{e^{-.1s}}{s(s+2)}$$

EXPERIMENTAL RESULTS

data-32

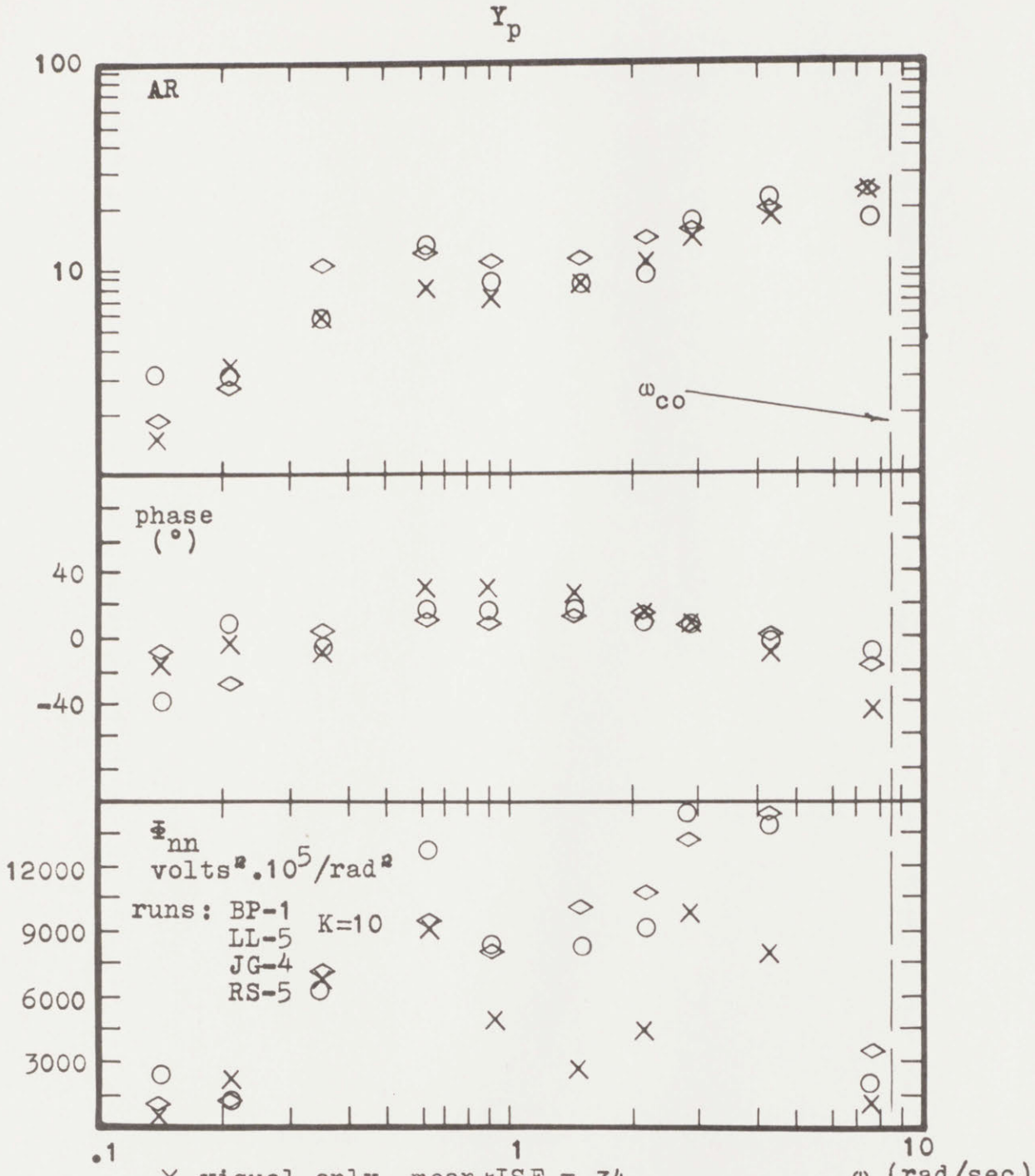

× visual only, mean rISE = .34
◇ motion only, mean rISE = .33
○ visual and motion, mean rISE = .24

ISI=1050

$$Y_c = \frac{e^{-.1s}}{s(s+4)}$$

EXPERIMENTAL RESULTS

data-33

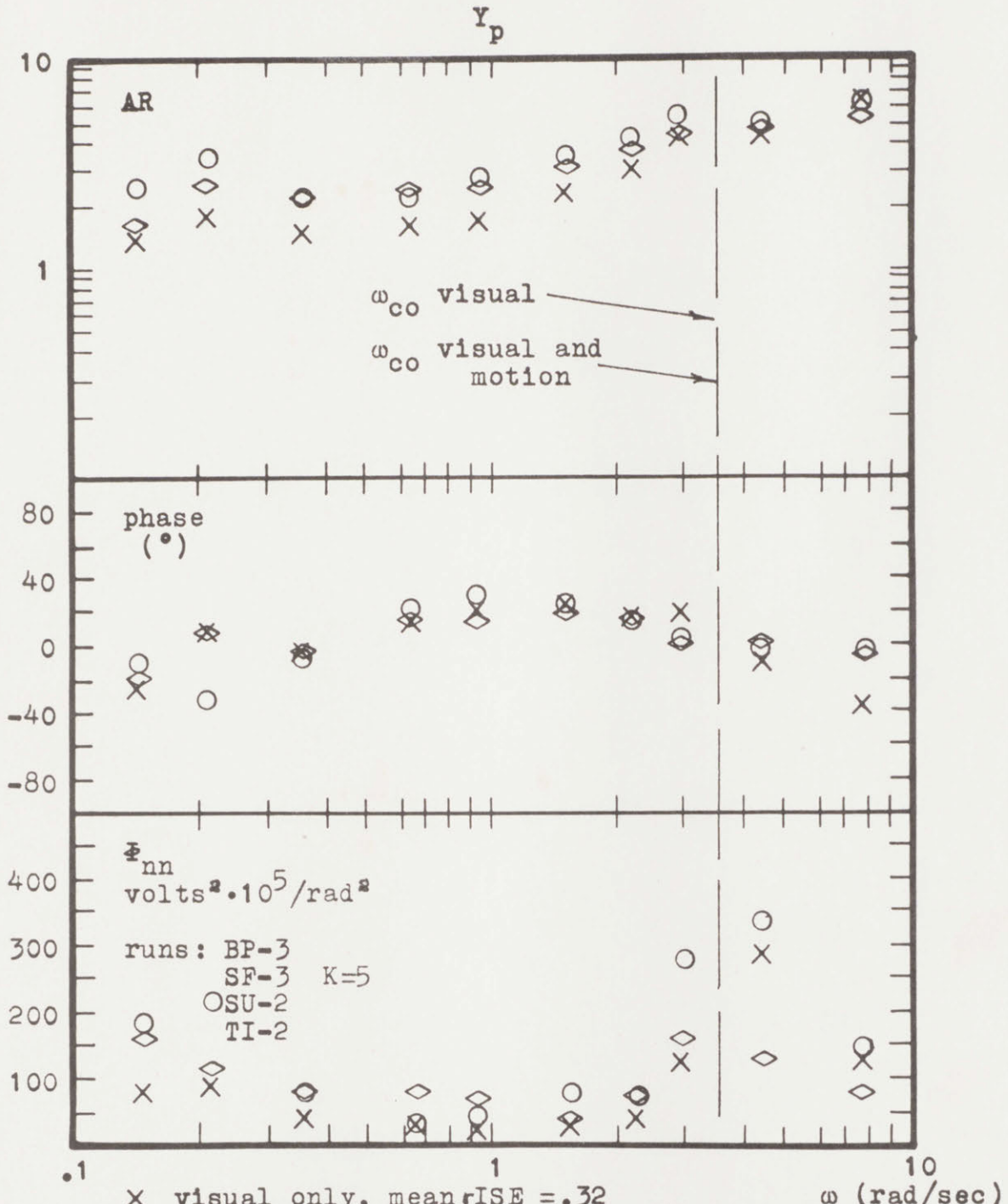

× visual only, mean rISE = .32
◇ motion only, mean rISE = .27
○ visual and motion, mean rISE = .23

ISI=1050

$$Y_c = \frac{e^{-.1s}}{s(.2s + 1)}, \quad K=5$$

EXPERIMENTAL RESULTS

data-34

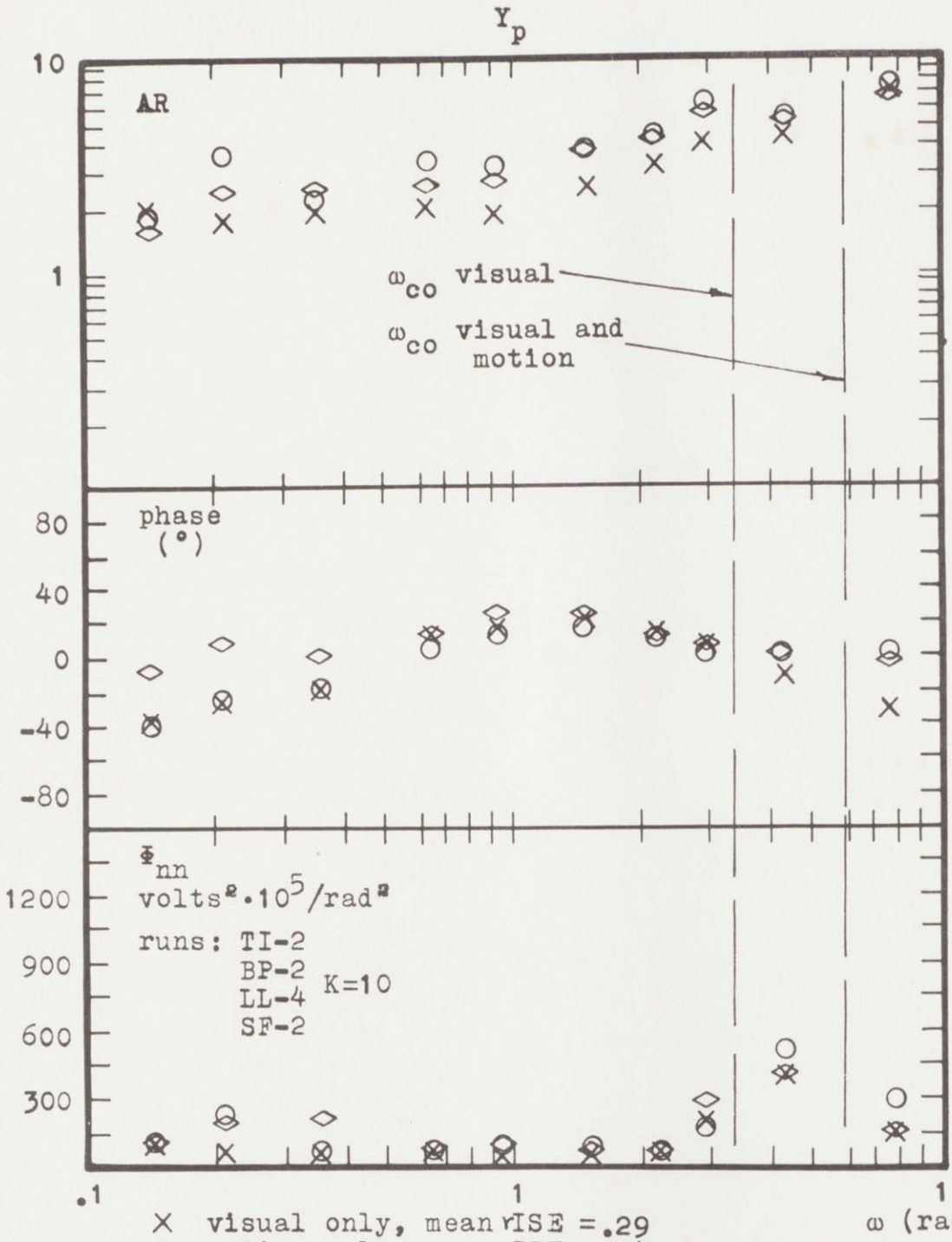

× visual only, mean rISE = .29
◇ motion only, mean rISE = .24
○ visual and motion, mean rISE = .19

ISI=1050

$$Y_c = \frac{e^{-.1s}}{s(.2s + 1)}, \quad K=10$$

EXPERIMENTAL RESULTS

data-35

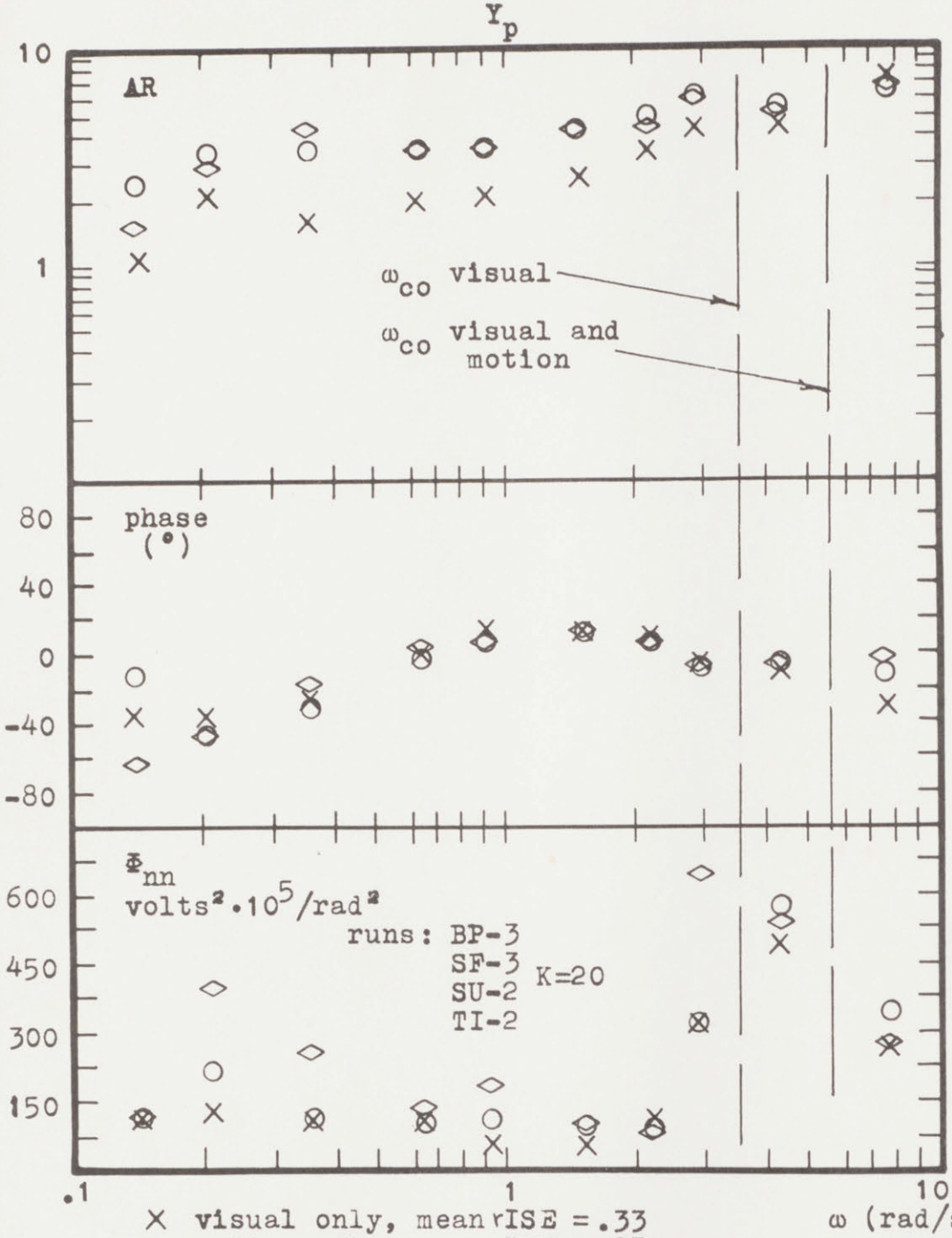

× visual only, mean rISE = .33
◇ motion only, mean rISE = .23
○ visual and motion, mean rISE = .21

ISI=1050

$$Y_c = \frac{e^{-.1s}}{s(.2s + 1)}, \quad K=20$$

EXPERIMENTAL RESULTS

data-36

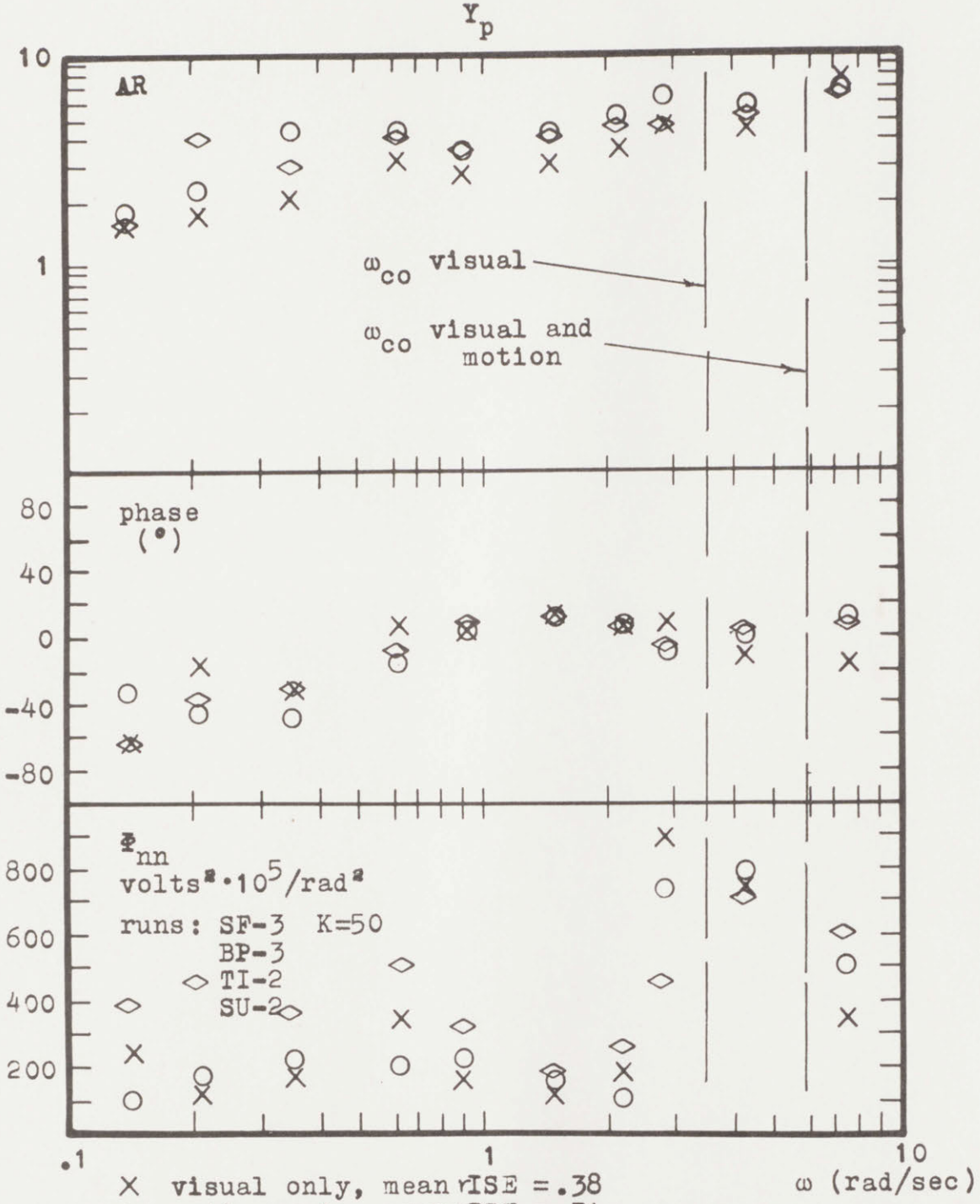

× visual only, mean rISE = .38
◇ motion only, mean rISE = .31
○ visual and motion, mean rISE = .22

$$Y_c = \frac{e^{-.1s}}{s(.2s + 1)}, \quad K=50$$

EXPERIMENTAL RESULTS

data-37

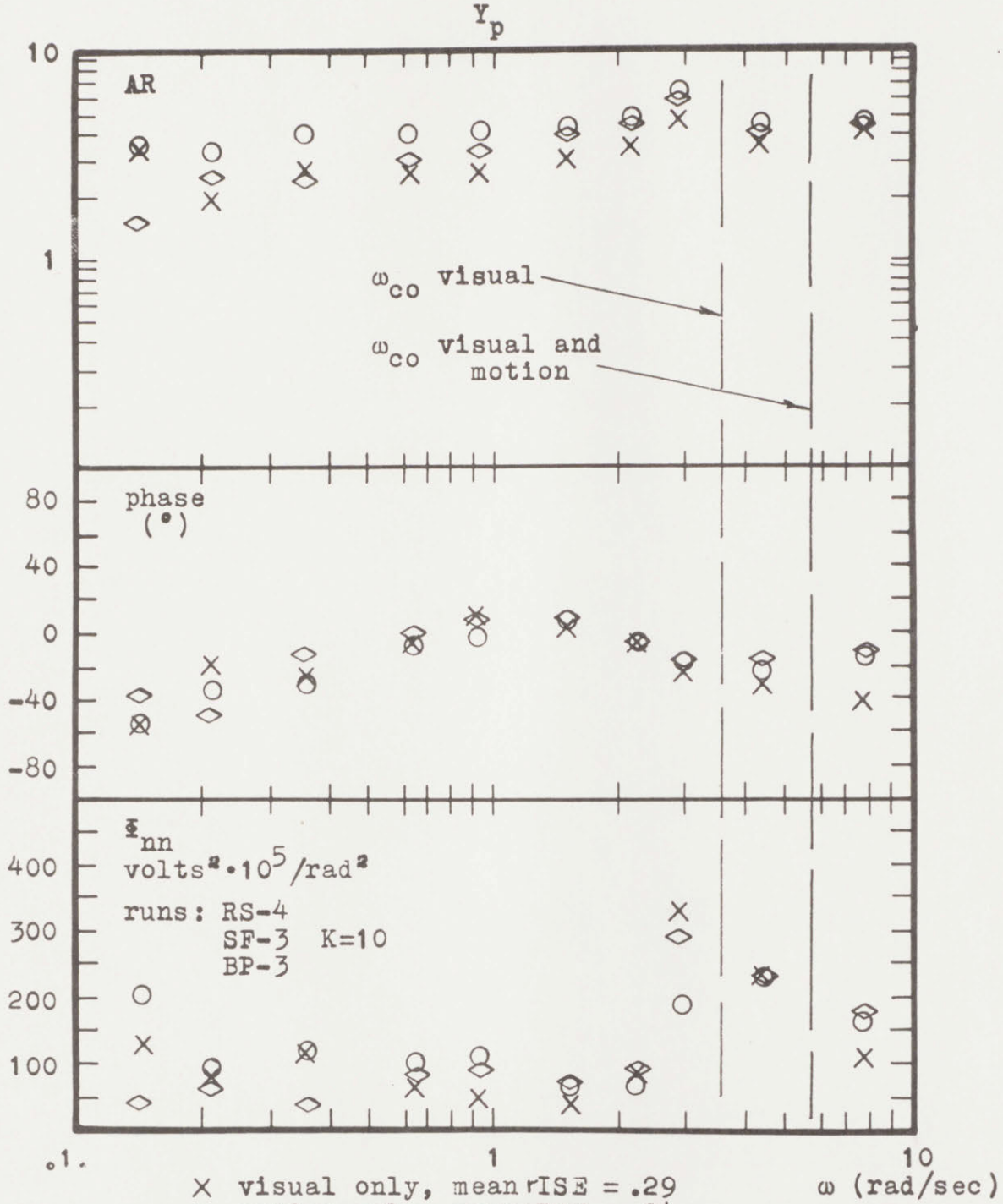

× visual only, mean rISE = .29
◇ motion only, mean rISE = .24
○ visual and motion, mean rISE = .19

ISI=1050

$$Y_c = \frac{e^{-.1s}}{s(.05s + 1)}, \quad K=10$$

EXPERIMENTAL RESULTS

data-38

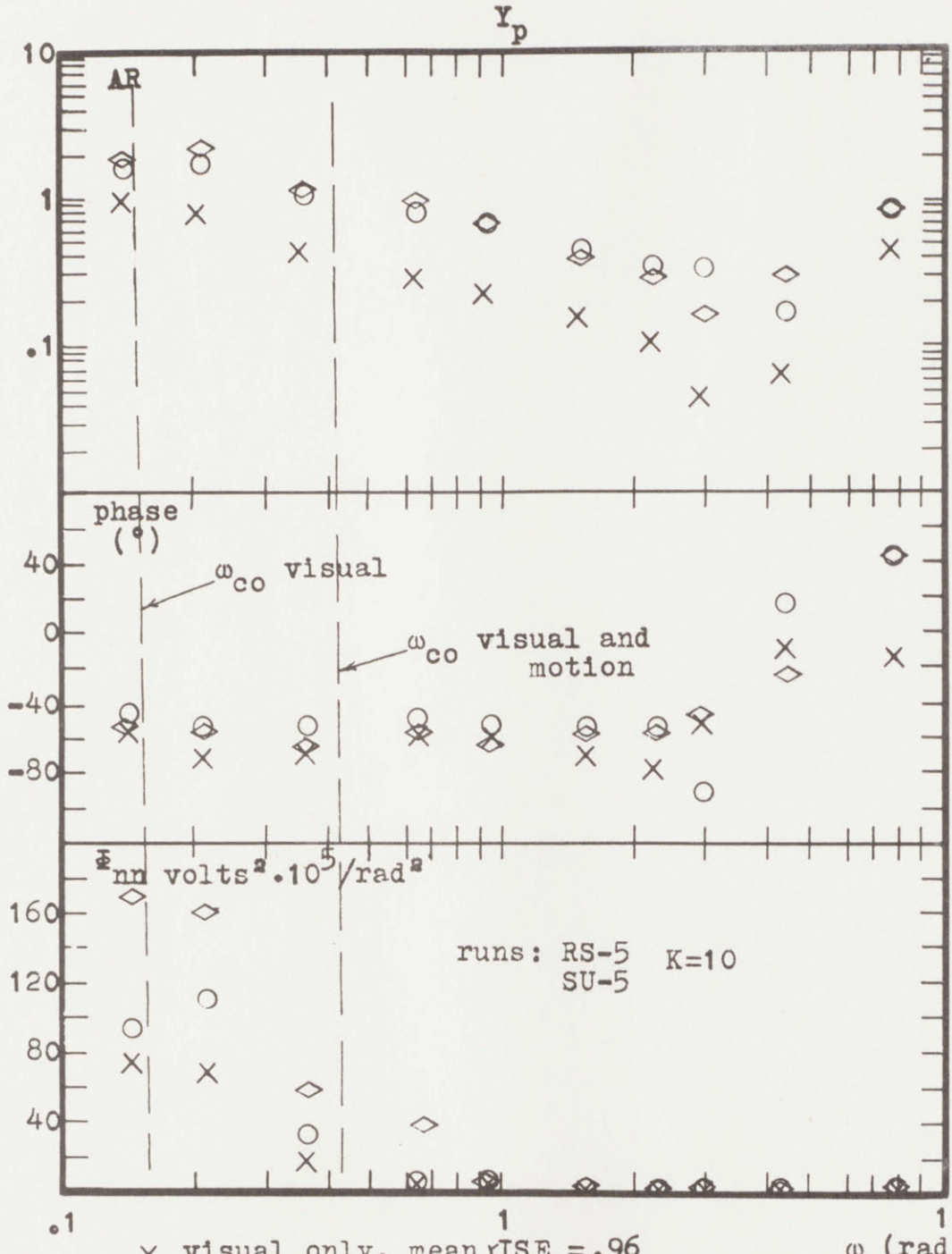

× visual only, mean rISE = .96
◇ motion only, mean rISE = .85
○ visual and motion, mean rISE = .64

ISI=1050

$$Y_c = \frac{20e^{-.1s}}{s^2 + 20}$$

EXPERIMENTAL RESULTS

data-39

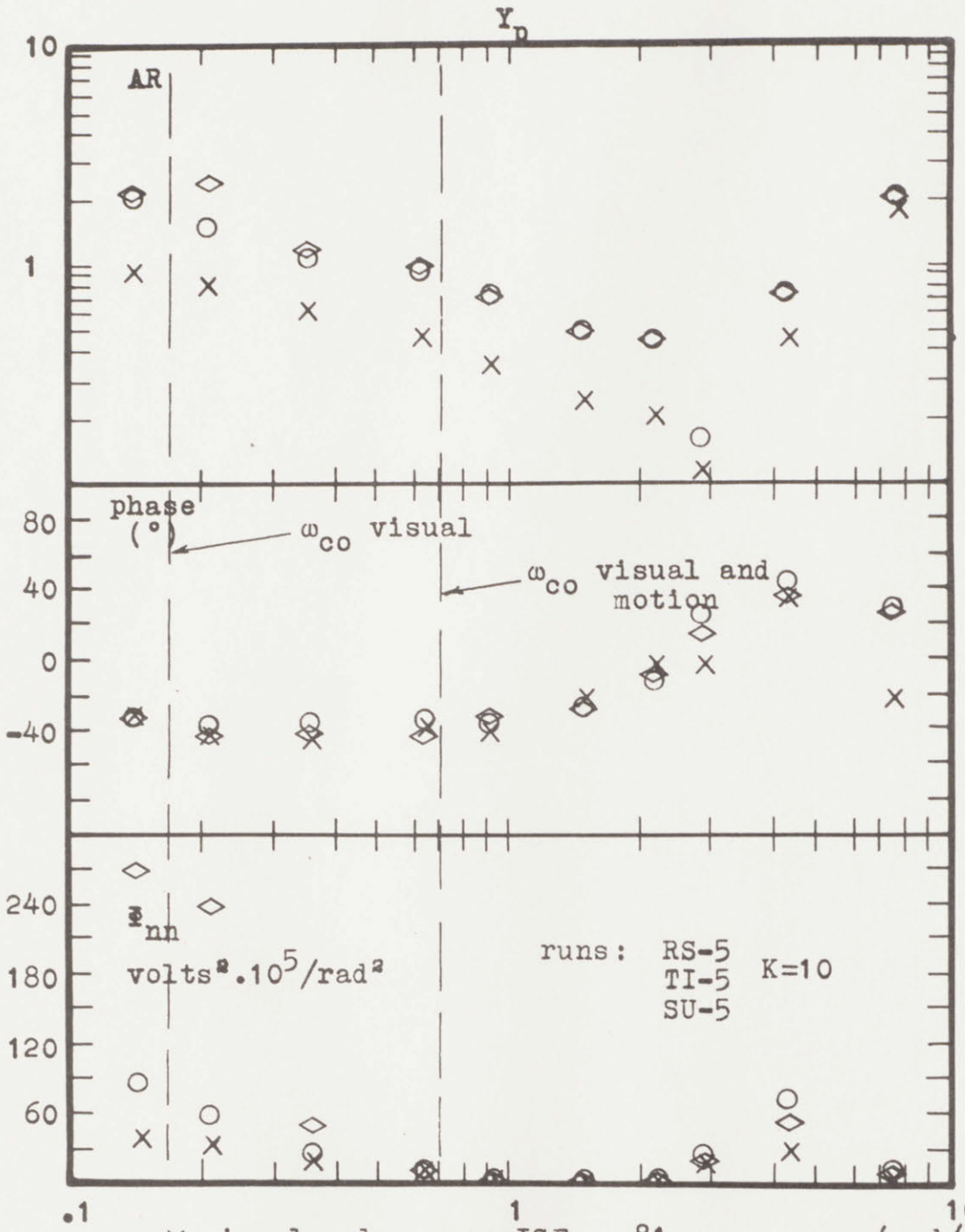

× visual only, mean rISE = .81
◇ motion only, mean rISE = .66
○ visual and motion, mean rISE = .53

$$Y_c = \frac{10e^{-.1s}}{s^2 + 10}$$

EXPERIMENTAL RESULTS

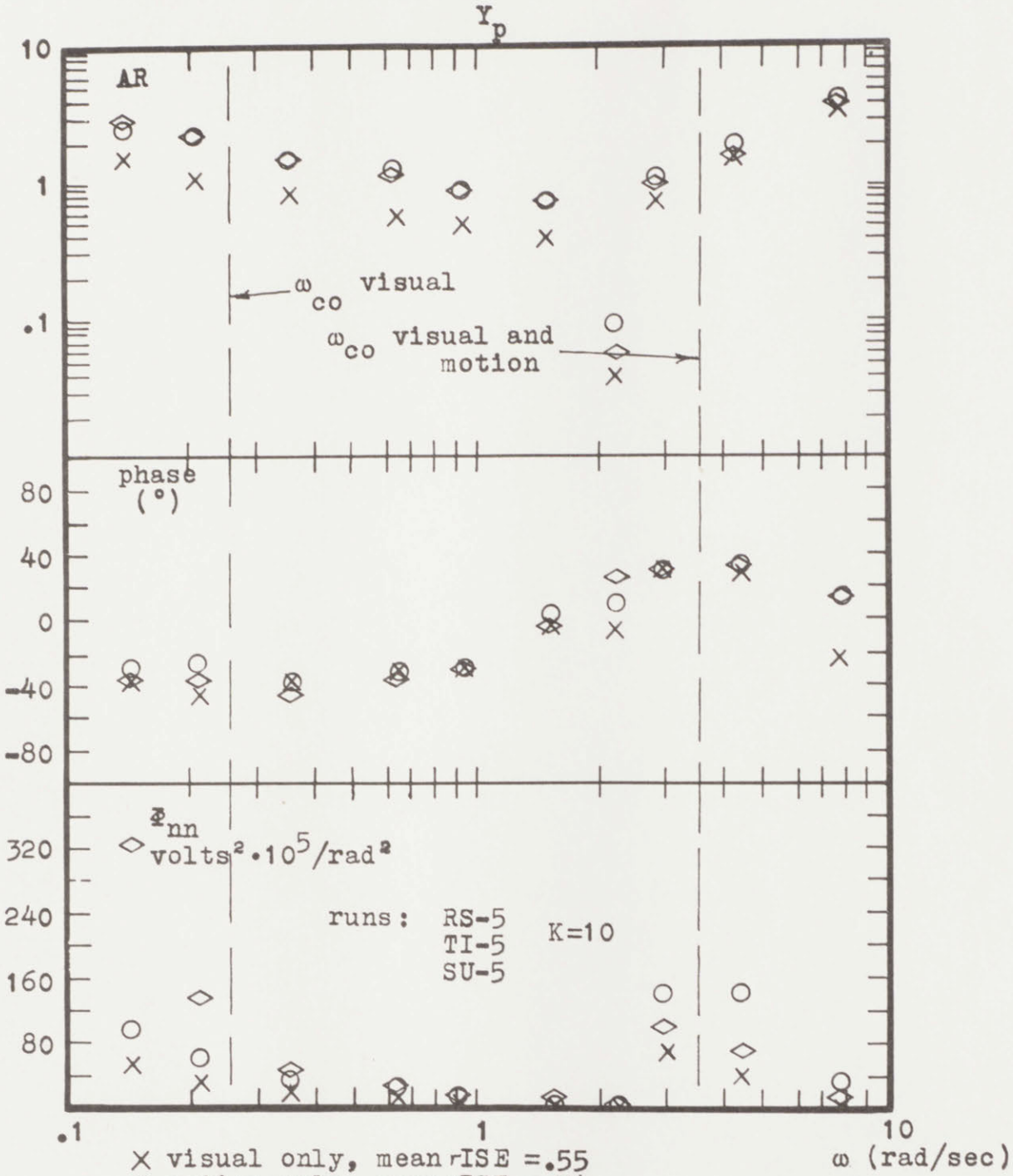

× visual only, mean rISE =.55
◇ motion only, mean rISE =.54
○ visual and motion, mean rISE =.39

ISI=1050

$$Y_c = \frac{5}{s^2 + 5} e^{-.1s}$$

EXPERIMENTAL RESULTS

data-41

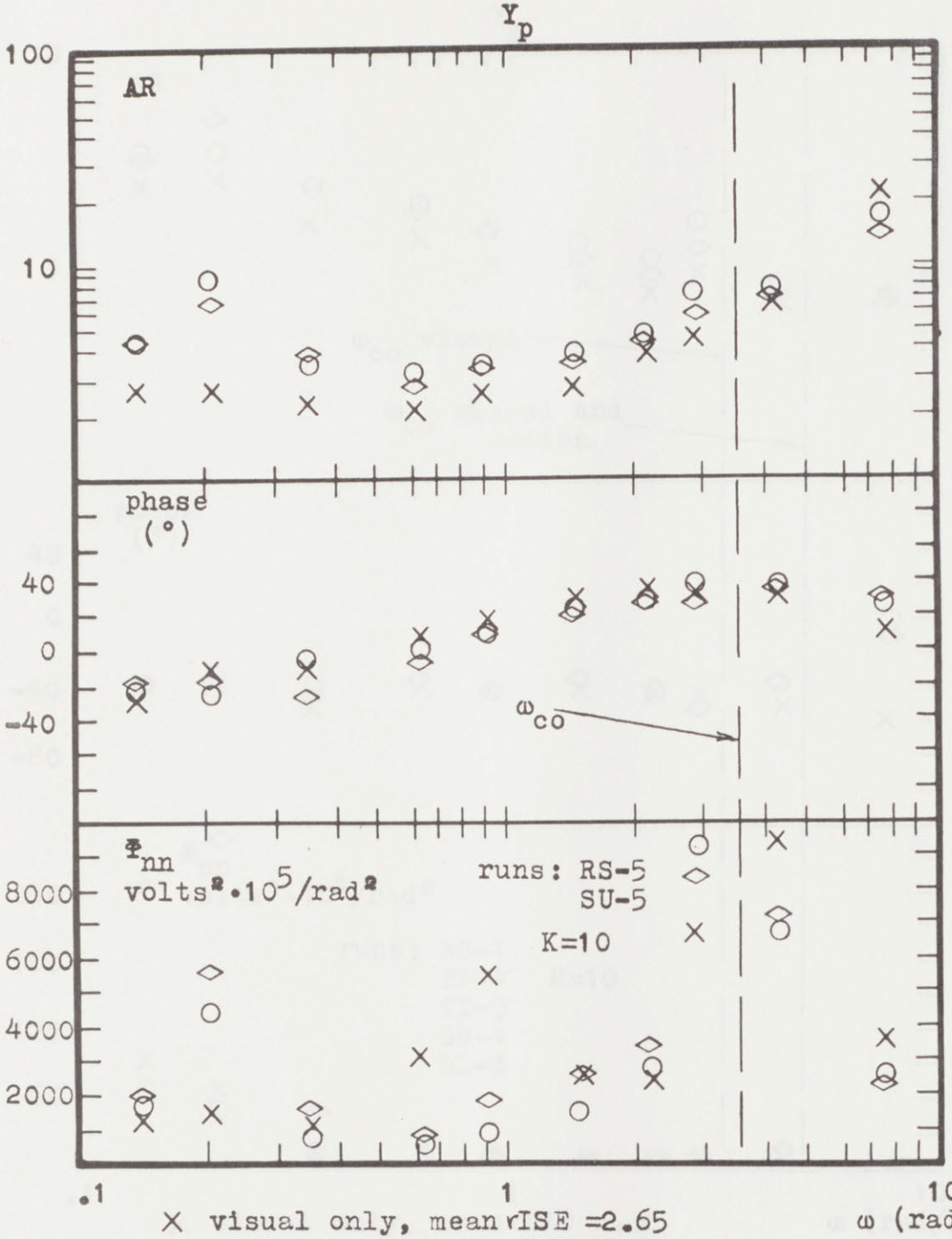

× visual only, mean rISE =2.65
◇ motion only, mean rISE =1.92
○ visual and motion, mean rISE = 1.24

$$Y_c = \frac{-2.5e^{-.1s}}{s^2 - 2.5}$$

EXPERIMENTAL RESULTS

data-42

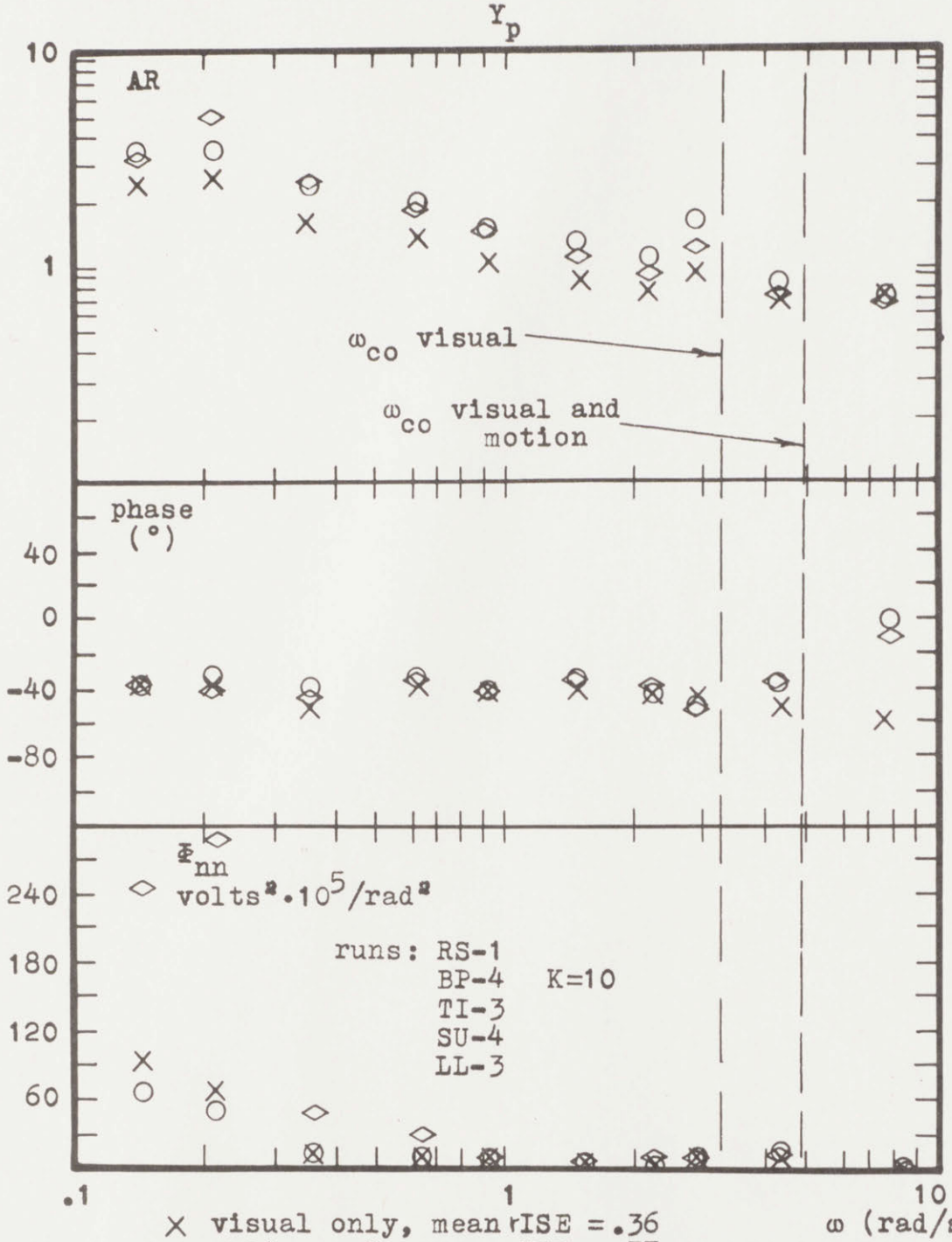

× visual only, mean rISE = .36
◇ motion only, mean rISE = .37
○ visual and motion, mean rISE = .24

$$Y_c = \frac{25e^{-.1s}}{s^2 + 5s + 25}$$

EXPERIMENTAL RESULTS

data-43

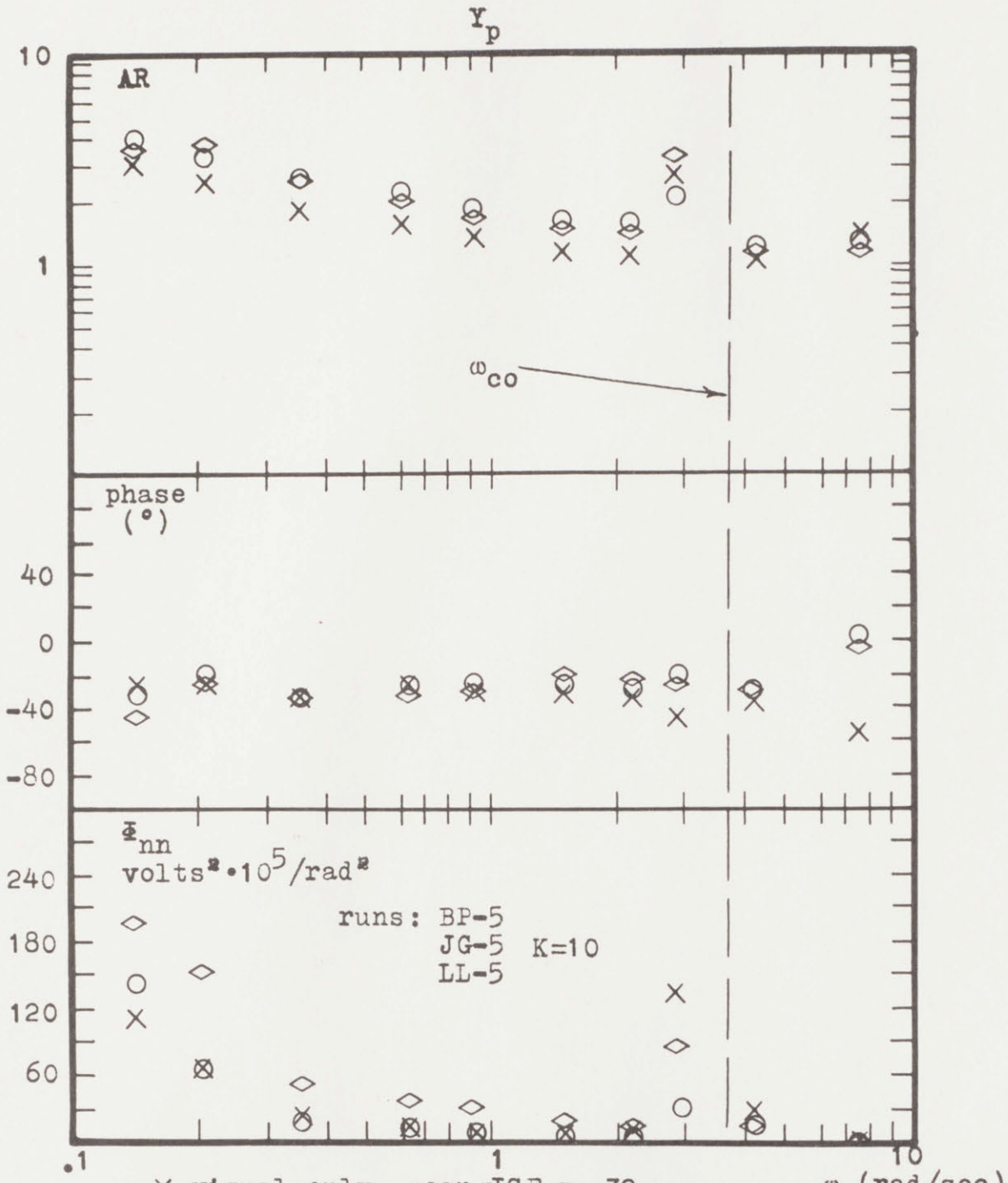

× visual only, mean rISE = .32
◇ motion only, mean rISE = .26
○ visual and motion, mean rISE = .20

$$Y_c = \frac{15e^{-.1s}}{s^2 + 5s + 15}$$

EXPERIMENTAL RESULTS

data-44

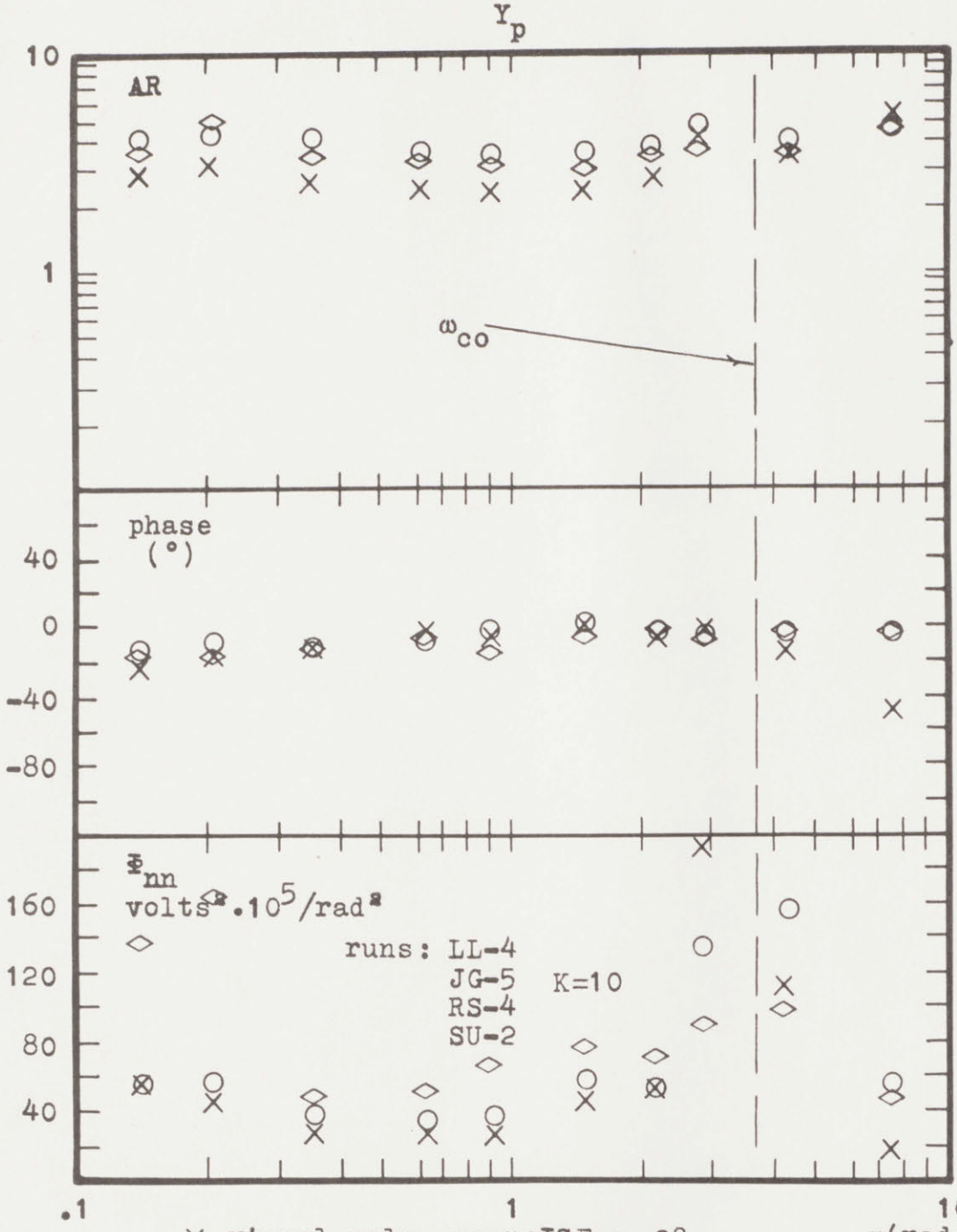

× visual only, mean rISE = .28
◇ motion only, mean rISE = .27
○ visual and motion, mean rISE = .20

ISI=1050

$$Y_c = \frac{5e^{-.1s}}{s^2 + 5s + 5}$$

EXPERIMENTAL RESULTS

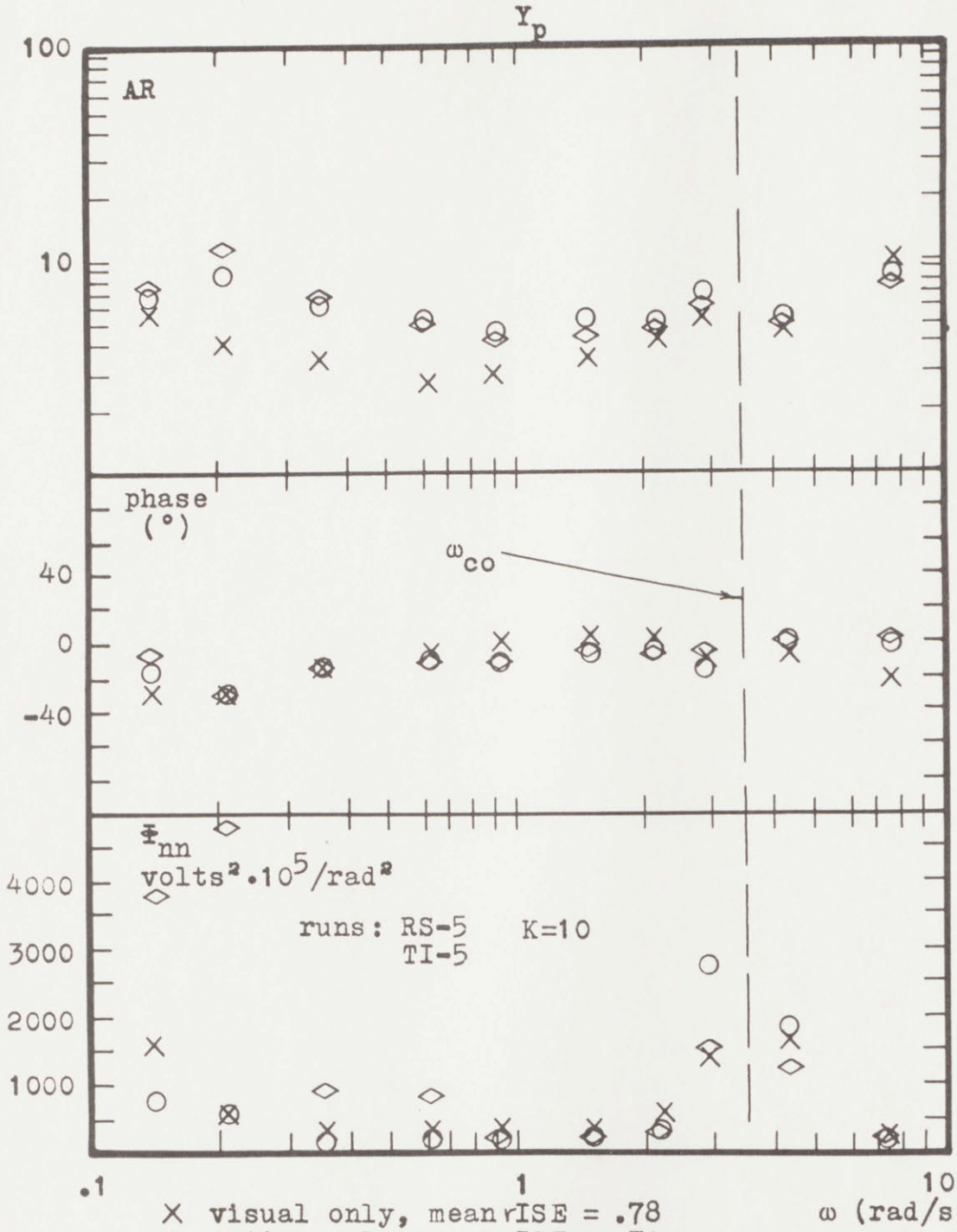

× visual only, mean rISE = .78
◇ motion only, mean rISE = .71
○ visual and motion, mean rISE = .43

ISI=1050

$$Y_c = \frac{-5e^{-.1s}}{s^2 + 5s - 5}$$

EXPERIMENTAL RESULTS

data-46

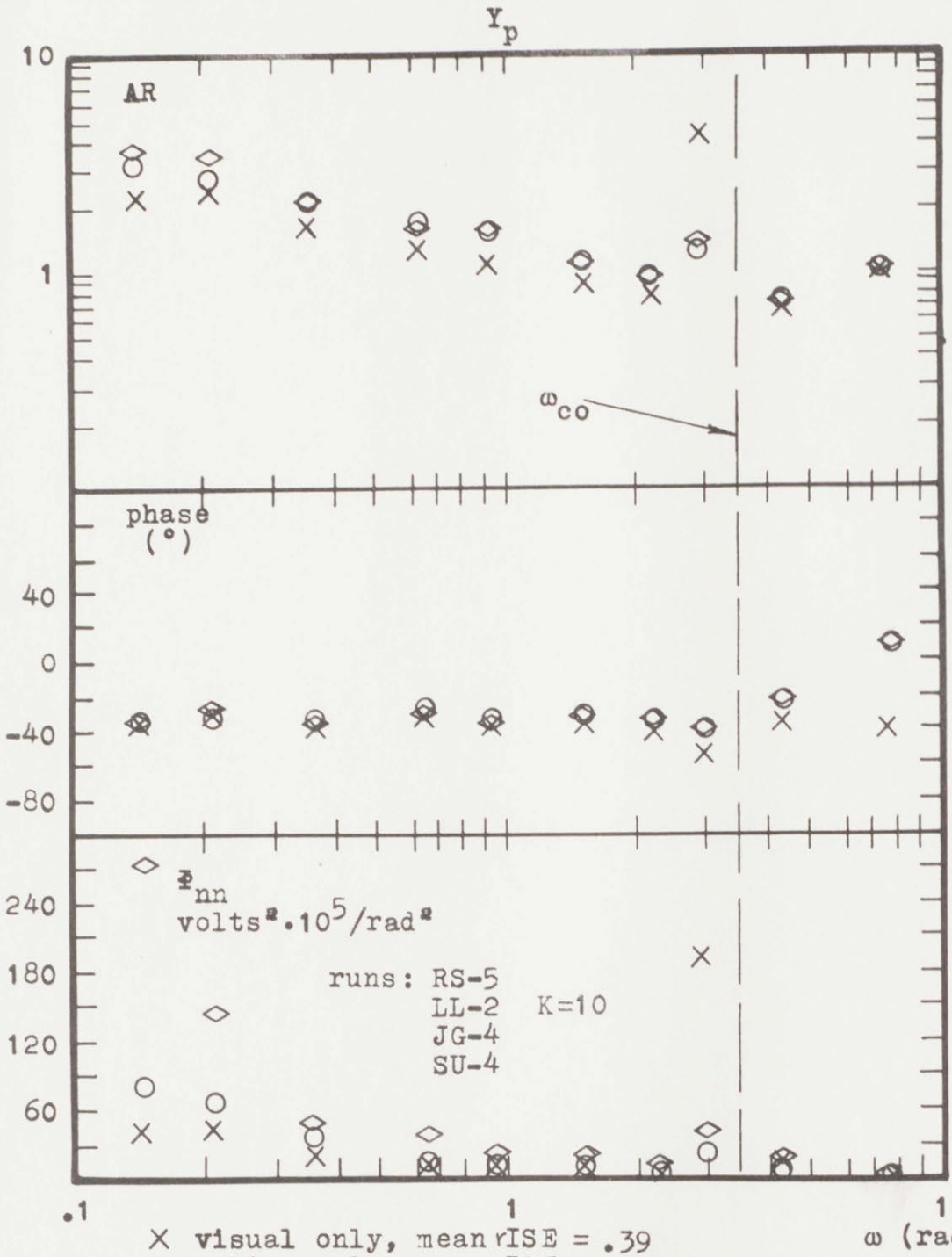

× visual only, mean rISE = .39
◇ motion only, mean rISE = .32
○ visual and motion, mean rISE = .30

ISI=1050

$$Y_c = \frac{15e^{-.1s}}{s^2 + 3s + 15}$$

EXPERIMENTAL RESULTS

data-47

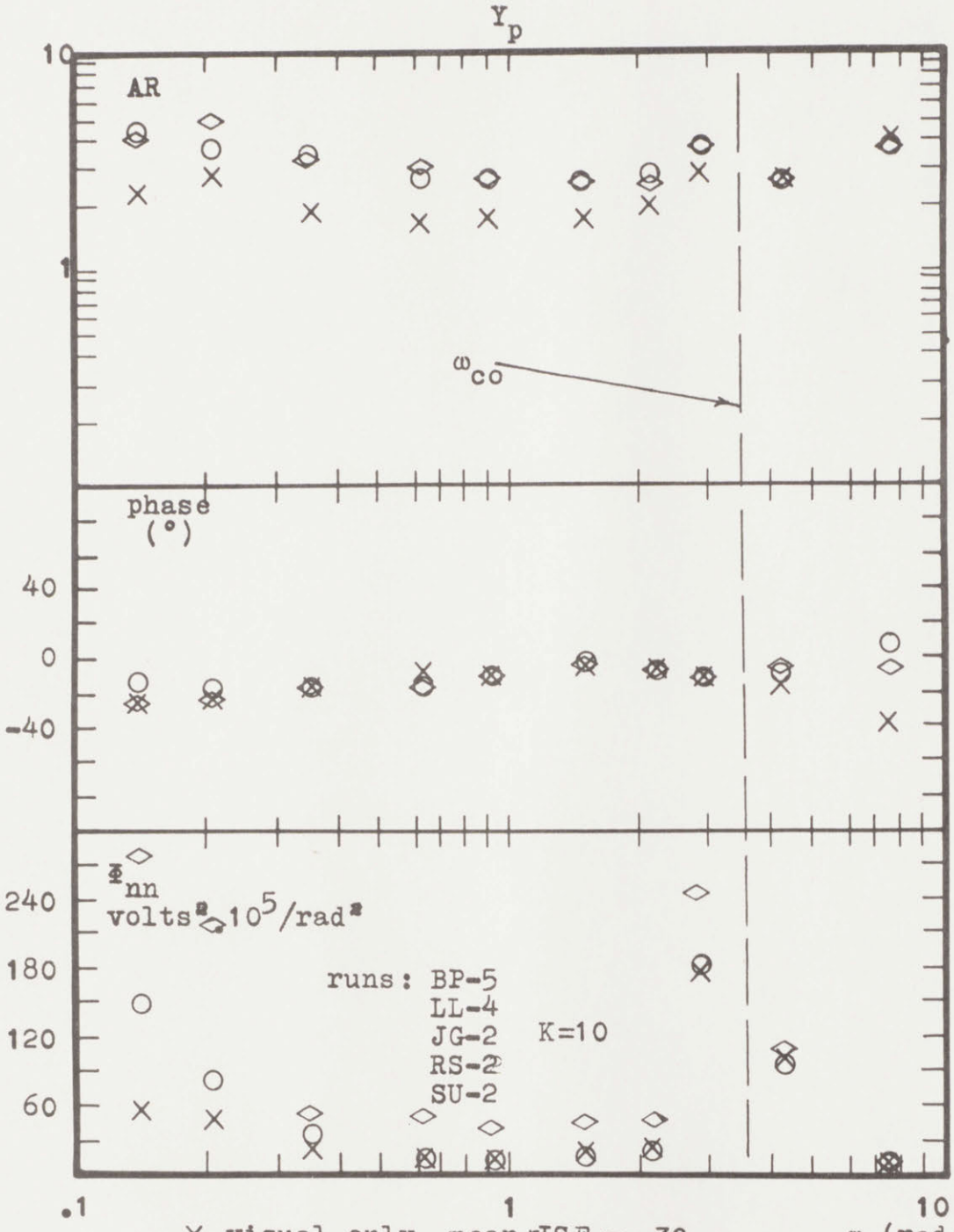

× visual only, mean rISE = .30
◇ motion only, mean rISE = .25
○ visual and motion, mean rISE = .20 ISI=1050

$$Y_c = \frac{5e^{-.1s}}{s^2 + 3s + 5}$$

EXPERIMENTAL RESULTS

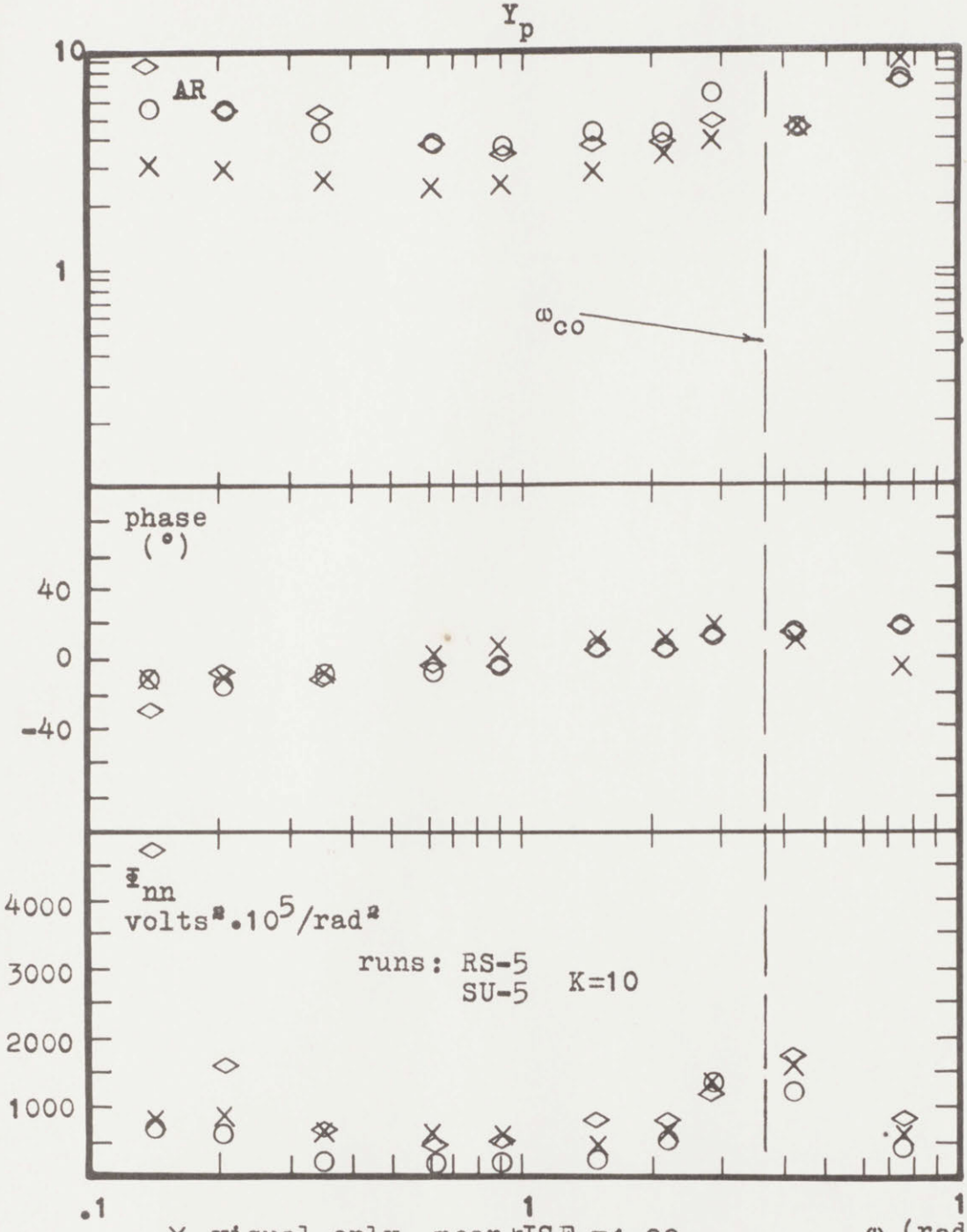

× visual only, mean rISE =1.29
◇ motion only, mean rISE =.69
○ visual and motion, mean rISE =.58

ISI=1050

$$Y_c = \frac{5e^{-.1s}}{s^2 + 3s - 5}$$

EXPERIMENTAL RESULTS

data-49

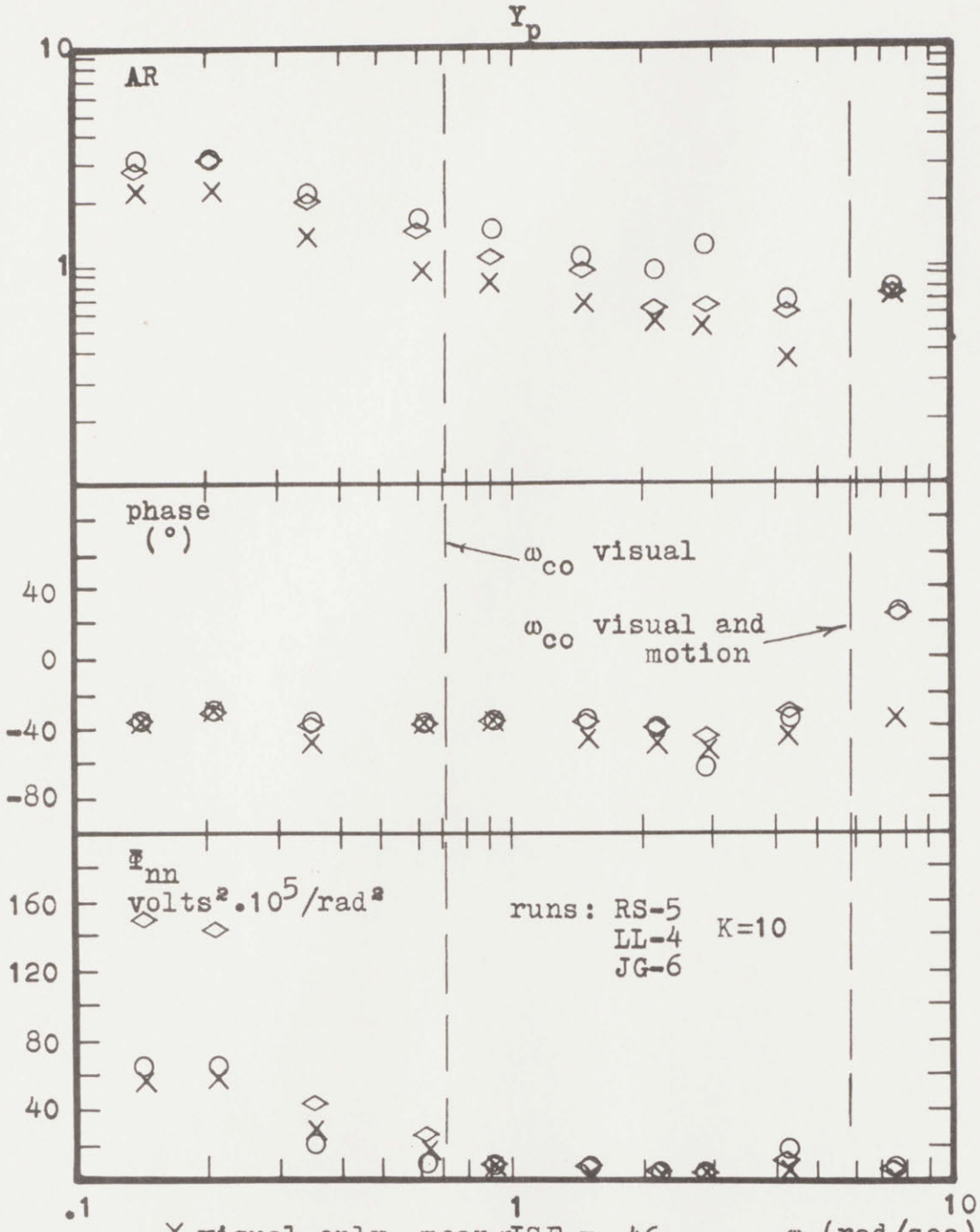

× visual only, mean rISE = .46
◇ motion only, mean rISE = .43
○ visual and motion, mean rISE = .30

$$Y_c = \frac{20e^{-.1s}}{s^2 + 2s + 20}$$

EXPERIMENTAL RESULTS

data-50

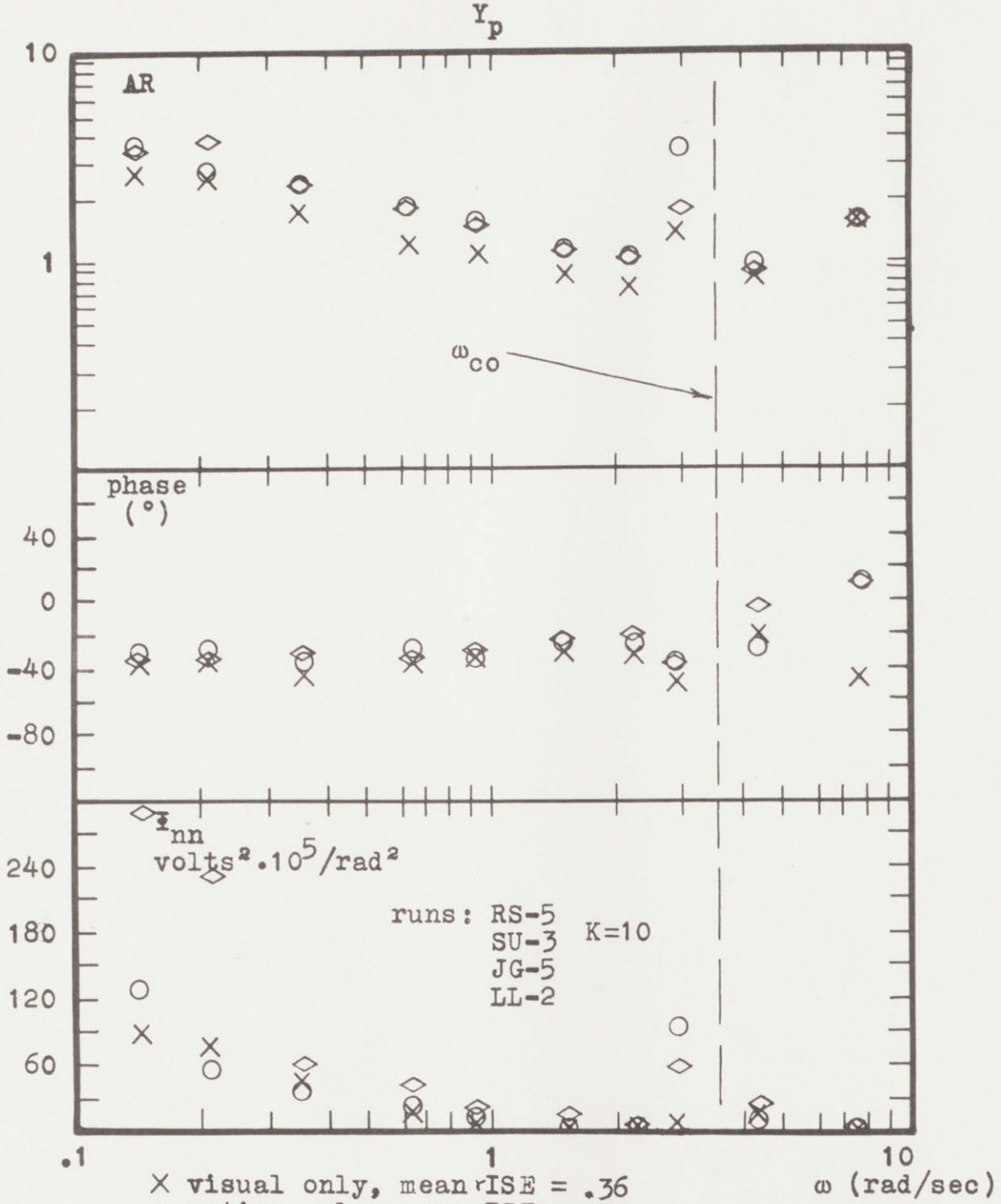

× visual only, mean rISE = .36
◇ motion only, mean rISE = .30
○ visual and motion, mean rISE = .27

ISI=1050

$$Y_c = \frac{10e^{-.1s}}{s^2 + 2s + 10}$$

EXPERIMENTAL RESULTS

data-51

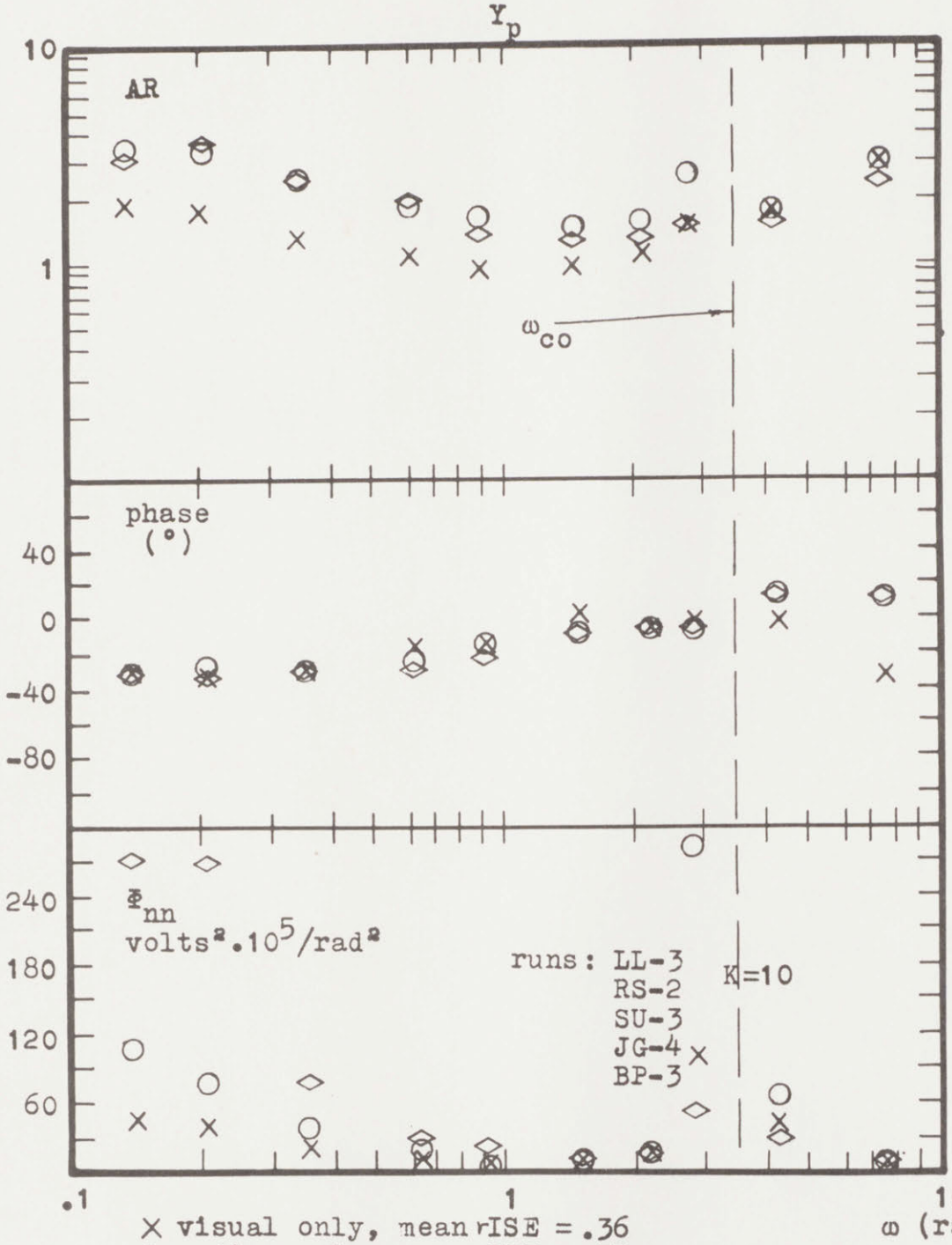

× visual only, mean rISE = .36
◇ motion only, mean rISE = .30
○ visual and motion, mean rISE = .24

ISI=1050

$$Y_c = \frac{5e^{-.1s}}{s^2 + s + 5}$$

EXPERIMENTAL RESULTS

data-52

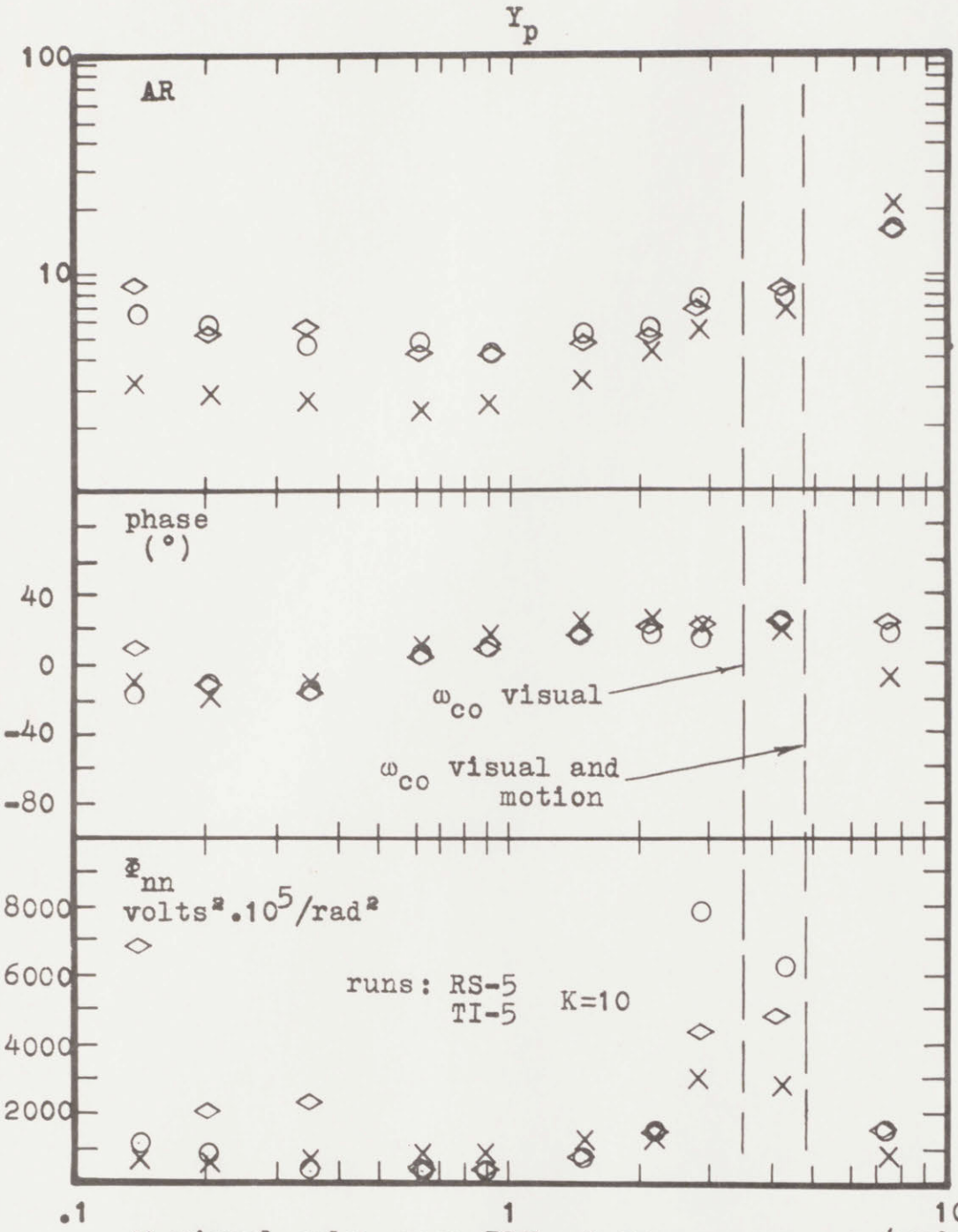

× visual only, mean rISE = 1.35
◇ motion only, mean rISE = 1.45
○ visual and motion, mean rISE = .73

ISI=1050

$$Y_c = \frac{-2.5e^{-.1s}}{s^2 + s - 2.5}$$

EXPERIMENTAL RESULTS

data-53

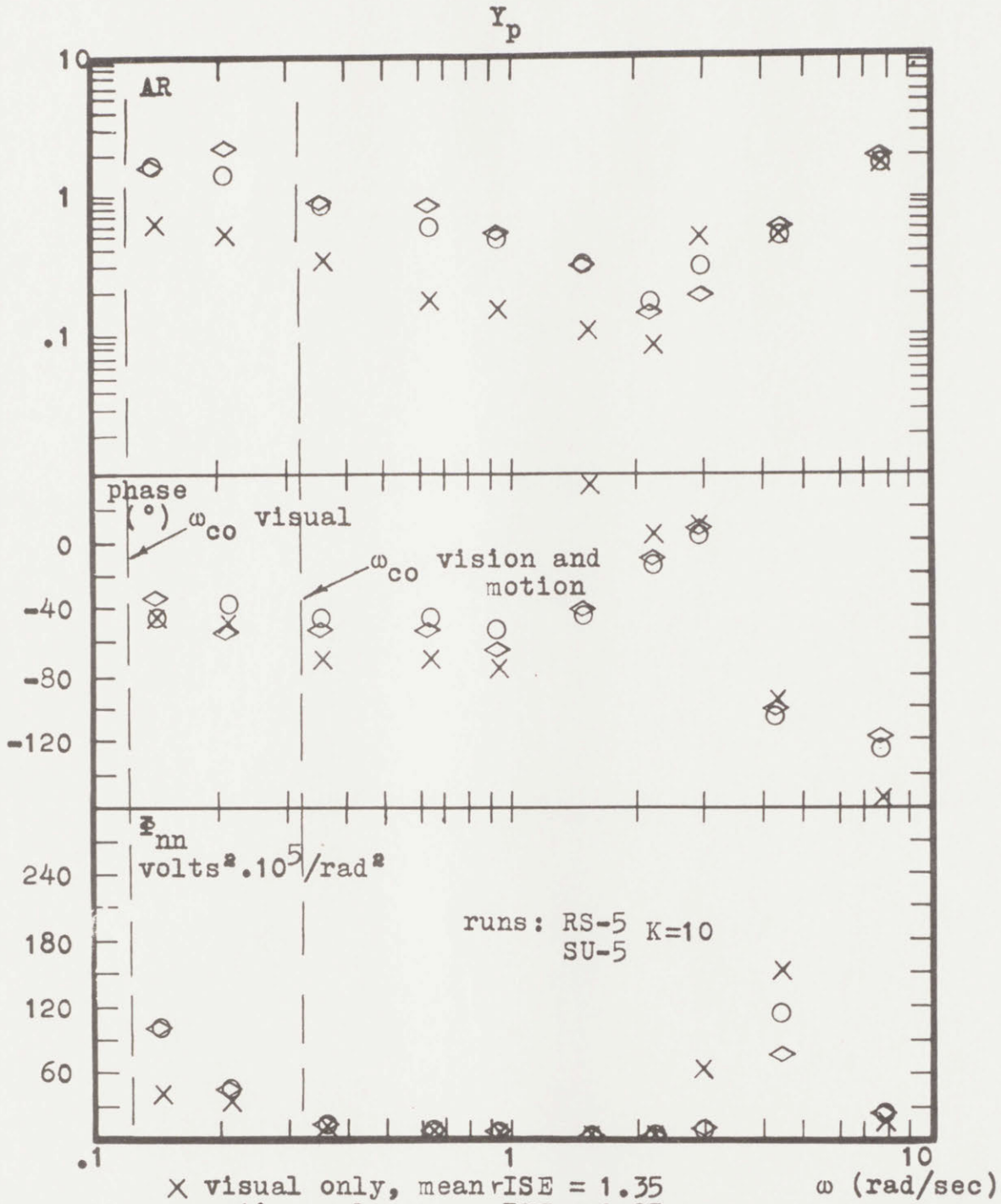

× visual only, mean rISE = 1.35
◇ motion only, mean rISE = 1.25
○ visual and motion, mean rISE = .84

ISI=1050

$$Y_c = \frac{15e^{-.1s}}{s^2 - s + 15}$$

EXPERIMENTAL RESULTS

data-54

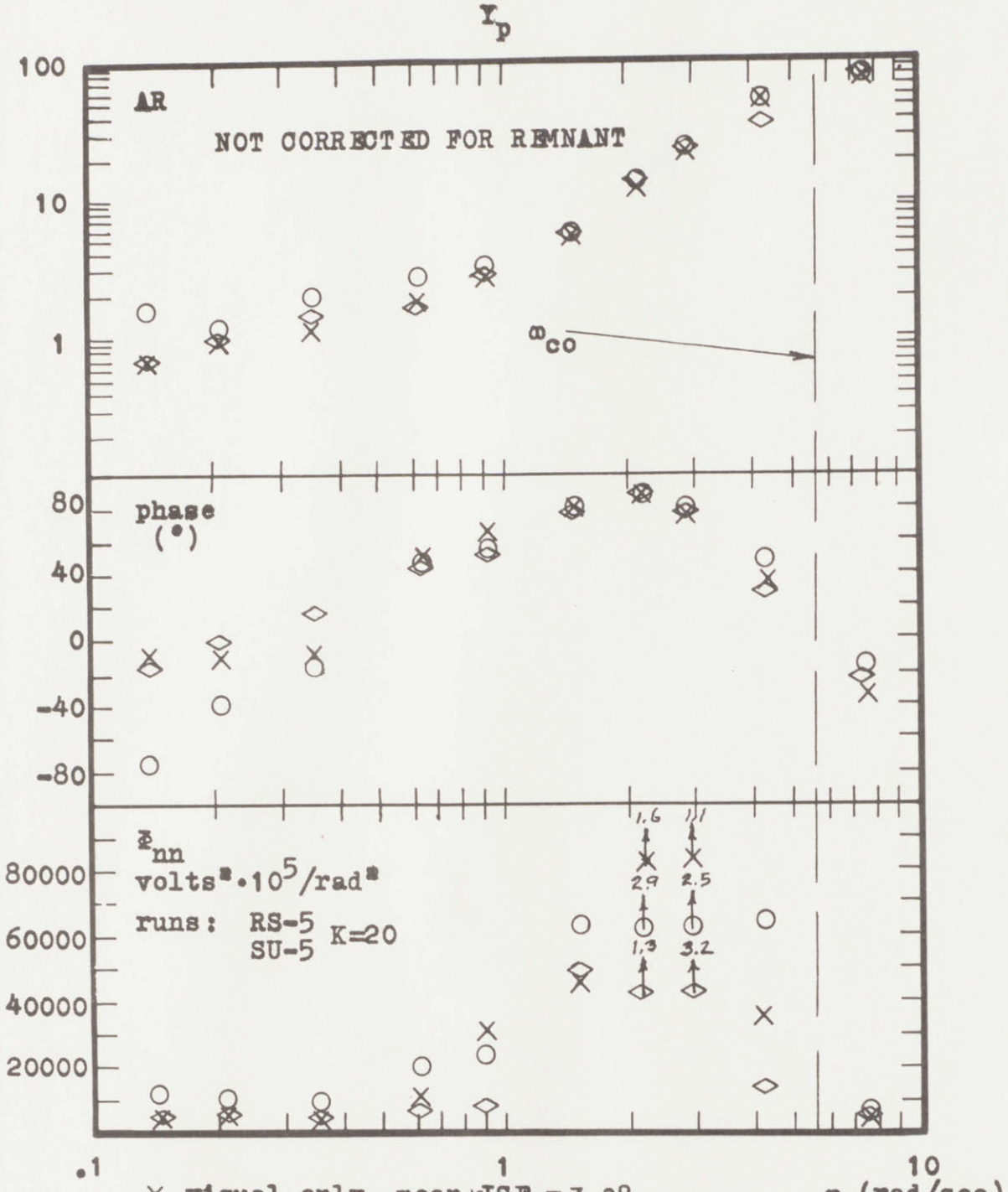

× visual only, mean rISE = 3.08
◇ motion only, mean rISE = 3.96
○ Visual and motion, mean rISE = 3.07

$$Y_c = \frac{2e^{-.1s}}{s^2(s+2)}, \quad K=20$$

EXPERIMENTAL RESULTS

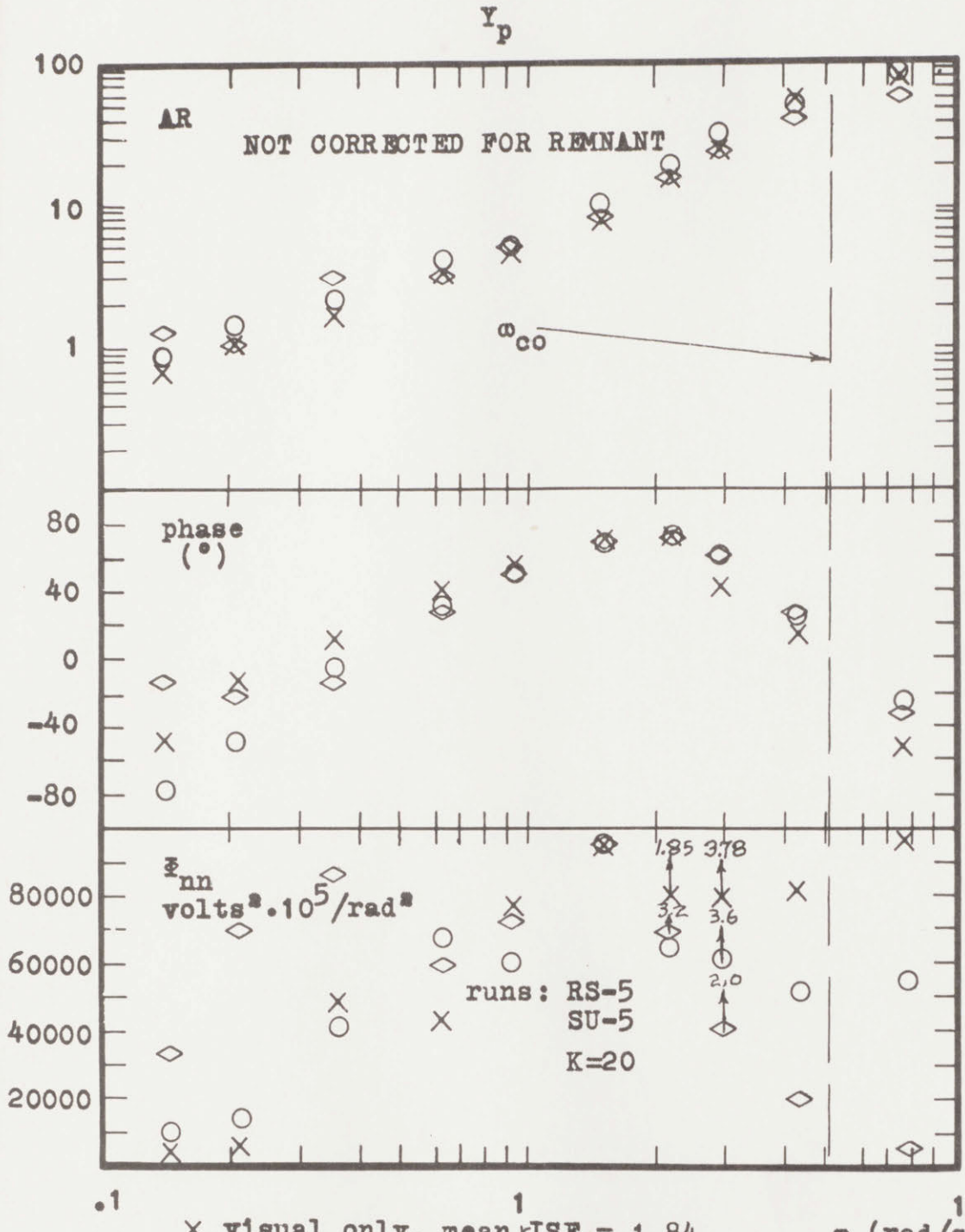

× visual only, mean rISE = 1.84
◇ motion only, mean rISE = 2.12
○ visual and motion, mean rISE = 1.84

ISI=1050

$$Y_c = \frac{4e^{-.1s}}{s^2(s+4)}, \quad K=20$$

EXPERIMENTAL RESULTS

data-56

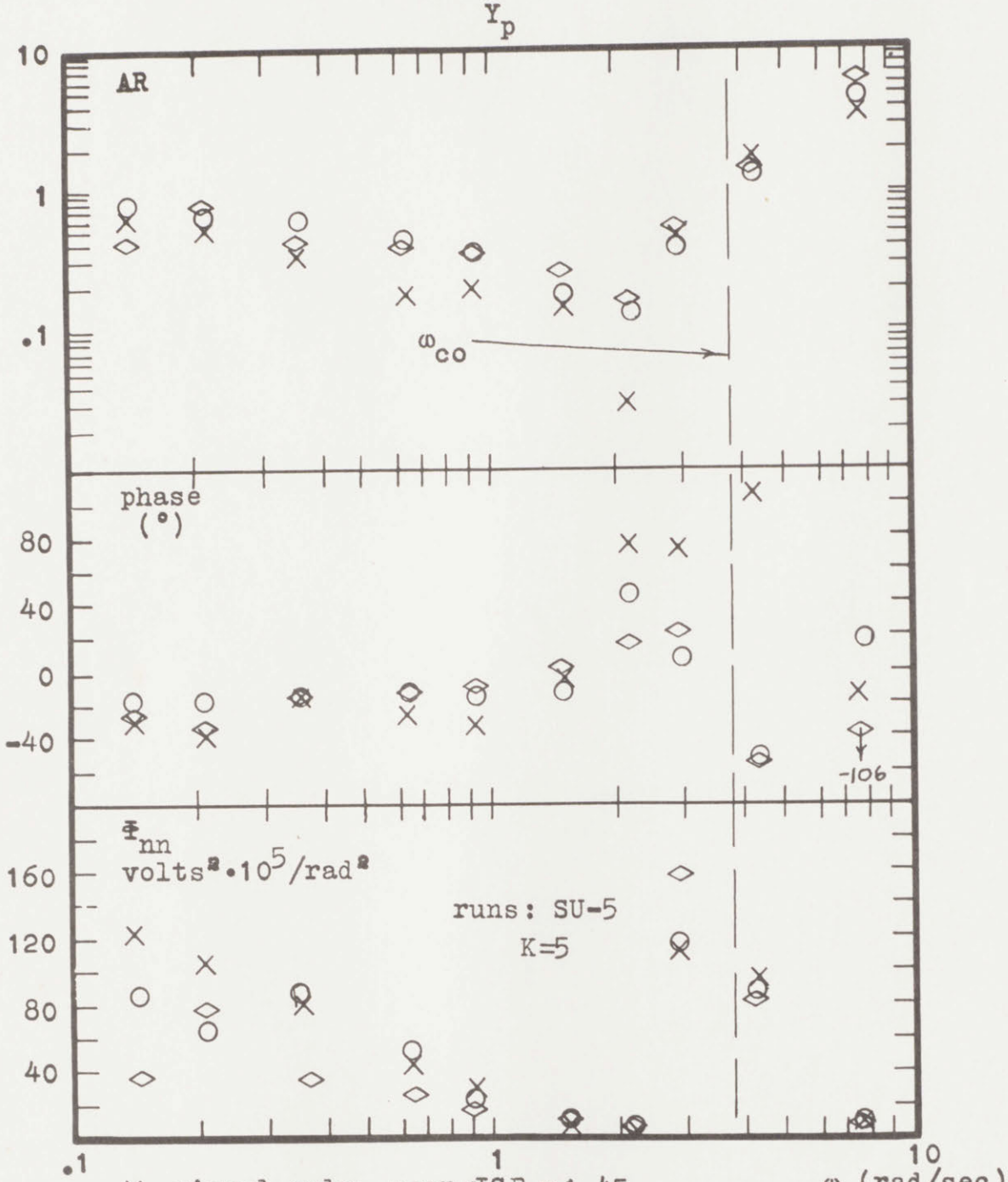

× visual only, mean rISE = 1.45
◇ motion only, mean rISE = .89
○ visual and motion, mean rISE = 1.05

$$Y_c = \frac{10e^{-.1s}}{s(s^2 + 10)}$$

EXPERIMENTAL RESULTS

data-57

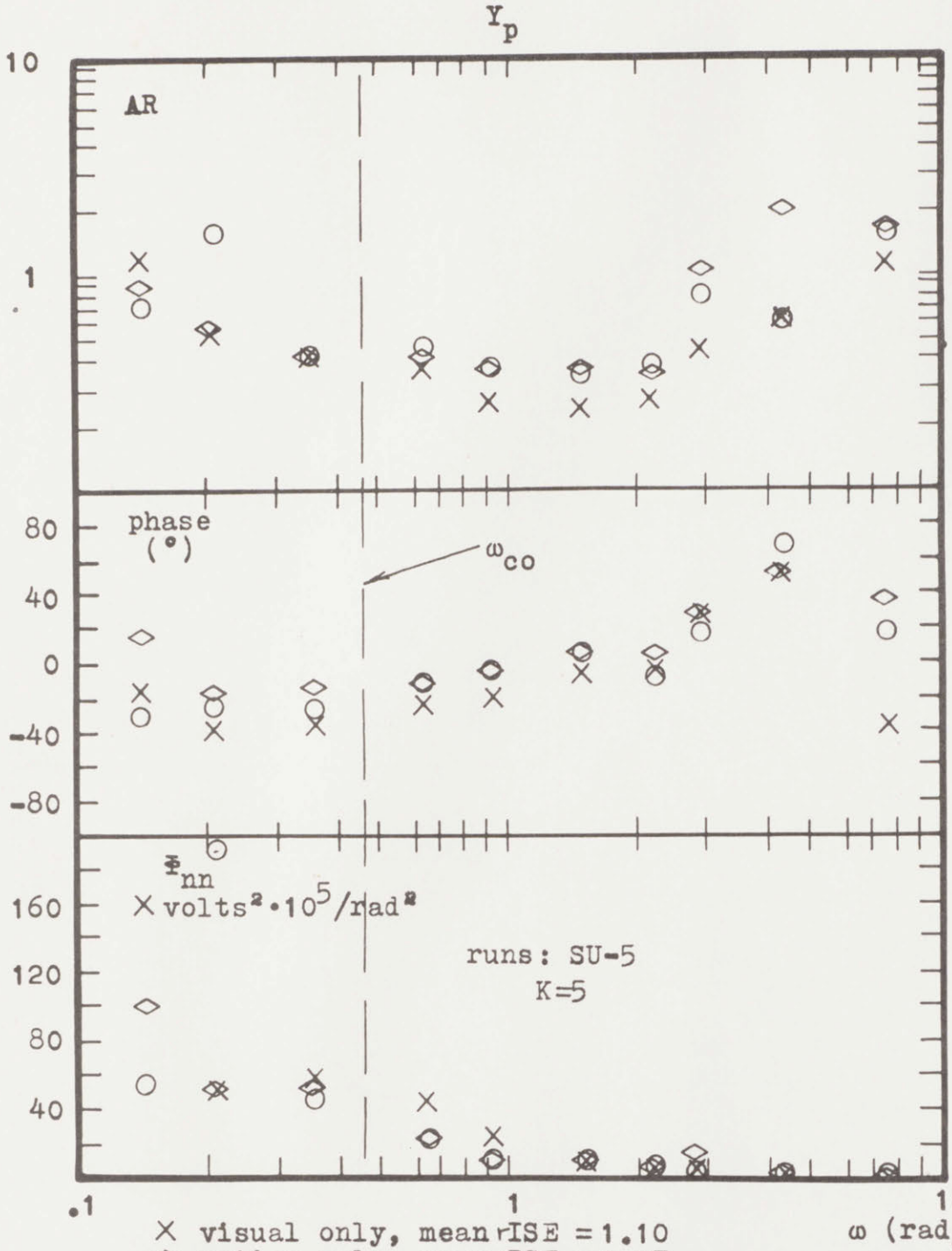

× visual only, mean rISE = 1.10
◇ motion only, mean rISE = 1.07
○ visual and motion, mean rISE = .97

ISI=1050

$$Y_c = \frac{20e^{-.1s}}{s(s^2 + .5s + 20)}$$

EXPERIMENTAL RESULTS

data-58

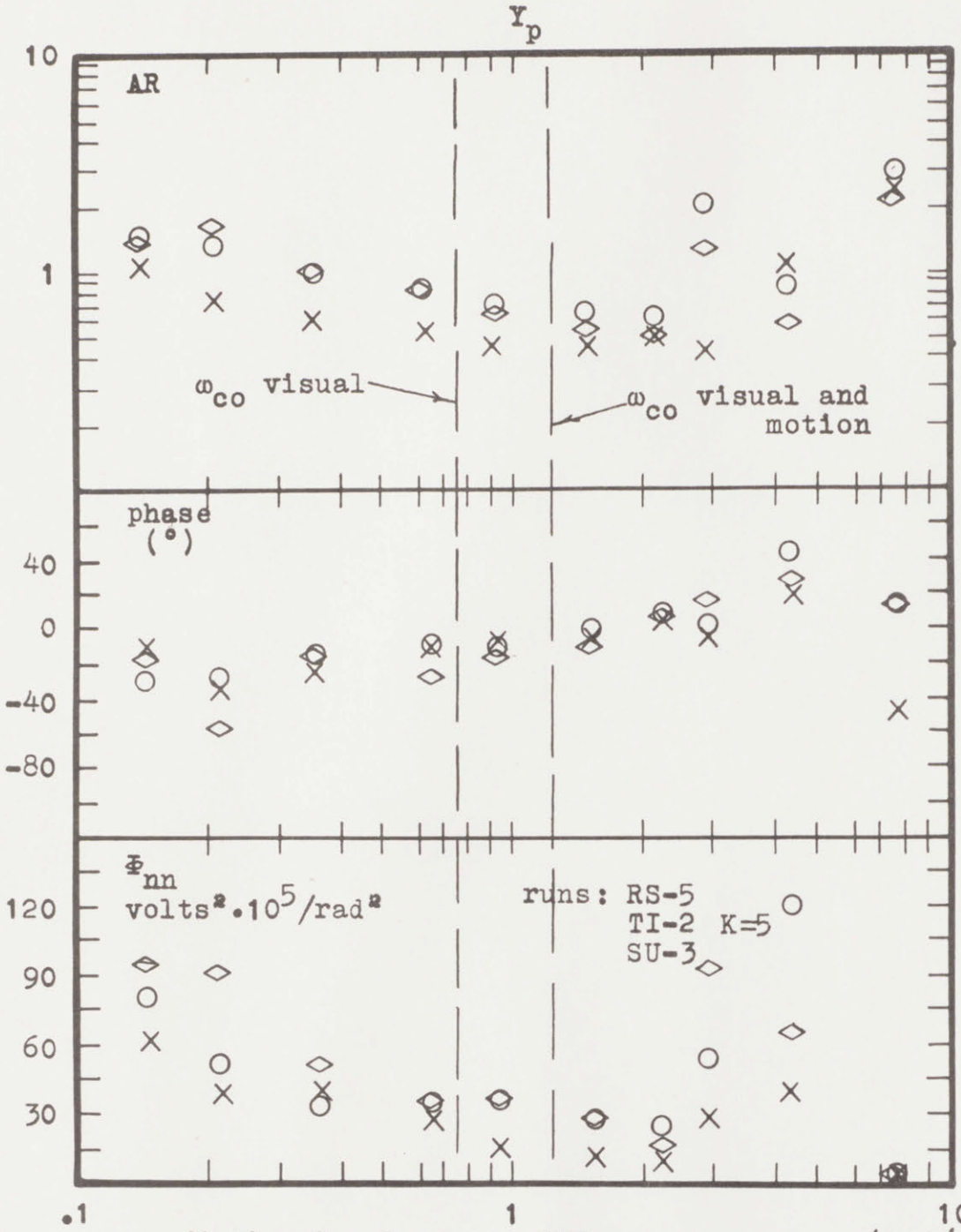

× visual only, mean rISE =.91
◇ motion only, mean rISE =.97
○ visual and motion, mean rISE = .79

ISI=1050

$$Y_c = \frac{15e^{-.1s}}{s(s^2 + s + 15)}$$

EXPERIMENTAL RESULTS

data-59

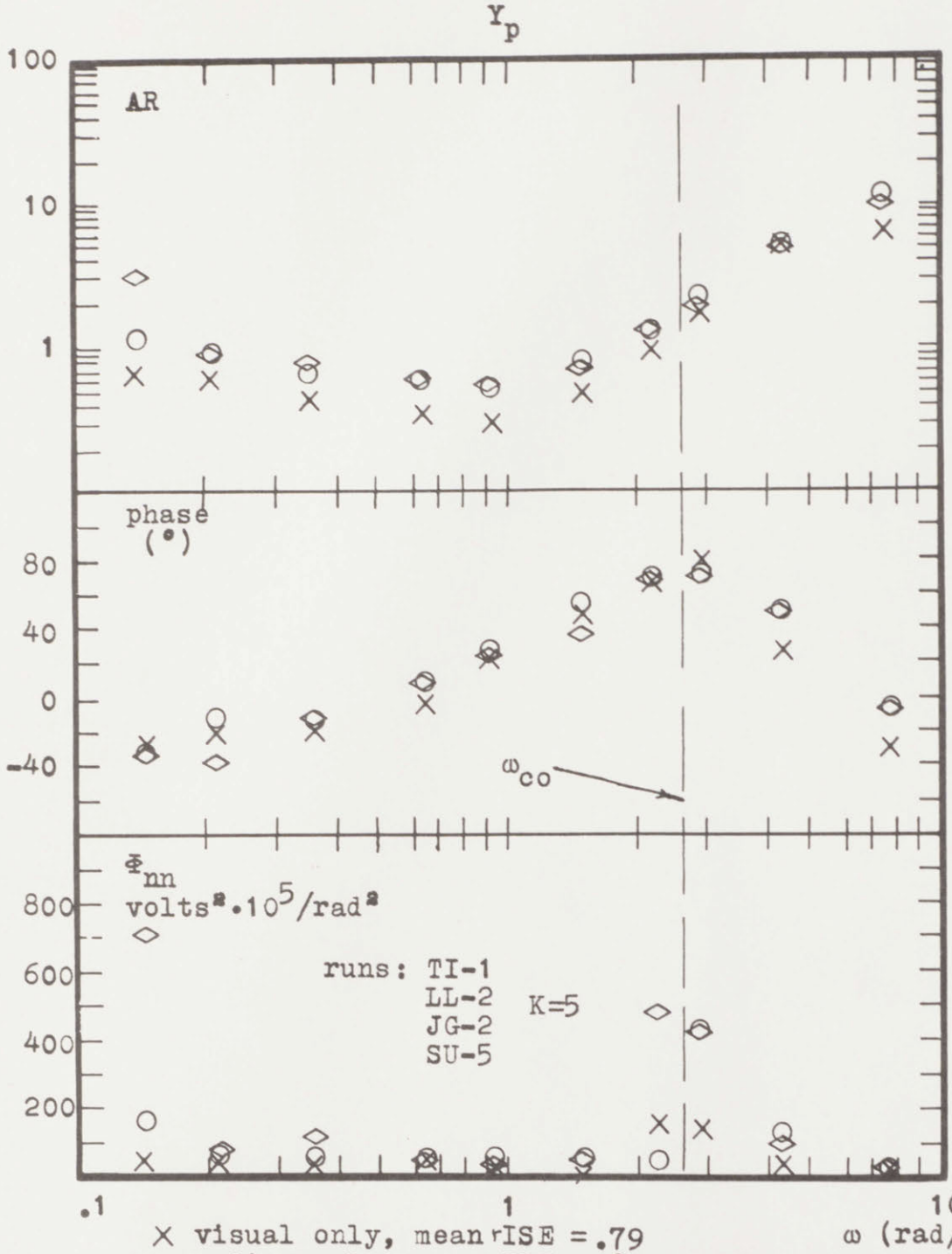

× visual only, mean rISE = .79
◇ motion only, mean rISE = .81
○ visual and motion, mean rISE = .62

ISI=1050

$$Y_c = \frac{5e^{-.1s}}{s(s^2 + s + 5)}$$

EXPERIMENTAL RESULTS

data-60

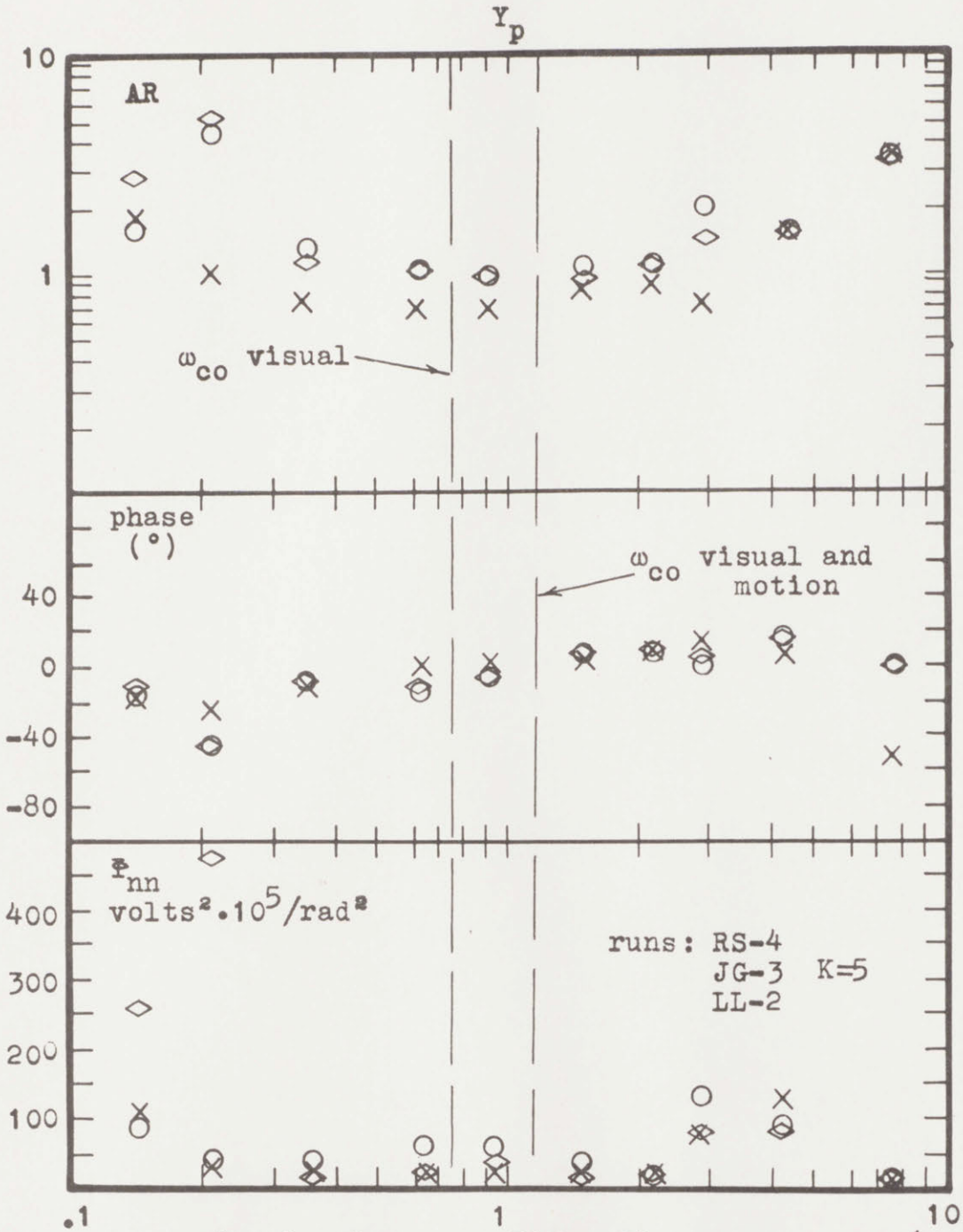

× visual only, mean rISE = .71
◇ motion only, mean rISE = .81
○ visual and motion, mean rISE = .61

ISI=1050

$$Y_c = \frac{20e^{-.1s}}{s(s^2 + 2s + 20)}$$

EXPERIMENTAL RESULTS

data-61

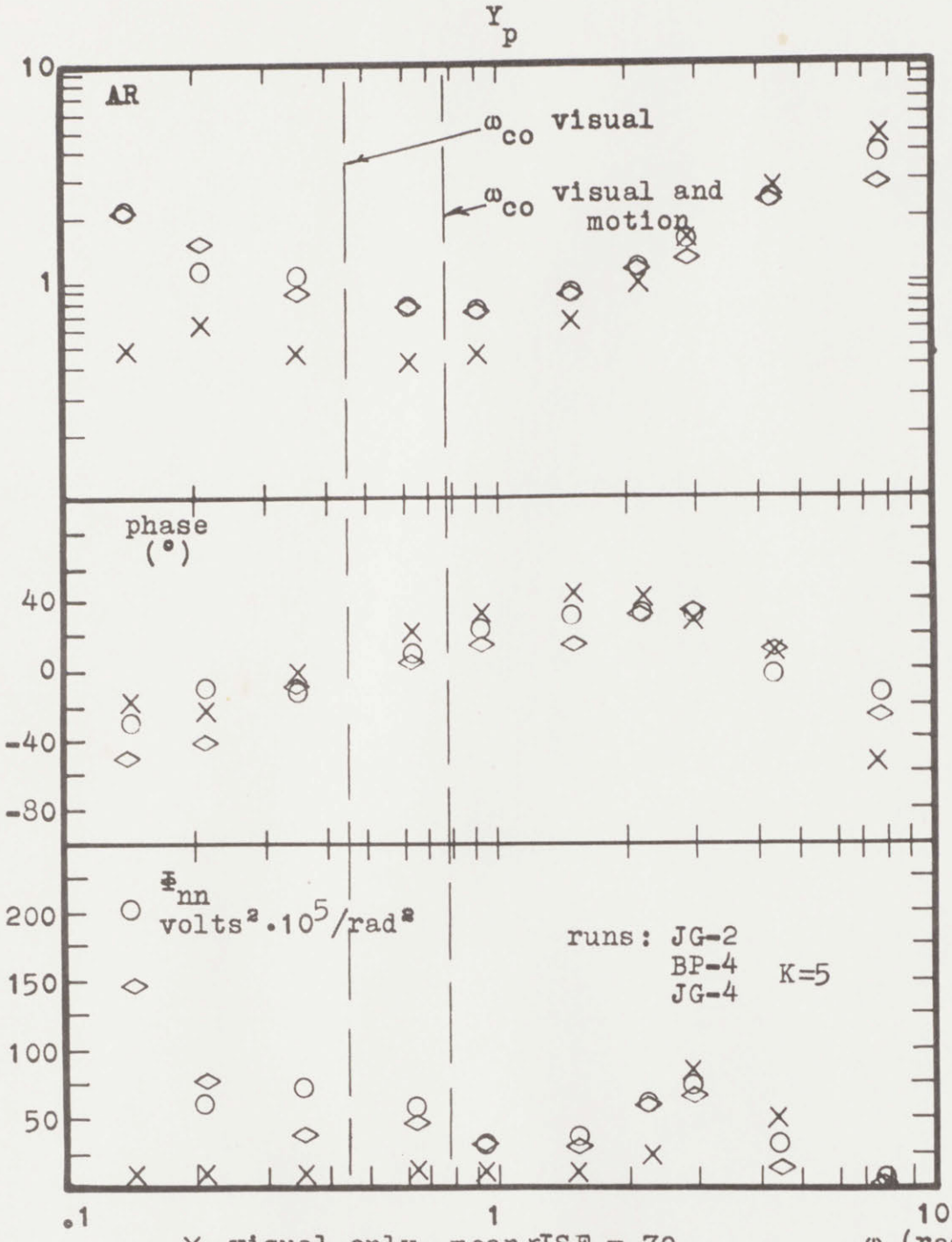

× visual only, mean rISE =.70
◇ motion only, mean rISE =.80
○ visual and motion, mean rISE =.70

ISI=1050

$$Y_c = \frac{10e^{-.1s}}{s(s^2 + 2s + 10)}$$

EXPERIMENTAL RESULTS

data-62

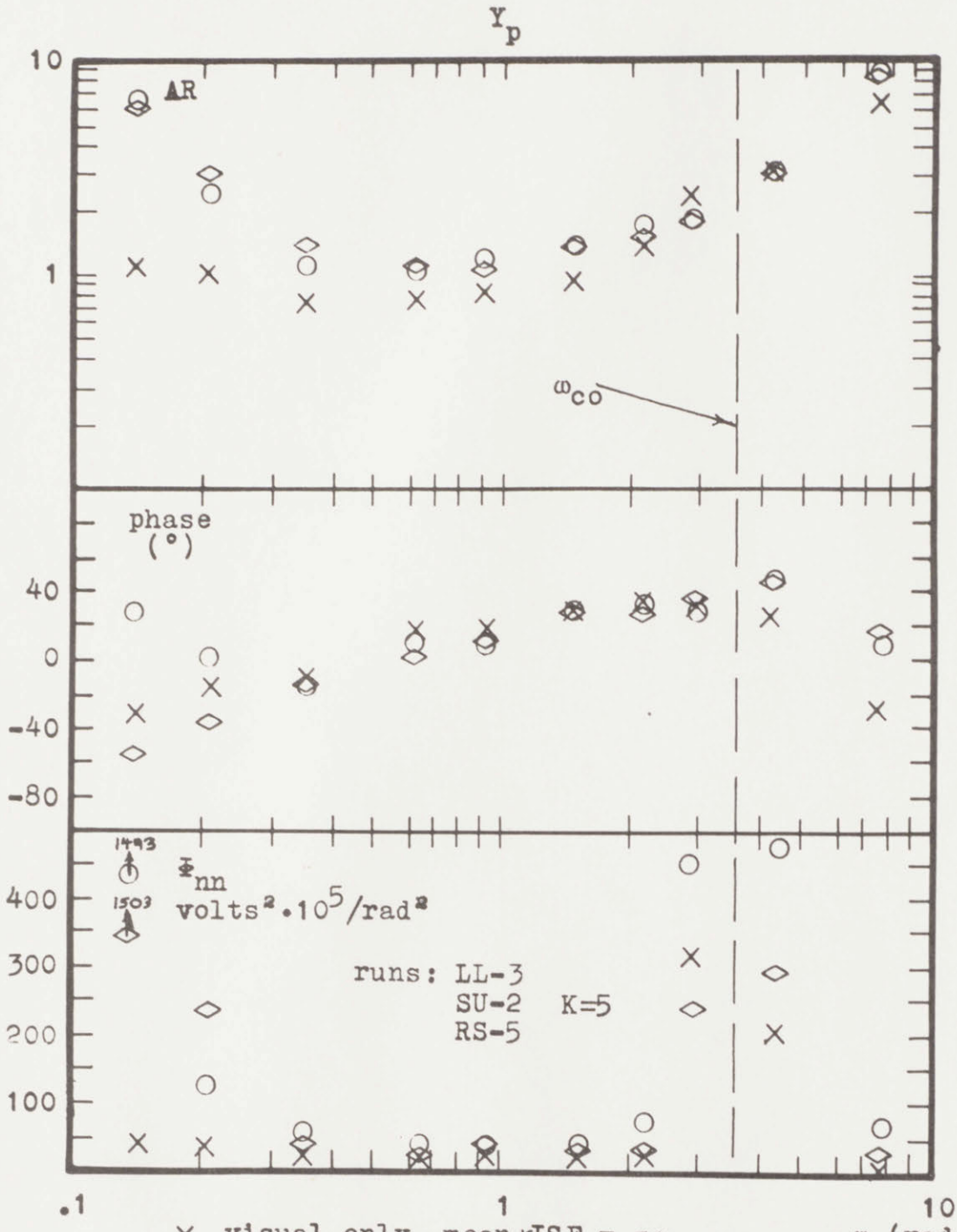

× visual only, mean rISE = .52
◇ motion only, mean rISE = .53
○ visual and motion, mean rISE = .49

ISI=1050

$$Y_c = \frac{15e^{-.1s}}{s(s^2 + 3s + 15)}$$

EXPERIMENTAL RESULTS

data-63

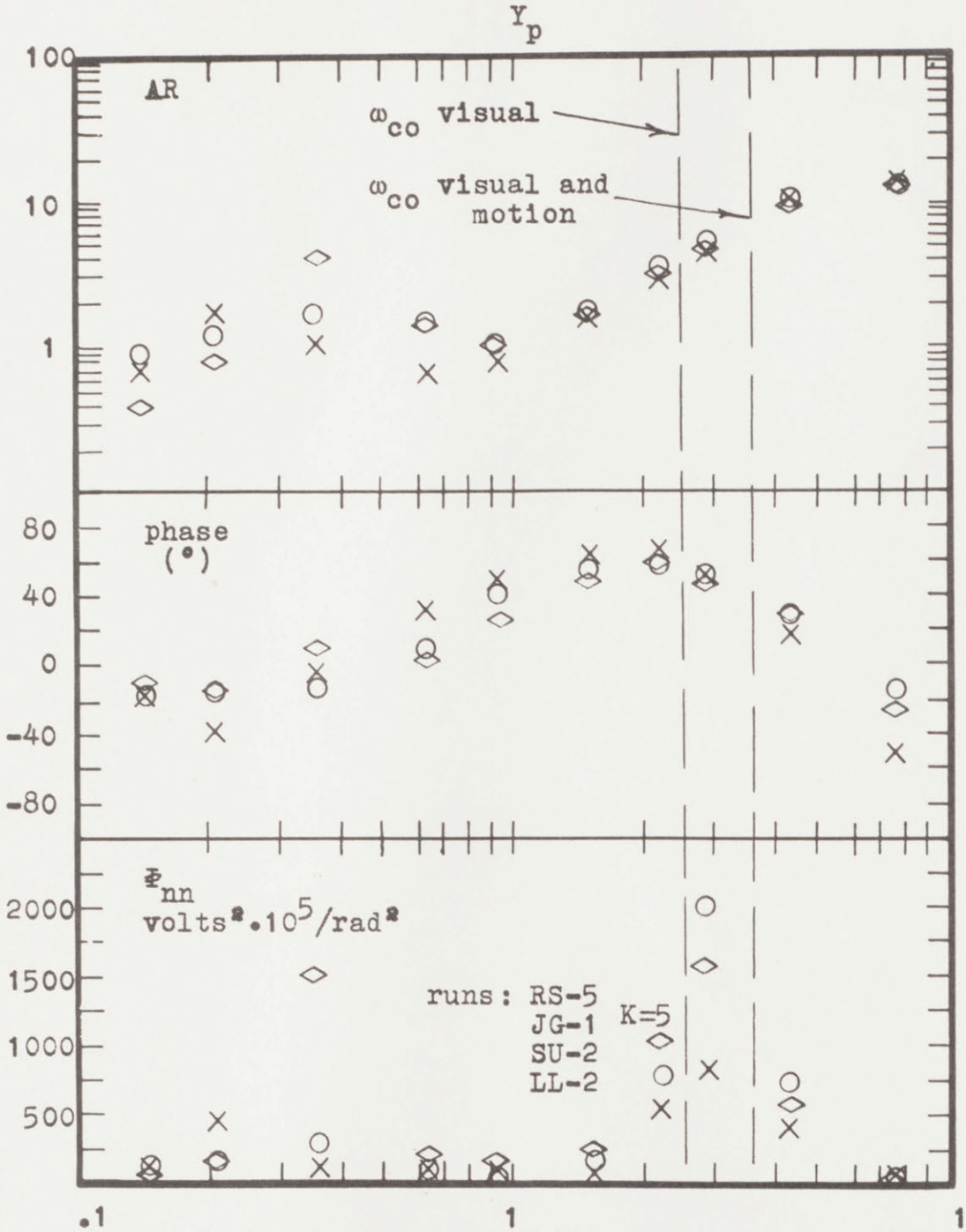

× visual only, mean rISE = .78
◇ motion only, mean rISE = .91
○ visual and motion, mean rISE = .78

ISI=1050

$$Y_c = \frac{5e^{-.1s}}{s(s^2 + 3s + 5)}$$

EXPERIMENTAL RESULTS

data-64

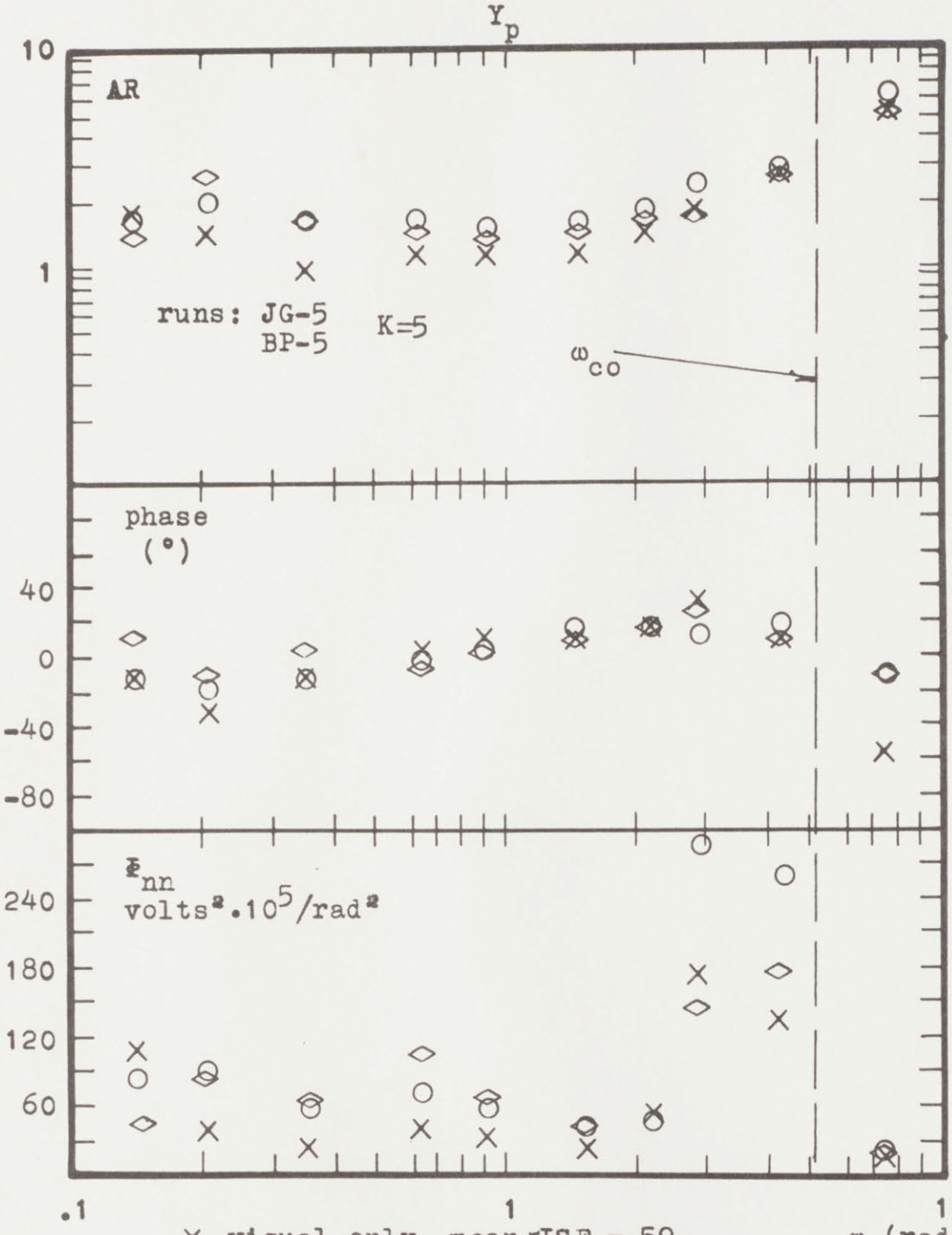

× visual only, mean rISE =.59
◇ motion only, mean rISE =.65
○ visual and motion, mean rISE = .52

ISI=1050

$$Y_c = \frac{20e^{-.1s}}{s(s^2 + 4s + 20)}$$

EXPERIMENTAL RESULTS

data-65

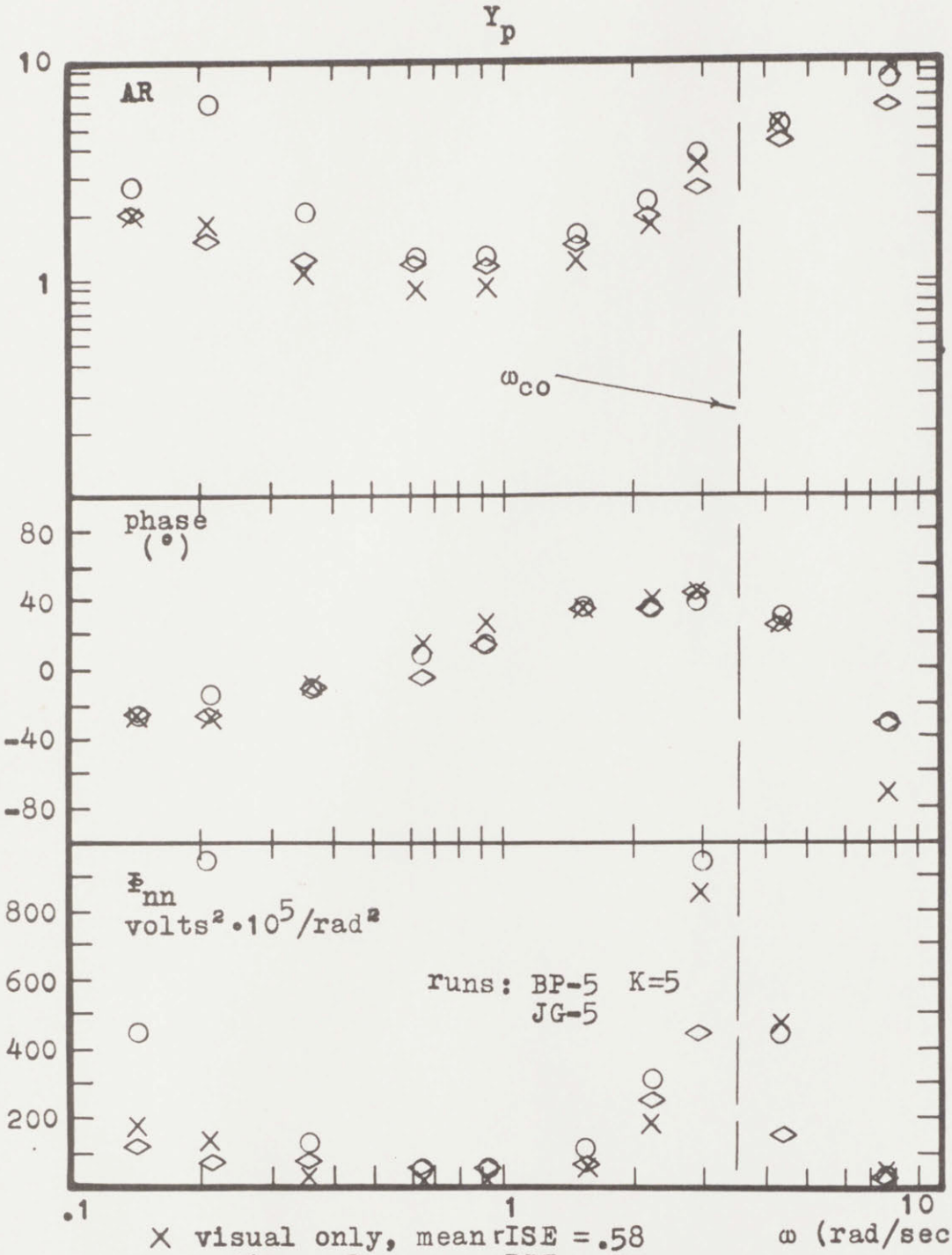

× visual only, mean rISE = .58
◇ motion only, mean rISE = .73
○ visual and motion, mean rISE = .45

ISI=1050

$$Y_c = \frac{10e^{-.1s}}{s(s^2 + 4s + 10)}$$

EXPERIMENTAL RESULTS

data-66

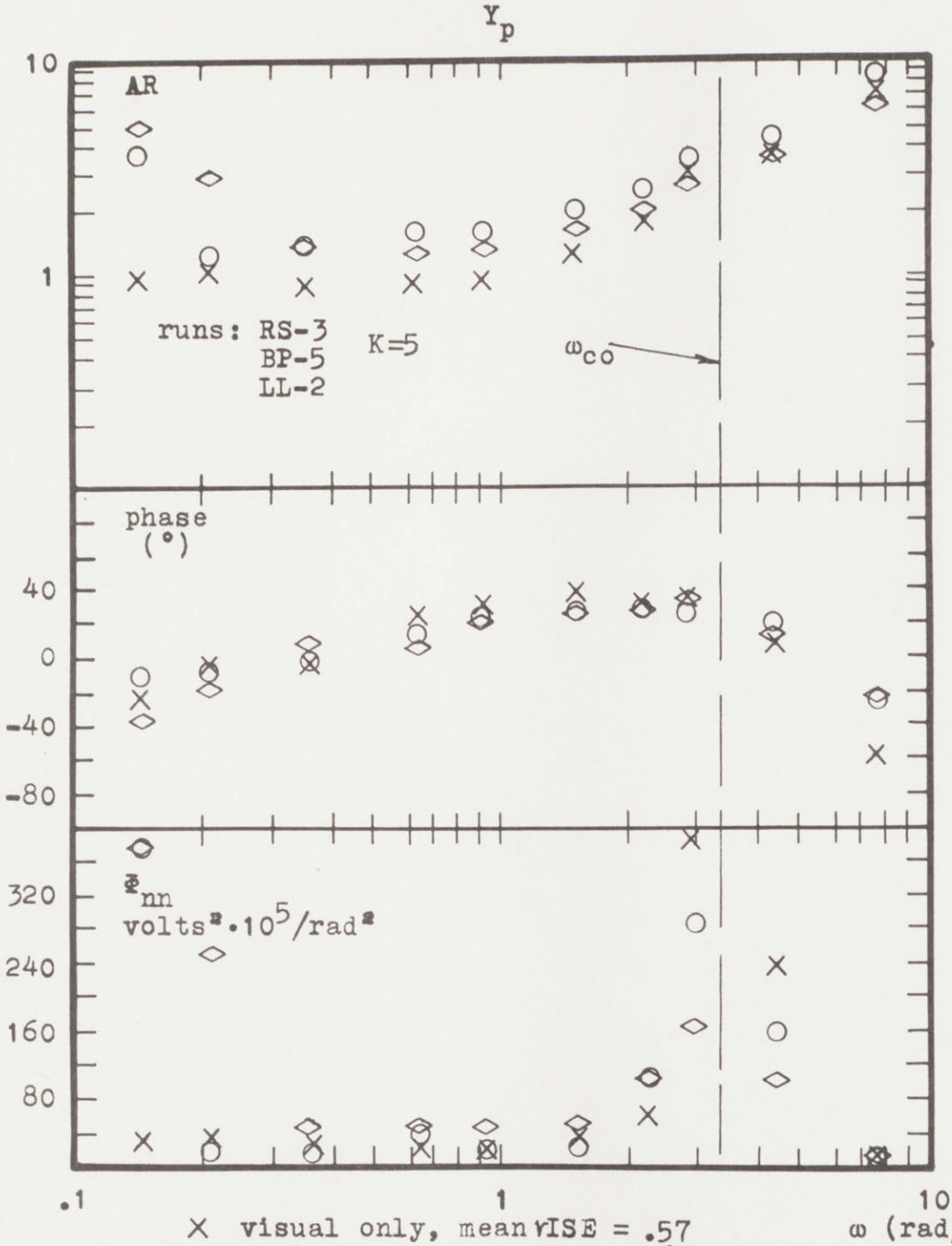

× visual only, mean rISE = .57

◇ motion only, mean rISE = .63

○ visual and motion, mean rISE = .45

ISI=1050

$$Y_c = \frac{15e^{-.1s}}{s(s^2 + 5s + 15)}$$

EXPERIMENTAL RESULTS

data-67

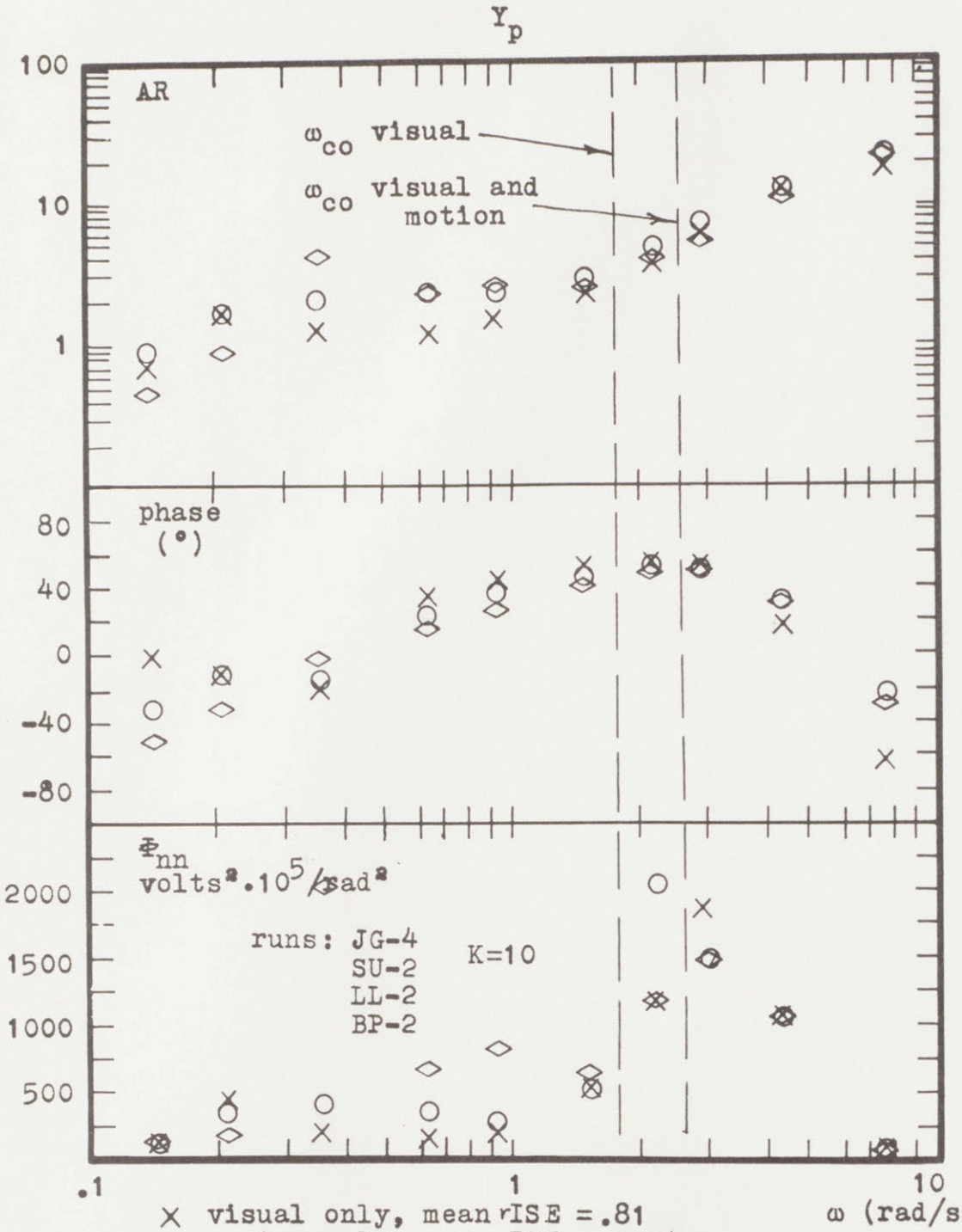

× visual only, mean rISE = .81
◇ motion only, mean rISE = 1.04
○ visual and motion, mean rISE = .71

ISI=1050

$$Y_c = \frac{5e^{-.1s}}{s(s^2 + 5s + 5)}$$

EXPERIMENTAL RESULTS

data-68

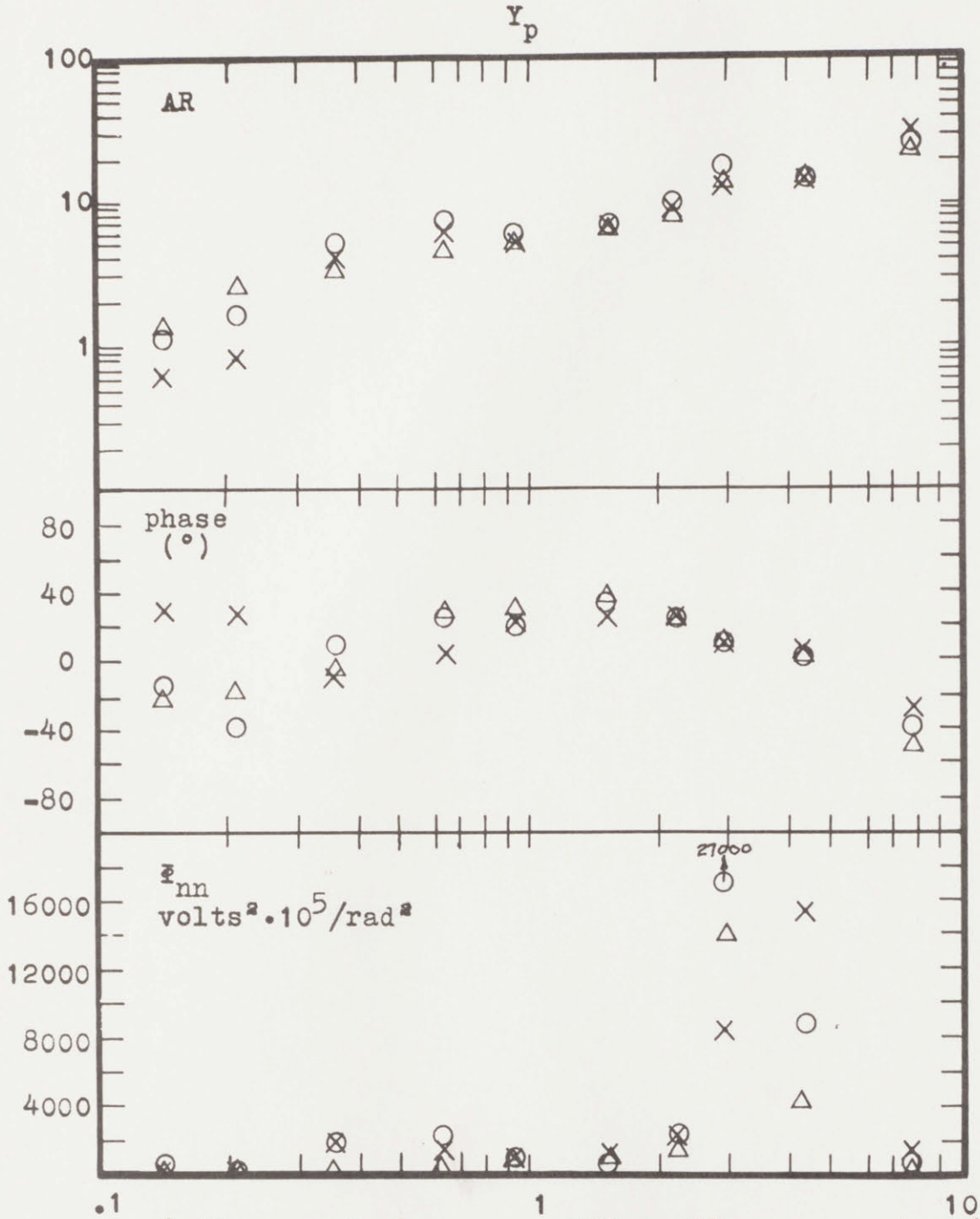

△ JG, mean 5 runs, mean rISE = .33
× TI, mean 5 runs, mean rISE = .33
○ RS, mean 5 runs, mean rISE = .32

visual cues only, $Y_c = \dfrac{2e^{-.1s}}{s(s+2)}$

SUBJECT TO SUBJECT COMPARISON

data-69

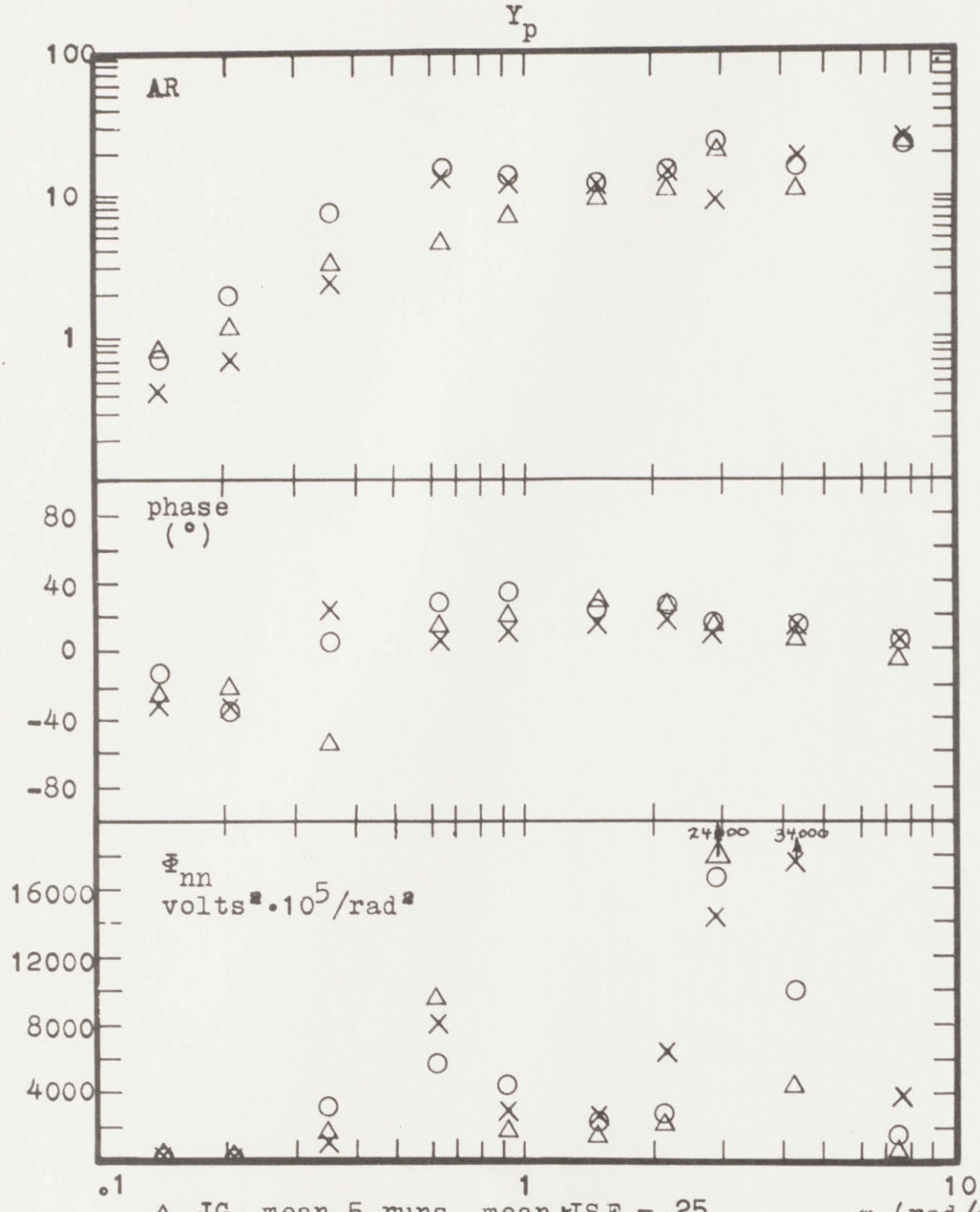

△ JG, mean 5 runs, mean rMSE = .25
× TI, mean 5 runs, mean rMSE = .27
○ RS, mean 5 runs, mean rMSE = .21

visual and motion cues, $Y_c = \dfrac{2e^{-.1s}}{s(s+2)}$

SUBJECT TO SUBJECT COMPARISON

data-70

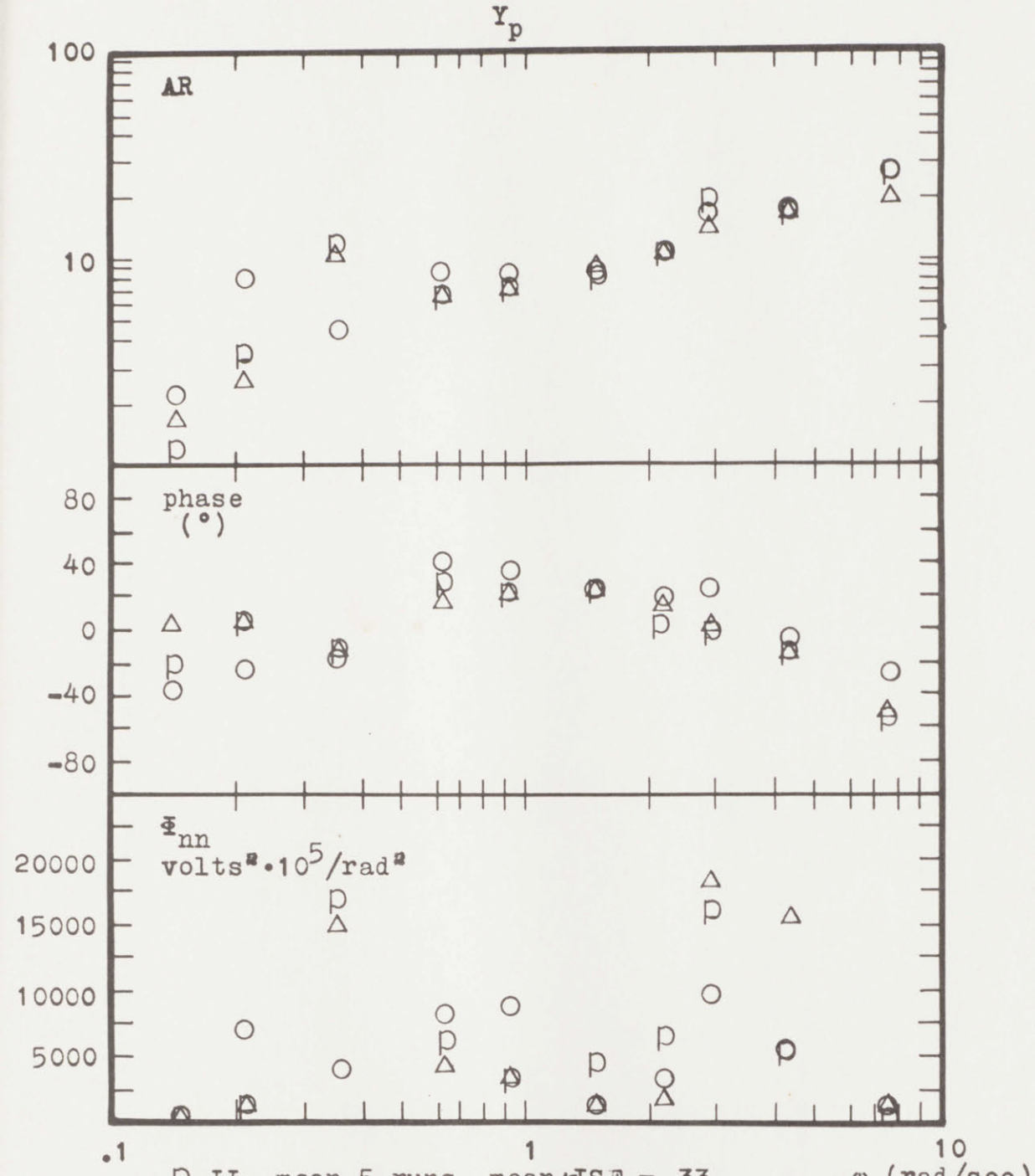

p LL, mean 5 runs, mean rISE = .33
△ JG, mean 4 runs, mean rISE = .33
○ RS, mean 5 runs, mean rISE = .34

visual cues only, $Y_c = \dfrac{4e^{-.1s}}{s(s+4)}$

SUBJECT TO SUBJECT COMPARISON

data-71

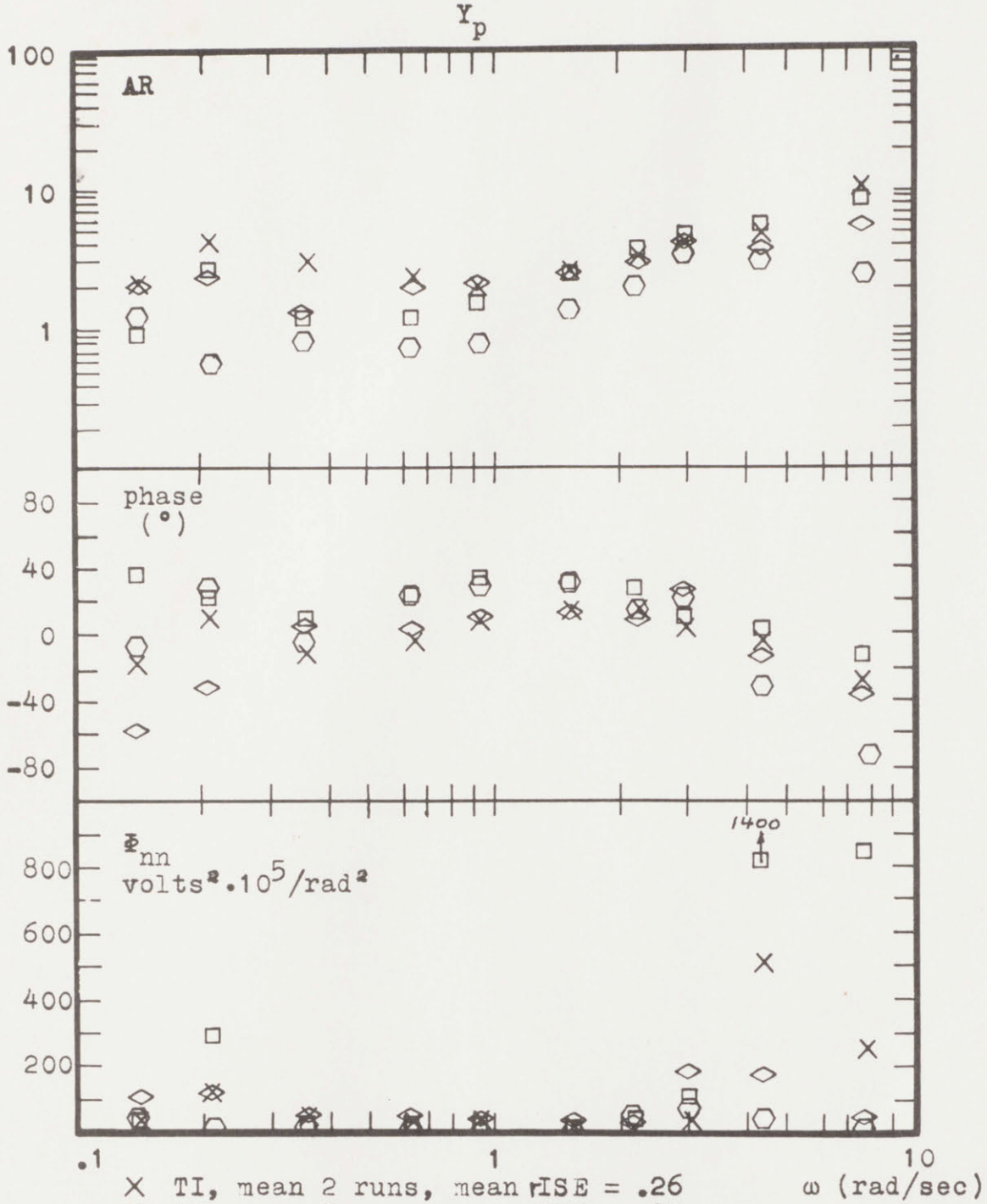

× TI, mean 2 runs, mean rISE = .26
□ SU, mean 2 runs, mean rISE = .23
◇ SF, mean 3 runs, mean rISE = .29
⬡ BP, mean 3 runs, mean rISE = .44

visual cues only, low control power, $Y_c = \frac{5e^{-.1s}}{s(s+5)}$

SUBJECT TO SUBJECT COMPARISON

data-73

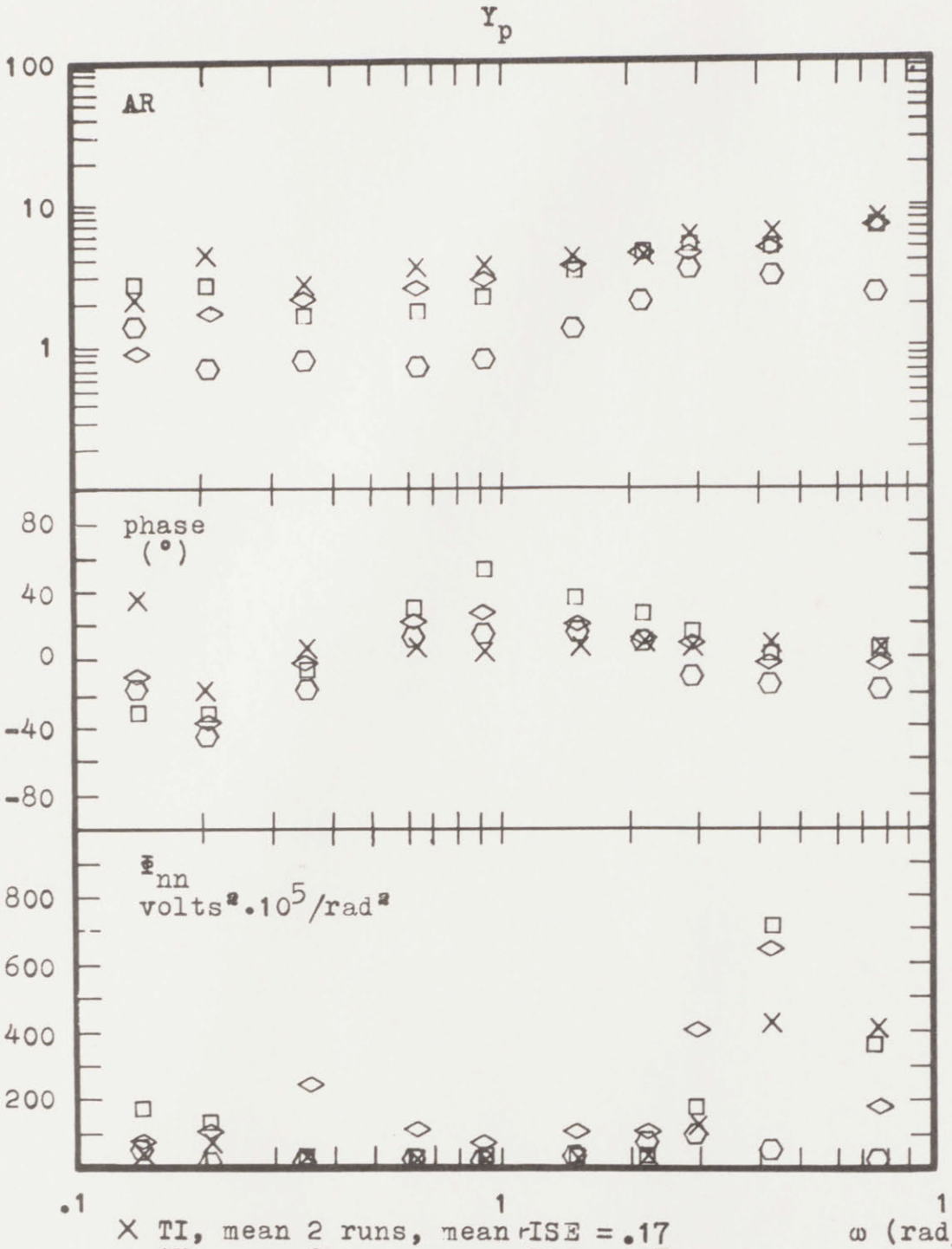

× TI, mean 2 runs, mean rISE = .17
□ SU, mean 2 runs, mean rISE = .17
◇ SF, mean 3 runs, mean rISE = .21
⬡ BP, mean 3 runs, mean rISE = .33

visual and motion cues, low control power, $Y_c = \frac{5e^{-.1s}}{s(s+5)}$

SUBJECT TO SUBJECT COMPARISON

data-74

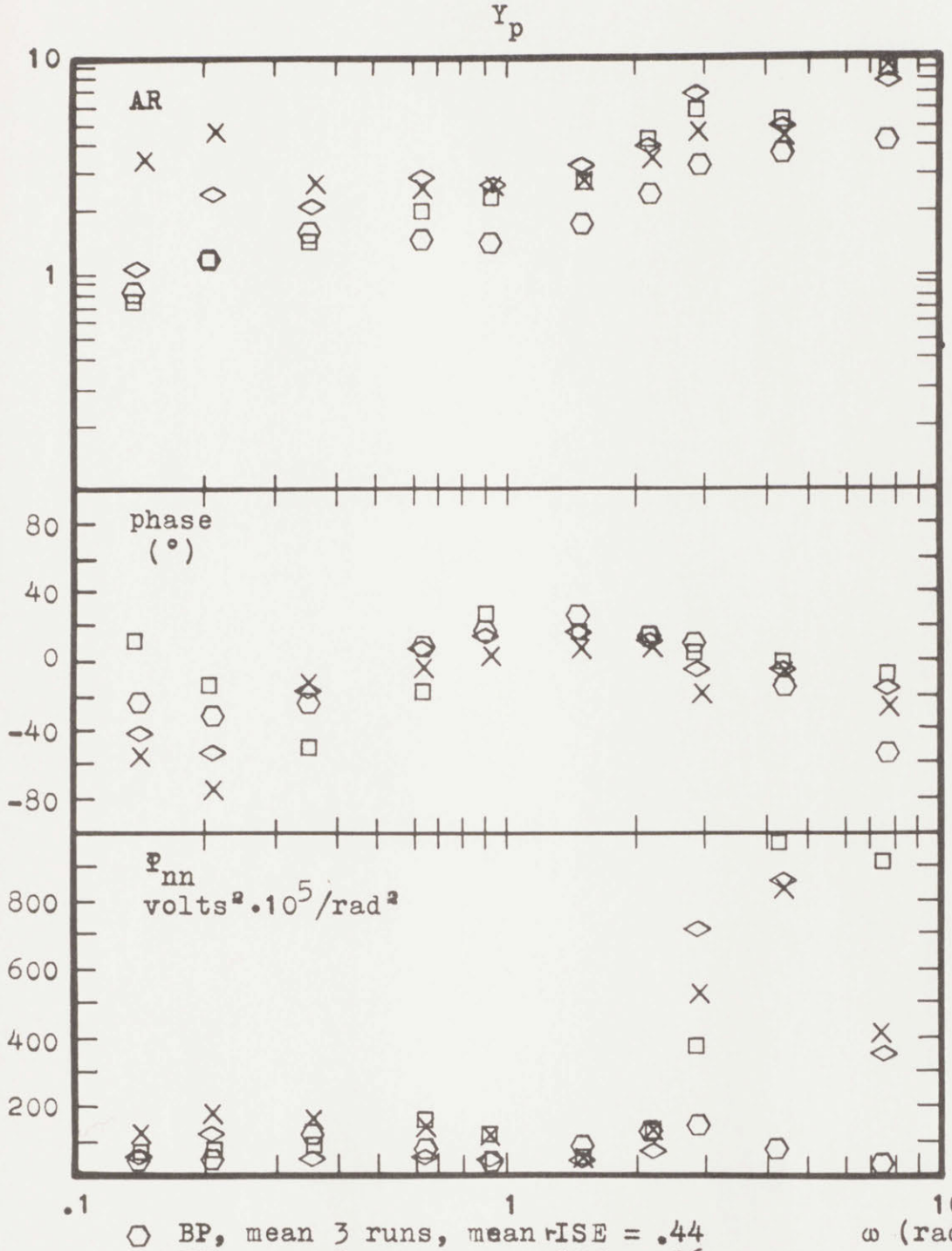

○ BP, mean 3 runs, mean rmsE = .44
◇ SF, mean 3 runs, mean rmsE = .26
□ SU, mean 2 runs, mean rmsE = .29
× TI, mean 2 runs, mean rmsE = .33

visual cues only, medium control power, $Y_c = \frac{5e^{-.1s}}{s(s+5)}$

SUBJECT TO SUBJECT COMPARISON

data-75

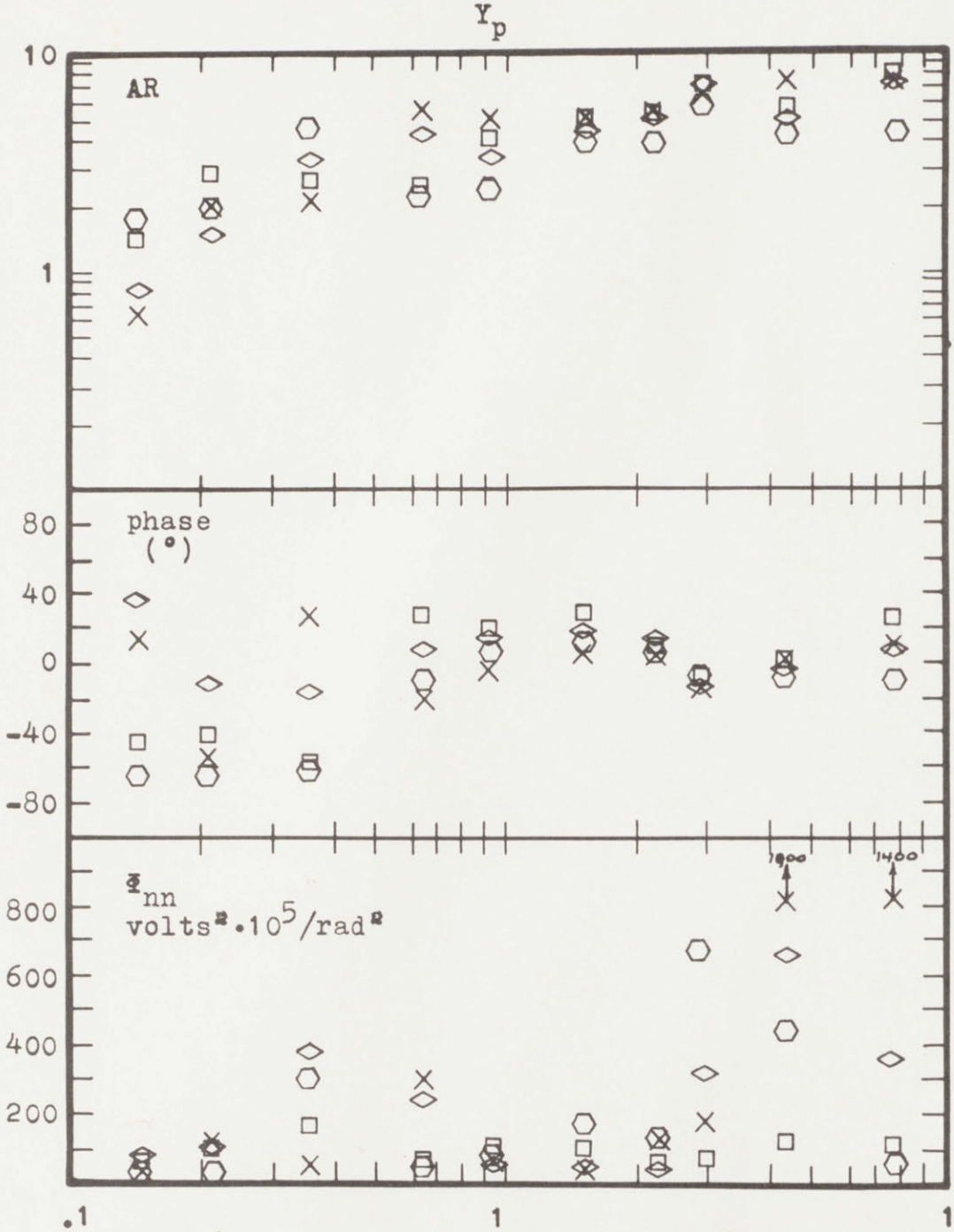

○ BP, mean 3 runs, mean rMSE = .26
◇ SF, mean 3 runs, mean rMSE = .20
□ SU, mean 2 runs, mean rMSE = .17
× TI, mean 2 runs, mean rMSE = .17

visual and motion cues, $Y_c = \dfrac{5e^{-.1s}}{s(s+5)}$
medium control power,

SUBJECT TO SUBJECT COMPARISON

data-76

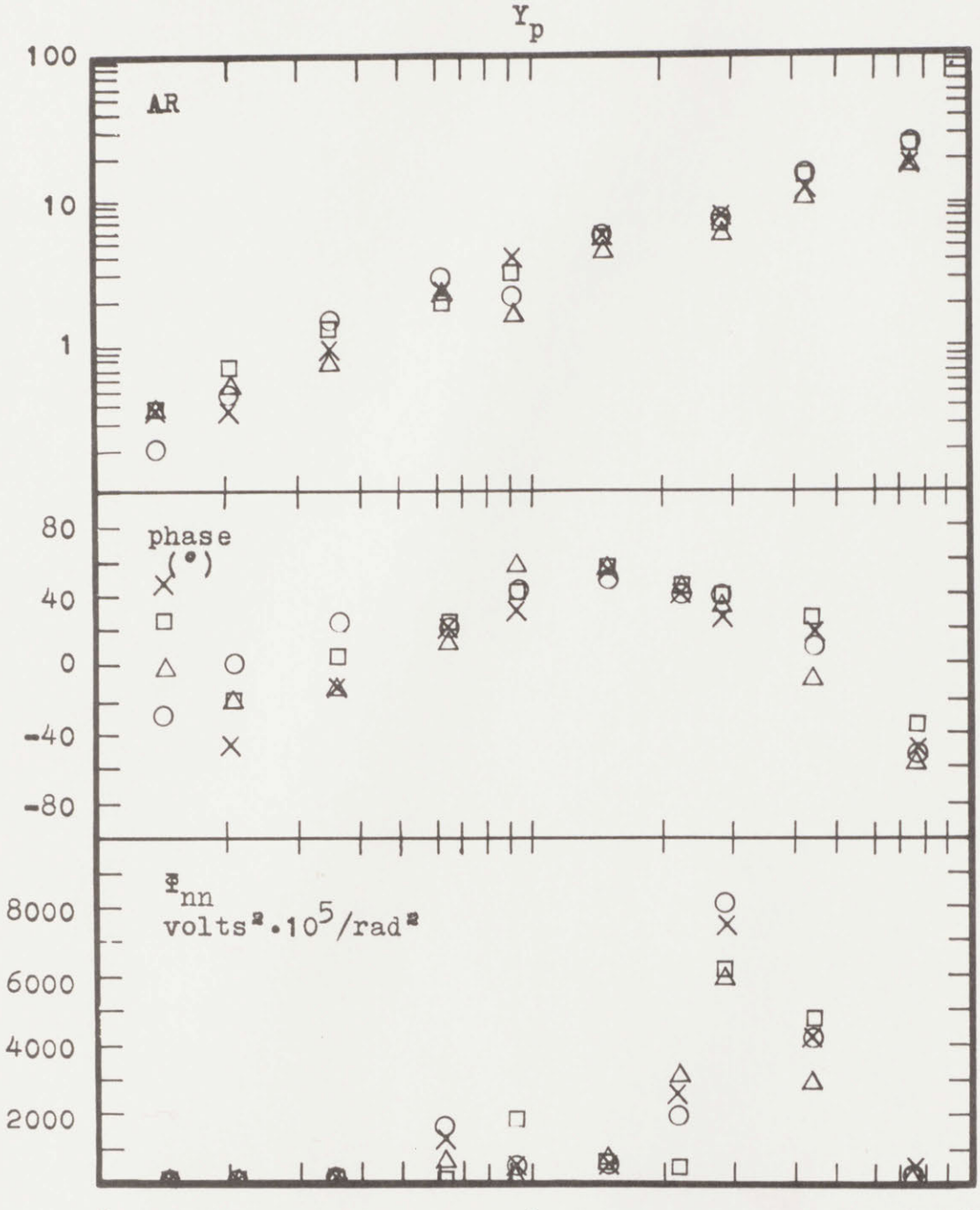

□ SU, mean 3 runs, mean rISE = .66
△ JG, mean 5 runs, mean rISE = 1.07
× TI, mean 2 runs, mean rISE = 1.04
○ RS, mean 5 runs, mean rISE = .88

visual cues only, $Y_c = \frac{e^{-.1s}}{s^2}$

SUBJECT TO SUBJECT COMPARISON

data-77

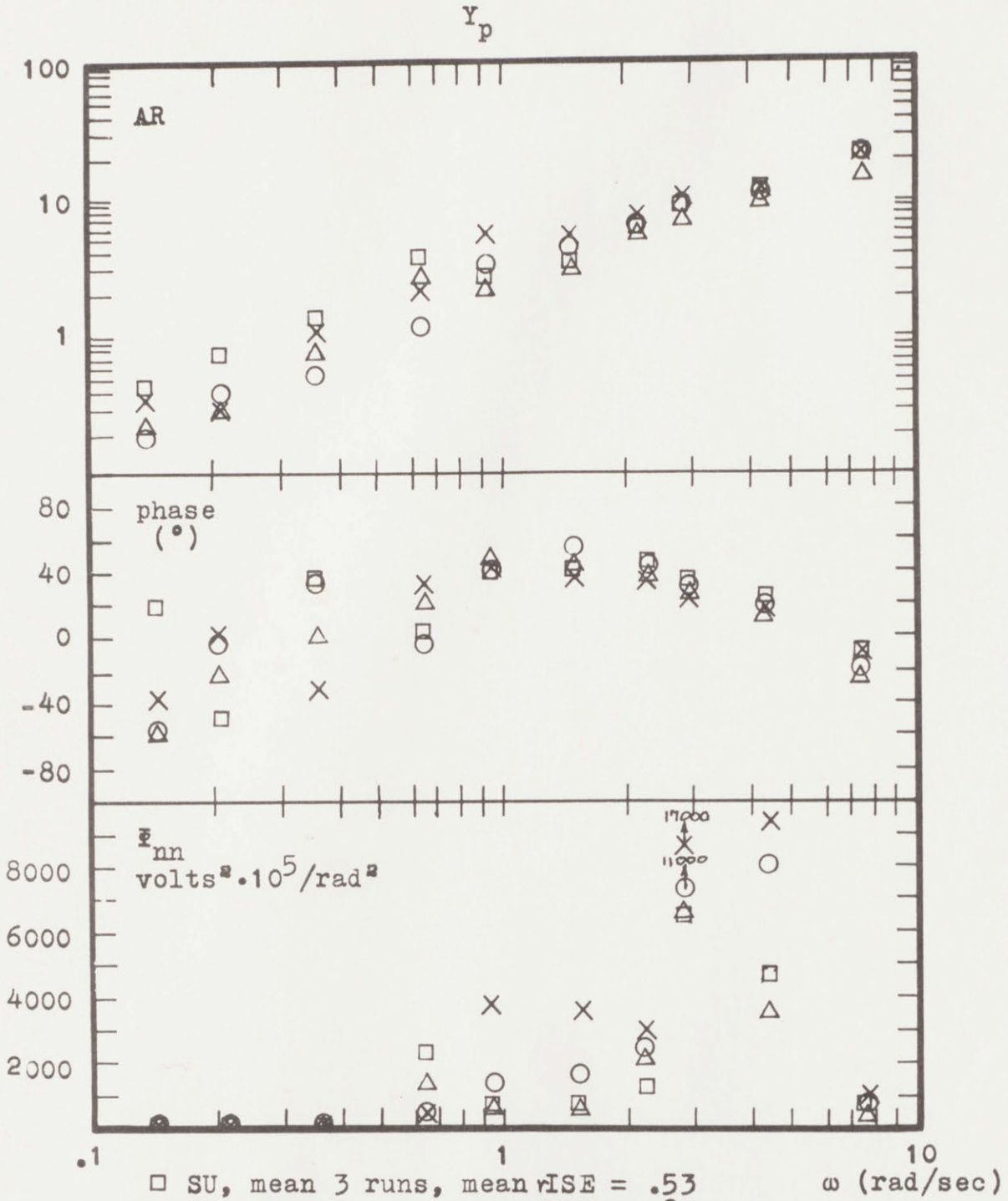

□ SU, mean 3 runs, mean rISE = .53
△ JG, mean 5 runs, mean rISE = .80
× TI, mean 2 runs, mean rISE = .79
○ RS, mean 5 runs, mean rISE = .82

visual and motion cues, $Y_c = \frac{e^{-.1s}}{s^2}$

SUBJECT TO SUBJECT COMPARISON

data-78

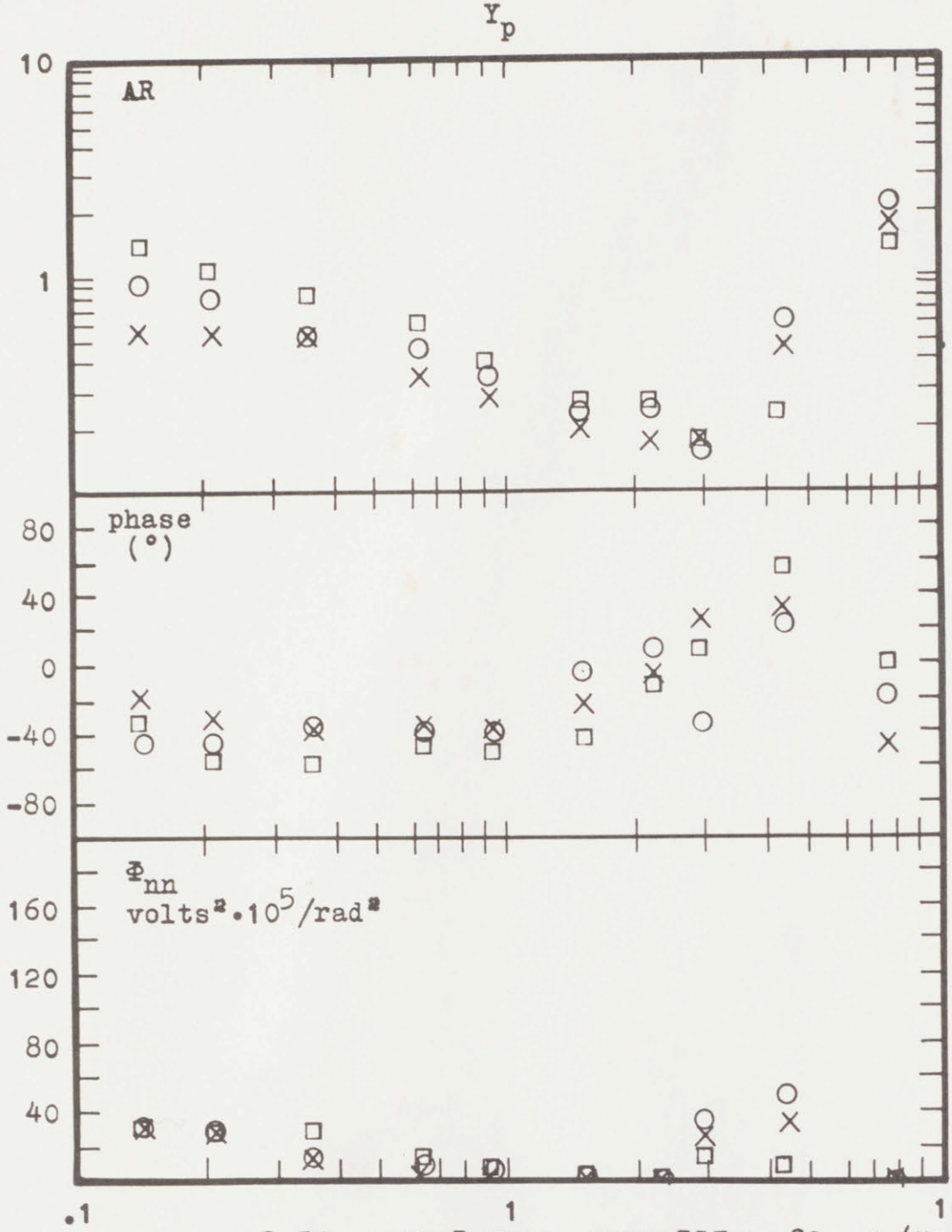

○ RS, mean 5 runs, mean rISE = .82
× TI, mean 5 runs, mean rISE = 1.03
□ SU, mean 5 runs, mean rISE = .60

visual cues only $Y_c = \frac{10e^{-.1s}}{s^2 + 10}$

SUBJECT TO SUBJECT COMPARISON

data-79

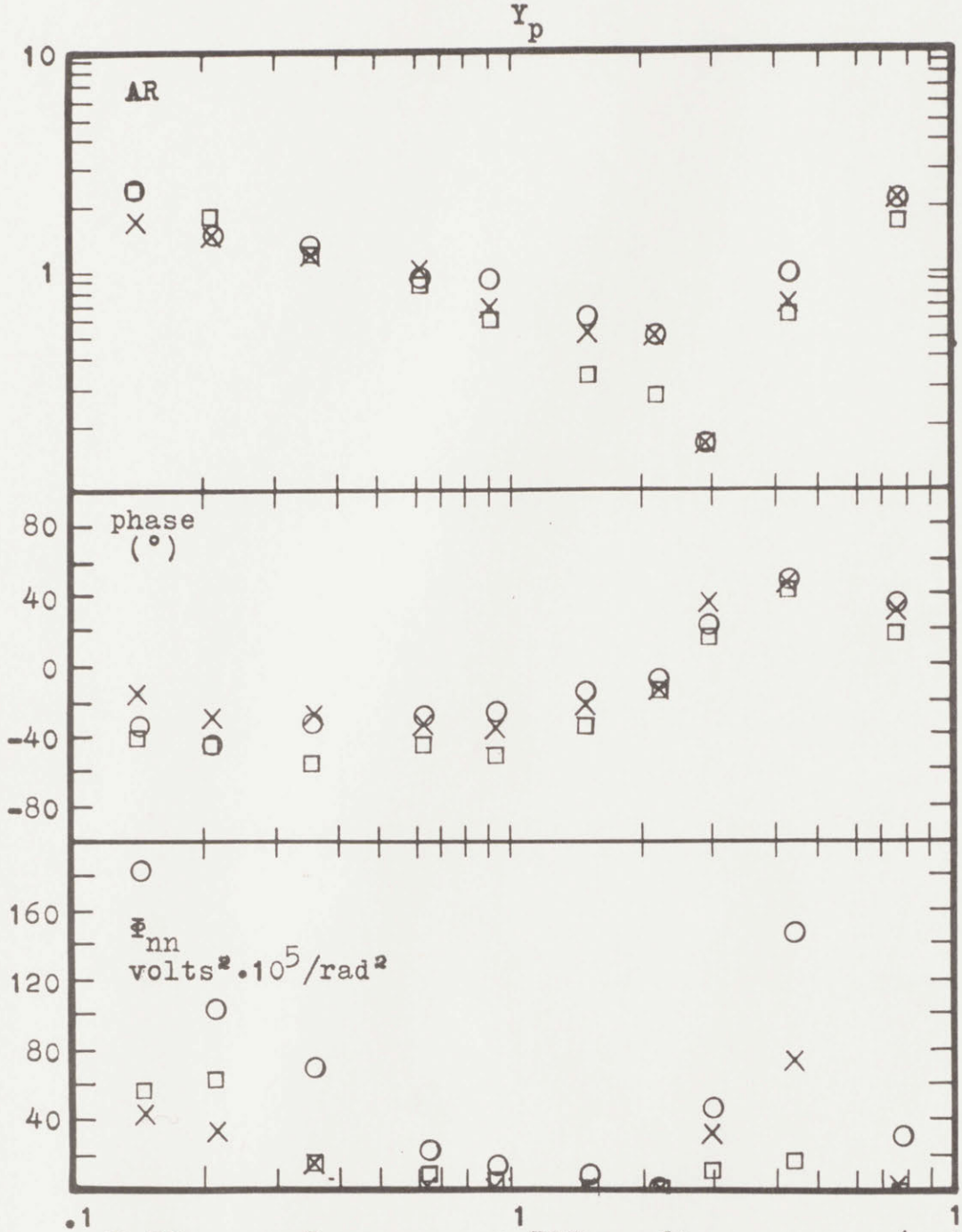

○ RS, mean 5 runs, mean rISE = .60
× TI, mean 5 runs, mean rISE = .51
□ SU, mean 5 runs, mean rISE = .48

visual and motion cues, $Y_c = \frac{10e^{-.1s}}{s^2 + 10}$

SUBJECT TO SUBJECT COMPARISON

data-80

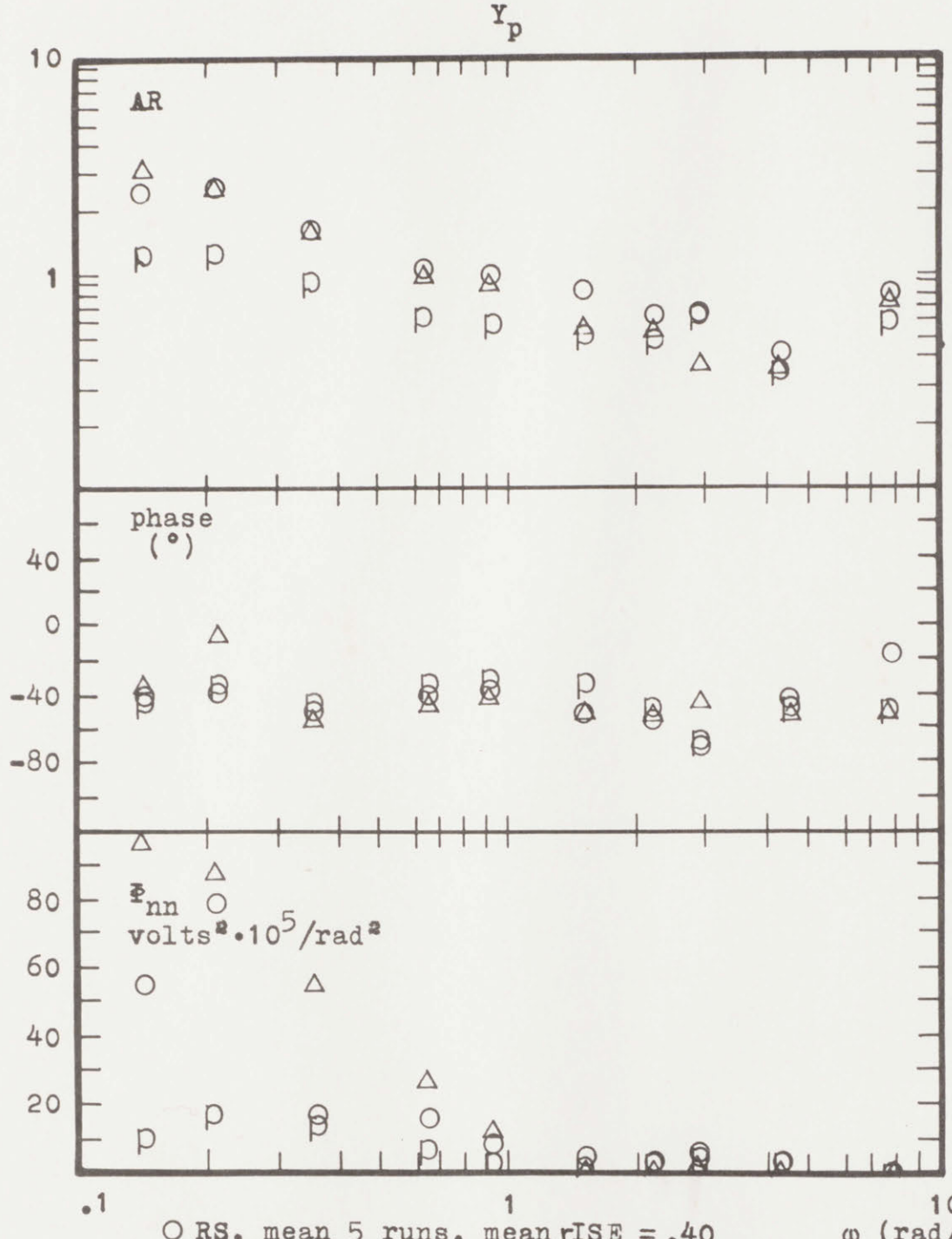

○ RS, mean 5 runs, mean rISE = .40
p LL, mean 4 runs, mean rISE = .52
△ JG, mean 6 runs, mean rISE = .46

visual cues only, $Y_c = \dfrac{20e^{-.1s}}{s^2 + 2s + 20}$

SUBJECT TO SUBJECT COMPARISON

data-81

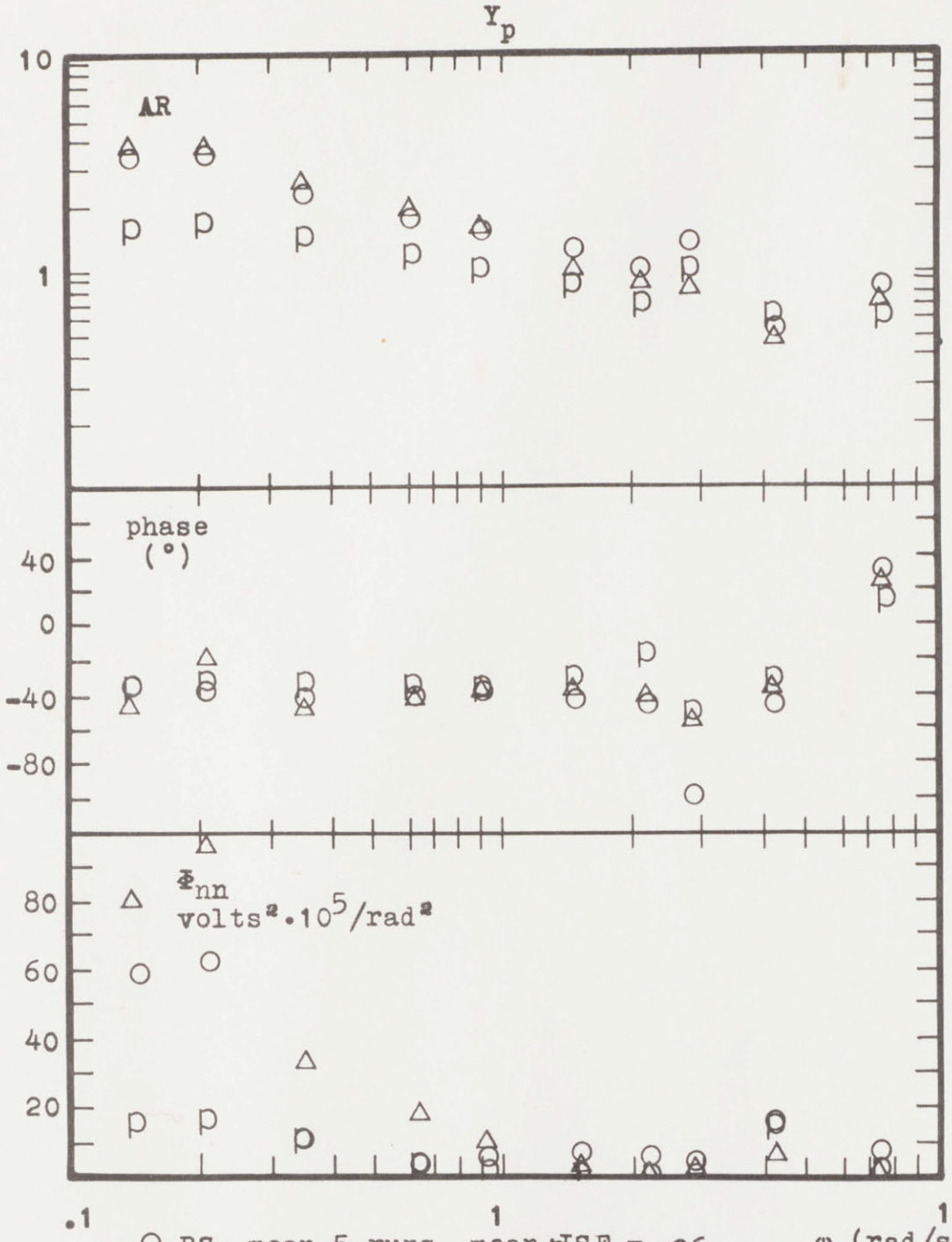

○ RS, mean 5 runs, mean rISE = .26
p LL, mean 4 runs, mean rISE = .35
△ JG, mean 6 runs, mean rISE = .29

visual and motion cues, $Y_c = \frac{20e^{-.1s}}{s^2 + 2s + 20}$

SUBJECT TO SUBJECT COMPARISON

data-82

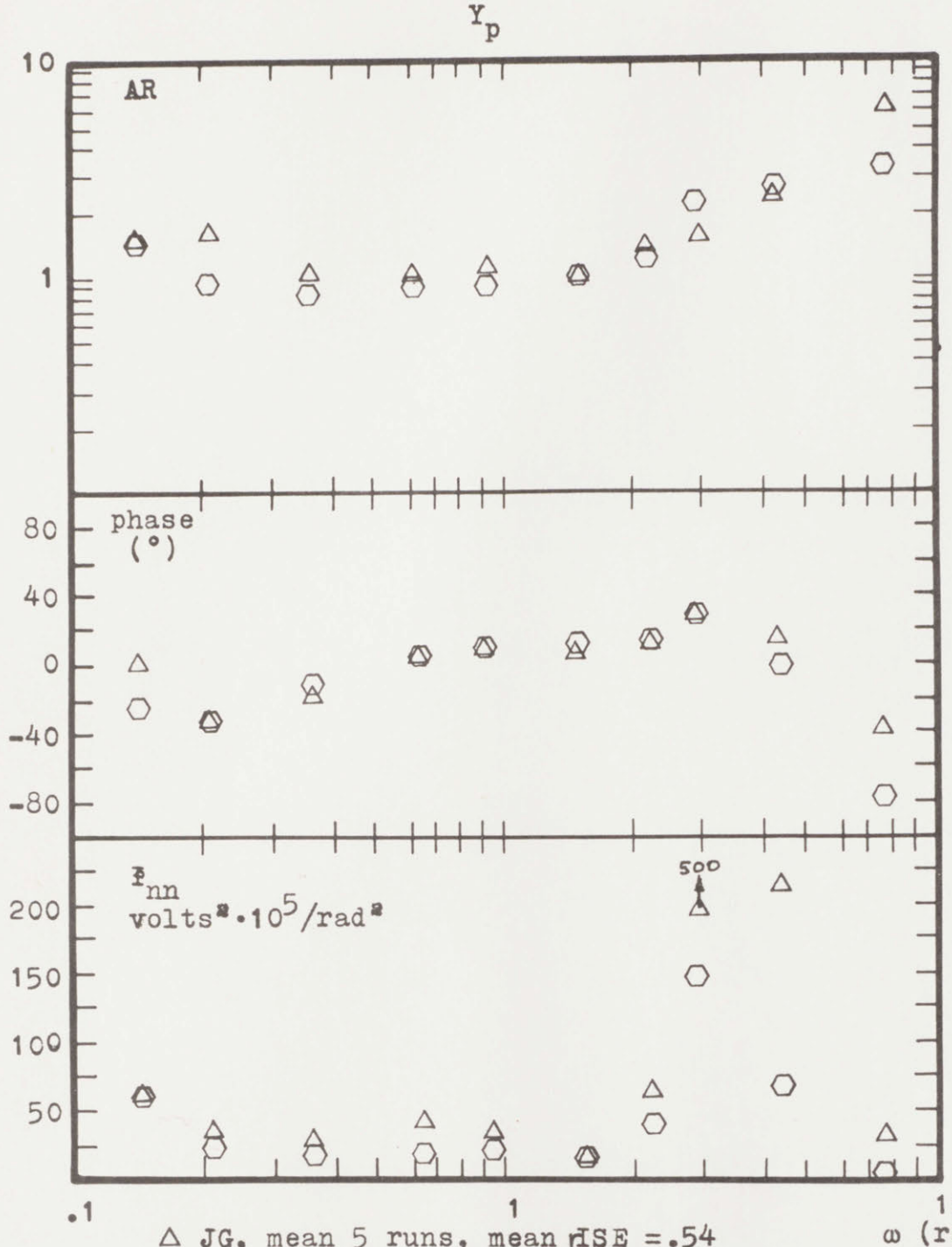

△ JG, mean 5 runs, mean rISE = .54
○ BP, mean 5 runs, mean rISE = .64

visual cues only, $Y_c = \dfrac{20e^{-.1s}}{s(s^2 + 4s + 20)}$

SUBJECT TO SUBJECT COMPARISON

data-83

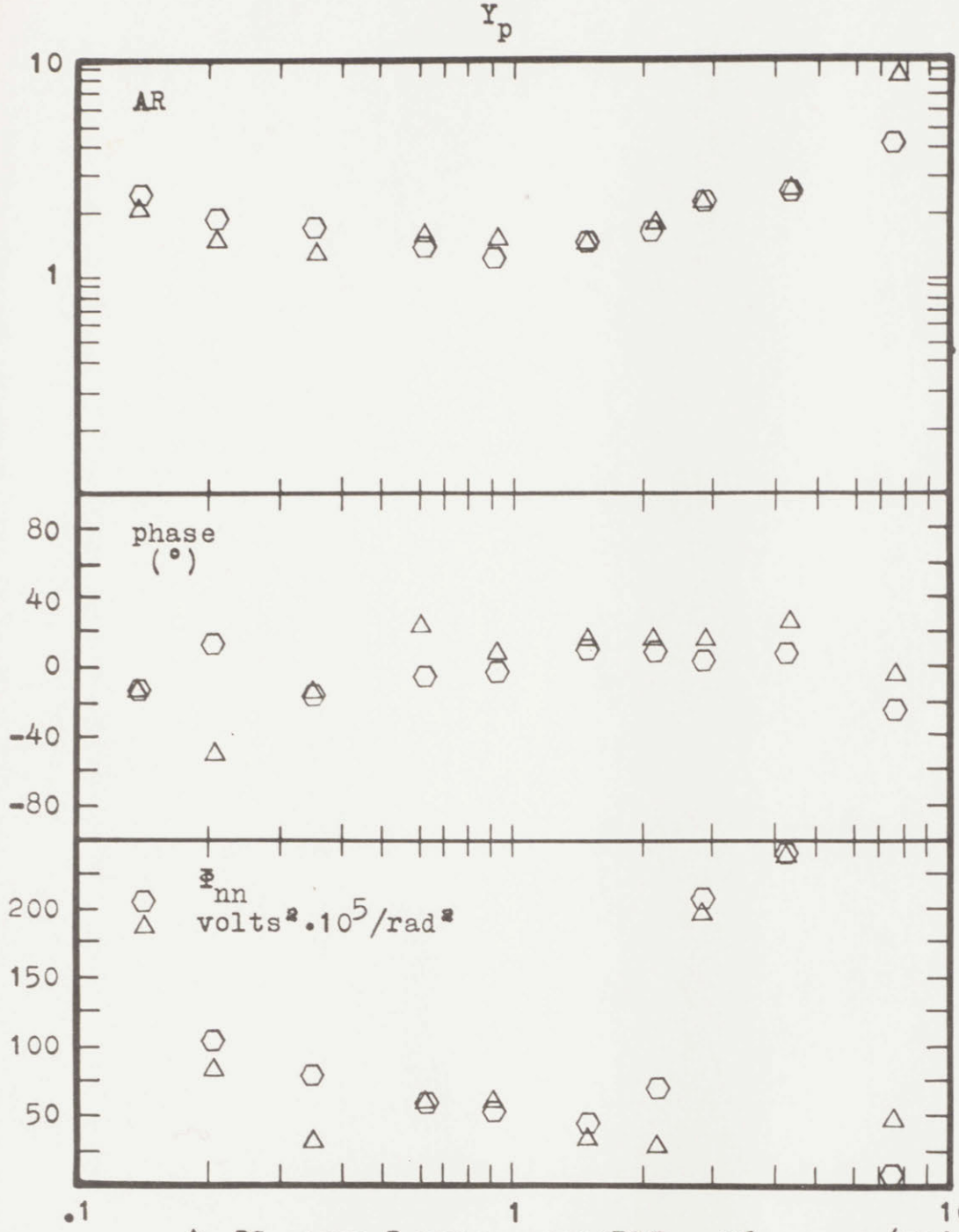

△ JG, mean 5 runs, mean rISE = .56

⬡ BP, mean 5 runs, mean rISE = .57

visual and motion cues, $Y_c = \dfrac{20e^{-.1s}}{s(s^2 + 4s + 20)}$

SUBJECT TO SUBJECT COMPARISON

data-84

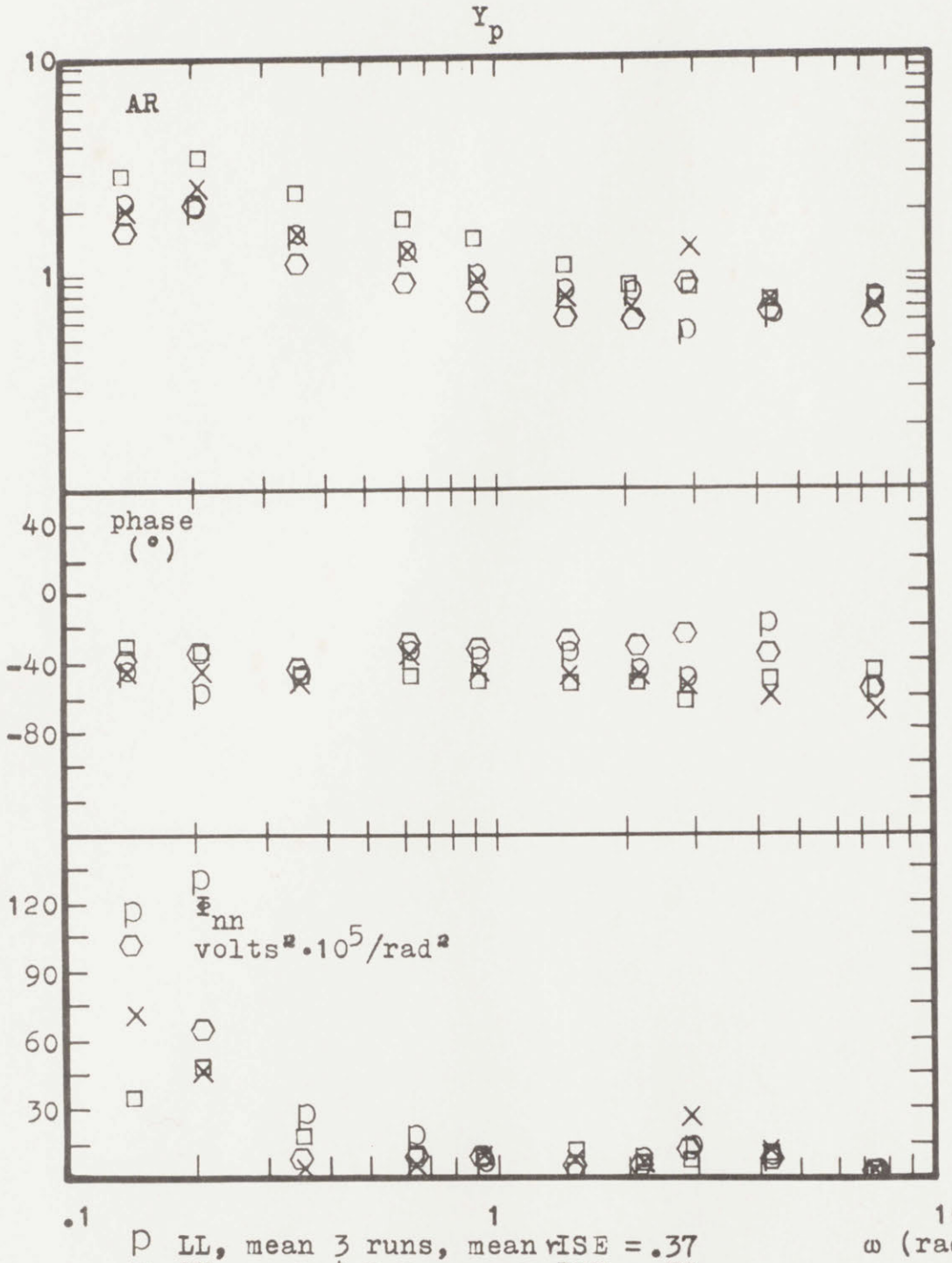

p LL, mean 3 runs, mean rISE = .37
□ SU, mean 4 runs, mean rISE = .32
× TI, mean 3 runs, mean rISE = .34
⬡ BP, mean 4 runs, mean rISE = .41

visual cues only, $Y_c = \dfrac{25e^{-.1s}}{s^2 + 5s + 25}$

SUBJECT TO SUBJECT COMPARISON

data-85

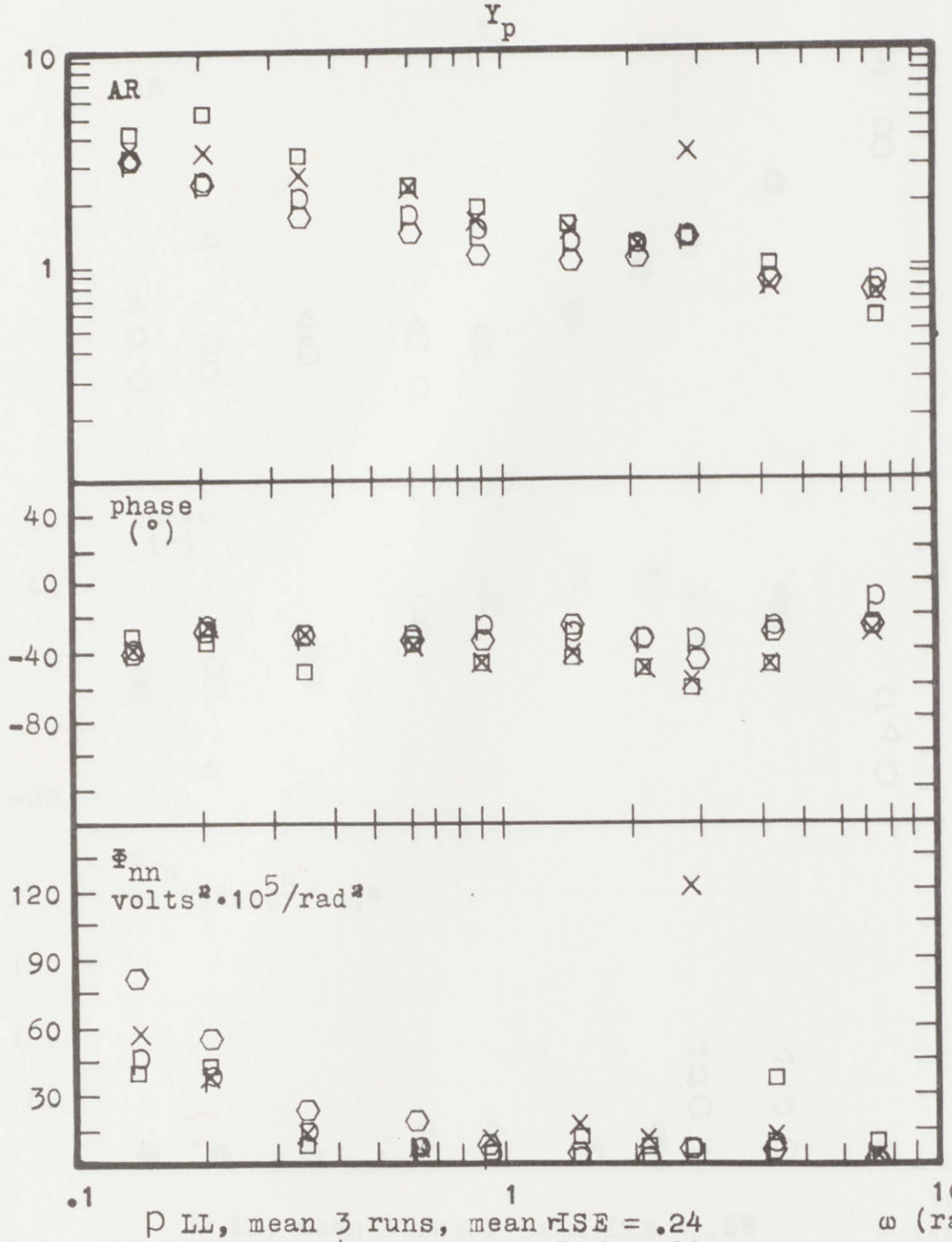

P LL, mean 3 runs, mean rISE = .24
□ SU, mean 4 runs, mean rISE = .22
X TI, mean 3 runs, mean rISE = .22
⬡ BP, mean 4 runs, mean rISE = .28

visual and motion cues, $Y_c = \dfrac{25e^{-.1s}}{s^2 + 5s + 25}$

SUBJECT TO SUBJECT COMPARISON

data-86

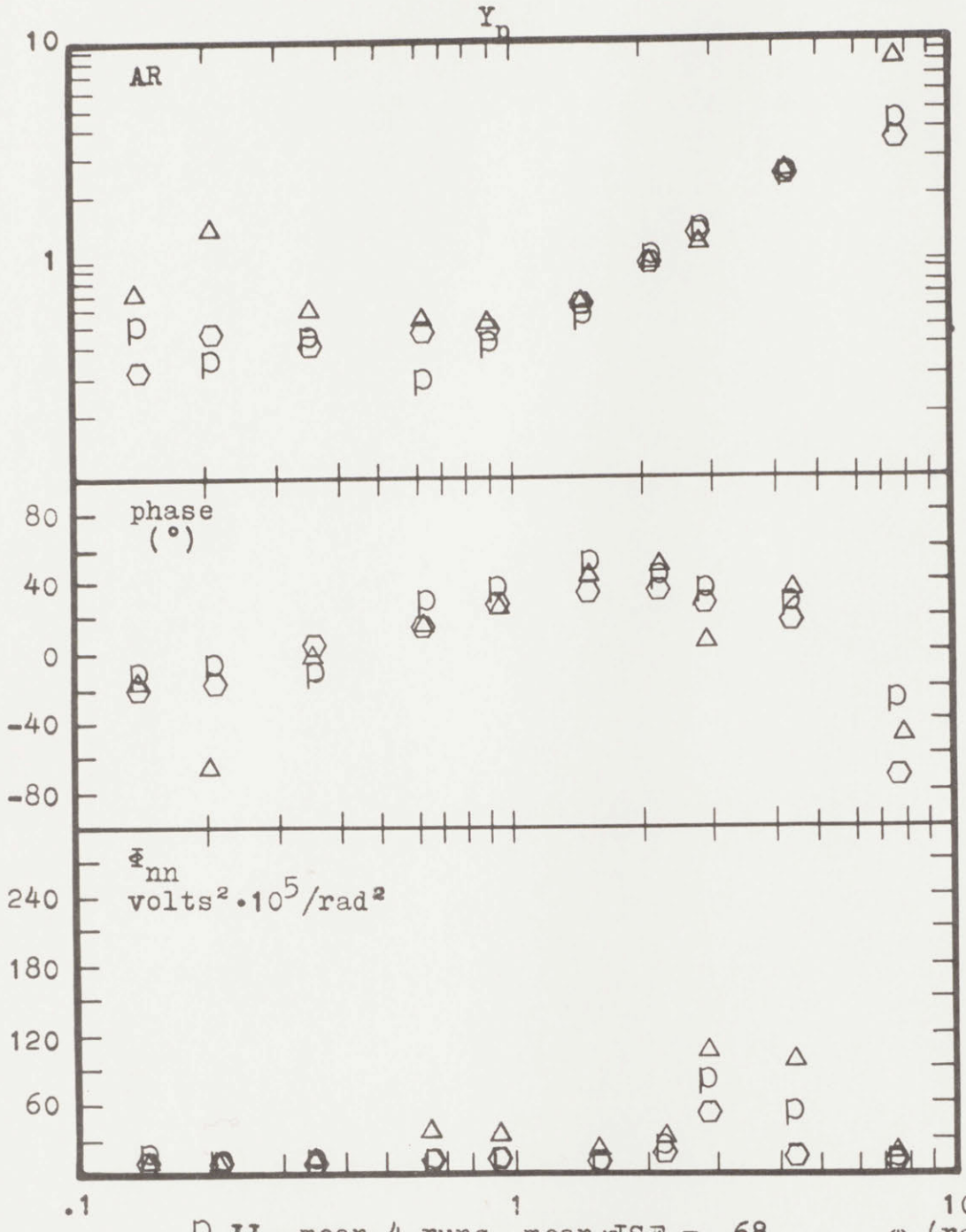

p LL, mean 4 runs, mean rISE = .68
⬡ BP, mean 4 runs, mean rISE = .73
△ JG, mean 2 runs, mean rISE = .70

visual cues only, $Y_c = \frac{10e^{-.1s}}{s(s^2 + 2s + 10)}$

SUBJECT TO SUBJECT COMPARISON

data-87

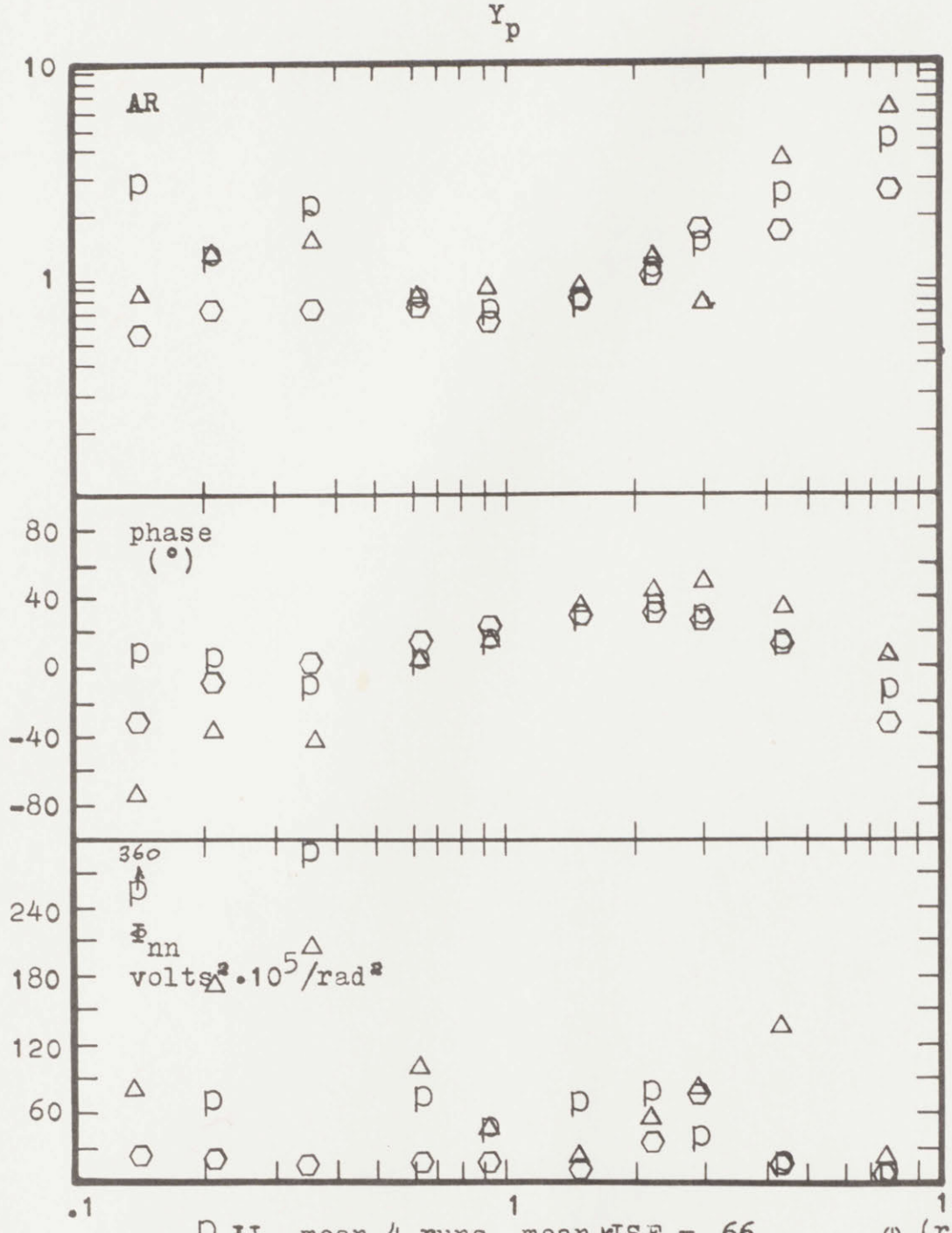

p LL, mean 4 runs, mean rISE = .66
⬡ BP, mean 4 runs, mean rISE = .67
△ JG, mean 2 runs, mean rISE = .82

visual and motion cues, $Y_c = \dfrac{10e^{-.1s}}{s(s^2 + 2s + 10)}$

SUBJECT TO SUBJECT COMPARISON

data-88

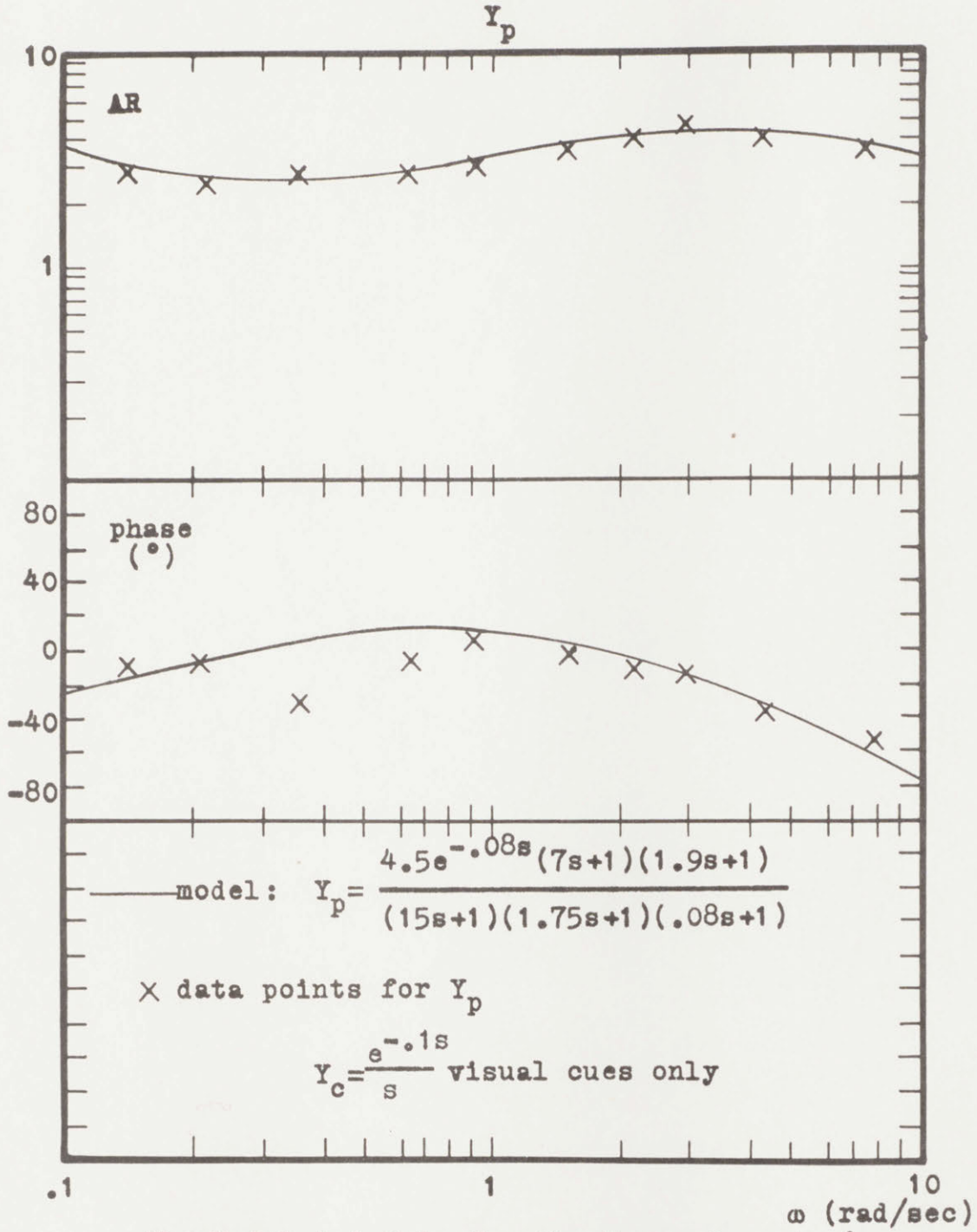

The Model And Data For The Human Operator's Describing Function

$$Y_c = \frac{e^{-.1s}}{s}$$

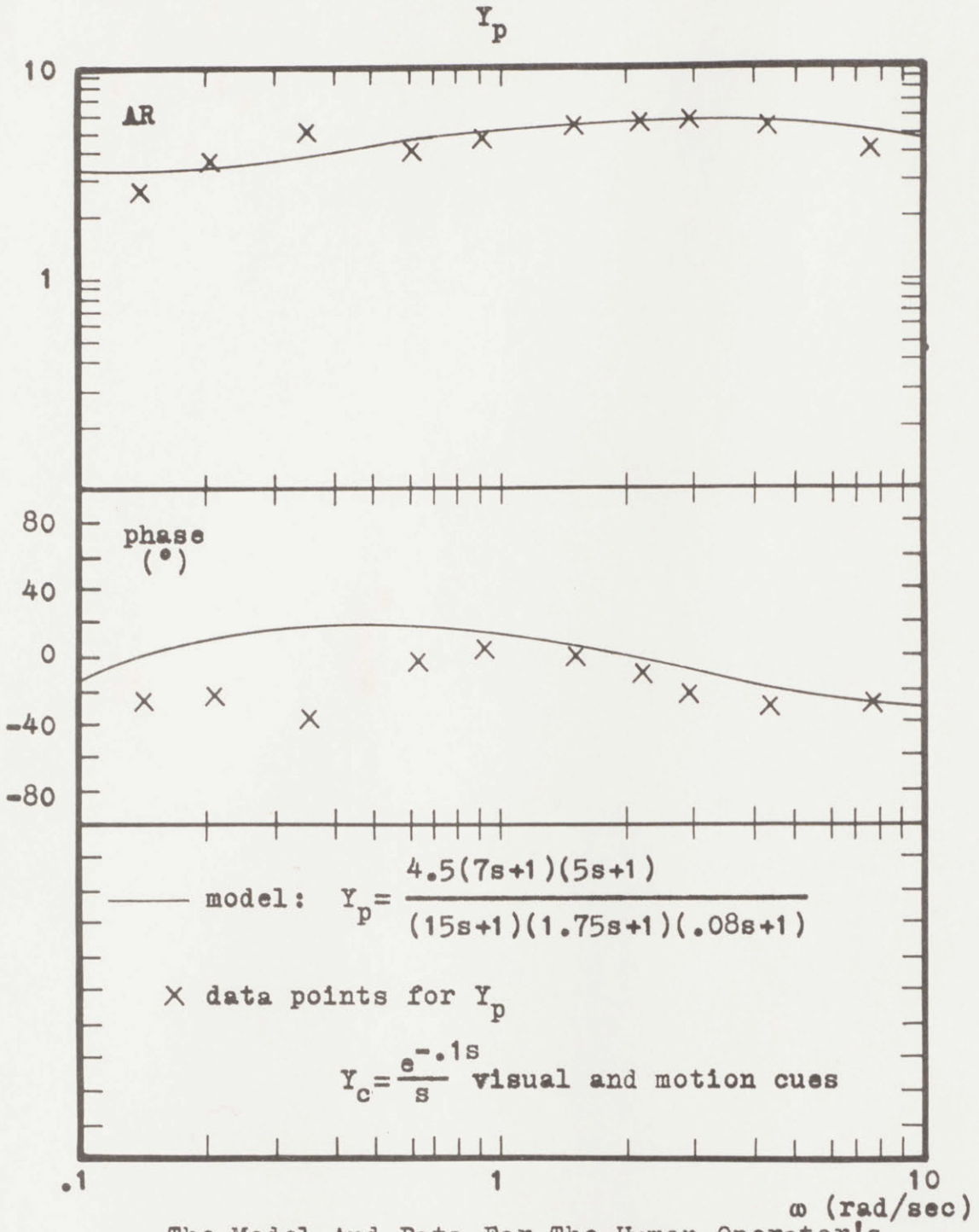

The Model And Data For The Human Operator's Describing Function

$$Y_c = \frac{e^{-.1s}}{s}$$

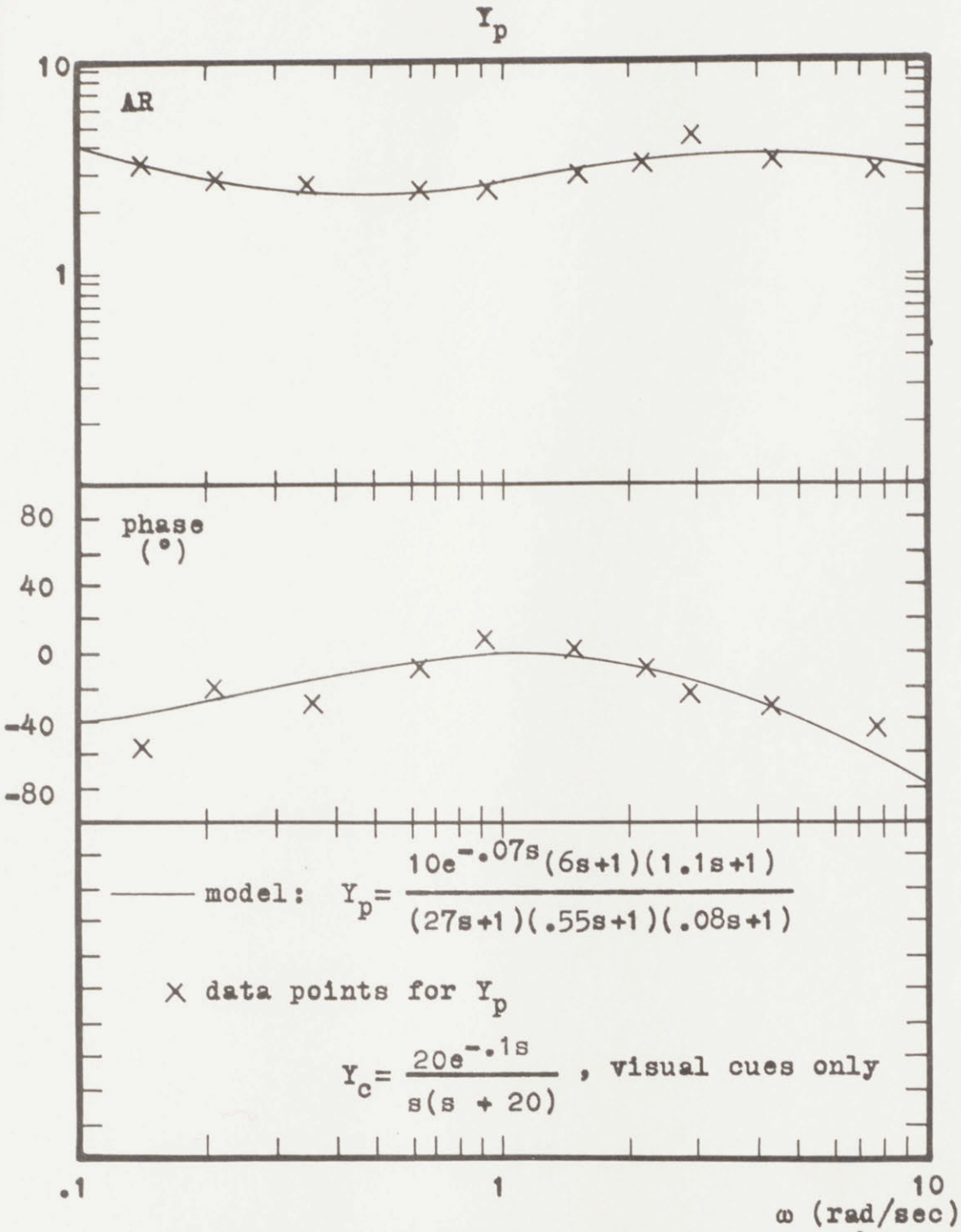

The Model And Data For The Human Operator's Describing Function

$$Y_c = \frac{20e^{-.1s}}{s(s+20)}$$

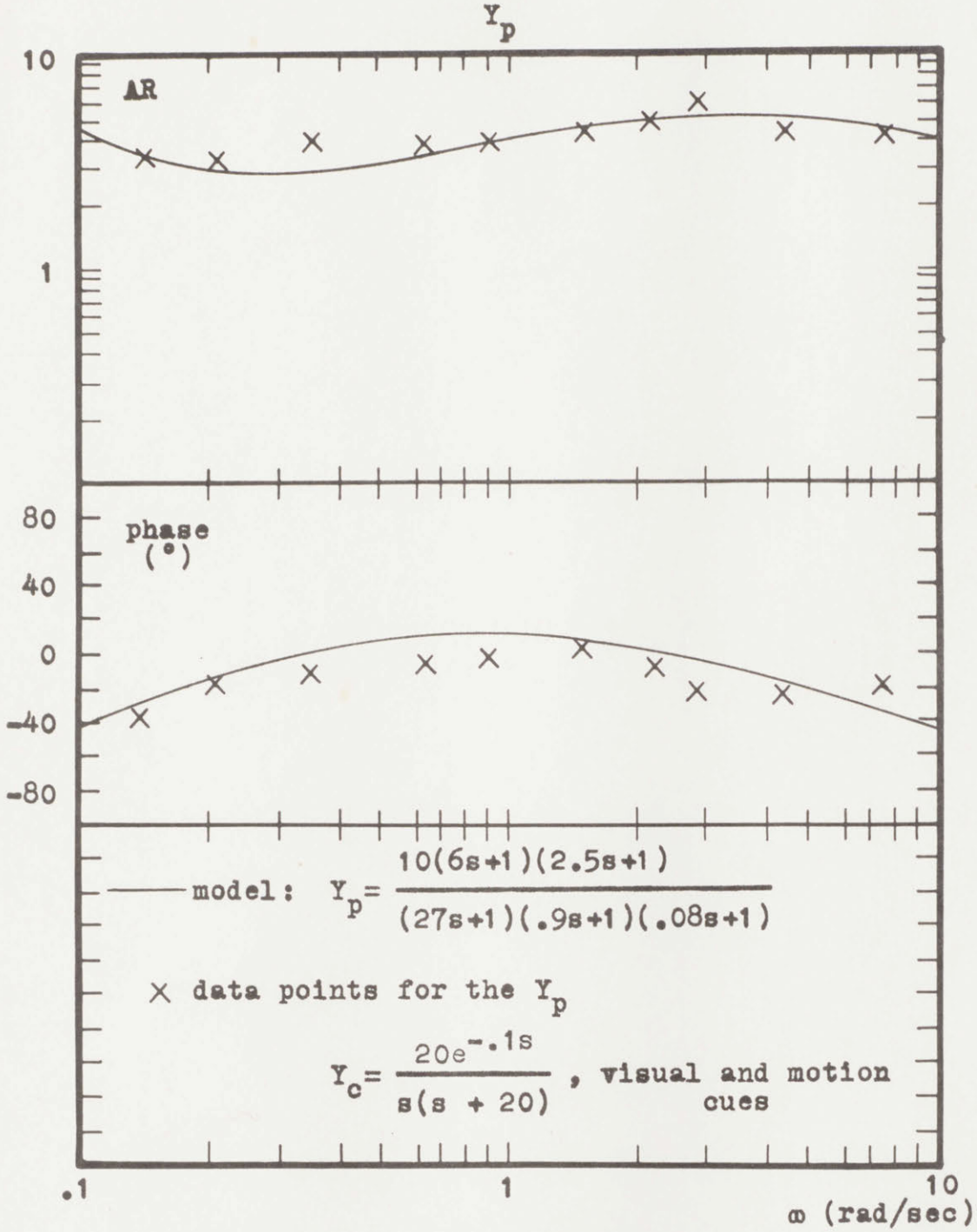

The Model And Data For The Human Operator's Describing Function

$$Y_c = \frac{20e^{-.1s}}{s(s+20)}$$

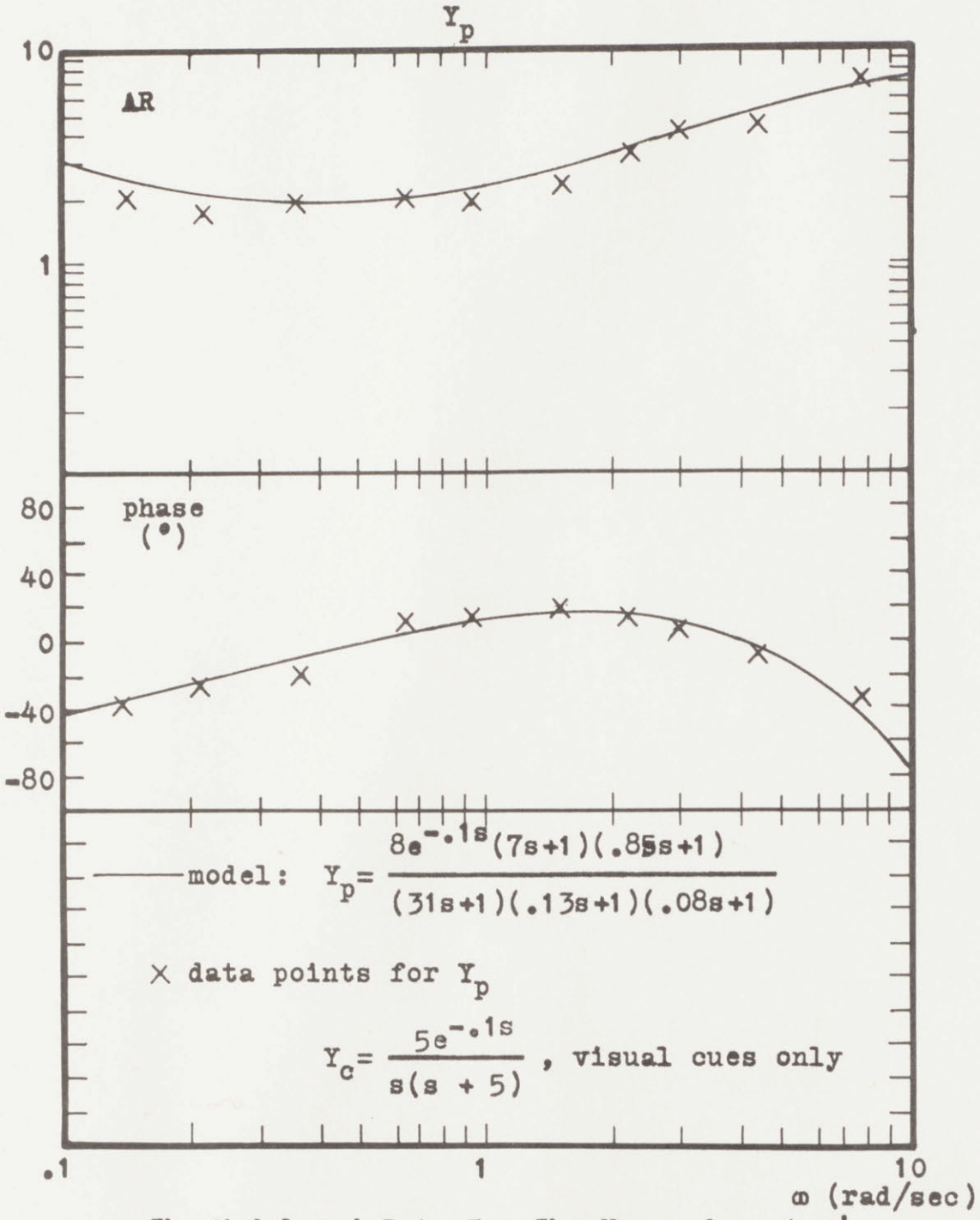

The Model And Data For The Human Operator's Describing Function

$$Y_c = \frac{5e^{-.1s}}{s(s+5)}$$

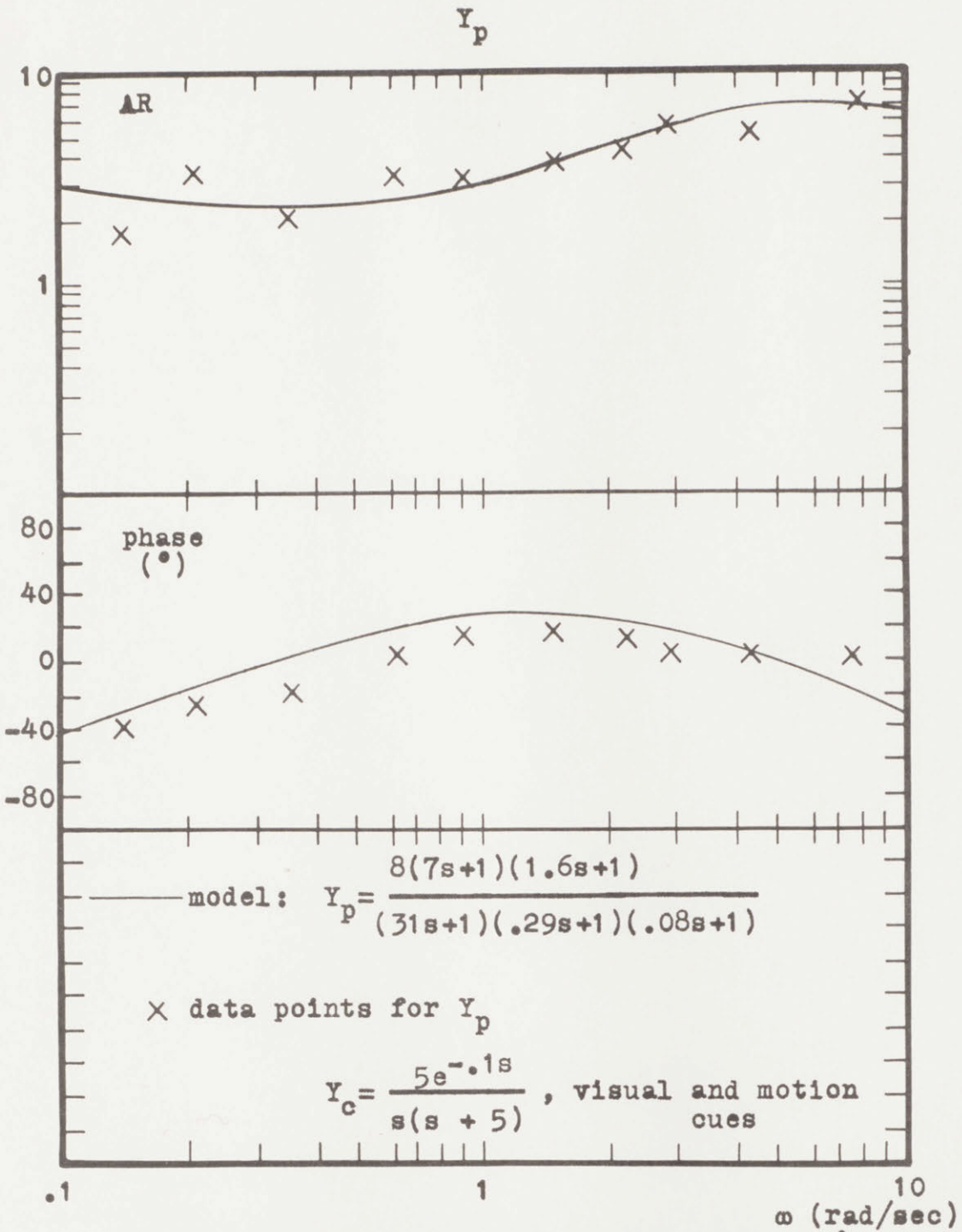

The Model And Data For The Human Operator's Describing Function

$$Y_c = \frac{5e^{-.1s}}{s(s+5)}$$

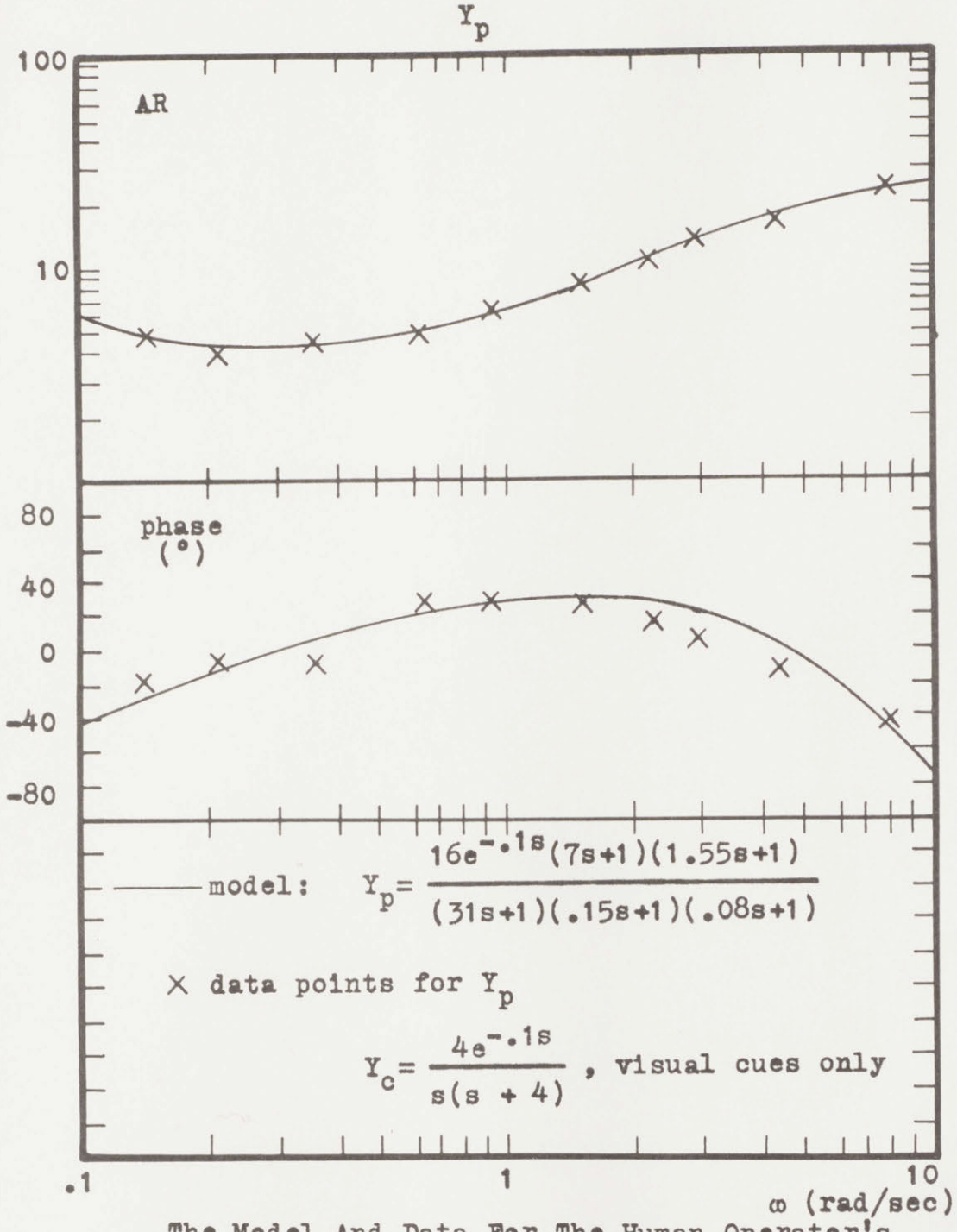

The Model And Data For The Human Operater's Describing Function

$$Y_c = \frac{4e^{-.1s}}{s(s+4)}$$

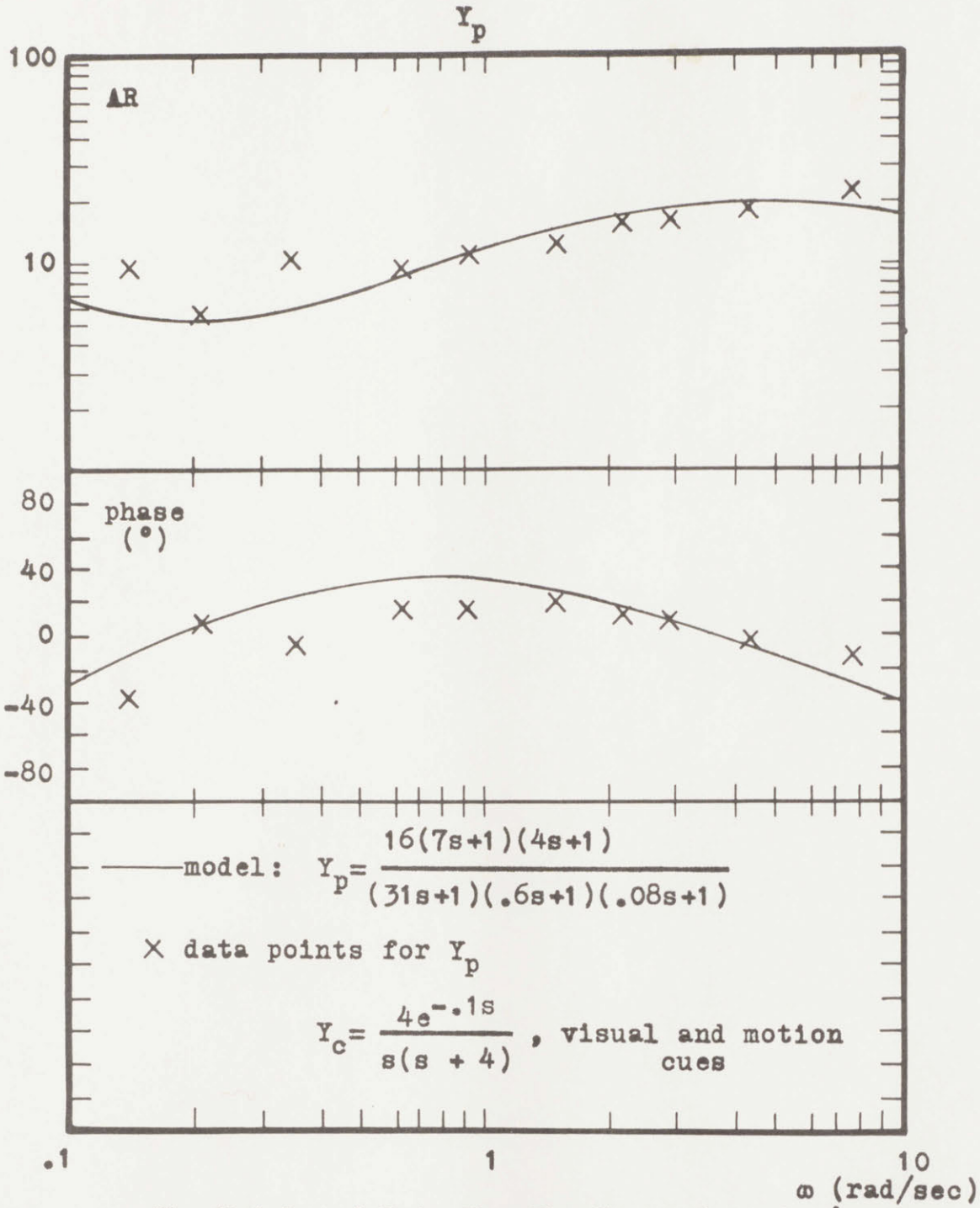

The Model And Data For The Human Operator's Describing Function

$$Y_c = \frac{4e^{-.1s}}{s(s+4)}$$

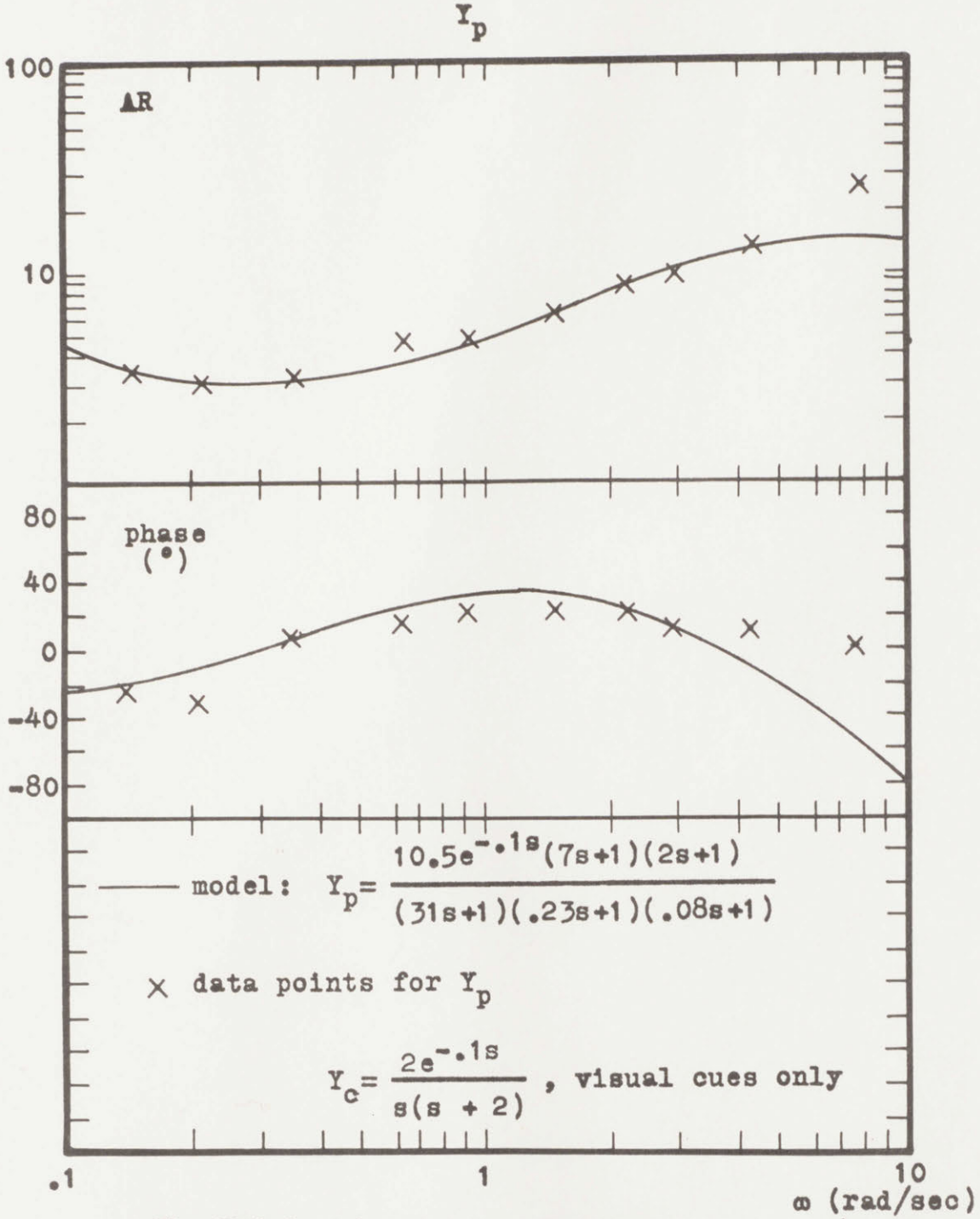

The Model And Data For The Human Operator's Describing Function

$$Y_c = \frac{2e^{-.1s}}{s(s+2)}$$

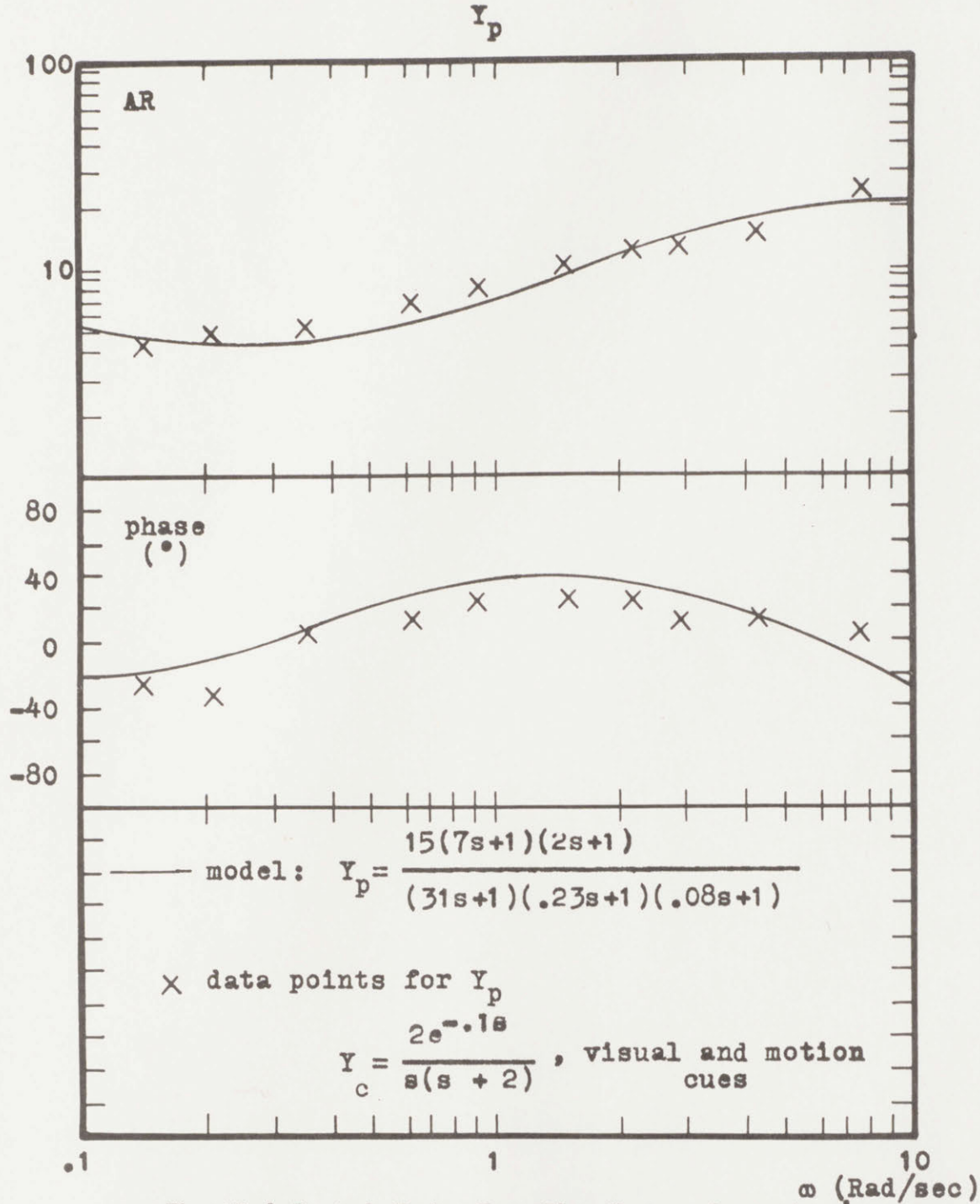

The Model And Data For The Human Operator's Describing Function

$$Y_c = \frac{2e^{-.1s}}{s(s+2)}$$

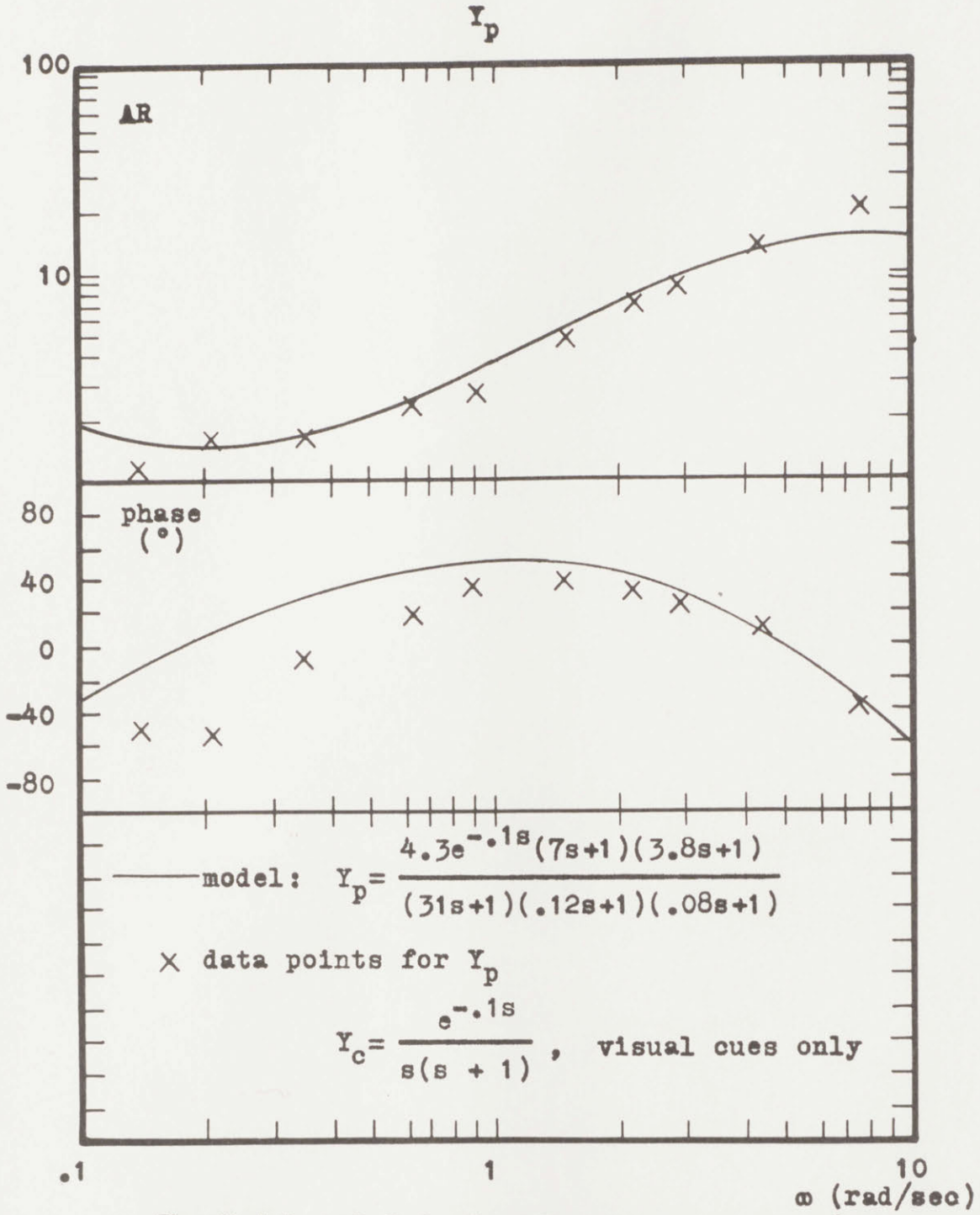

The Model And Data For The Human Operater's Describing Function

$$Y_c = \frac{e^{-.1s}}{s(s+1)}$$

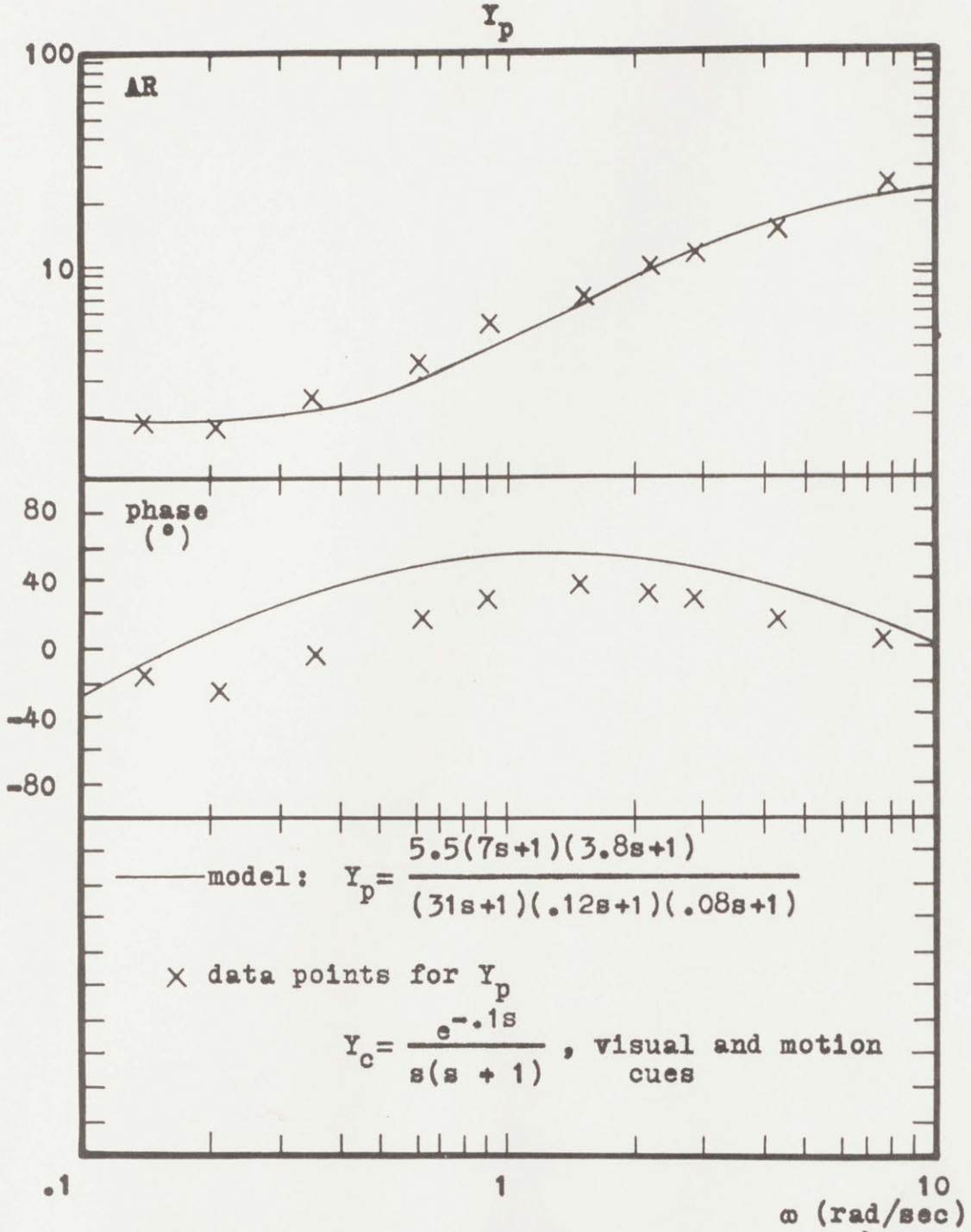

The Model And Data For The Human Operator's Describing Function

$$Y_c = \frac{e^{-.1s}}{s(s+1)}$$

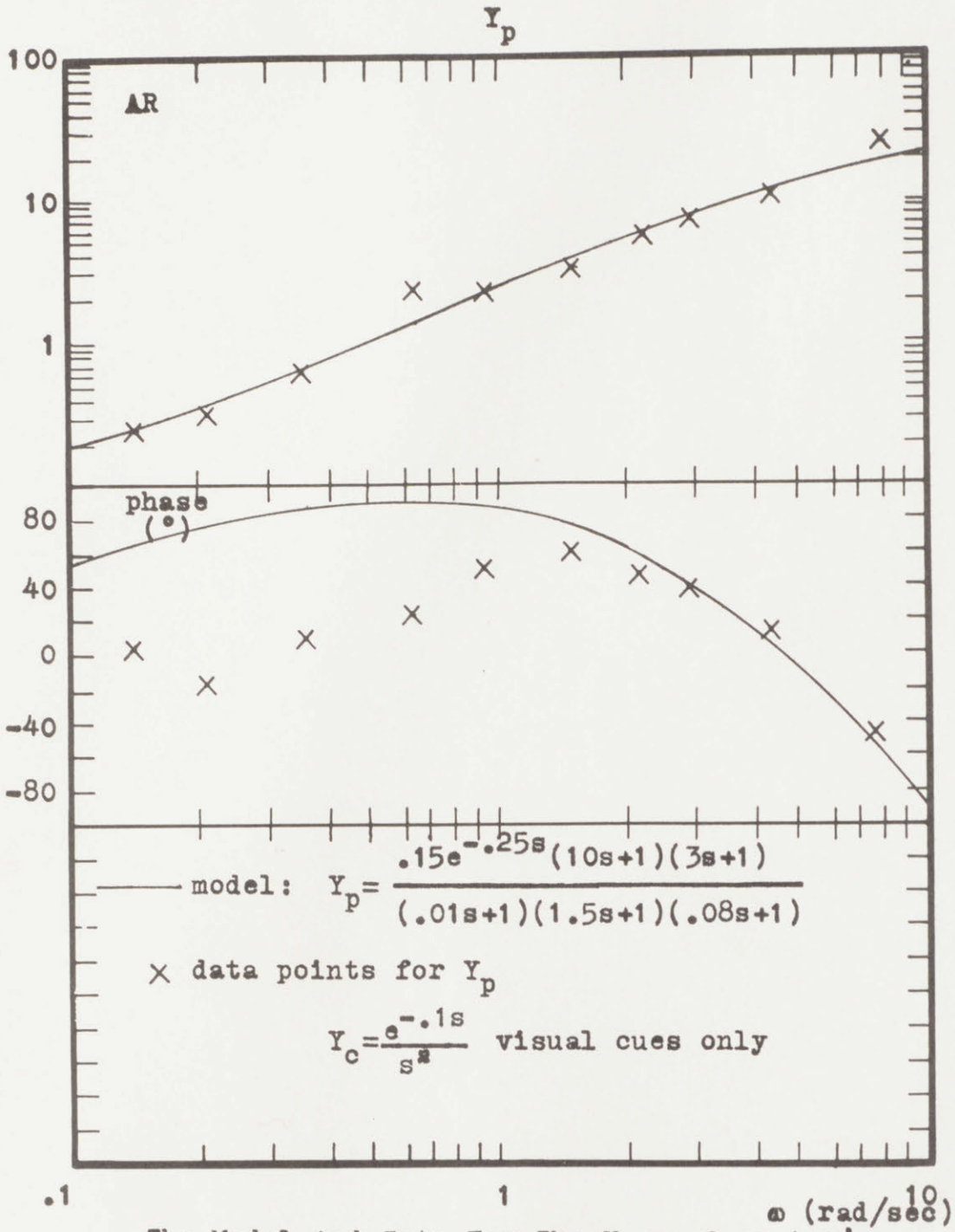

The Model And Data For The Human Operator's Describing Function

$$Y_c = \frac{e^{-.1s}}{s^2}$$

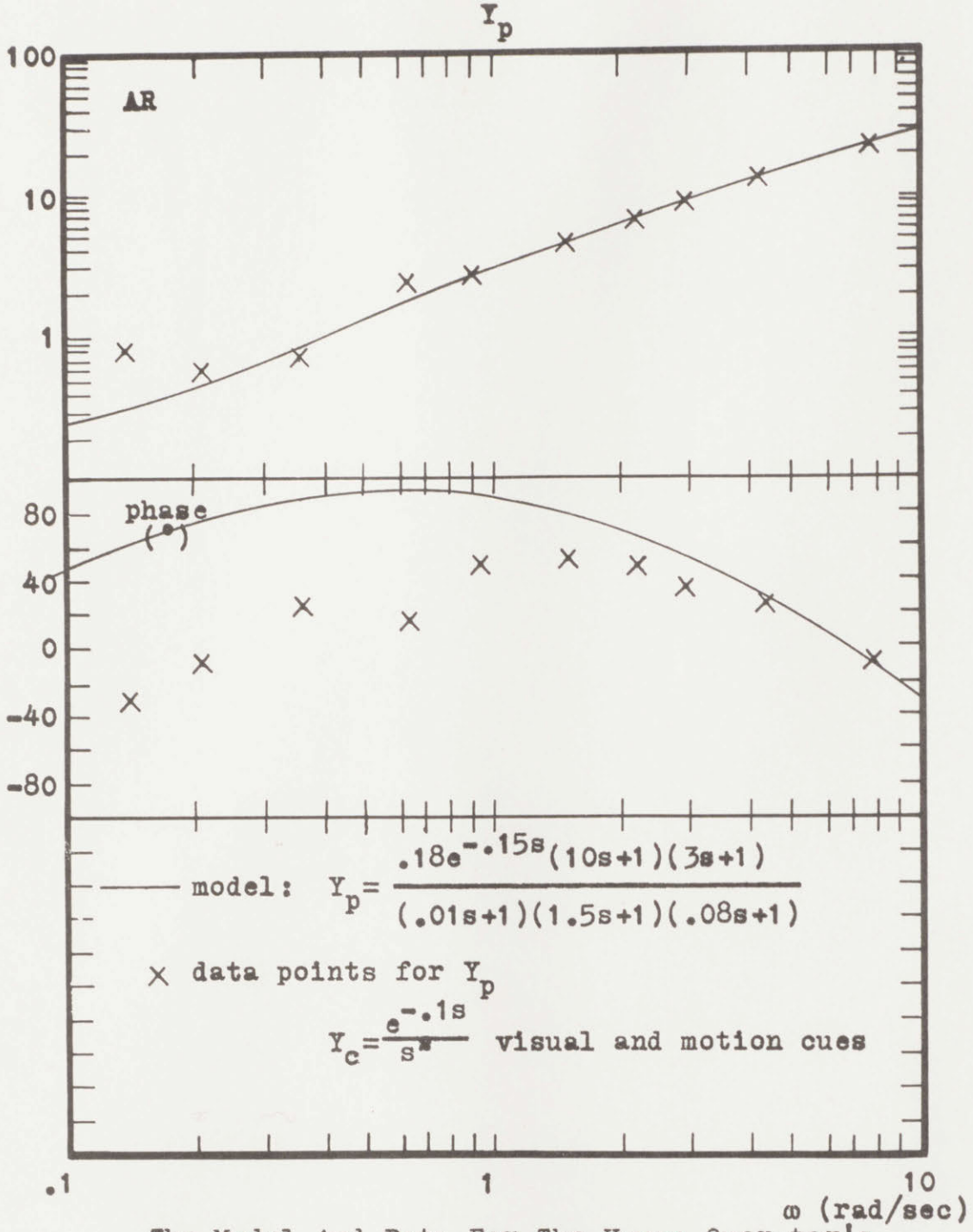

The Model And Data For The Human Operator's Describing Function

$$Y_c = \frac{e^{-.1s}}{s^2}$$

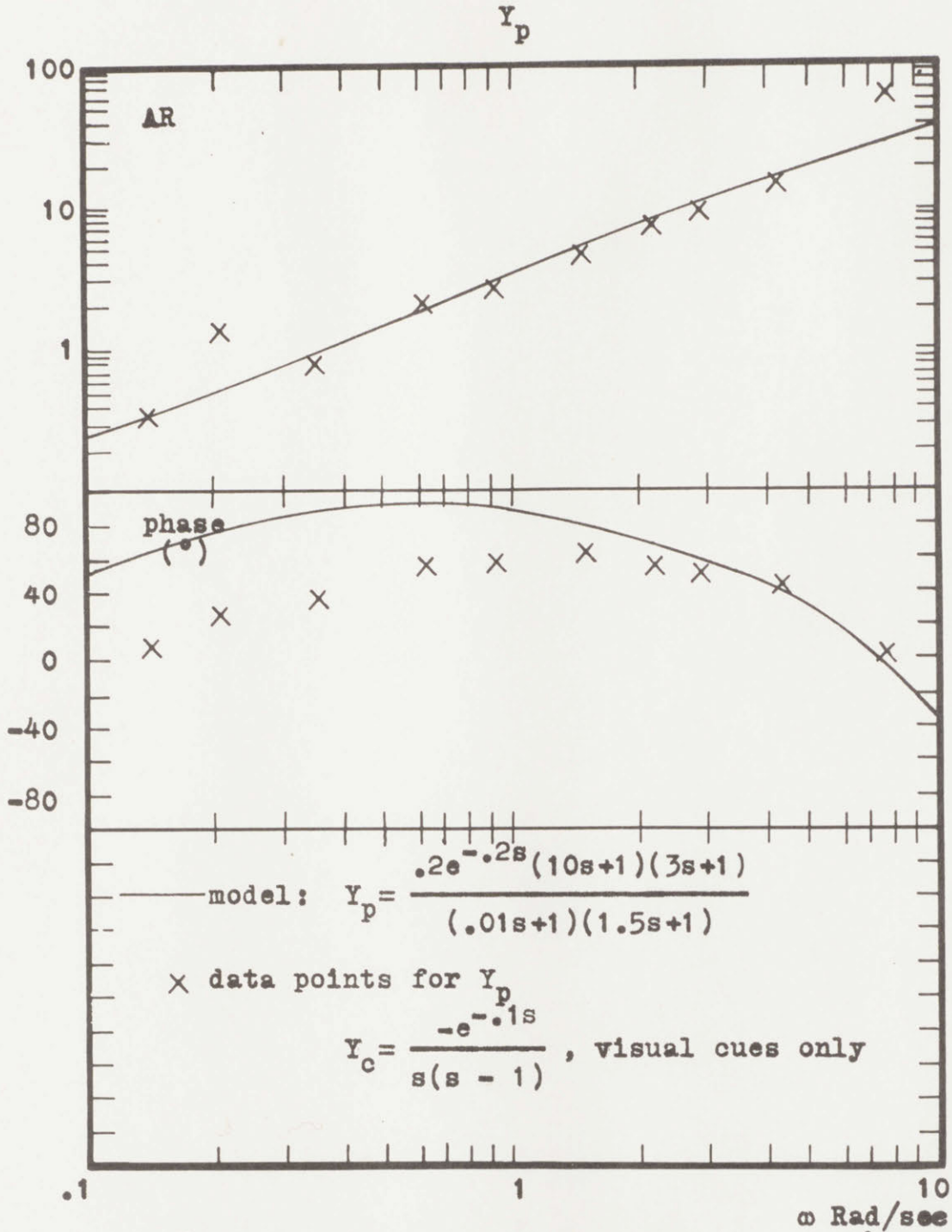

The Model And Data For The Human Operator's Describing Function

$$Y_c = \frac{-e^{-.1s}}{s(s-1)}$$

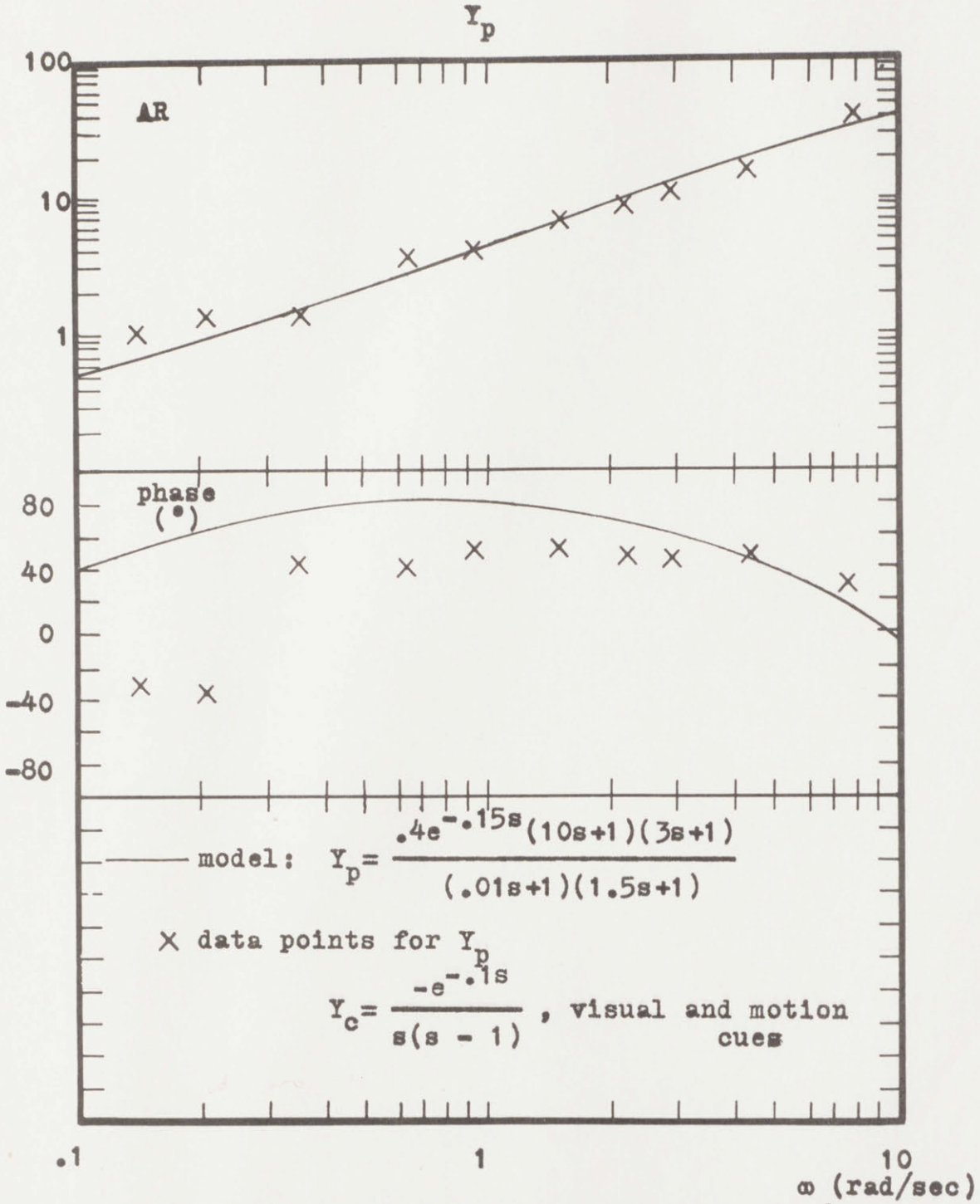

The Model And Data For The Human Operator's Describing Function

$$Y_c = \frac{-e^{-.1s}}{s(s-1)}$$

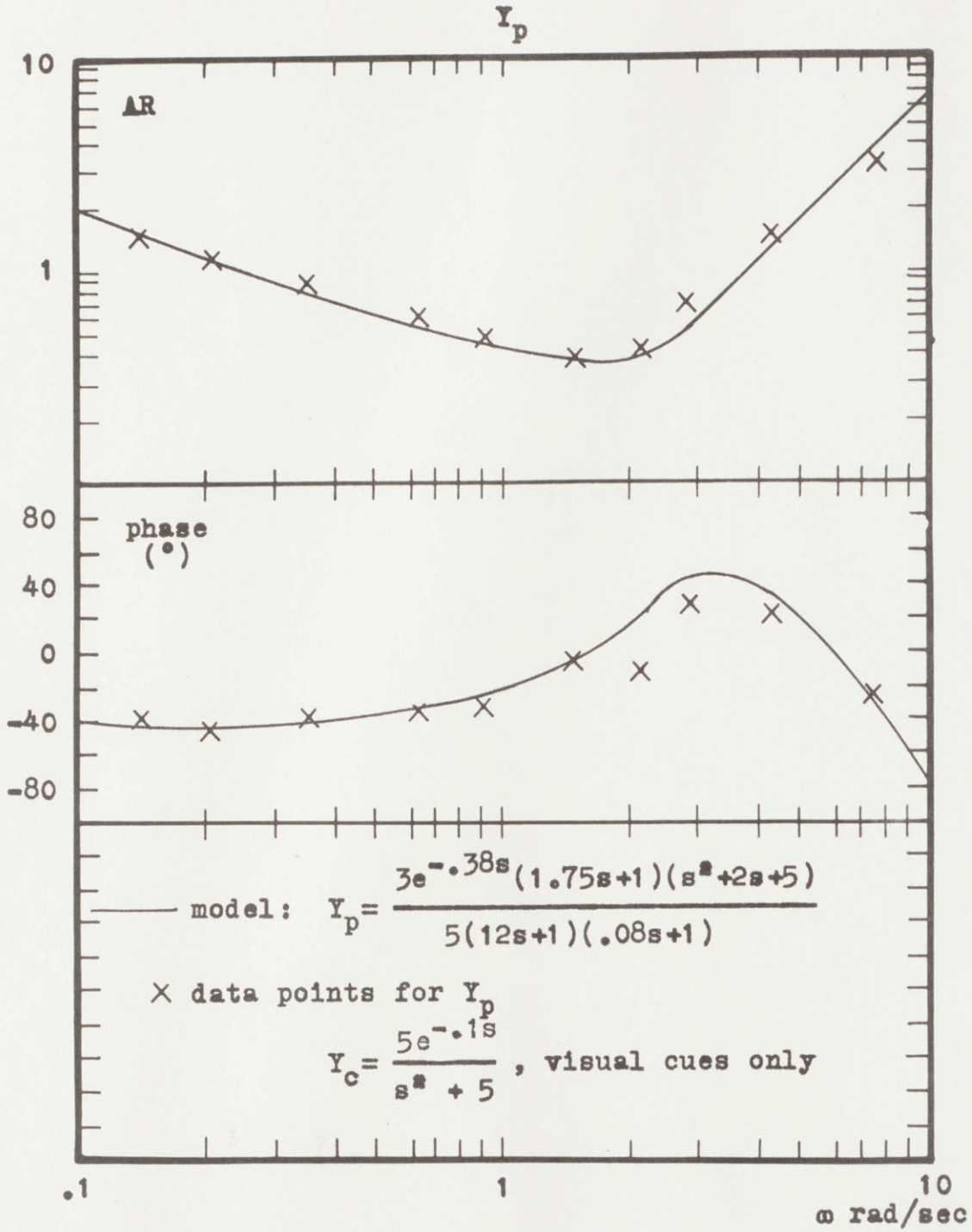

The Model And Data For The Human Operator's Describing Function

$$Y_c = \frac{5e^{-.1s}}{s^2+5}$$

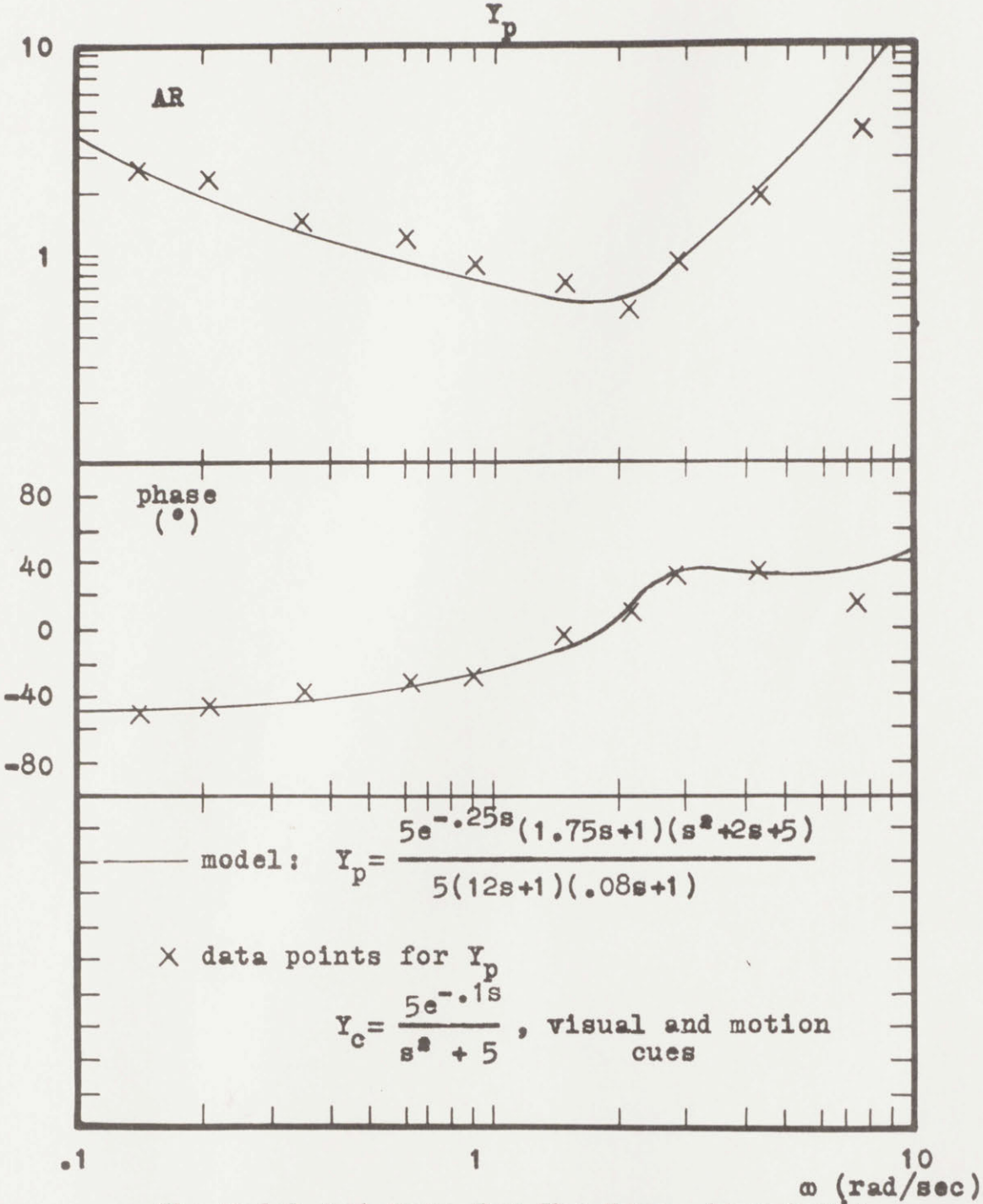

The Model And Data For The Human Operator's Describing Function

$$Y_c = \frac{5e^{-.1s}}{s^2+5}$$

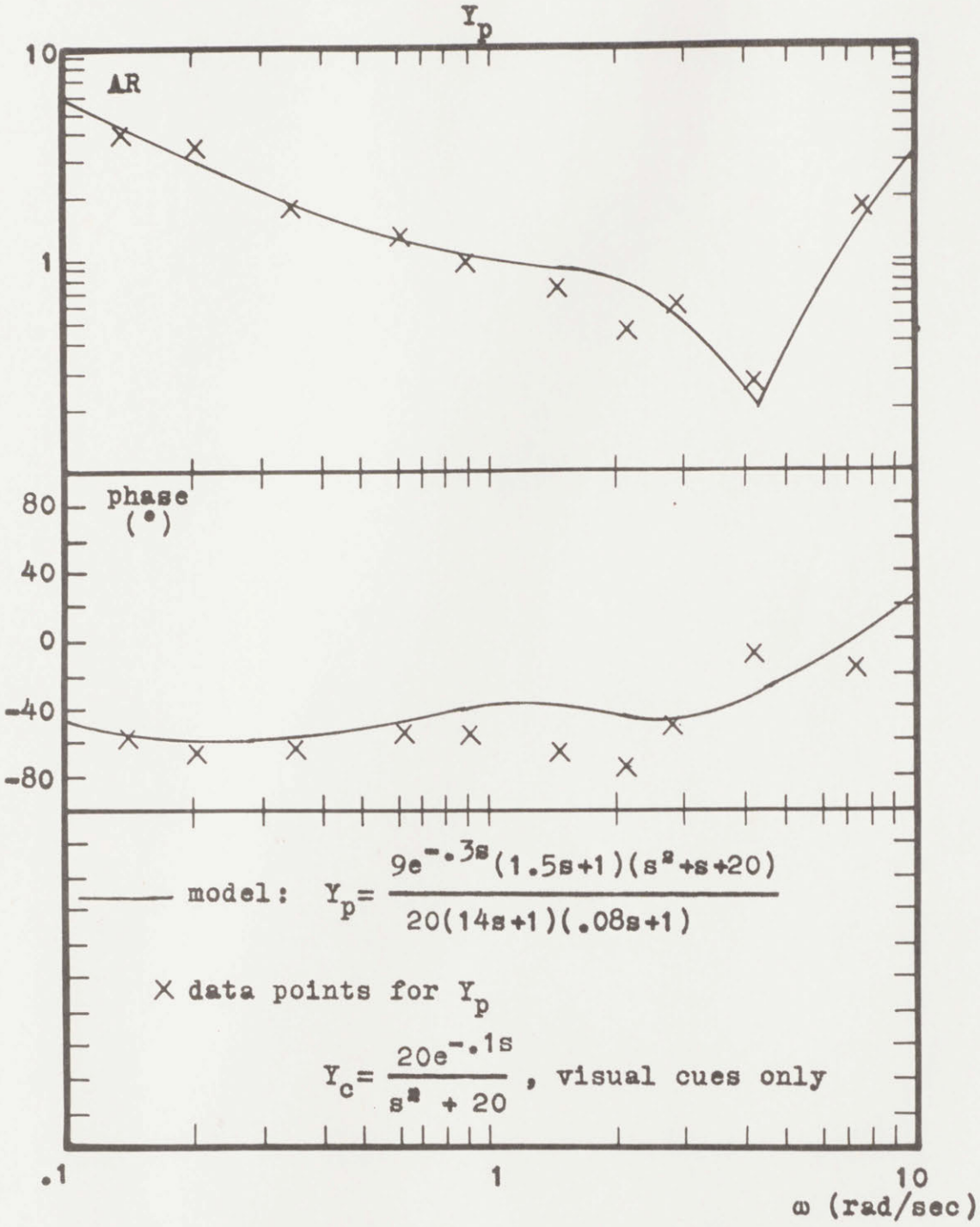

The Model And Data For The Human Operator's Describing Function

$$Y_c = \frac{20e^{-.1s}}{s^2 + 20}$$

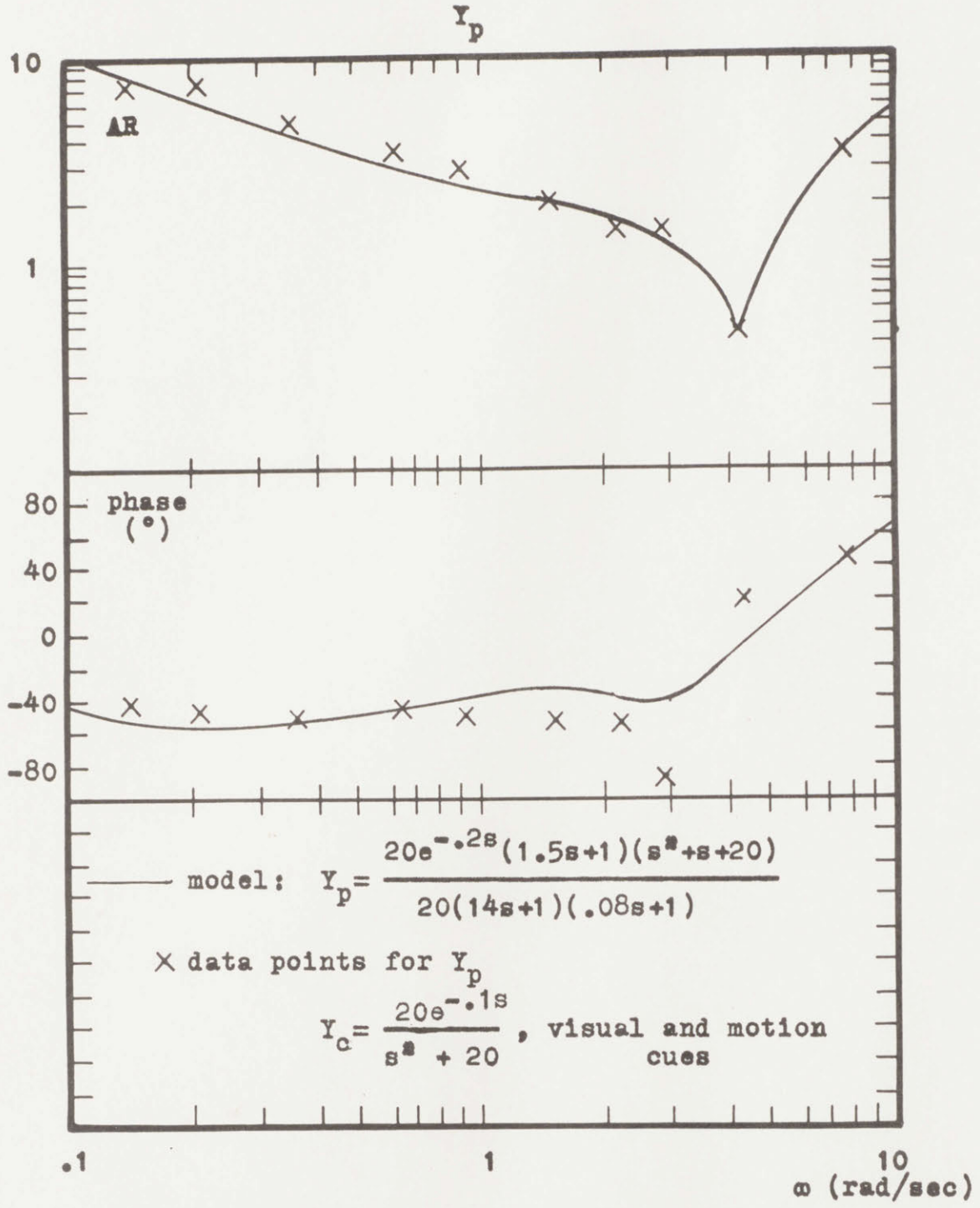

The Model And Data For The Human Operator's Describing Function

$$Y_c = \frac{20e^{-.1s}}{s^2 + 20}$$

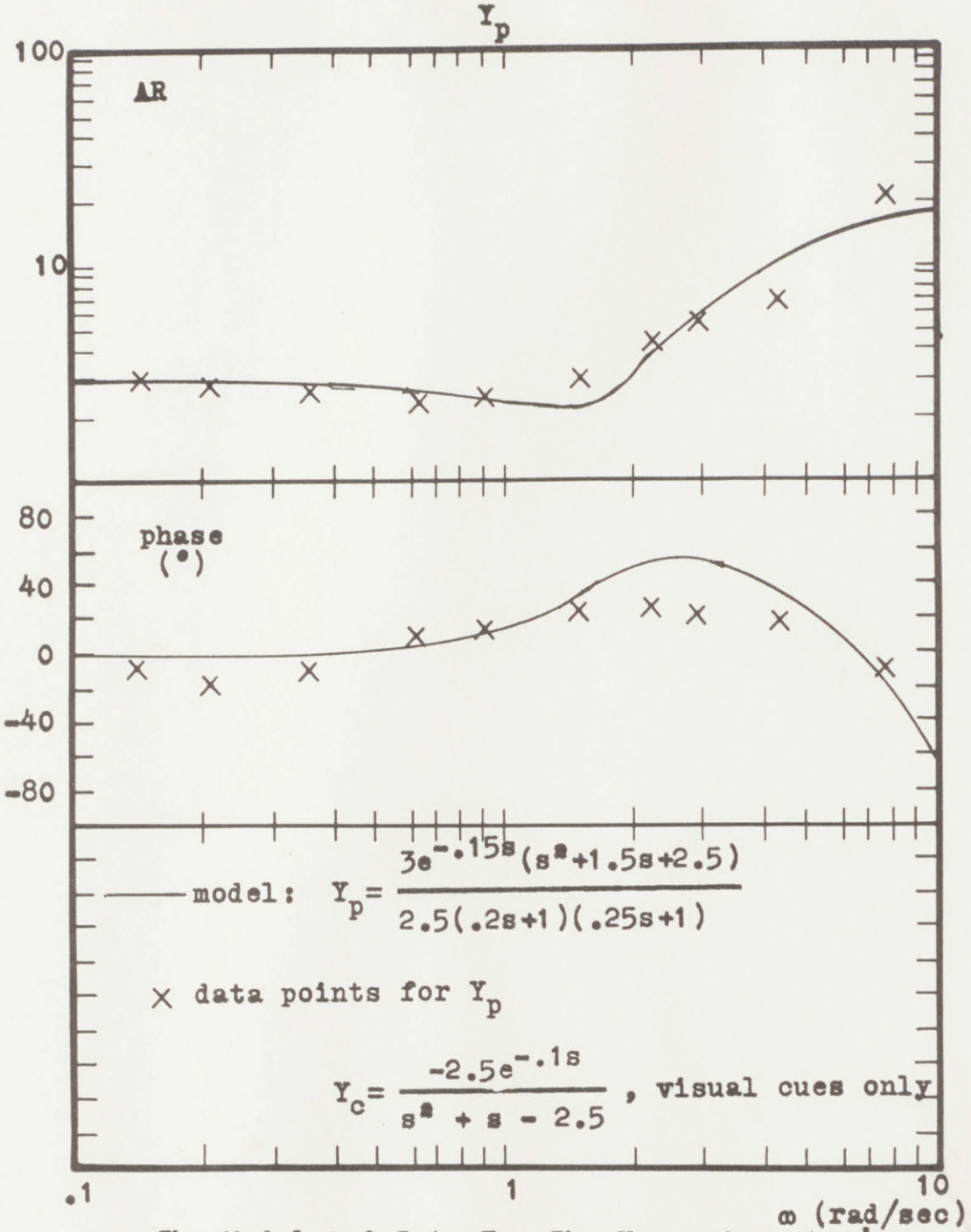

The Model And Data For The Human Operator's Describing Function

$$Y_c = \frac{-2.5e^{-.1s}}{s^2 + s - 2.5}$$

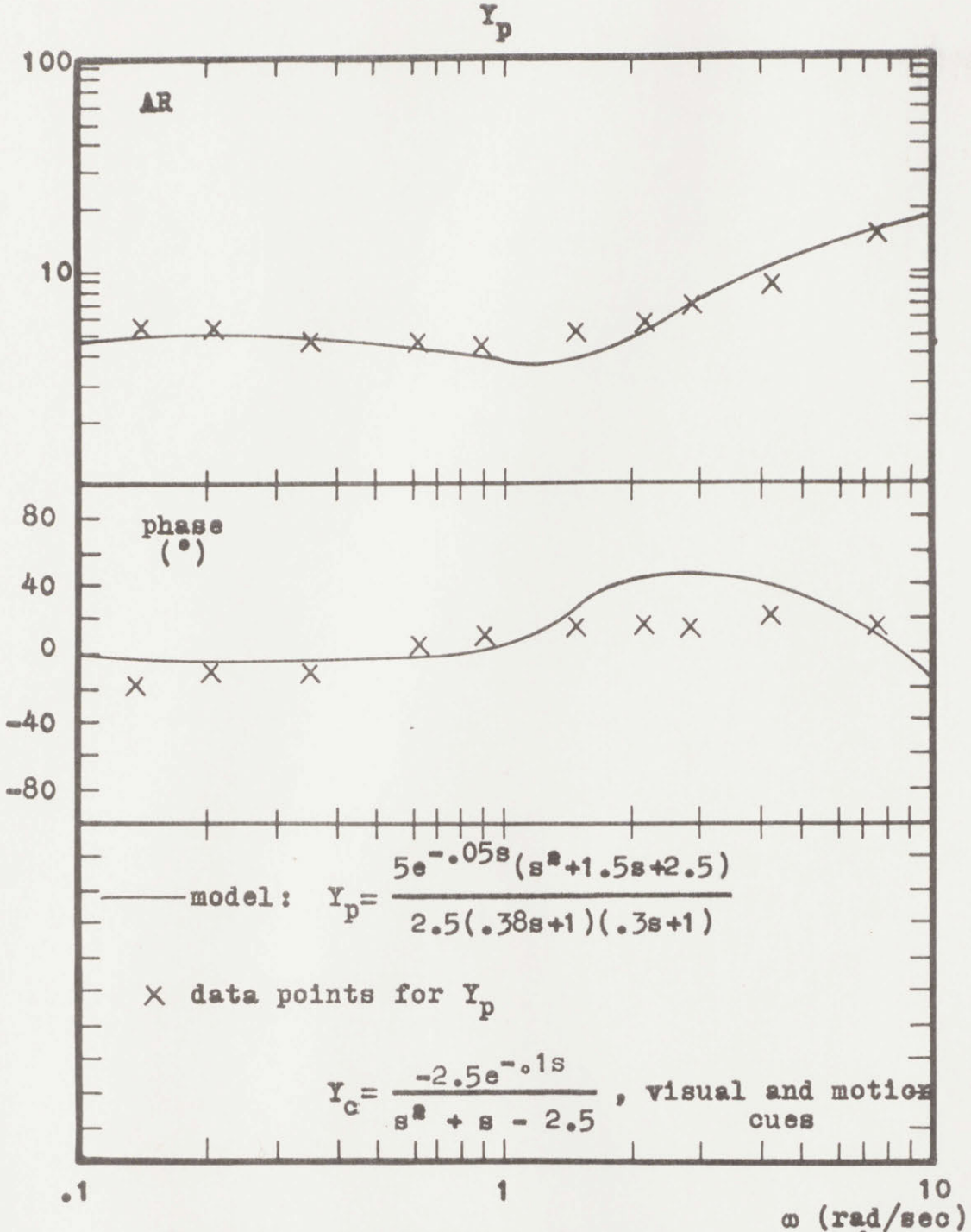

The Model And Data For The Human Operator's Describing Function

$$Y_c = \frac{-2.5e^{-.1s}}{s^2 + s - 2.5}$$

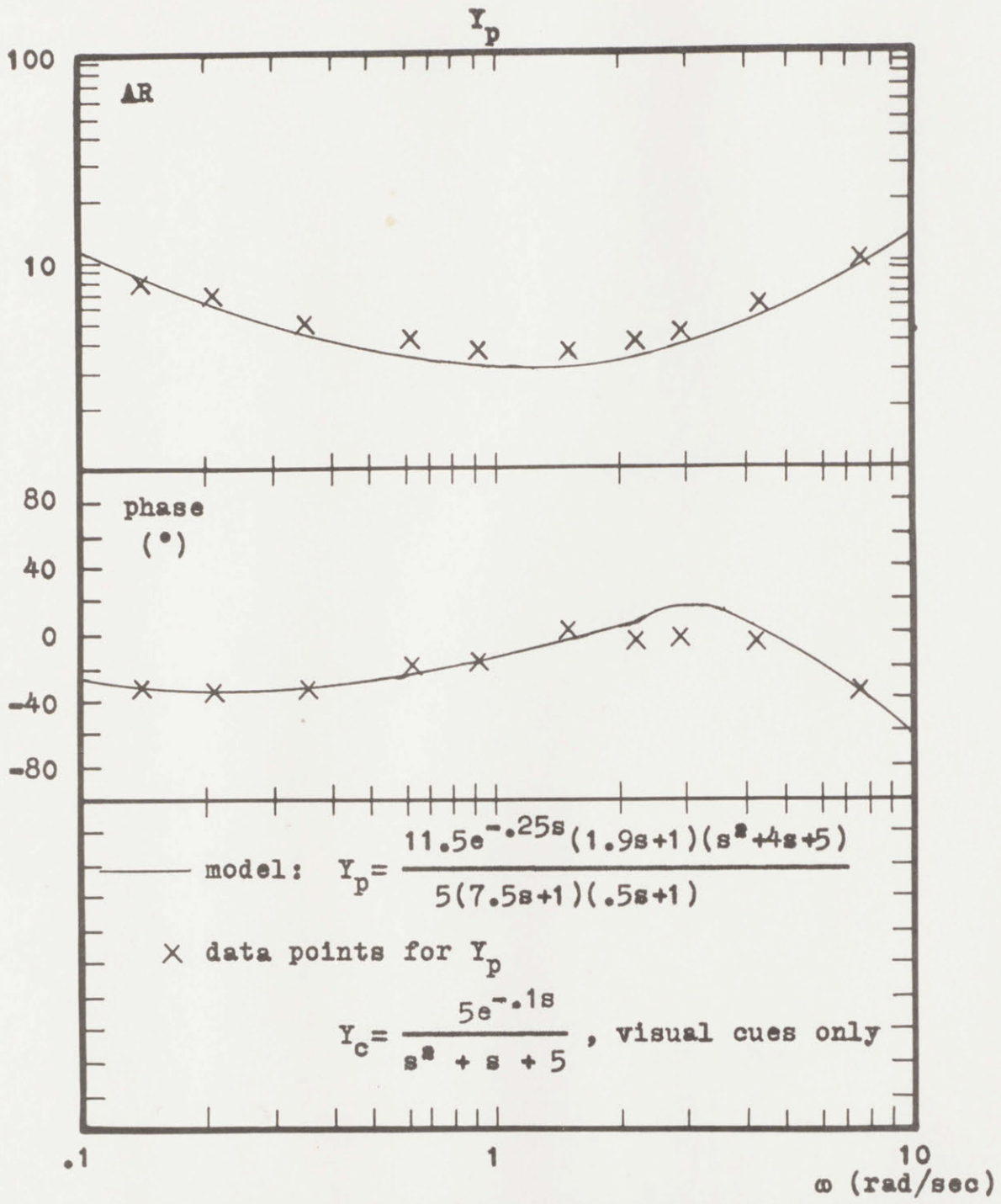

The Model And Data For The Human Operator's Describing Function

$$Y_c = \frac{5e^{-.1s}}{s^2 + s + 5}$$

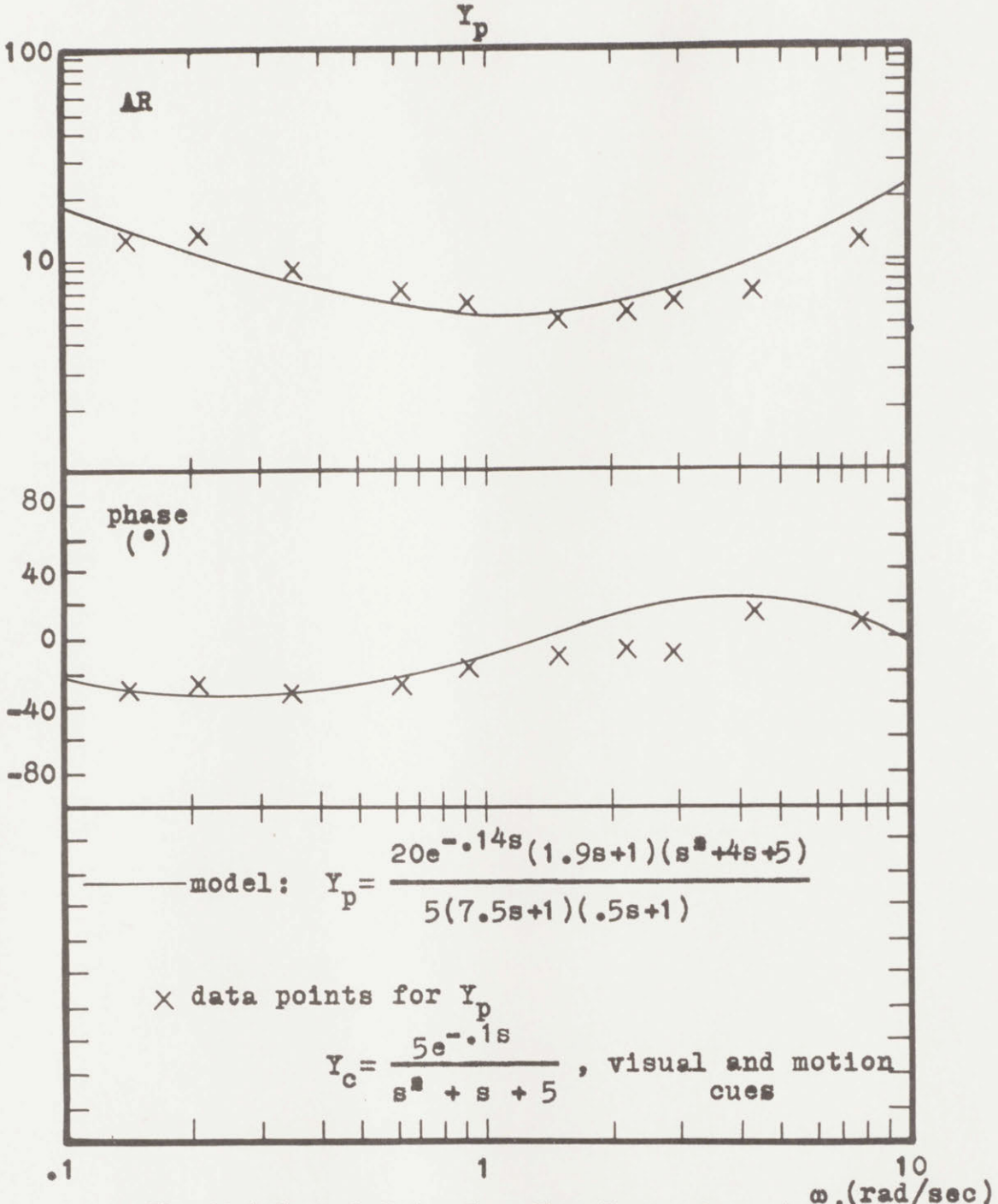

The Model And Data For The Human Operator's Describing Function

$$Y_c = \frac{5e^{-.1s}}{s^2+s+5}$$

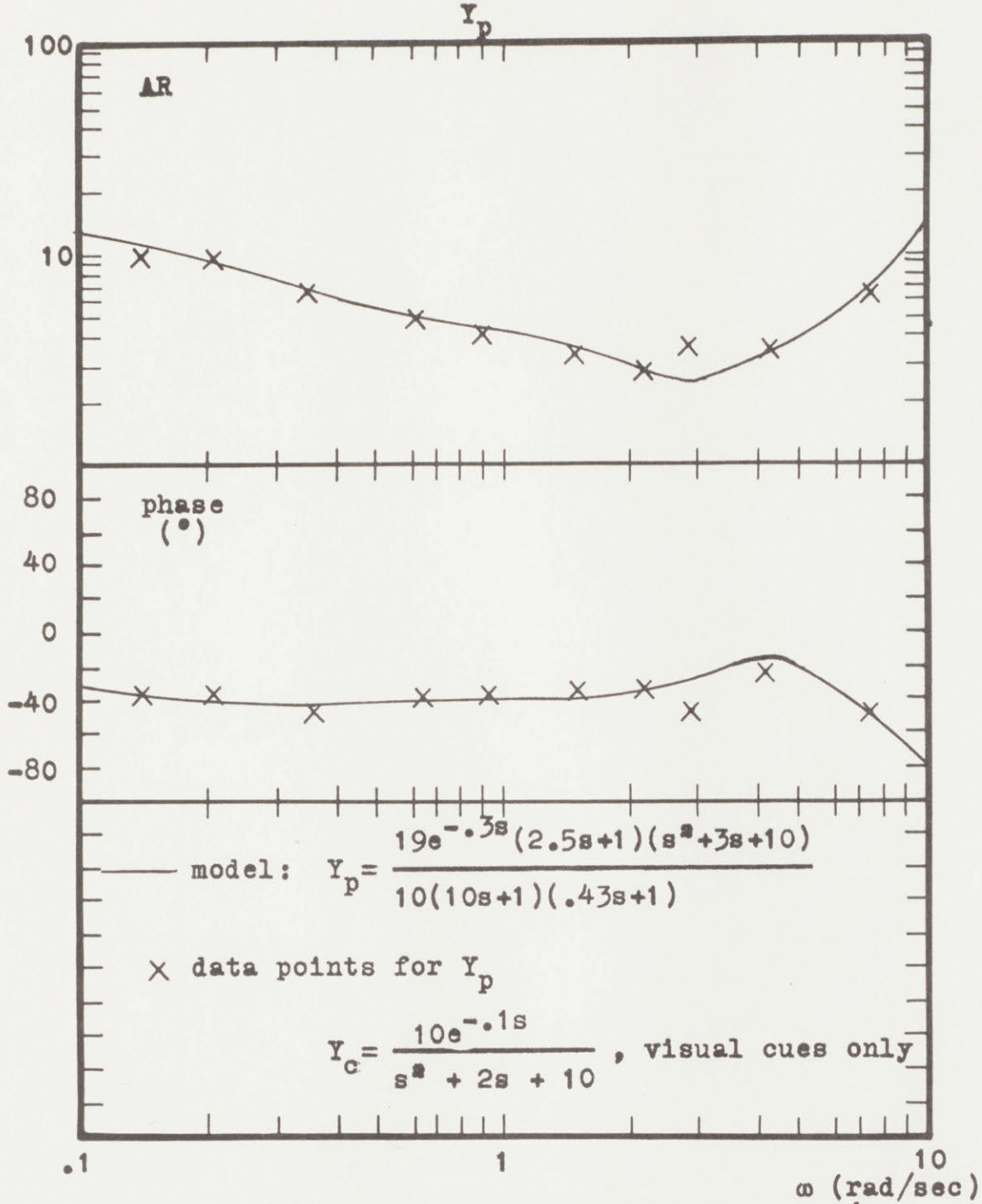

The Model And Data For The Human Operator's Describing Function

$$Y_c = \frac{10e^{-.1s}}{s^2 + 2s + 10}$$

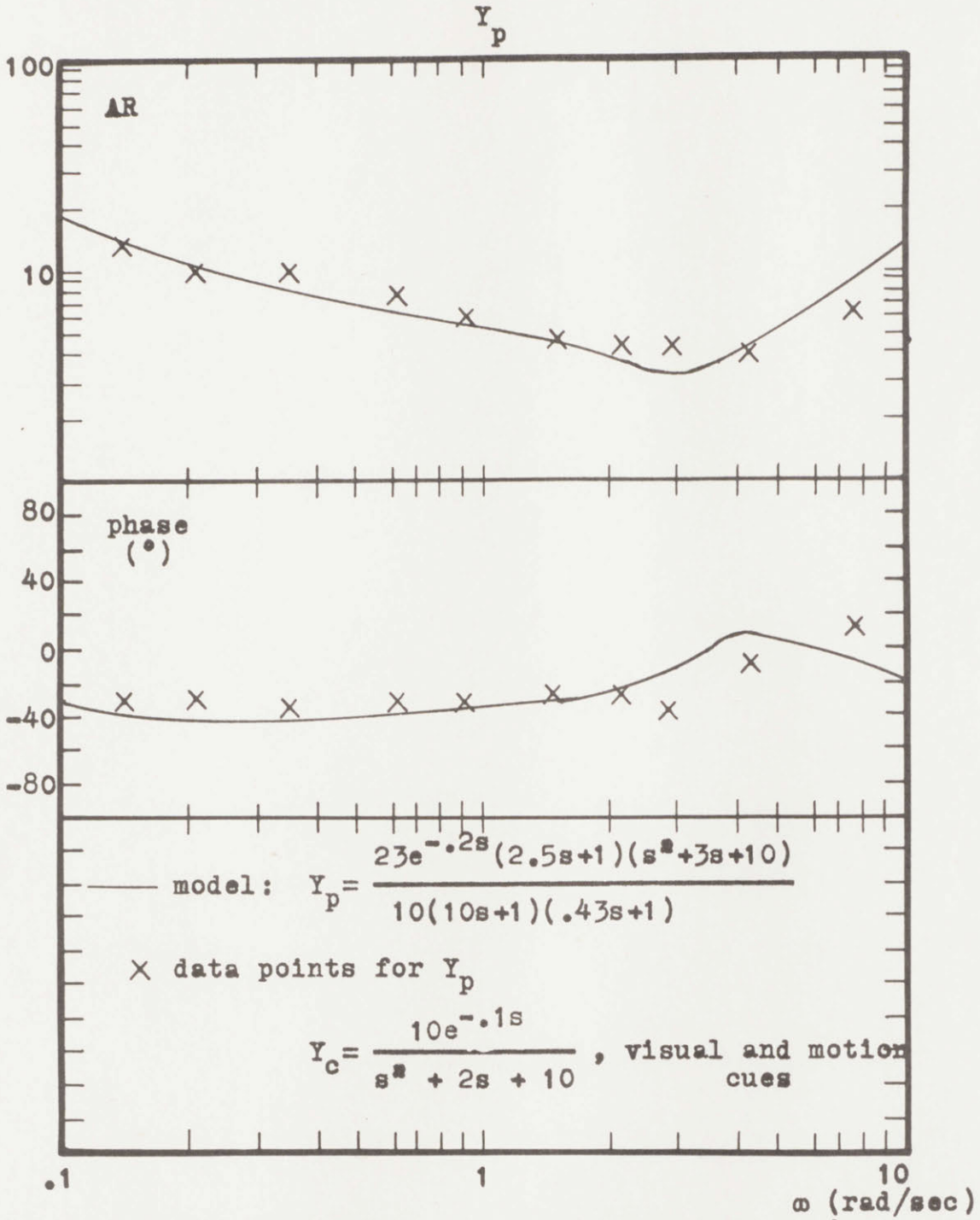

The Model And Data For The Human Operator's Describing Function

$$Y_c = \frac{10e^{-.1s}}{s^2 + 2s + 10}$$

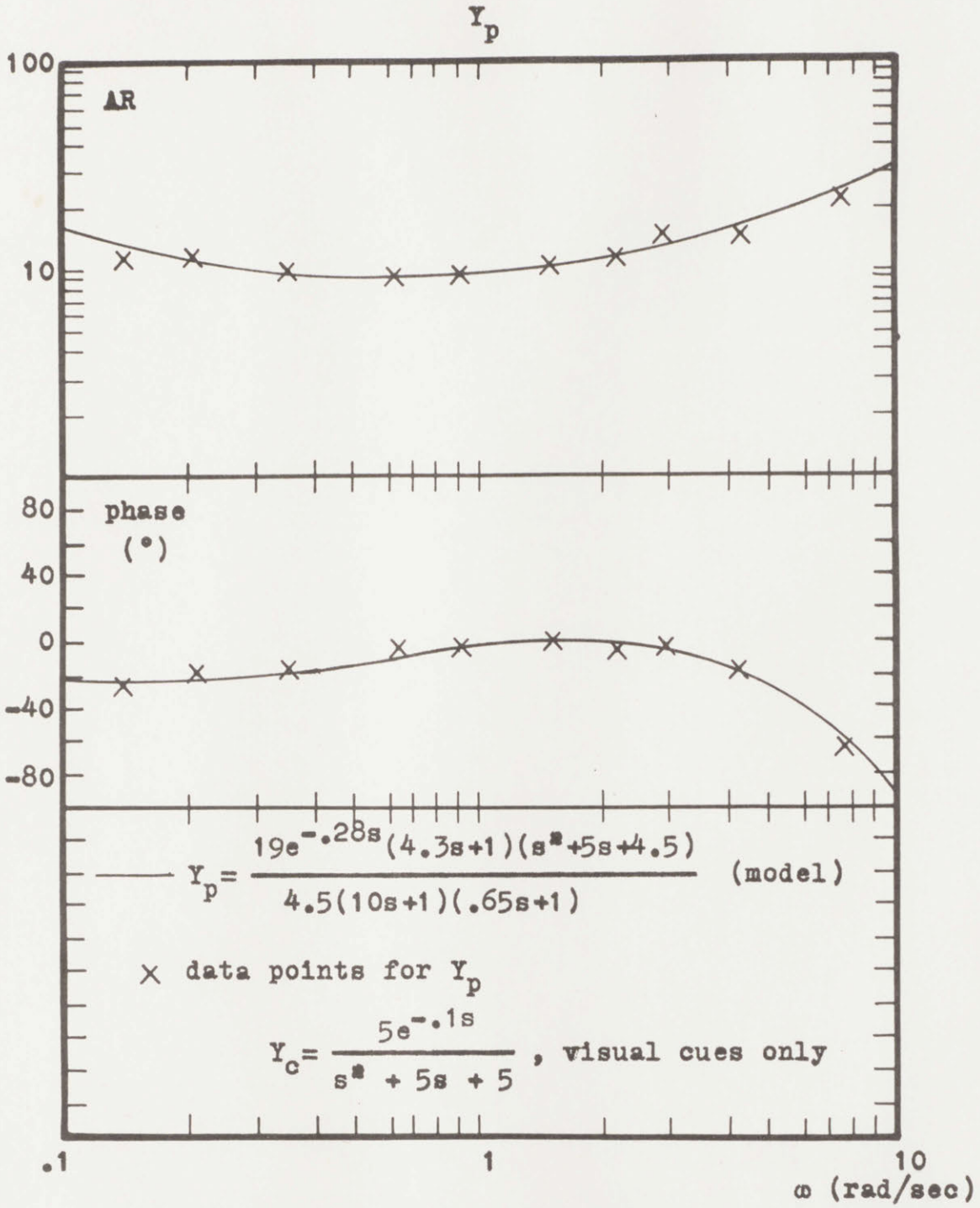

The Model And Data For The Human Operator's Describing Function

$$Y_c = \frac{5e^{-.1s}}{s^2 + 5s + 5}$$

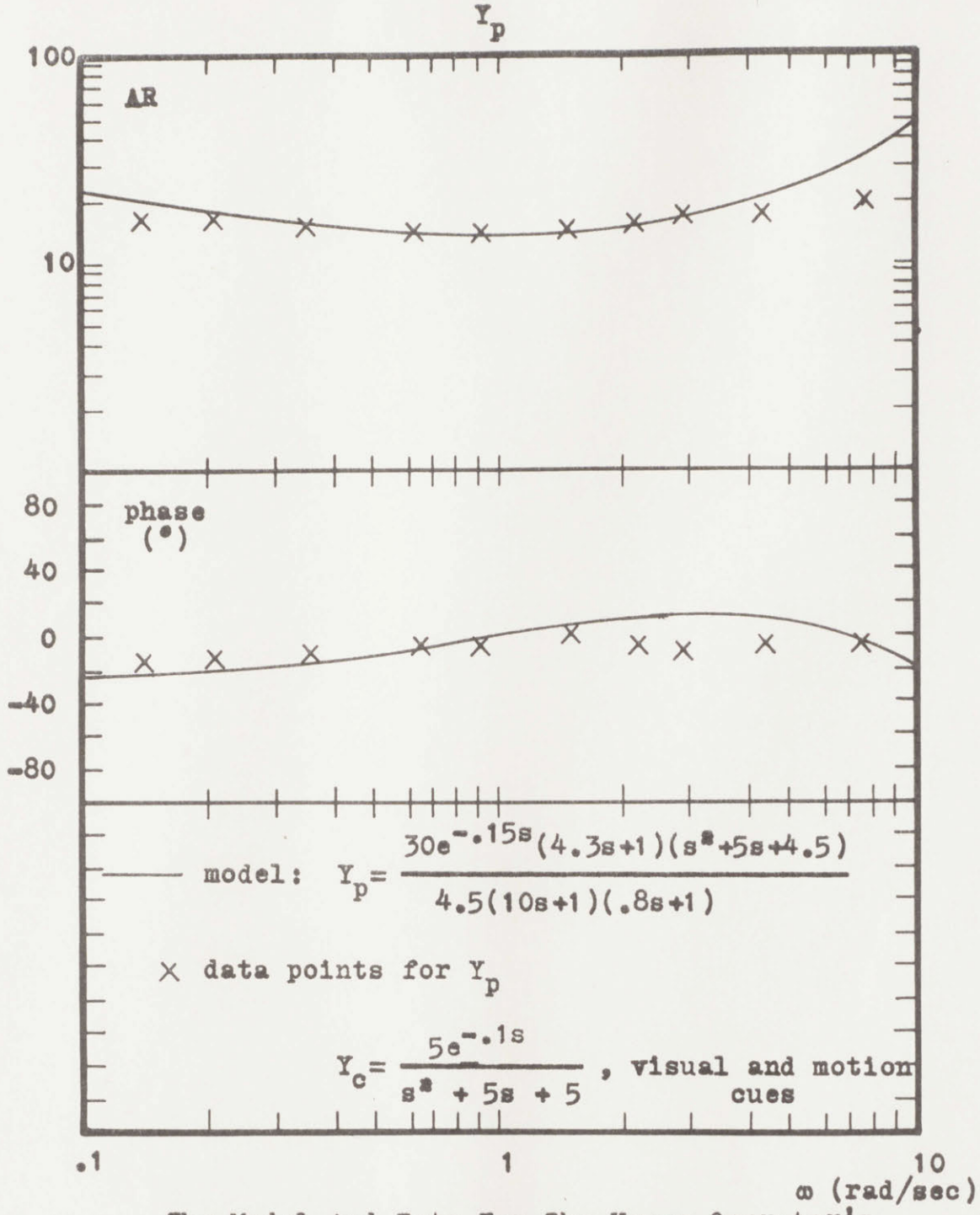

The Model And Data For The Human Operator's Describing Function

$$Y_c = \frac{5e^{-.1s}}{s^2 + 5s + 5}$$

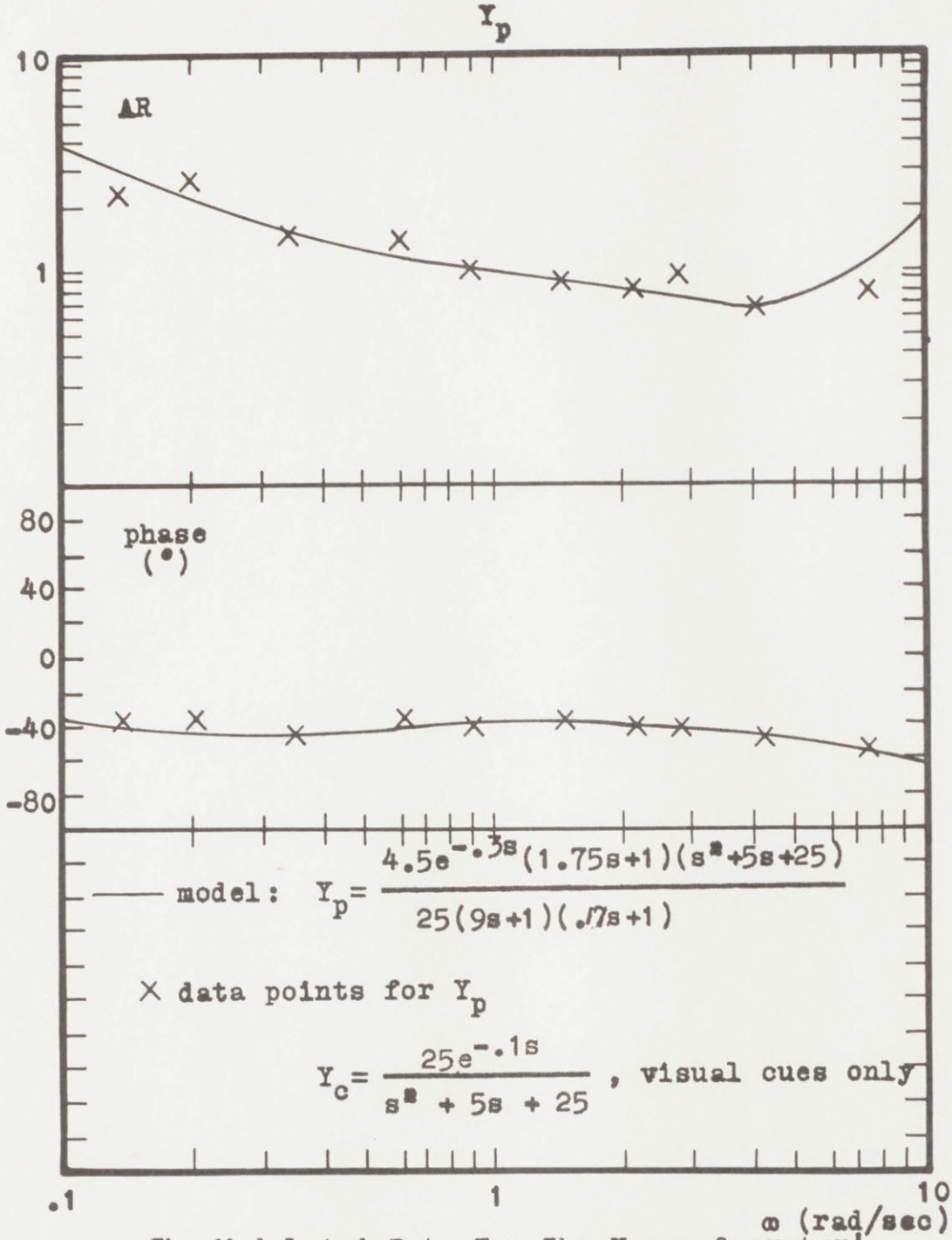

The Model And Data For The Human Operator's Describing Function

$$Y_c = \frac{25e^{-.1s}}{s^2 + 5s + 25}$$

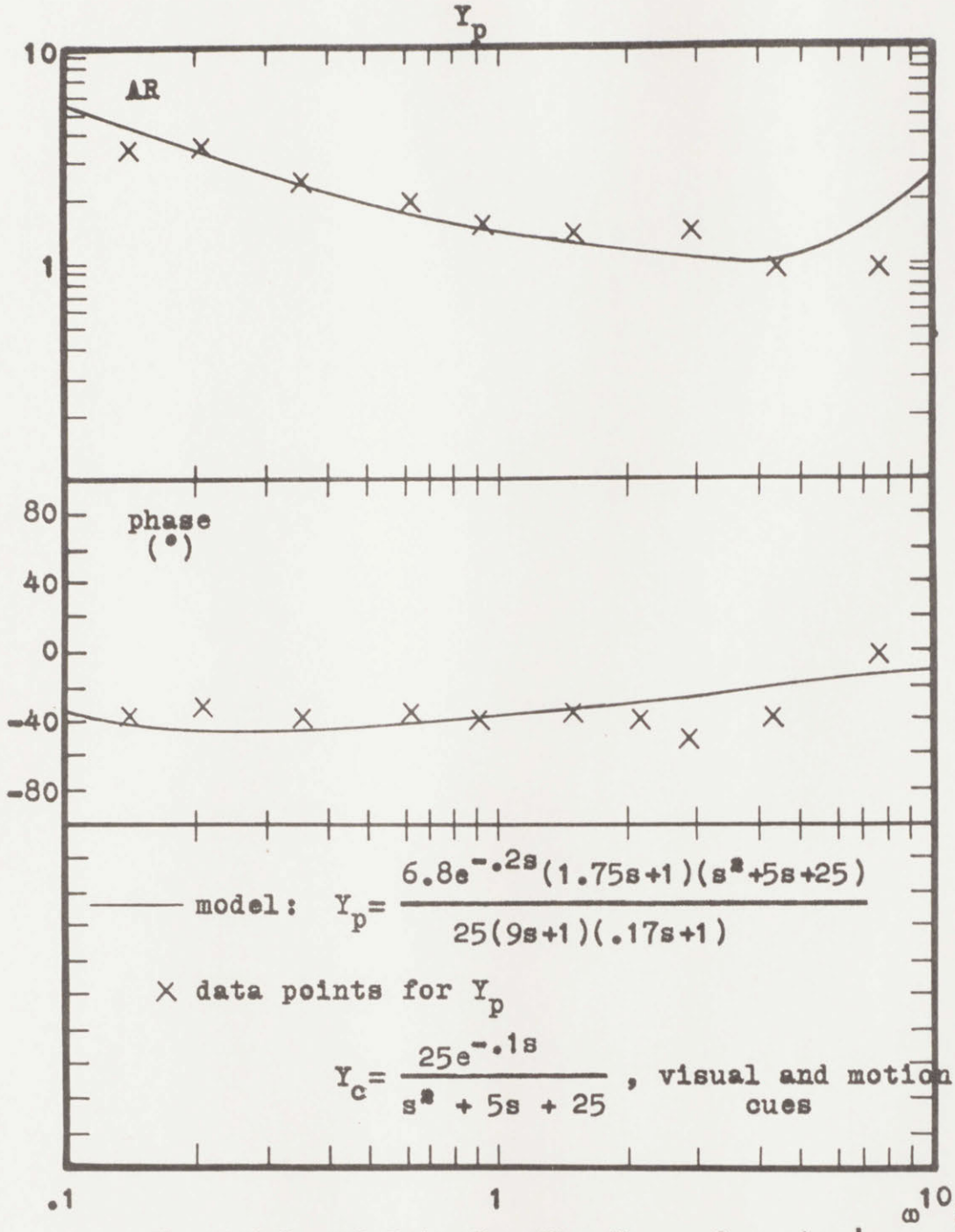

The Model And Data For The Human Operator's Describing Function

$$Y_c = \frac{25e^{-.1s}}{s^2 + 5s + 25}$$

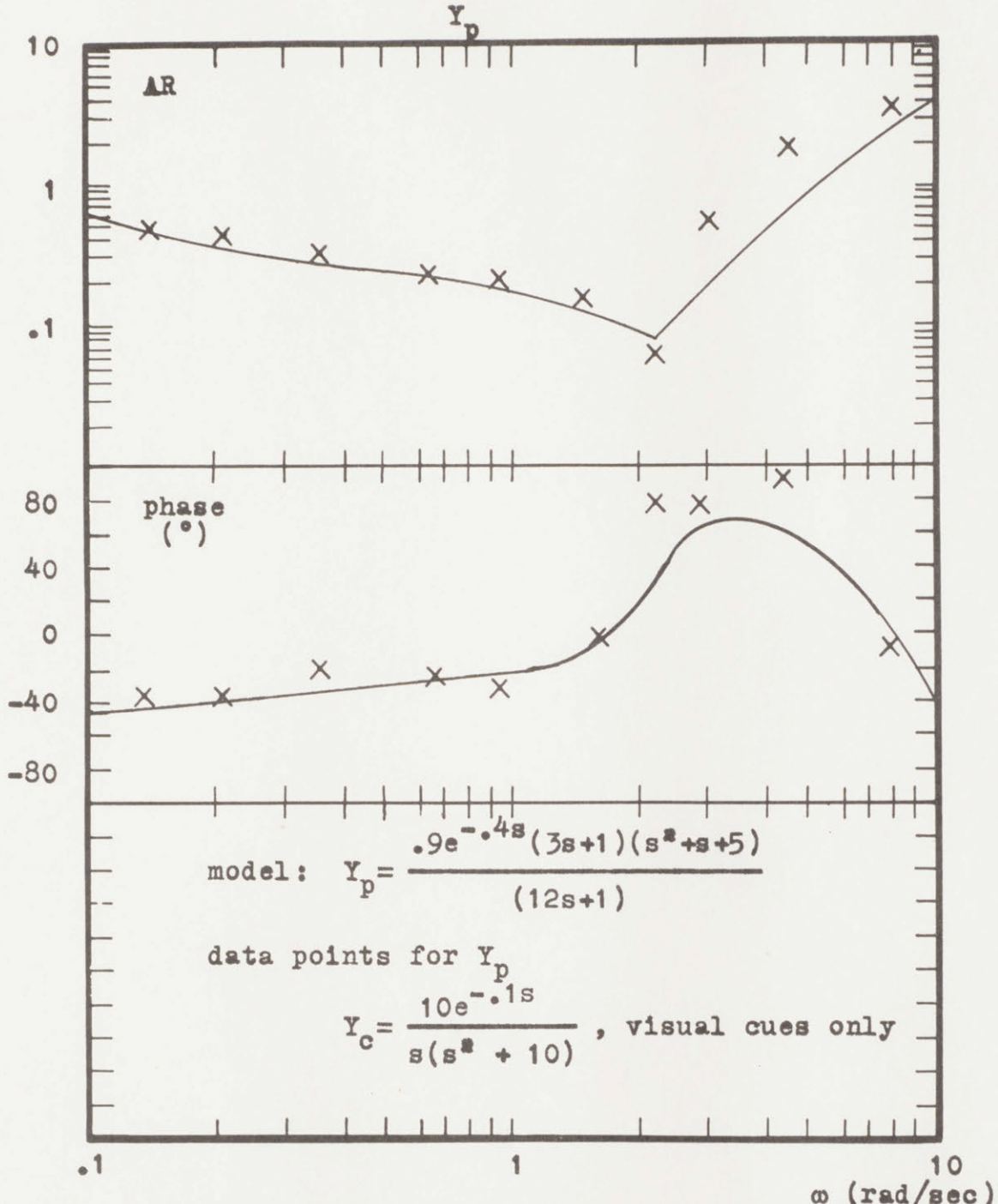

The Model And Data For The Human Operator's Describing Function

$$Y_c = \frac{10e^{-.1s}}{s(s^2+10)}$$

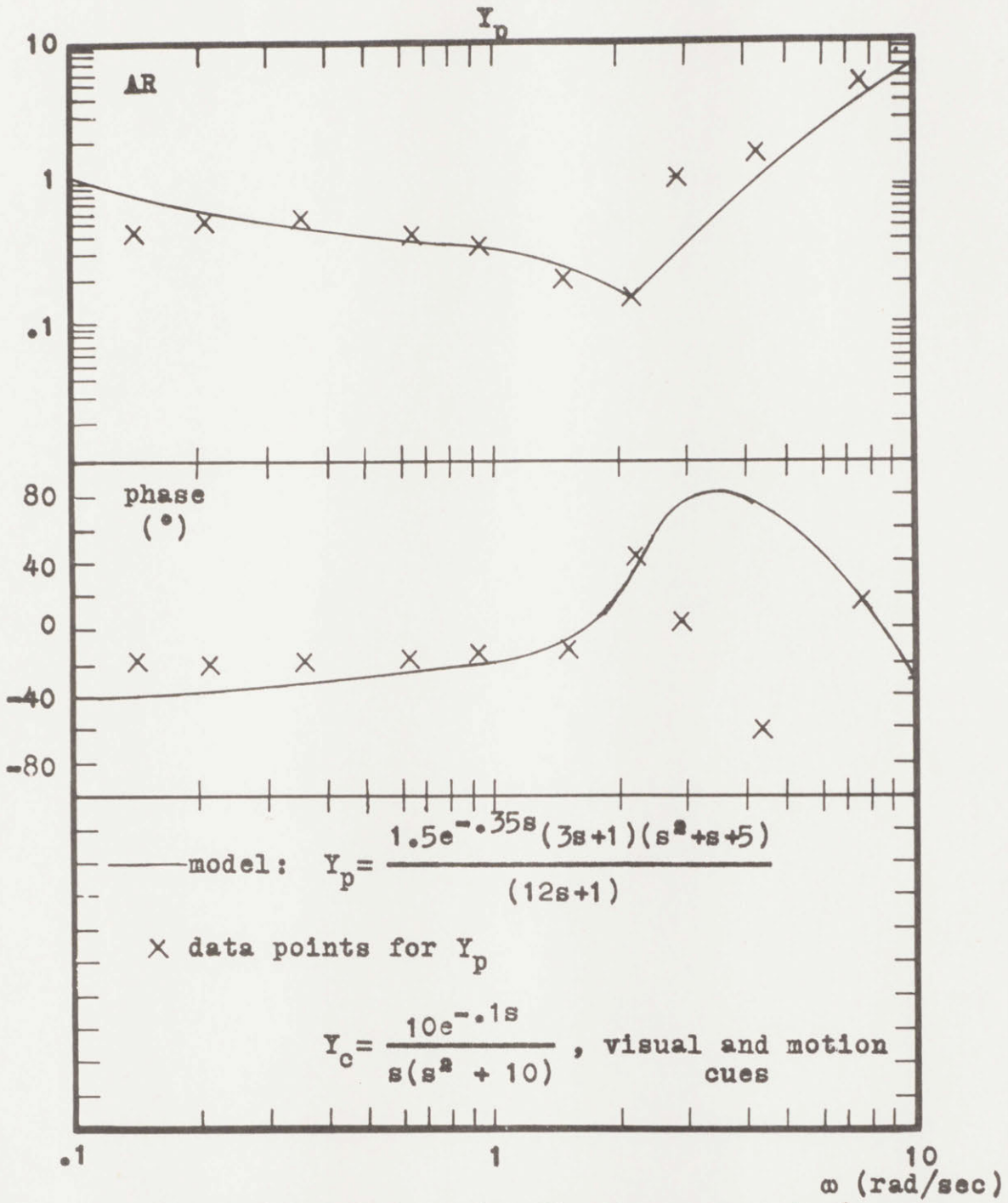

The Model And Data For The Human Operator's Describing Function

$$Y_c = \frac{10e^{-.1s}}{s(s^2 + 10)}$$

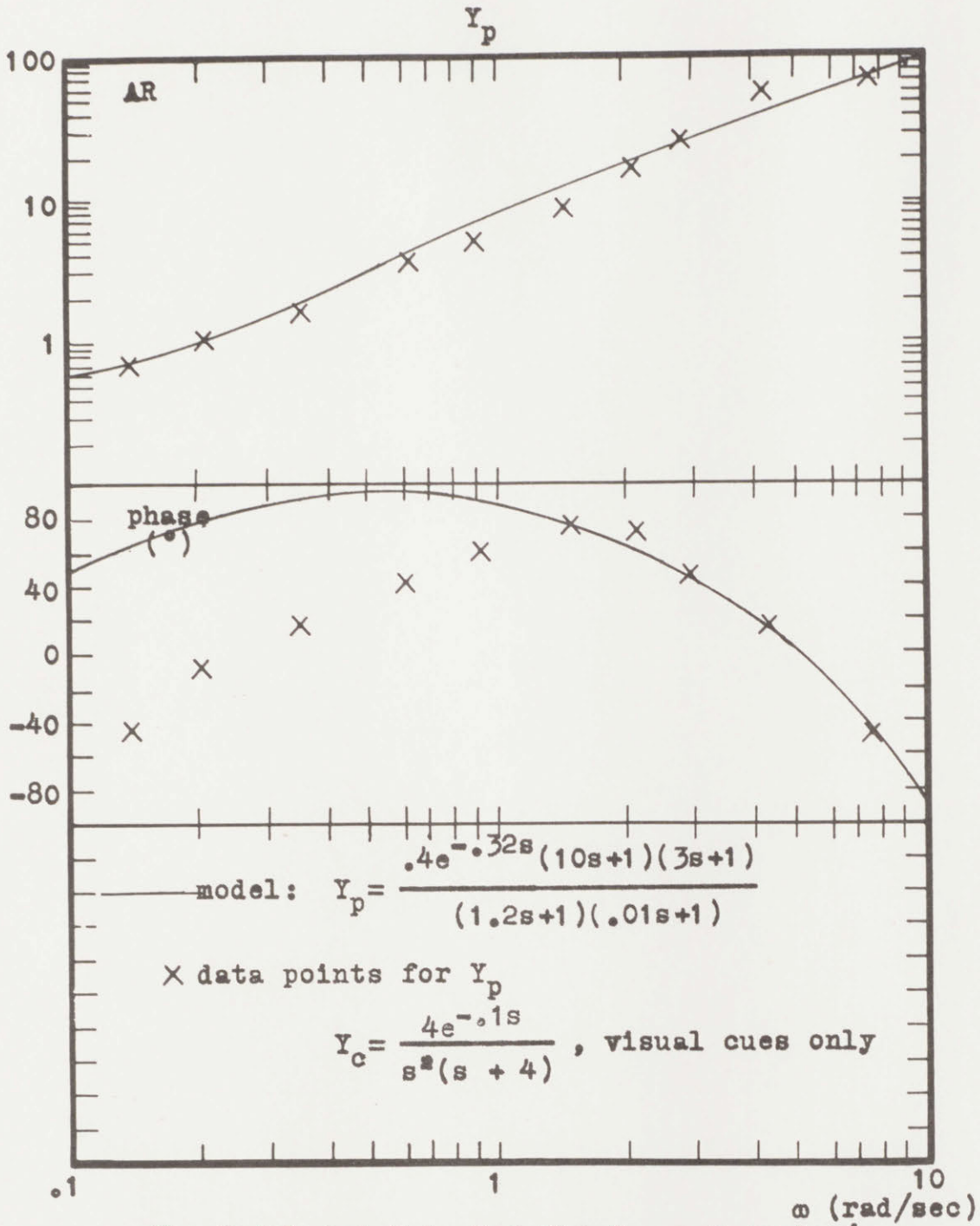

The Model And Data For The Human Operator's Describing Function

$$Y_c = \frac{4e^{-.1s}}{s^2(s+4)}$$

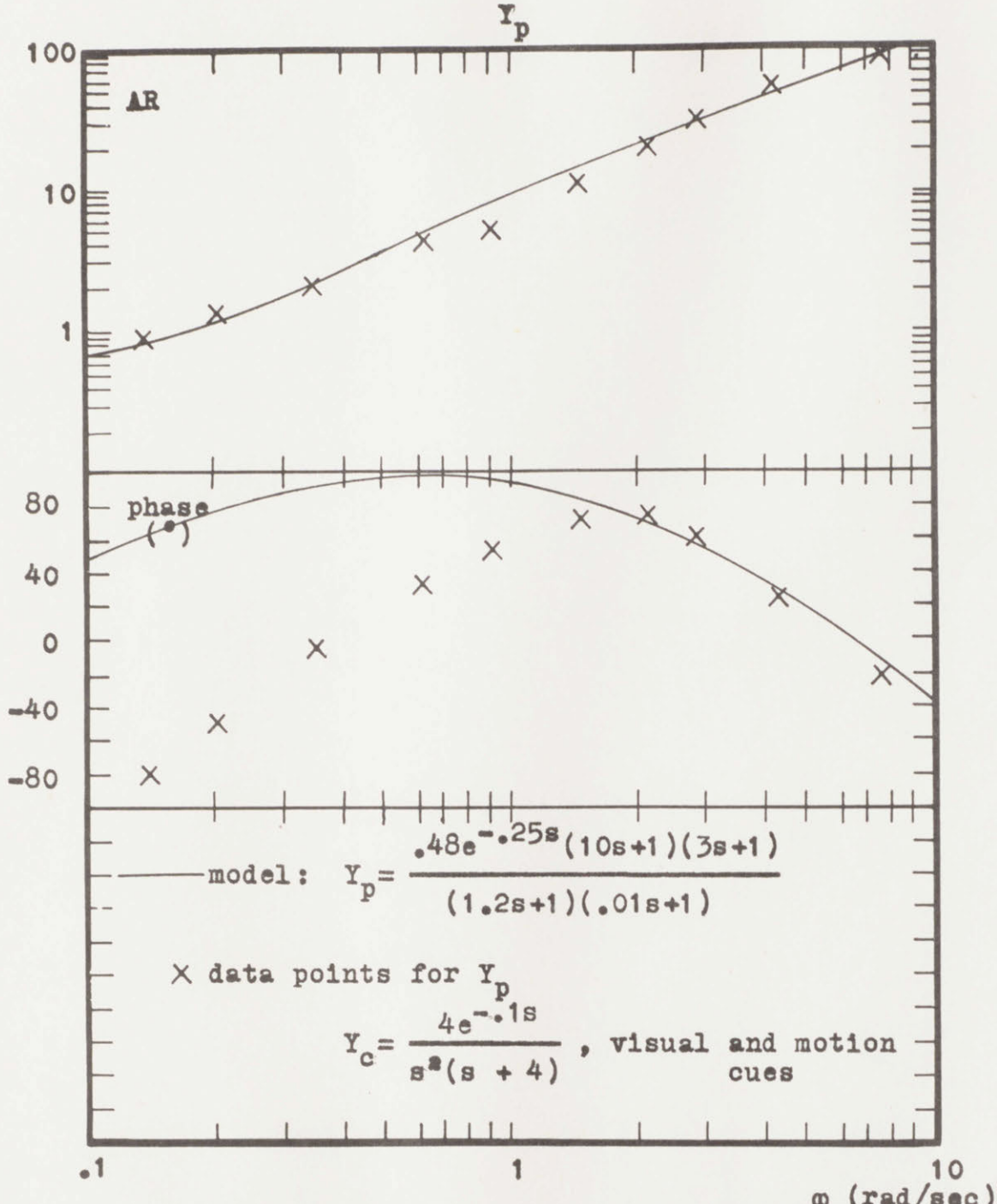

The Model And Data For The Human Operator's Describing Function

$$Y_c = \frac{4e^{-.1s}}{s^2(s+4)}$$

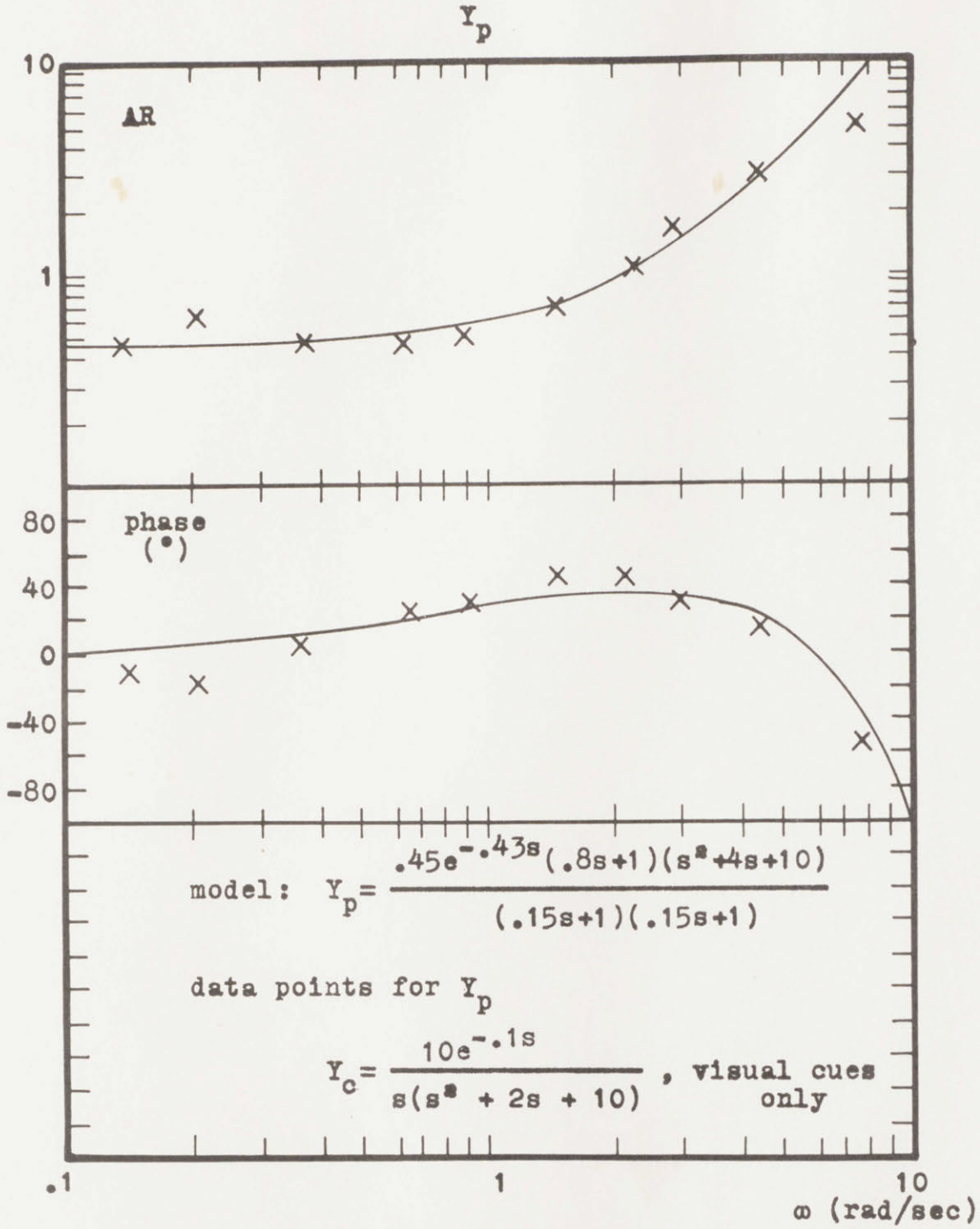

The Model And Data For The Human Operator's Describing Function

$$Y_c = \frac{10e^{-.1s}}{s(s^2 + 2s + 10)}$$

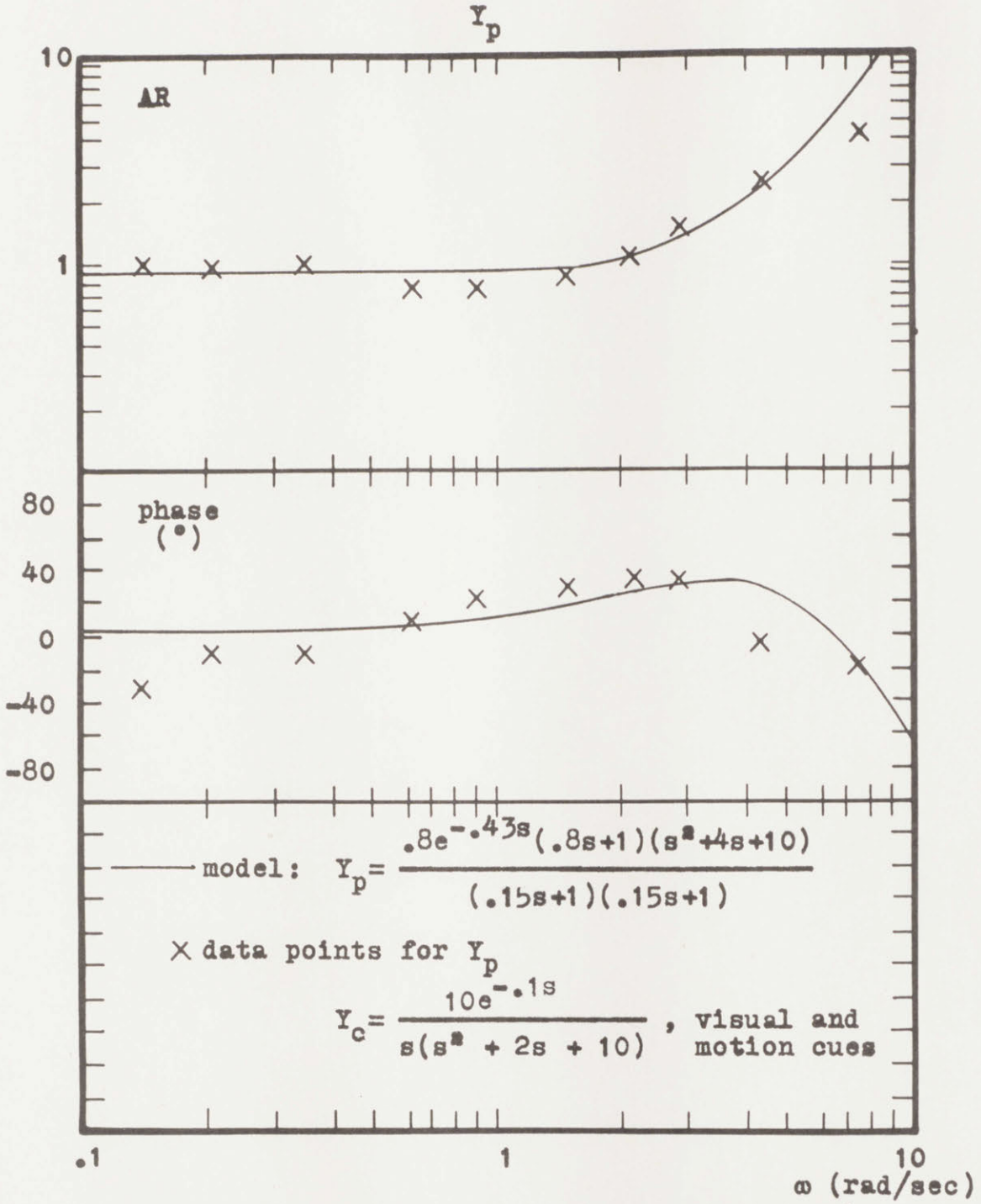

The Model And Data For The Human Operator's Describing Function

$$Y_c = \frac{10e^{-.1s}}{s(s^2 + 2s + 10)}$$

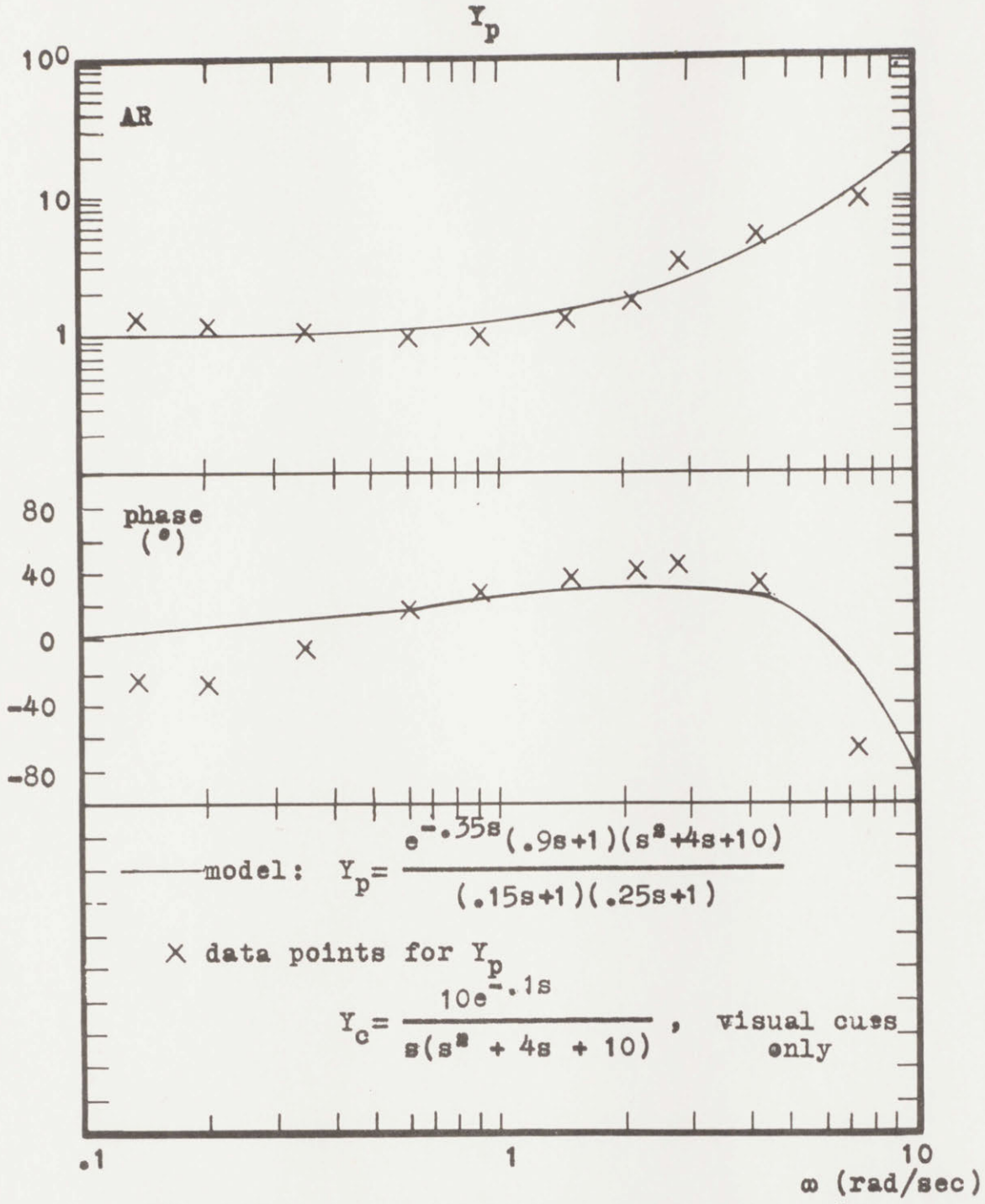

The Model And Data For The Human Operator's Describing Function

$$Y_c = \frac{10e^{-.1s}}{s(s^2+4s+10)}$$

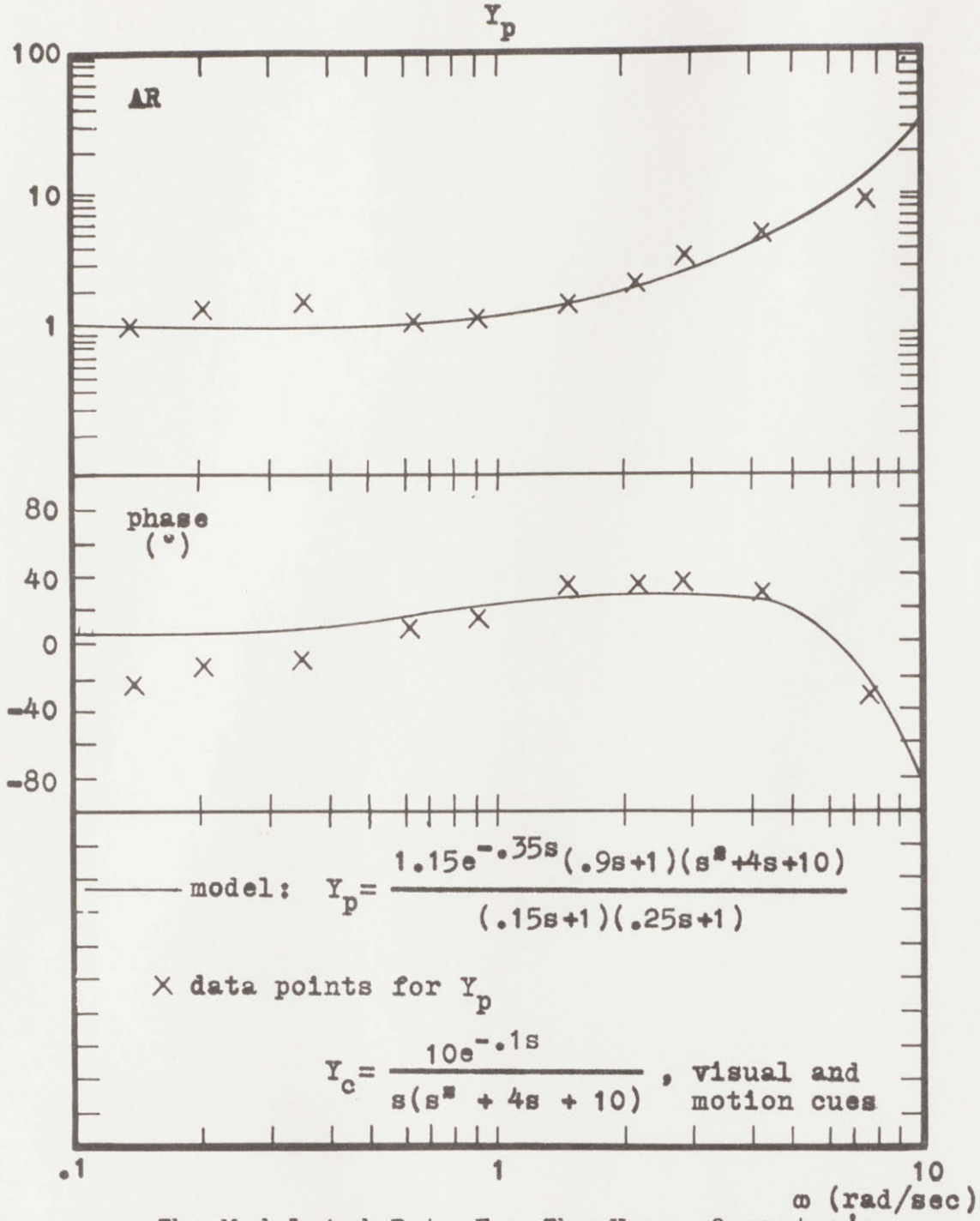

The Model And Data For The Human Operator's Describing Function

$$Y_c = \frac{10e^{-.1s}}{s(s^2+4s+10)}$$

BIBLIOGRAPHY

1. Belsley, S.E., "Man-Machine Simulation For Flight Vehicles", IEEE Trans. On Human Factors In Electronics, Vol. HEE-4, No. 1, pp 4-14, 1963.

2. Benjamin, P., "Visual And Motion Cues In Helicopter Flight", MIT Man-Vehicle Control Lab Rept., No. T-66-1, Jan., 1966.

3. Brown, P.B., H.I. Johnson, and R.G. Murgall, "Simulator Motion Effects On A Pilot's Ability To Perform A Precise Longitudinal Flying Task", NASA TN D-367, 1960.

4. Chang, S.L., Synthesis Of Optimal Control Systems, McGraw-Hill Book Co., Inc., 1961.

5. Dolkas, C.B., and J.D. Stewart, "Effect of Combined Linear and Oscillatory Acceleration On Pilot Attitude-Control Capabilities", NASA TN D-2710, 1965.

6. Elkind, J.I., "Characteristics Of Simple Manual Control Systems", MIT Lincoln Laboratory, TR-11, April 6, 1956.

7. Gerdes, R.M., "A piloted Motion Simulator Investigation Of VTOL Height-Control Requirements", NASA TN D-2451, 1964.

8. Hardy, G.H., J.V. West, and R.W. Gunderson, "Evaluation Of Pilot's Ability To Stabilize A Flexible Launch Vehicle During First-Stage Boost", NASA TN D-2807, May, 1965.

9. Harper, R.P., Jr., "Flight Evaluations Of Various Longitudinal Handling Qualities In A Variable-Stability Jet Fighter", WADC Tech. Rept. 55-299, 1955.

10. Holleman, E.C., N.A. Armstrong, and W.H. Andrews, "Utilization Of The Pilot In The Launch And Injections Of A Multistage Orbital Vehicle", IAS Paper No. 60-16, 1960.

11. Kilpatrick, P.S., "Bending Mode Acceleration Influence On Pilot Control Of Flexible Booster Dynamics", MIT Man-Vehicle Control Lab Rept., No. T-65-2, Sept., 1965.

12. Kuehnel, H.A., "Human Pilot's Dynamic Response Characteristics Measured In Flight And On A Non-moving Simulator", NASA TN D-1229, 1962.

BIBLIOGRAPHY (continued)

13. Mason, S.J., and H.J. Zimmerman, Electronic Circuits, Signals, and Systems, John Wiley and Sons, Inc., New York, 1960.

14. McFadden, N.M., R.F. Vomaske, and D.R. Heinle, "Flight Investigation Using Variable-Stability Airplanes Of Minimum Stability Requirements For High-Speed, High-Altitude Vehicles", NASA TN D-779, 1961.

15. McNemar, Q., Psychological Statistics, John Wiley and Sons, Inc., New York, 1965.

16. McRuer, D., D. Graham, E. Krendel, and W. Reisener, Jr., "Human Pilot Dynamics In Compensatory Systems", Tech. Rept. Nr. AFFDL-TR-65-15, July, 1965.

17. Meiry, J.L., "The Vestibular System And Human Dynamic Space Orientation", MIT Man-Vehicle Control Lab Rept., No. T-65-1, June, 1965, (ScD Thesis, MIT)

18. Sadoff, M., and C.W. Harper, "Piloted Flight-Simulator Research: A Critical Review", Aerospace Engrs., Vol. 21, No. 9, pp 50-63, 1962.

19. Sadoff, M., N.M. McFadden, and D.R. Heinle, "A Study Of Longitudinal Control Problems At Low And Negative Damping and Stability With Emphasis On Effects Of Motion Cues", NASA TN D-348, 1961.

20. Sadoff, M., "A Study Of Pilot's Ability To Control During Simulated Stability Augmentation System Failures", NASA TN D-1229, 1962.

21. Sadoff, M., "Effects Of High Sustained Acceleration On Pilot's Performance And Dynamic Response", NASA TN D-2067, 1964.

22. Seckel, E., I.A.M. Hall, D.T. McRuer, and D.H. Weir, "Human Pilot Dynamic Response In Flight And Simulator", WADC Tech. Rept. 57-520, 1958.

23. Smith, O.J.M., "Improved Regulation Of Loops With Flow Time", ISA Instrumentation And Control Symposium, May, 1957, Berkeley, Calif.

24. Smith, R.H., "On The Limits Of Manual Control", IEEE Transactions On Human Factors In Electronics, No. 1, Vol. HFE-4, Sept., 1963, pp 56-59.

BIBLIOGRAPHY (continued)

25. Sommers, L.G., and A.A. Burrows, "Human Tracking Performance Under Transverse Acceleration", NASA CR-21, 1964.

26. Taylor, L.W., and R.E. Day, "Flight Controllability Limits And Related Human Transfer Functions As Determined From Simulator And Flight Tests", NASA TN D-746, 1961

27. Vuorikari, V.O., "Human Role In The Control Loop Of The Automatic Landing Aircraft", S.M. Thesis, MIT, 1965.

28. Young, L.R., "Some Effects Of Motion Cues On Manual Tracking", Journal of Spacecraft and Rockets, October, 1967, pp 1300-1303.

29. Young, L.R., and J.L. Meiry, "A Revised Dynamic Otolith Model", 3rd Symposium On The Role Of The Vestibular Organs In Space Exploration, Pensacola, Florida, January 23-27, 1967.

30. Young, L.R., and J.L. Meiry, "Manual Control Of An Unstable System With Visual And Motion Cues", IEEE International Convention Record, Vol. 13, Part 6, 1965, pp 123-127.

BIOGRAPHICAL SKETCH

Richard Sargent Shirley was born on May 6, 1940, in New York City, New York. He entered the Massachusetts Institute of Technology, Cambridge, Massachusetts, in 1958 and received an S.B. and S.M. in Aeronautical and Astronautical Engineering in 1963.

From 1963 to 1967 Mr. Shirley was employed as a teaching assistant and a research assistant in the Department of Aeronautics and Astronautics at M.I.T., first at the M.I.T. Instrumentation Laboratory, and finally at the Man-Vehicle Control Laboratory, where this research was carried out.

Mr. Shirley is a member of Sigma Gamma Tau.